A COMPUTER AIDED BROAD BAND IMPEDANCE MATCHING TECHNIQUE USING A COMPARISON REFLECTOMETER

A THESIS

Presented to

The Faculty of the Division of Graduate Studies and Research

by

Robert Stephen Gordy

In Partial Fulfillment

of the Requirements for the Degree

Doctor of Philosophy

in the School of Electrical Engineering

Georgia Institute of Technology

July, 1972

A COMPUTER AIDED BROAD BAND IMPEDANCE MATCHING TECHNIQUE USING A COMPARISON REFLECTOMETER

A THESIS

Presented to

The Faculty of the Division of Graduate Studies and Research

by

Robert Stephen Gordy

In Partial Fulfillment

of the Requirements for the Degree

Doctor of Philosophy

in the School of Electrical Engineering

Georgia Institute of Technology

July, 1972

A COMPUTER AIDED BROAD BAND

IMPEDANCE MATCHING TECHNIQUE

USING A COMPARISON REFLECTOMETER

Approved:

_____

G. P. Rodrigue, Chairman

_____

R. W. Larson

_____

H. A. Ecker

Date approved by Chairman: ____

ACKNOWLEDGEMENTS

I wish to express my sincere appreciation to my thesis advisor, Dr. G. P. Rodrigue, for his guidance, assistance, and interest during the development of this thesis. I also wish to thank Dr. R. W. Larson, for his guidance and patience during the many hours of discussions, and Dr. H. A. Ecker, for his service as a member of the reading committee.

I also wish to thank the National Aeronautics and Space Administration for the Trainee Fellowship and to Dr. S. L. Dickerson for his interest and administration of the fellowship.

To Dr. A. P. Sheppard, Jr. and Dr. R. C. Johnson and Mr. R. M. Goodman, Jr. and the staff of the Systems and Techniques Department, Georgia Institute of Technology Experiment Station, go a special thank you for the facilities, financial support of this research, and the many helpful discussions, all of which helped make this endeavor successful.

My deepest appreciation goes to my wife, Kitty, to whom this thesis is dedicated, for her patience, understanding, and encouragement during the difficult times of intensive work.

TABLE OF CONTENTS

TABLE OF CONTENTS

LIST OF TABLES

LIST OF TABLES
(Continued)

LIST OF ILLUSTRATIONS

LIST OF ILLUSTRATIONS
(Continued)

LIST OF ILLUSTRATIONS
(Continued)

LIST OF ILLUSTRATIONS
(Continued)

LIST OF ILLUSTRATIONS
(Continued)

LIST OF ILLUSTRATIONS
(Continued)

LIST OF ILLUSTRATIONS
(Continued)

LIST OF ILLUSTRATIONS
(Continued)

SUMMARY

The object of this thesis research has been to develop an improved broad band impedance matching technique. The technique is capable of resolving points in the waveguide which generate reflected energy. A version of the comparison reflectometer has been developed and fabricated to determine the mean amplitude of the reflection coefficient excited at points in the guide as a function of distance, and the complex reflection coefficient of a specific discontinuity in the guide as a function of frequency. An impedance matching computer program has been developed which is capable of impedance matching the characteristics of each disturbance independent of other reflections in the guide.

The characteristics of four standard matching elements have been compiled, and their associated curves of reflection coefficient and shunt susceptance as a function of frequency are presented in Appendix A. The characteristics of the four standard matching elements (symmetrical capacitive iris, asymmetrical inductive iris, inductive metal post, and dielectric post) are also programmed into the impedance matching program listed in Appendix B.

A sample of each of the four standard matching elements have been fabricated, and results measured by both the

comparison reflectometer and a slotted line setup have been compared with theoretical predictions. The measurements made by the comparison reflectometer on the sample standard matching elements have shown agreement within the accuracy of the comparison reflectometer.

A shunt slot radiator was fabricated, and its characteristics were measured and impedance matched to demonstrate the computer aided broad band impedance matching technique. The shunt slot radiator was impedance matched over a 2 GHz bandwidth to a VSWR of 1.16 to 1.0. A theoretical dimensional perturbation has been made on the matching element to determine the extent of the sensitivity of the impedance match to machining tolerance.

As a result of this research, an economical, fast, and reliable impedance matching technique has been established which can provide broad band impedance matches.

CHAPTER I

INTRODUCTION

Motivation for Problem

For many years impedance matching at spot frequencies has been practiced, and the Smith chart is a well known tool for narrow band impedance matching. In most cases the matching element is placed some distance from the disturbance to be matched. In such a configuration the phase angle of the generalized reflection coefficient resulting from the matching element and the discontinuity to be matched varies as 2 βL, where β is the propagation constant and L is the distance between the matching element and the mismatch. The propagation constant can be expressed in the form,

$$\beta = (\omega^2 \mu \varepsilon - K^2)^{\frac{1}{2}} = 2\pi/\lambda_g \qquad (1)$$

where: λ_g is the wavelength in the waveguide, K is defined for dominant mode propagation in the rectangular waveguide by $K^2 = \pi^2/a^2$, a being the width of the guide, ω is the angular frequency in radians per second, μ is the permeability, ε is the permittivity.

Equation (1) shows that β is frequency dependent and

as a result complete cancellation of waves generally extends only over a narrow-band. The greater the distance L the narrower the bandwidth of the impedance match. If the distance L were reduced to zero then there would be no variation in phase angle due to the electrical length separating the discontinuities, and two discontinuities having reflection coefficients of equal magnitude and opposite sign, Appendix C, would present a broad-band match.

In recent years there has been a need to use many microwave devices over a large portion of a waveguide bandwidth. As an example, some antenna systems which transmit swept signals require matching over a large percentage of a waveguide band. All components which make up this transmitting system and handle the microwave energy, such as ferrite circulators and phase shifters, couplers, modulators, and many other components, must also have a large band pass. Without good impedance matching over the band of interest, large quantities of energy are reflected back towards the generator and must be absorbed in isolators or attenuators. As a result, excessive amounts of energy are demanded from the generator in order to supply the load with the desired energy. Many times these excessive energy demands are economically prohibitive and never desirable.

Usually broad band impedance matching is done without much insight into the unmatched component. The location of reflections and the number of these reflections have

in most cases been left unknown, exceptions being only in the simplest cases. Therefore, impedance matching of complex components has been largely trial and error. The end result is often neither very satisfying nor very economical.

The location of the discontinuity in the waveguide and the complex reflection coefficient of the disturbance as a function of frequency need to be known in order to gain insight into the problem of impedance matching. In this work a version of the comparison reflectometer [1] is used to determine these parameters within limits. In some cases there may be some difficulty determining a discontinuity which will identically cancel out the effect of the original mismatch. However, the impedance matching technique described provides the engineer with a powerful tool to obtain broad band impedance matches that are practically acceptable.

Definition of the Problem

Discontinuities in an otherwise uniform transmission line cause the excitation of a reflected wave in order to satisfy the boundary conditions on the electric and magnetic fields at the discontinuity. The reflected wave generally represents a reduction in transmitted power and is described as arising from a mismatch in the characteristic impedance of the line. An additional discontinuity placed in the transmission line in such a way as to cancel the original

reflected wave is said to impedance match the transmission line. This general technique provides a good match for lossless mismatches if the reflection coefficients of the mismatch and the matching discontinuity represent waves which cancel identically and if the discontinuities are located equal distances from the generator. If, however, the mismatch and matching element are not located the same distance from the generator, the match will be frequency dependent, and therefore of a narrow band nature.

Most mismatches that occur in practice are in fact reflections arising from multiple discontinuities and generally cannot be broad band impedance matched by a single matching element. Successful matching of multiple reflections requires that the location of each reflection should be known and that the contribution of each reflecting point to the total reflection coefficient be known.

The objective of this research has been to develop an improved broad band impedance matching technique. The technique is capable of resolving points in the waveguide which generate reflected energy. A version of the comparison reflectometer has been developed and fabricated to determine the mean amplitude of the reflected wave excited at a point in the guide as a function of distance, and the complex reflection coefficient of a specific discontinuity in the guide as a function of frequency.[1] An impedance matching computer program has been developed which is capa-

ble of impedance matching each disturbance independent of other reflections in the guide. The justification for the impedance matching procedure is given in Appendix C.

The characteristics of four standard matching elements have been compiled, and their associated curves of reflection coefficient and shunt susceptance as a function of frequency are presented in Appendix A. The curves take the form of plots of shunt susceptance, and plots of magnitude and phase angle of the current reflection coefficient.

CHAPTER II

BACKGROUND OF IMPEDANCE MATCHING AND OF REFLECTOMETRY

Impedance Matching

Reflected waves are generally undesirable and are to be avoided in waveguides. One method of minimizing reflections in a waveguide is to design the system such that the load impedance will completely absorb the incident fields without reflections. This load corresponds to a characteristic impedance termination in a transmission line. A second approach to the problem is to create a reflected wave near the load that is equal in magnitude but opposite in phase from the wave reflected by the load. The two reflected waves therefore cancel each other as shown by Equation (C-14). Both methods of impedance matching are usually used simultaneously. The system is initially fabricated so that the load provides as good an impedance match as is possible to obtain with a reasonable effort. The reflected wave that still remains is eliminated by the use of an impedance matching system that creates a compensating reflection. Many waveguide arrangements have been devised for generating a controllable reflection. Some of these are analogous to the impedance matching arrangements employed in transmission lines, while others are unique to

waveguides.

The shorted stub so commonly used in transmmission lines has a waveguide analogue, the stub guide or E-H tuner. In Figure 1 there are two types of tuners, the series tuner and shunt tuner. The series and shunt tuner can be used to impedance match a discontinuity or mismatched load over a narrow band of frequencies. To achieve this match the length of the stub as well as the distance from the load are critical dimensions. An analysis of this matching procedure is given in many electromagnetics texts.[2]

A second important procedure used frequently to impedance match over a narrow band of frequencies is the quarter wave transformer. The impedance transformer consists of a length of line of impedance Z_t that begins a quarter wavelength from the load, as indicated in Figure 2. The proper impedance of the quarter wave transformer Z_t is given by Equation (1) as[3]:

$$Z_t = (Z_o Z_r)^{\frac{1}{2}} . \qquad (1)$$

When the impedance Z_t satisfies Equation (1) the impedance looking to the load at point P will be equal to the characteristic impedance of the line, Z_o. It should be noted that the impedance matching just described is exact only for the frequency corresponding to the waveguide wavelength λ_{go}. Once this match is achieved at a particular

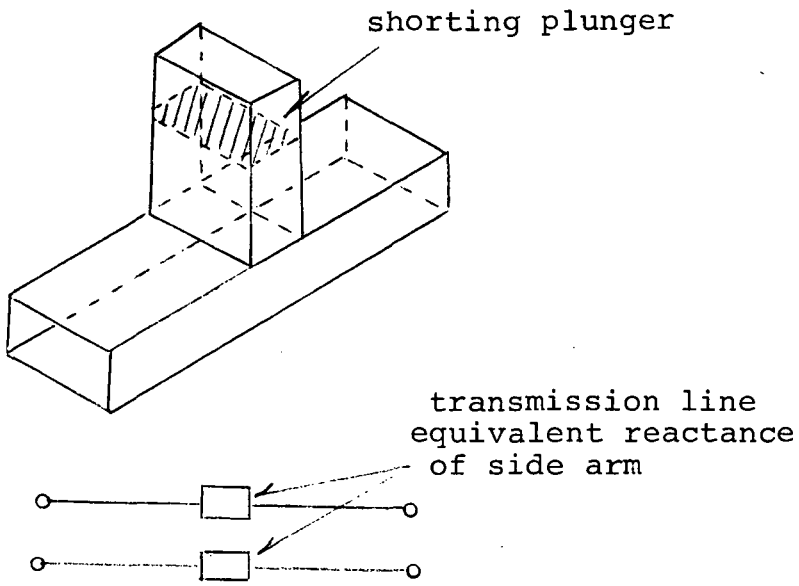

(a) Series T

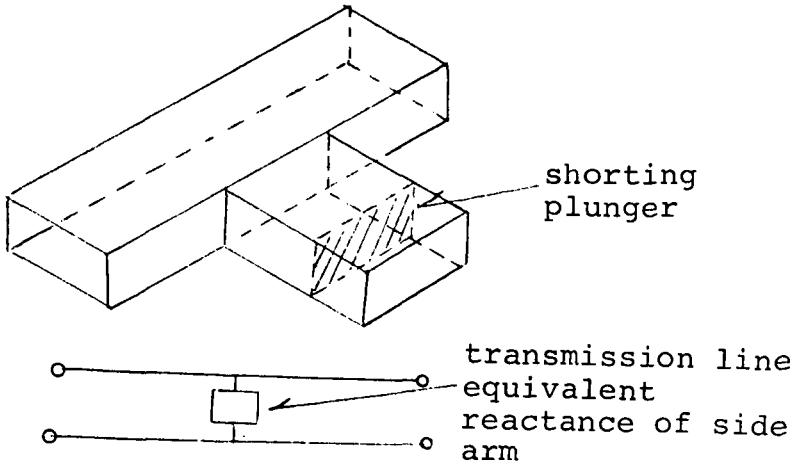

(b) Shunt T

Figure 1. Series and Shunt Tuners

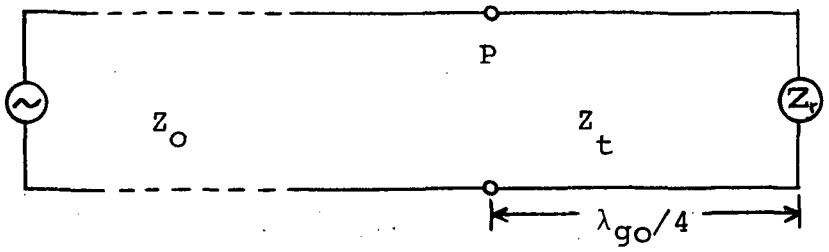

Figure 2. Quarter Wave Transformer

λ_{go}, the match does not hold for a general $\lambda_g \neq \lambda_{go}$. This results in a narrow band impedance match. There are many such techniques giving restricted matches.

Reflectometry

The basic function of a reflectometer consists of sampling an incident wave and a reflected wave and determining the ratio of the two. The ratio of the reflected to the incident electric field is defined as the voltage reflection coefficient Γ, and has both real and imaginary parts.

The general procedure[4] uses two directional couplers located back to back as in Figure 3. The incident energy is coupled into the directional coupler D1 and the reflected energy is coupled into the reversed directional coupler D2. Each directional coupler is terminated in a square law detector. These detectors provide a D.C. voltage output which is proportional to the square of the electric field intensity. If the incident detector is used to provide a feedback signal which enables a high frequency oscillator to maintain a constant power level, then the

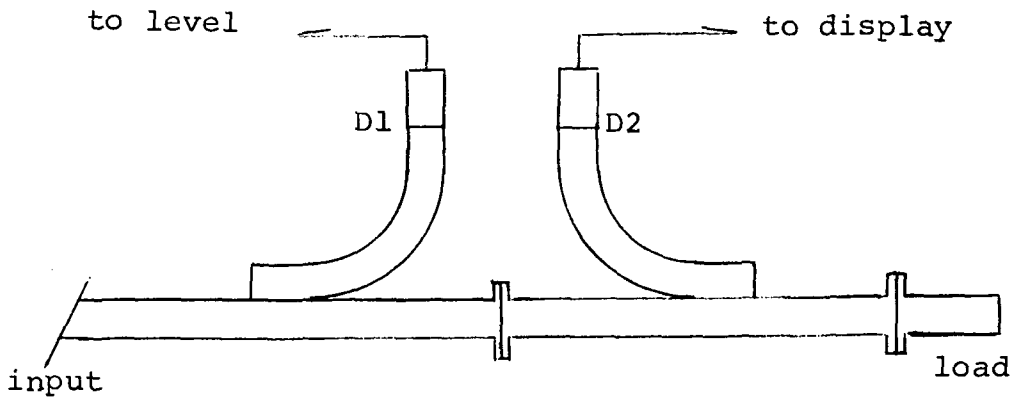

(a) Leveled Reflectometer

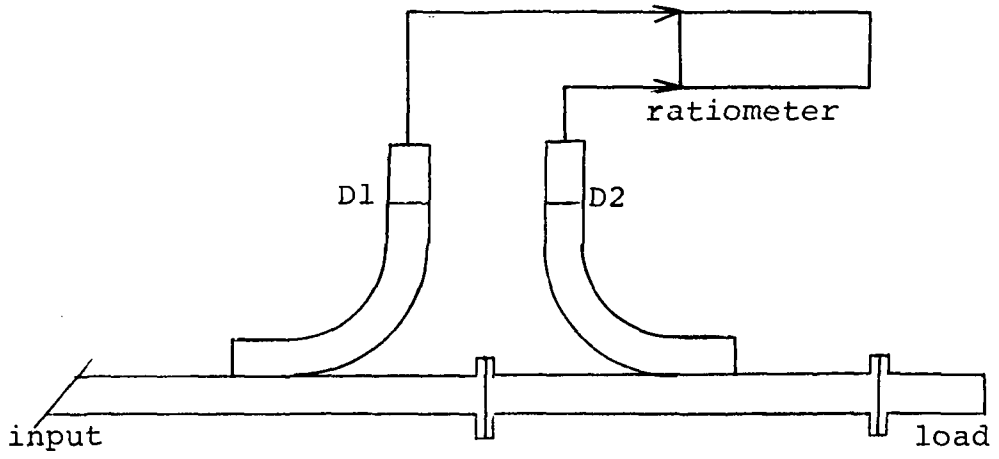

(b) Unleveled Reflectometer

Figure 3. Reflectometer Systems

magnitude squared of the reflection coefficient is proportional to the output of the detector D2, Equation (2):

$$|\Gamma|^2 = T\ E_r\ , \qquad (2)$$

where T is a proportionality constant, and E_r is the voltage output of the square law detector.

Alternatively, if the output of both detectors are used as inputs to a ratio meter than the reading of this device is a function of the magnitude of the reflection coefficient squared.[5] The ratio meter can be calibrated to provide magnitude of reflection coefficient or voltage standing wave ratio (VSWR). The use of a swept oscillator in either of the above two cases will provide a display of the magnitude of reflection coefficient as a function of frequency.

It is well to note that these techniques do not provide phase information. Since the phase information is unknown, there is no assurance that two discontinuities will in fact provide a cancellation of waves even though the curves of the magnitude of the reflection coefficient $|\Gamma|$ are equivalent. Therefore, impedance matching using these reflectometers is largely trial and error.

Reflecto "meter"

A technique which takes a different approach to

reflectometry was introduced by F. C. deRonde.[6] This system called the reflecto "meter" utilizes three detectors in the main transmission line, Figure 4, instead of the two directional couplers as in Figure 3. The advantage of this device is improved accuracy of the modulus of reflection coefficient, but the setup is more difficult to fabricate than the reflectometer composed of directional couplers. The common disadvantage is that it gives no phase information and cannot resolve individual discontinuities in a waveguide.

It is desirable when impedance matching to have both the phase information and the magnitude information of the reflection coefficient, as indicated in Appendix C. This information can be obtained using slotted line techniques,[7,8] but this procedure is extremely time consuming when dealing with the many data points needed to cover a large frequency range. In addition, the slotted line technique has no provision for the separation of reflection coefficients generated by different discontinuities.

Time Domain Reflectometer

Time Domain Reflectometer (TDR) is an approach which can determine the location of discontinuities in a transmission line. TDR is an application of a pulse reflection technique.[9,10] A pulse of energy is transmitted down a transmission line. If there exists an impedance discontinuity in the transmission line, energy will be reflected

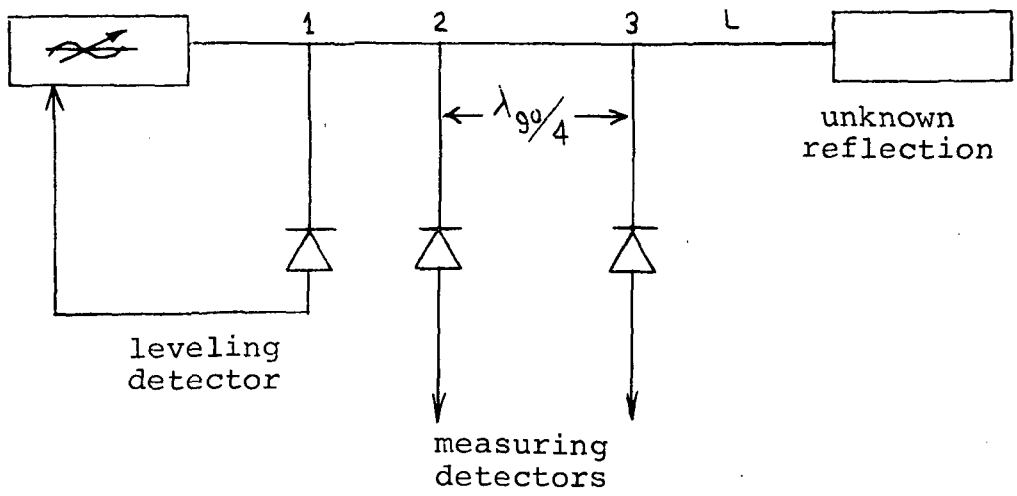

Figure 4. Reflecto "meter"

back toward the generator. The location of the discontinuity can be determined by measuring the round trip time delay for reception of reflected pulses. The narrowness of the pulse and the quality of the measuring equipment determine the resolution capabilities of the TDR. The narrowband TDR is used when measuring waveguide structures.[10] The amplitude of the reflected pulse is related to impedance, so any slight deviation from the characteristic impedance level of the output of the TDR can easily be recognized and measured.

Time Domain Reflectometry has been applied to open transmission lines, coaxial cable and recently to waveguide structures. For the waveguide structures a step modulated carrier is used[10] to remain within the confines of the waveguide passband. Generally, the true value of the narrowband TDR is in applications where long runs of waveguide are used. The locating accuracy for this device is of the order of ±3 percent of the distance measured, depending on the quality of the leading edge of the transmitted pulse.

Network Analyzer

Recently, the network analyzer has been introduced.[11] This device characterizes microwave components in terms of their scattering matrix. This characterization allows the microwave device to be modeled and more efficiently used in complex networks. The network analyzer is an important impedance matching tool, as a result of its modeling ability.

However, the network analyzer lacks one important quality, it cannot measure the effect of individual discontinuities independent of adjacent disturbances. Therefore, the impedance matching of the composite discontinuities of the microwave device remains a difficult problem requiring a composite of matching elements. If however, the composite reflection coefficients of microwave devices could be broken down into an ensemble of simpler reflections, then it is reasonable to assume that the simpler reflections would be easier to impedance match individually. The net result is an overall impedance matched device.

Comparison Reflectometer

The comparison reflectometer[1] is another technique which provides the location of a disturbance in the guide. If there is more than one disturbance in the guide these disturbances are shown as separate disturbances and their locations are displayed. The comparison reflectometer also can provide a curve of magnitude and phase of the reflection coefficient as a function of frequency for each discontinuity in the guide.

In using the comparison reflectometer inaccuracies in the waveguide components are largely cancelled out due to the technique of taking measurements, as described in Chapter III. This cancelling effect enables a background reflection coefficient noise level typically less than 0.00005 to be measured, as shown in Figure 31. Because

of these attributes a comparison reflectometer has been chosen as the basis of the computer aided impedance matching technique, and has been fabricated to take the measurements used in this research.

CHAPTER III

APPROACH TO IMPEDANCE MATCHING

Introduction

The computer aided broad band impedance matching technique, Figure 5, consists of first collecting data to determine the combined complex reflection coefficient of both a reference step and a test discontinuity. The location of the disturbance to be impedance matched is then determined and the complex reflection coefficient is calculated. The physical dimensions and the relative location of a preselected matching element are calculated by the impedance matching computer program. The result is the impedance matched disturbance. If additional matching is required, a second matching element may be selected. The physical parameters of this element are again calculated by the impedance matching program.

Two sets of data are taken by the comparison reflectometer at 50 MHz intervals from 7.975 GHz through 12.425 GHz. One set of data is taken with the reference step terminated in a matched load, Figures 6 and 7. The second set of measurements is taken with the reference step terminated by the test disturbance. These data are processed by two computer programs. The first, Test 1,

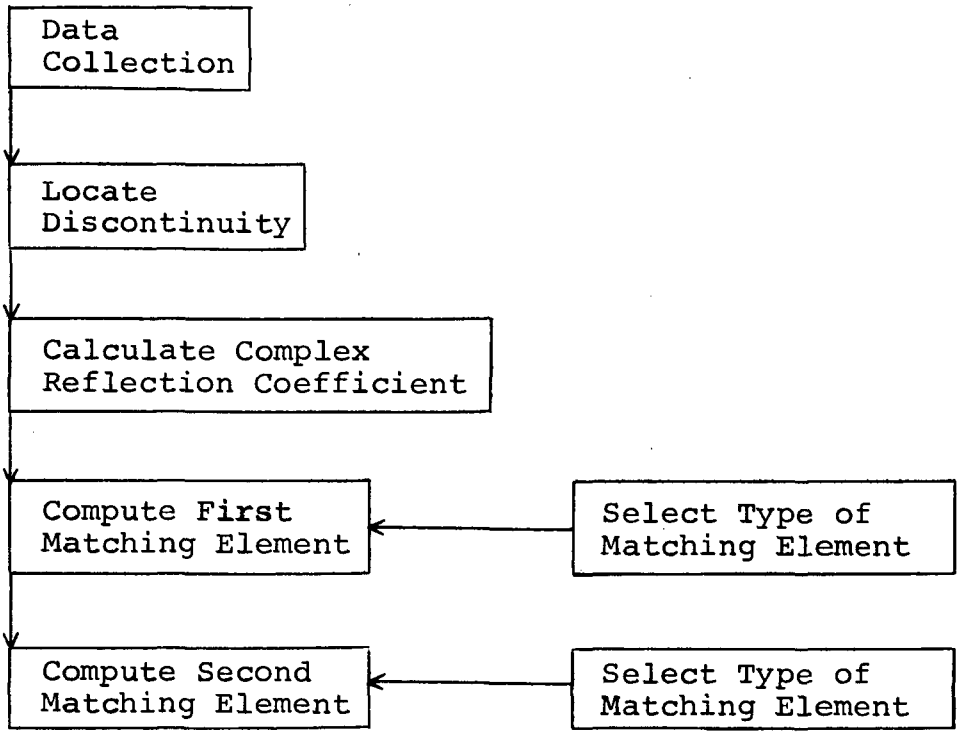

Figure 5. Flow Chart of the Impedance Matching Technique

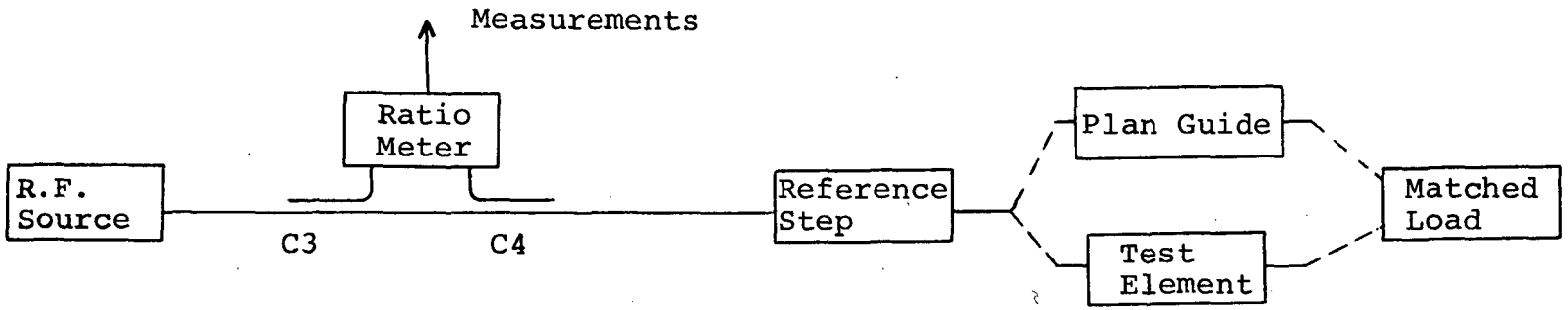

Figure 6. Comparison Reflectometer Functional Flow Graph

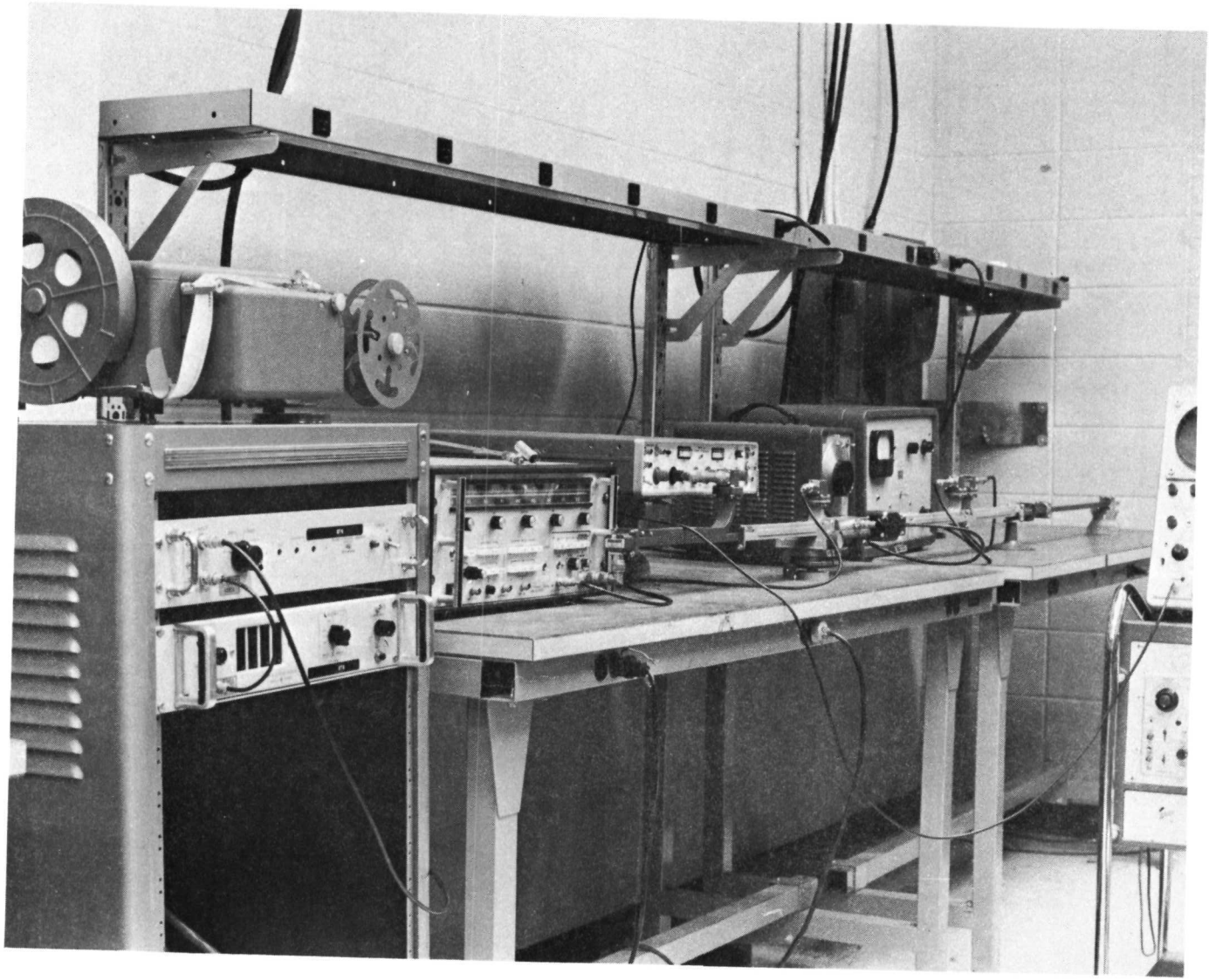

Figure 7. Photograph of Comparison Reflectometer System

determines the mean magnitude of the reflection coefficient as a function of distance as shown in Figure 8. This curve locates discontinuities relative to the reference plane. The second program, Test 2, calculates the complex current reflection coefficient as a function of frequency at a predetermined location in the waveguide, Figure 9. This complex reflection coefficient characterizes the measured disturbance in the impedance matching program.

The impedance matching computer program developed as part of this thesis determines the physical dimensions of a matching element and an appropriate location with respect to the original mismatch. The program provides the best impedance match over the bandwidth of interest in the root mean square sense. This "best" impedance match is dependent on the matching element and the method of choosing its parameters. The input data for the matching program are the results of the comparison reflectometer program, Test 2. All of these programs discussed are listed in Appendix B.

Theory of Operation of a Comparison Reflectometer

Introduction

The comparison reflectometer first introduced by D. L. Hollway,[1] is an instrument designed to locate and measure the characteristics of reflections in waveguides and transmission-line systems. It is particularly suitable for measuring small reflections in microwave components up to

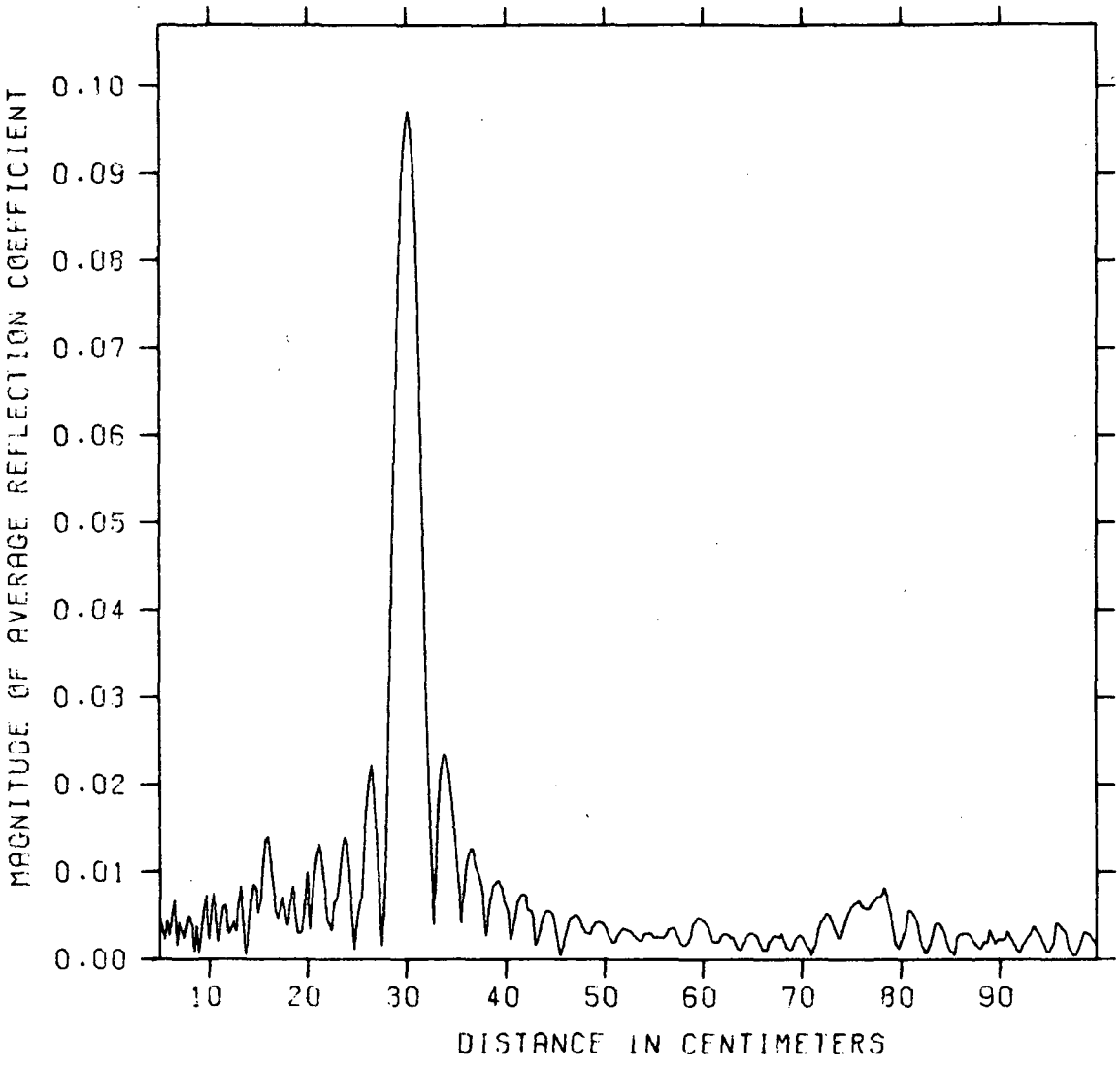

Figure 8. Typical Locating Plot

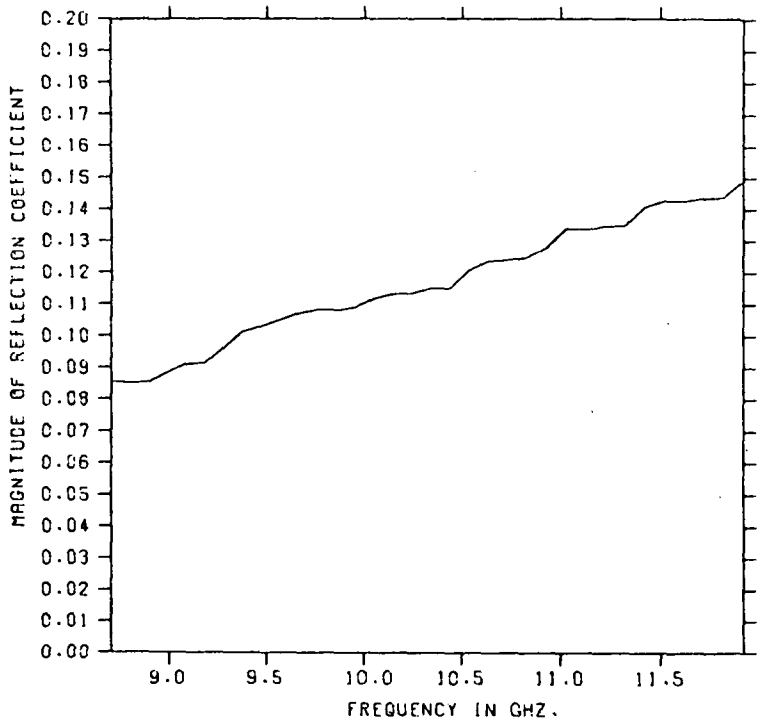

(a) Magnitude

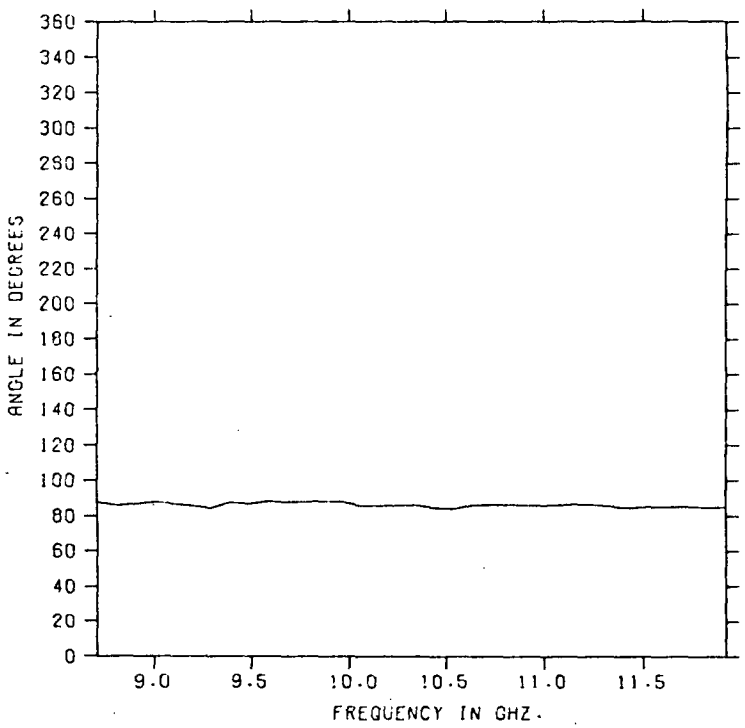

(b) Phase

Figure 9. Typical Plot of Magnitude and Phase of the Current Reflection Coefficient

one meter in length.

The principle of operation is the comparison of the total magnitude of reflection coefficient of a known reference disturbance and a test disturbance with that of the known reference disturbance. From this comparison the location of the test mismatch can be determined, and its complex reflection coefficient as a function of frequency calculated. A high speed digital computer is used to perform the necessary calculations.

Governing Equations

Consider a waveguide system shown in Figure 6. A component having a single reflection $|\Gamma_1|\exp[j\theta]$ is connected to a reference reflection having the scattering coefficients shown in Figure 10. The reflection coefficient of the combination may be written,

$$b_1/a_1 = (S_{22}(1-S_{33}\Gamma_1)+S_{32}\Gamma_1 S_{23})/(1-S_{33}\Gamma_1) \qquad (1)$$

$$b_1/a_1 = \left[S_{22} - \Gamma_1(S_{22}\,S_{33} - S_{32}\,S_{23})\right]/(1-S_{33}\Gamma_1). \qquad (2)$$

Generally, the reflection to be measured will be located at some distance L_1 from the reference plane, so that the value of Γ_1 measured at this plane will be,

$$\Gamma_1 = |\Gamma_1|\ \exp\ [j(\theta-2\beta L_1)]\ . \qquad (3)$$

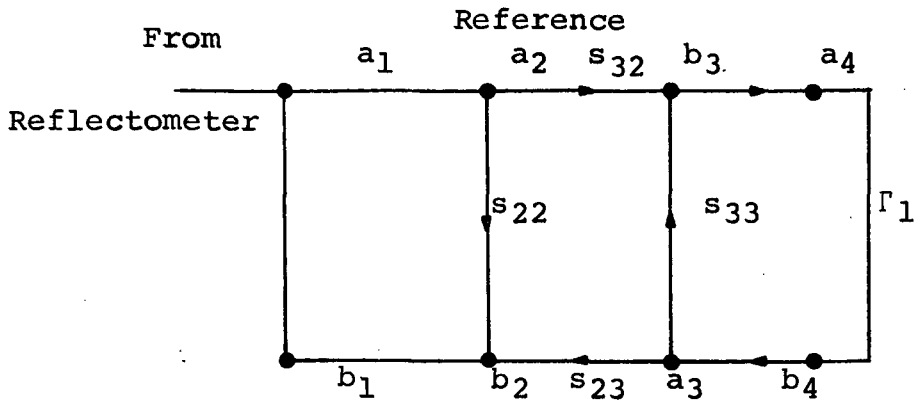

Figure 10. Scattering Representation of a Single Reflection Connected to a Reference Connection

The theory and computations are simplified, and the accuracy of the results improved if a reference reflection is used having a reflection coefficient which is essentially constant in magnitude and phase throughout the frequency band at a stationary reference plane. A design which has been found by D. L. Hollway[12] to be superior to others in this respect consists of a symmetrical E-plane taper, having only negligibly small reflections followed by a sudden step back to full guide height.

If we ignore for later simplicity the small correction required for the step capacitance, the step reflection, shown in Figure 11a, may be considered as a lossless transformer[1], having turns ratio N, set in the guide at the reference plane as in Figure 11b.

Let Γ_r be the voltage reflection coefficient of this reference as seen from the generator side, then

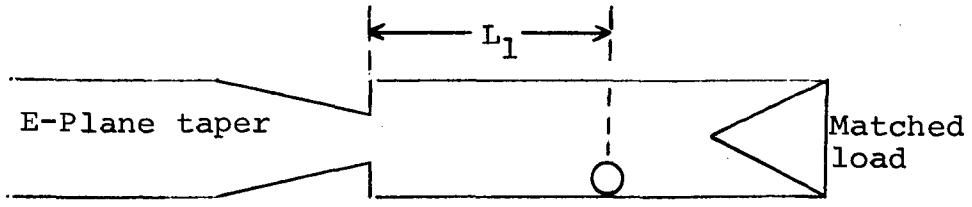

(a) Reference Step and Typical Disturbance

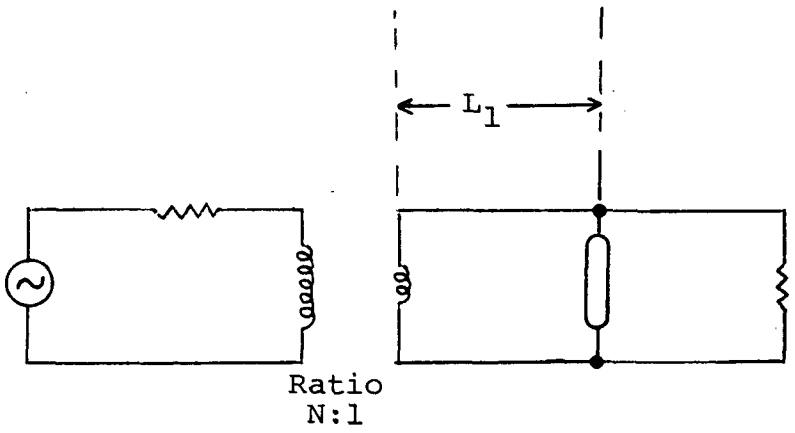

(b) Transformer Model

Figure 11. A Model for the E-Plane Taper and a Typical Disturbance

$$\Gamma_r = S_{22} = (N^2-1)/(N^2+1) \tag{4}$$

and $$S_{33} = (1-N^2)/(1+N^2) \tag{5}$$

and $$S_{32} = S_{23} = 2N/(1+N^2) \tag{6}$$

Since Γ_r has been chosen to have zero phase it will be written without a modulus sign.[1]

The total reflection coefficient at the reference plane is found by substituting Equations (4), (5), (6) into Equation (2), the result being

$$\Gamma = b_1/a_1 = (\Gamma_r(1+\Gamma_r\Gamma_1) + S_{23}S_{32}\Gamma_1)/(1+\Gamma_r\Gamma_1) \tag{7}$$

but $$S_{32} \cdot S_{23} = 1-\Gamma_r^2$$

therefore $$\Gamma = (\Gamma_r + \Gamma_1)/(1+\Gamma_r\Gamma_1)$$

$$= \left(\Gamma_r+|\Gamma_1|\exp\{j(\theta-2\beta L)\}\right)/\left(1+\Gamma_r|\Gamma_1|\exp\{j(\theta-2\beta L)\}\right) \tag{8}$$

A measured curve of the total reflection coefficient Γ is shown in Figure 12 for a fabricated capacitive iris and the fabricated reference step. The oscillations in the waveform as a function of frequency is in part a function of separation distance L as described by Equation (8).

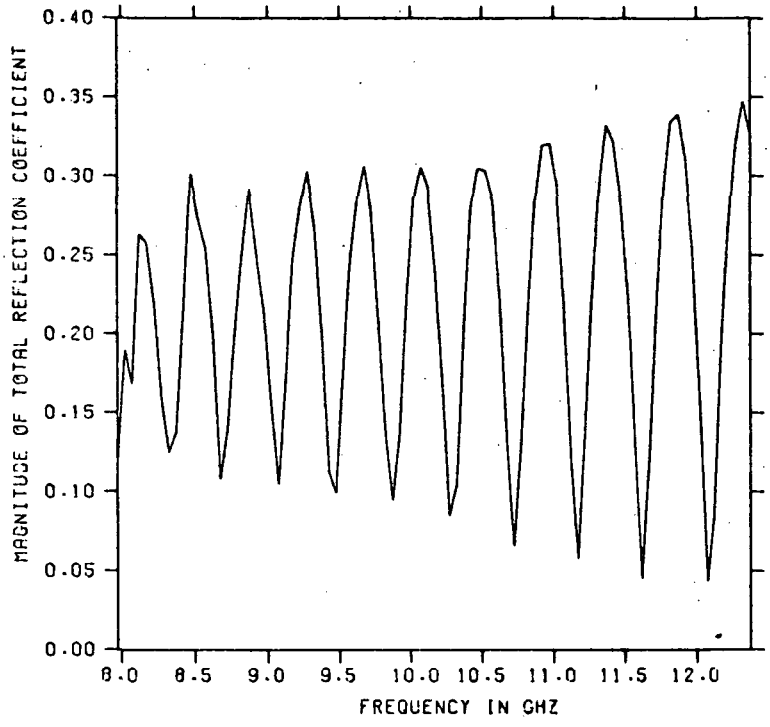

Figure 12. Total Magnitude of Reflection Coefficient for a Capacitive Iris 27.0 Centimeters from the Reference Step

Let $$c = |\Gamma_1|\cos(\theta-2\beta L) \tag{9}$$

$$s = |\Gamma_1|\sin(\theta-2\beta L) \tag{10}$$

Substituting Equations (9), (10) into (8),

$$\Gamma = [(\Gamma_r+c+js)]/[1+\Gamma_r(c+js)] \tag{11}$$

$$\Gamma=[\Gamma_r(1+|\Gamma_1|^2)+c(1+\Gamma_r^2)+js(1-\Gamma_r^2)]/[1+2\Gamma_r c+\Gamma_r^2|\Gamma_1|^2] \tag{12}$$

Part of the return wave passes through the directional coupler C4, Figure 6, and produces a DC voltage which is independent of the phase of Γ. The output of the crystal detector at C3 is proportional to $|\Gamma|^2$. Therefore, squaring the magnitude of (12),

$$|\Gamma|^2 = [\Gamma_r^2(1+|\Gamma_1|^2)^2 + 2c\Gamma_r(1+|\Gamma_1|^2)(1+\Gamma_r^2)$$

$$+c^2(1+\Gamma_r^2)^2+s^2(1-\Gamma_r^2)^2]/(1+2c\Gamma_r$$

$$+\Gamma_r^2|\Gamma_1|^2)^2 \quad . \tag{13}$$

We are concerned chiefly with small reflections, therefore terms such as $\Gamma_r^3|\Gamma_1|^3$ are small compared to unity. If $\Gamma_r = .2$ and $|\Gamma_1| = .1$ then $\Gamma_r^3|\Gamma_1|^3$ is equal to 8×10^{-6}. Ignoring these and terms containing cos $(2\theta - 4\beta L)$ for later simplicity, the denominator of Equation (13) may be written as:

$$(1+2c\Gamma_r+\Gamma_r^2|\Gamma_1|^2)^2$$

$$\cong 1/(1-4c\Gamma_r+4\Gamma_r^2|\Gamma_1|^2), \tag{14}$$

with these approximations,

$$|\Gamma|^2 \cong \Gamma_r^2+|\Gamma_1|^2-2\Gamma_r^2|\Gamma_1|^2+2\Gamma_r|\Gamma_1|$$

$$\cdot(1-\Gamma_r^2-|\Gamma_1|^2+\Gamma_r^2|\Gamma_1|^2)\cos(\theta-2\beta L) \qquad (15)$$

In order to compute $|\Gamma_1|\cos(\theta-2\beta L)$, (15) may be rearranged,

$$|\Gamma_1|\cos(\theta-2\beta L) = \frac{|\Gamma|^2-\Gamma_r^2+|\Gamma_1|^2-2\Gamma_r^2|\Gamma_1|^2}{2\Gamma_r(1-\Gamma_r^2-|\Gamma_1|^2+\Gamma_r^2|\Gamma_1|^2)} \qquad (16)$$

Let $$\Lambda \equiv (1-\Gamma_r^2-|\Gamma_1|^2+\Gamma_r^2|\Gamma_1|^2), \qquad (17)$$

and $$G(\nu) \equiv |\Gamma|^2/2\Gamma_r\Lambda. \qquad (18)$$

Then (16) can be rewritten as,

$$|\Gamma_1|\cos(\theta-2\beta L) = G(\nu)-(\Gamma_r^2+|\Gamma_1|^2-2\Gamma_r^2|\Gamma_1|^2)/2\Gamma_r\Lambda \qquad (19)$$

The term $G(\nu)$ is a function of wavenumber and is to be determined from the readings of the digital volt meter as will be described in the next sections. Λ is a correction term near unity.

Up to this point in the derivation only one reflection has been considered in addition to the reference. In general, the components being measured will contain more than one reflection, Γ_1, Γ_2 $\cdots\Gamma_n$, at distances L_1, L_2 $\ldots.L_n$, and

these must be computed from the data $G(\nu)$.

Assume that interactions between adjacent test reflections may be neglected, then by superposition,

$$G(\nu) = \sum_{n=1}^{\infty} |\Gamma_n| \cos(\theta_n - 4\pi L_n \nu) \tag{20}$$

The above equation may be written as a Fourier series,

$$G(\nu) = \sum_{n=1}^{\infty} [a_n \cos(4\pi n L' \nu) + b_n \sin(4\pi n L' \nu)] \tag{21}$$

where $L_n = nL'$ and L' is the unit length.

The component reflections are found by taking the finite Fourier transforms.

$$a_n = 1/\nu' \int_{\nu_1}^{\nu_2} G(\nu) \cos(n\pi\nu/\nu') d\nu \tag{22}$$

and

$$b_n = 1/\nu' \int_{\nu_1}^{\nu_2} G(\nu) \sin(n\pi\nu/\nu') d\nu \tag{23}$$

where $2\nu' = \nu_2 - \nu_1$, the range of wavenumber interval in which the $G(\nu)$ is measured. And $L' = \frac{\nu'}{4}$

From (20) a_n and b_n are also equal to

$$a_n = |\Gamma_n| \cos\theta_n \tag{24}$$

$$b_n = |\Gamma_n| \sin\theta_n \tag{25}$$

using the trig expansion,

$$\cos (x - y) = \cos x \cos y + \sin x \sin y \ .$$

Therefore, $$|\Gamma_n| = (a_n^2 + b_n^2)^{\frac{1}{2}} \tag{26}$$

and $$\theta_n = \arctan (b_n/a_n) . \tag{27}$$

The phase angle of the total voltage reflection coefficient was lost when the r.f. signals were rectified by the detector crystals, however, both the magnitude and phase angle of the measured component may be computed from the transforms. It is well to point out that $|\Gamma|$ is the magnitude of the total voltage reflection coefficient when the reference step and the unknown device to be measured are attached in the guide.

Substituting $L' = \frac{\nu'}{4}$ into the sine and cosine argument of Equations (22) and (23),

$$n\pi\nu/\nu' = 4\pi L_n \nu. \tag{28}$$

Since $$L_n = n/2(\nu_2-\nu_1), \tag{29}$$

for an arbitrary distance L the wavenumber range $\nu_2 - \nu_1$ must be adjusted. The message here is that for an arbitrary distance along the waveguide, the angle traversed by the arguments of the sine and cosine terms of the Fourier transforms (22), (23) must be an integral multiple of 2π. This is important to recognize since the computer program will be calculating the Fourier integrals for an arbitrary distance L. Therefore the limits of the wavenumber range must be adjusted to satisfy Equation (22) and (23).

Method of Measuring $G(\nu)$. The Hewlett-Packard Model 416B ratio meter has been used, Figure 6. This particular ratio meter requires inputs of 1 KHz signals from two square law detectors. Two sets of measurements are taken, one with Γ_1 measured and a second with Γ_2 measured. The corresponding voltages out E_1 and E_2, obey the equation,

$$|\Gamma_1|^2/|\Gamma_2|^2 = \tan(CE_1)/\tan(CE_2), \tag{30}$$

where C is a constant peculiar to the ratio meter used and can be related to a conduction angle, i.e., time lag between pulses generated in the ratio meter. Consider now that if we take one set of readings with the reference step terminated in a matched load, then $|\Gamma_2| = \Gamma_r$. Then consider that the

second set of measurements are taken with the reference step terminated by the unknown device to be measured. Using this approach Equation (30) may be rewritten as:

$$|\Gamma|^2 = \Gamma_r^2 \tan(CE)/\tan(CE_r). \tag{31}$$

The quantities Γ_r and C are known from previous measurements. The quantities E and E_r are measured for each unknown. Using Equation (31), Equations (22) and (23) may be rewritten as

$$a_n = \Gamma_r/2\nu'\Lambda \int_{\nu_1}^{\nu_2} [\tan(CE)/\tan(CE_r)]\cos(2\pi L\nu)d\nu \tag{32}$$

and

$$b_n = \Gamma_r/2\nu'\Lambda \int_{\nu_1}^{\nu_2} [\tan(CE)/\tan(CE_r)]\sin(2\pi L\nu)d\nu. \tag{33}$$

Equations (32) and (33) are the equations which are used by the digital computer to calculate the reflection coefficient as a function of distance.

At a particular distance corresponding to the location of a discontinuity in the guide, the complex reflection coefficient as a function of frequency is determined by integrating Equation (32) and (33) over small overlapping wavenumber ranges and selecting the frequency corresponding to the wavenumber in the center of each range as the frequency of the particular integration, Figure 13. Each subinterval initially has ten data points or 500 MHz bandwidth

and is staggered two data points or 100 MHz. Each subinterval must satisfy Equation (29) for the location down the waveguide. Since this location is an arbitrary number, the wavenumber range must be appropriately adjusted such that an even interger multiple of it is equal to L_n, the distance location. This adjustment is done from the low side of the subinterval.

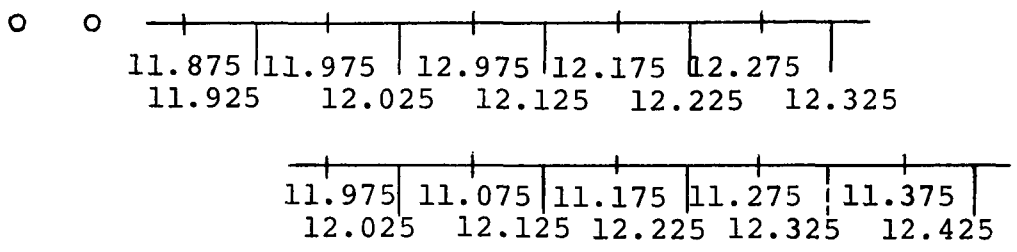

Figure 13. Wavenumber Subintervals Given in GHz

As a result of the overlapping procedure and the subinterval adjustment, the calculated results of complex reflection coefficient* are known at unequal frequency intervals of approximately 100 MHz. While the reflectometer data is taken at equal frequency intervals, the integrals are in terms of wavenumber, $1/\lambda_g$,** which does not correspondingly occur at equal intervals. The method used in pro-

---

*At this point the complex voltage reflection coefficient Γ is transformed to the complex current reflection coefficient Γ_I by the equation $\Gamma_I = -\Gamma$.

**The usual definition, $2\pi/\lambda_g$ is not used here for convenience.

gramming the integrals (32) and (33) is a point by point calculation of the area under the curve formed by the argument of the integrals.[12] This is discussed further in Appendix B.

Selected Waveguide Discontinuities

Introduction

Four waveguide discontinuities were selected as a library of matching elements. Families of curves of the characteristics of these elements, the symmetrical capacitive iris, the asymmetrical inductive iris, the solid metal inductive post, and the dielectric post, are given in Appendix A. The above elements also serve as matching elements for the impedance matching computer program. The equations which model the matching elements are programmed in the matching program and are called upon to impedance match the discontinuities measured by the comparison reflectometer.

Symmetrical Capacitive Iris

The symmetrical capacitive iris shown in Figure 14a is modeled by the circuit in Figure 14b. This iris is formed by obstacles of small but finite thickness with edges perpendicular to the electric field (H_{10} - mode in rectangular guide). The equations used are given by N. Marcuvitz[13] and are in terms of the physical dimensions of the iris. Figure 14, on the next page, shows this arrangement.

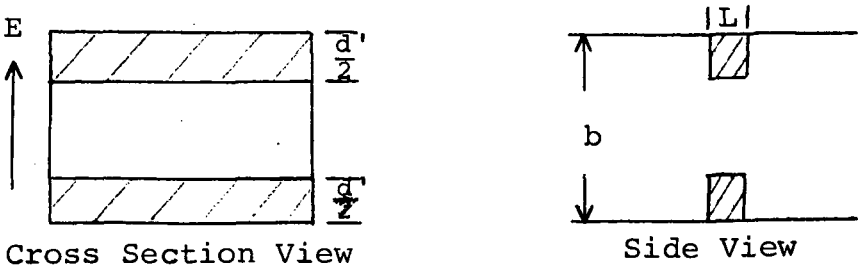

(a) Symmetrical Capacitive Iris

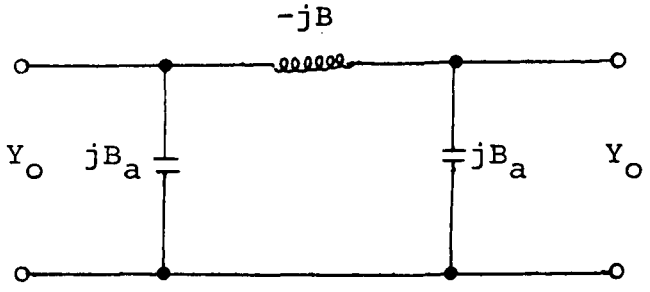

(b) Equivalent Circuit

Figure 14. Symmetrical Capacitive Iris and Equivalent Circuit

Consider now the equivalent circuit of Figure 14b. B_b is given by:

$$B_b/Y_o = \frac{b}{d}\csc(2\pi L/\lambda_g) \tag{34}$$

and

$$B_a/Y_o = B_1/Y_o + \frac{b}{d}\tan(\pi L/\lambda_g) \tag{35}$$

where

$$B_1/Y_o = \frac{2b}{\lambda_g}\left\{\ln\sec\left(\frac{\pi d'g}{2b}\right) - \frac{\pi d'L}{2bd} + \frac{A\sin^4\left(\frac{\pi d'}{2b}\right)}{1+A\cos^4\left(\frac{\pi d'}{2b}\right)} + \frac{1}{16}\left(\frac{b}{\lambda_g}\right)^2\left(1-3\cos^2\left(\frac{\pi d'}{2b}\right)^2\right)\sin^4\left(\frac{\pi d'}{2b}\right)\right\} \tag{36}$$

and

$$A = \left(1/\sqrt{1-\left(\frac{b}{\lambda_g}\right)^2}\right) - 1 \tag{37}$$

Where the physical parameters b, d', L, and d are shown in Figure 14a, and λ_g is the guide wavelength.

Equations (34) to (37) are programmed in the impedance matching program. They were also programmed in order to calculate the library of families of curves in Appendix A.

Restrictions. The equivalent circuit is valid in the wavelength range $b/\lambda_g < 1$, where Equation (34) is in error by less than 2 percent. Equation (36) is in error by less than 5 percent when $d'/b < 0.5$ and $1/d < 0.5$. A comparison of calculated and measured results are made in Chapter V.

Asymmetrical Inductive Iris

The asymmetrical inductive iris shown in Figure 15a is modeled by the circuit in Figure 15b. This inductive iris is formed by an obstacle of small but finite thickness with edges parallel to the electric field (H_{10} - mode in rectangular guide). The equations used are given by N. Marcuvitz[13] and are in terms of the physical dimensions of the inductive iris.

Consider now the equivalent circuit of Figure 14b. Where:

$$X_a/Z_o = (4a/\lambda_g)(a/\pi D')^2 , \quad \pi D'/\lambda << 1, \tag{38}$$

and

$$X_b/Z_o = (a/16\lambda_g)(\pi D_1/a)^2, \quad \pi D_1/\lambda << 1 \tag{39}$$

where

$$D' \cong \frac{d'}{\sqrt{2}}\left[1+\frac{L}{\pi d'}\,\mathrm{In}\left(\frac{4\pi d'}{eL}\right)\right], \quad \frac{L}{d'} << 1, \tag{40}$$

and

$$D_1 \cong (4Ld'^3/3\pi)^{1/4} , \quad L/d' << 1. \tag{41}$$

Where the physical parameters b, d', L and a are shown in Figure 15a. The free space wavelength is λ and the guide width is a. Equations (38) through (41) are programmed as part of the impedance matching program. They were also programmed in order to calculate the library of curves in Appendix A.

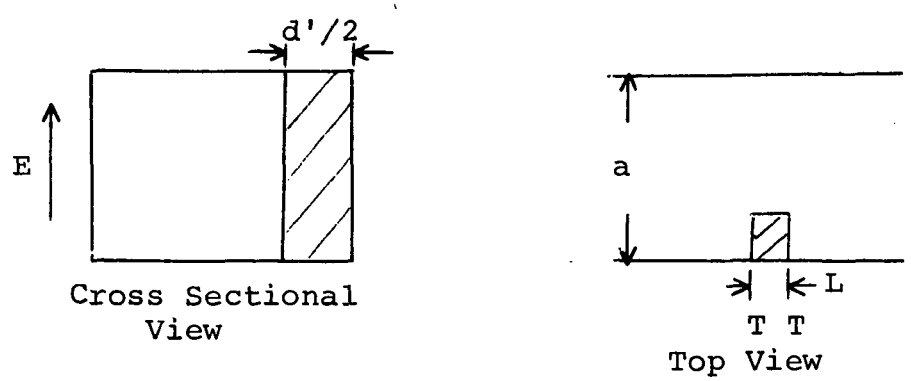

(a) Asymmetrical Inductive Iris

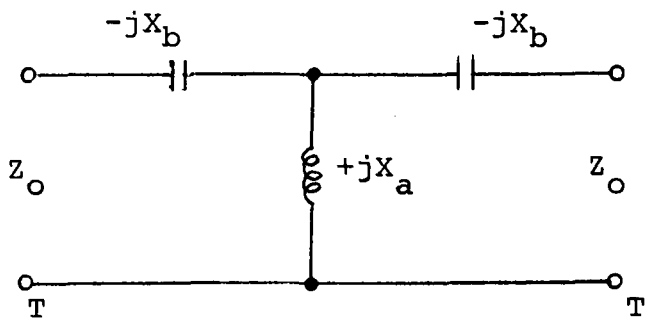

(b) Equivalent Circuit

Figure 15. Asymmetrical Inductive Iris and Equivalent Circuit

Restrictions. The equivalent circuit is valid in the wavelength range $a < \lambda < 2a$. For D', $D_1 < 0.2a$ and $a < \lambda$ Equation (38) through (41) are estimated to be in error by less than 10 percent. A comparison of calculated and measured results are made in Chapter V.

Solid Inductive Post

A solid metallic post of circular cross section with axis parallel to the electric field (H_{10} - mode in rectangular guide) is shown in Figure 16a with the equivalent circuit in Figure 16b. The equations used are given by N. Marcuvitz[13] and are in terms of the physical parameters of the inductive post.

Consider now the equivalent circuit of Figure 16b. Where:

$$X_a/Z_o - X_b/2Z_o = \left(\frac{a}{2\lambda_g}\right)\left[S_o - \left(\frac{\pi d}{2\lambda}\right)^2 - \left(\frac{\pi d}{2a}\right)^2 (S_o \cot\left(\frac{\pi x}{a}\right) - S_1)^2\right] \csc^2\left(\frac{\pi x}{a}\right) \qquad (42)$$

and

$$\frac{X_b}{Z_o} = \frac{a}{\lambda_g}\left(\frac{\pi d}{a}\right)^2 \sin^2\left(\frac{\pi x}{a}\right), \qquad (43)$$

where

$$S_o = \ln\left[\frac{4a}{\pi d}\sin\frac{\pi x}{a}\right] - 2\sin\left(\frac{2\pi x}{a}\right)$$

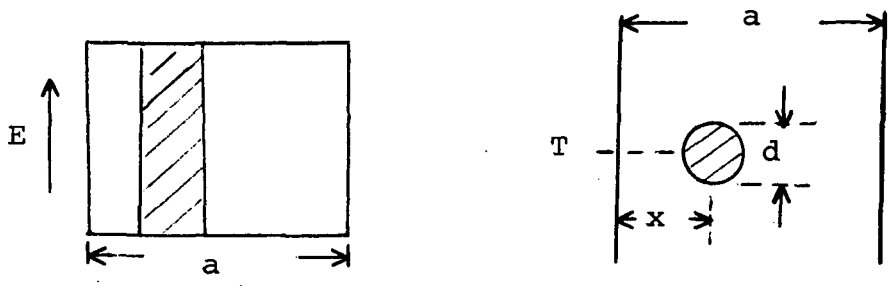

(a) Solid Metal Inductive Post

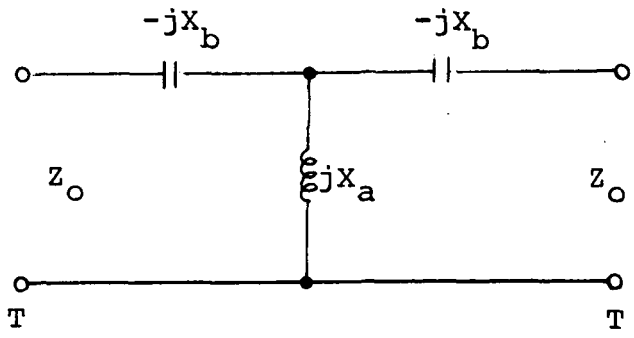

(b) Equivalent Circuit Parameters

Figure 16. Solid Metal Inductive Post and Equivalent Circuit

$$+2\sum_{n=2}^{\infty}\left[\frac{1}{\sqrt{n^2-\left(\frac{2a}{\lambda}\right)^2}}-\frac{1}{n}\right]\sin^2\left(\frac{n\pi x}{a}\right), \tag{44}$$

and

$$S_1 = \frac{1}{2}\cot\left(\frac{\pi x}{a}\right)-\sin\left(\frac{2\pi x}{a}\right)$$

$$+\sum_{n=2}^{\infty}\left[\frac{n}{\sqrt{n^2-\left(\frac{2a}{\lambda}\right)^2}}-1\right]\sin\left(\frac{2n\pi x}{a}\right). \tag{45}$$

The physical parameters x, d, and a are shown in Figure 16a. Equations (42) through (45) are programmed as part of the impedance matching program. They were also programmed in order to calculate the library consisting of families of curves in Appendix A.

Restrictions. The equivalent circuit is applicable in the wavelength range $a < \lambda < 2a$. The results are reliable to within a few percent for $d/a < 0.1$ and $0.8 > x/a > 0.2$. A comparison of calculated and measured results will be made in Chapter V.

Dielectric Post

A cylindrical dielectric obstacle of circular cross section aligned parallel to the electric field, (H_{10} - mode in rectangular guide), is shown in Figure 16a with the equivalent circuit in Figure 17b. The equations used are given by N. Marcuvitz[13] and are in terms of the physical parameters of the inductive post.

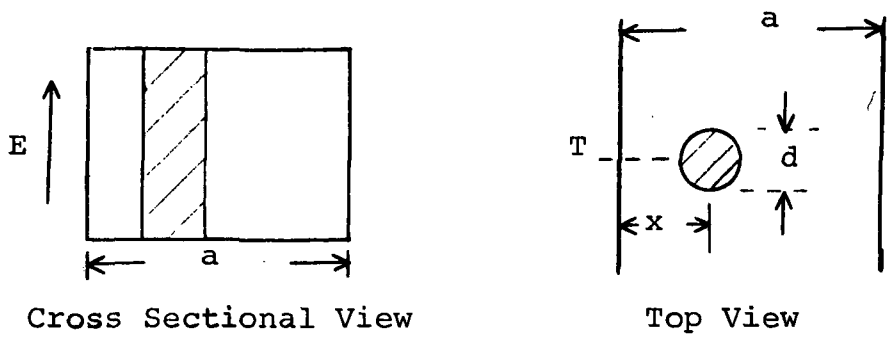

(a) Dielectric Post

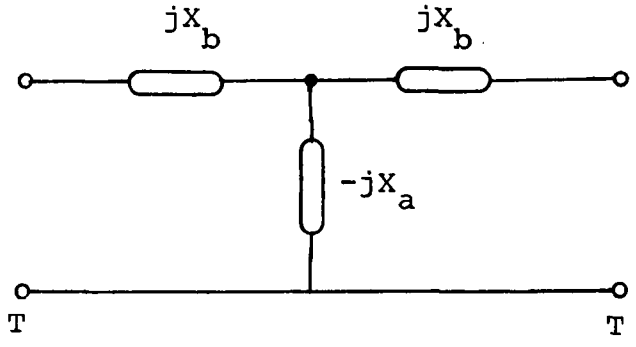

(b) Equivalent Circuit

Figure 17. Dielectric Post and Equivalent Circuit

Consider now the equivalent circuit of Figure 17b.

$$\frac{X_b}{Z_o} = \frac{(2a/\lambda_g)(\pi d/a)^2 \sin^2(\pi x/a)}{\frac{\alpha^2 J_1(\beta)}{J_1(\alpha)} \frac{1}{\alpha J_o(\alpha)J_1(\beta) - \beta J_o(\beta)J_1(\alpha)} - 2} \tag{46}$$

$J_0(B)$ and $J_1(B)$ are the bessel functions of the first kind with orders 0 and 1 respectively.

and $$\alpha = \pi d/\lambda \ , \ \beta = \sqrt{\varepsilon'}\ \pi d/\lambda .$$

$$X_a/Z_o - X_b/Z_o = (a/2\lambda_g)\csc^2(\pi x/a)\Big[J_o(\beta)/J_o(\alpha) \cdot \frac{1}{\beta J_o(\alpha)J_1(\beta) - \alpha J_o(\beta)J_1(\alpha)} - S_o + \alpha^2/4\Big] \tag{47}$$

where $$S_o = \ln\left[\frac{4a}{\pi d}\sin\frac{\pi x}{a}\right] - 2\sin^2\frac{\pi x}{a} + 2\sum_{n=2}^{\infty}\left[\frac{1}{\sqrt{n^2-\left(\frac{2a}{\lambda}\right)^2}} - \frac{1}{n}\right]\sin^2\left(\frac{n\pi x}{a}\right), \tag{48}$$

where the dielectric constant $\varepsilon' = \frac{\varepsilon}{\varepsilon_o}$, and ε_o is the free space dielectric constant. For an obstacle with a complex dielectric constant, $\varepsilon' - j\varepsilon'' = \frac{\varepsilon}{\varepsilon_o}$, the above formulas are still valid provided ε', X_a/Z_o and X_b/Z_o are replaced by $\varepsilon' - j\varepsilon''$ and

$j(X_a/Z_o)$, and $-j(X_b/Z_o)$ respectively. It should be noted that resonant effects occur for large values of ε' with attendant changes in sign of the circuit elements. Only low loss dielectrics are considered herein and only the real part of the dielectric constant will be considered in this research.

Restrictions. The equivalent circuit is applicable in the wavelength range $2a > \lambda > a$, and for the centered cylinder ($x = a/2$) in a wider range $2a > \lambda > 2a/3$. Equations (46) through (48) are estimated to be in error by only a few percent in the range $d/a < 0.15$ and $0.2 < x/a < 0.8$ provided that neither X_a/Z_o nor X_b/Z_o are too close to resonance. Since this research is concerned with reflection coefficient values $\leq .2$ the above resonance criterion presents no problem. A comparison of calculated and measured results are made in Chapter V.

Matching Computer Program

Introduction

The computer program which calculates the physical dimensions of the matching element and its location from the mismatch is referred to here as the matching program. This matching program uses an iterating technique to determine the desired physical dimensions. The criterion which has been used is the least root mean square of the resultant

mismatch (LRMS).* The RMS of the mismatch reflection coefficient has been used as the matching criterion in this research to reduce the net energy reflected over the bandwidth. This criterion does not always lead to the lowest peak VSWR over the matched band. If it is important to decrease the upper limit of the VSWR obtained by using the RMS criterion then the criterion described in the recommendations section of Chapter VI may be used at the possible expense of increasing the average VSWR over the matched bandwidth. The term resultant mismatch is used here to identify the reflection coefficient observed by the generator when a matching element is present in the waveguide.

In order to assist in the selection of a matching element, a library of selected matching elements has been compiled and is given in Appendix A. The selected matching elements consist of the symmetrical capacitive iris, the asymmetrical inductive iris, the solid metal inductive post, and the dielectric post. Information is presented in the form of plots of magnitude of current reflection coefficient and phase angle as a function of frequency. Also, plots of shunt susceptance are given, normalized to the characteristic impedance, as a function of frequency.

---

*RMS $\equiv \frac{1}{M} \sum_{n=1}^{M} \sqrt{(\text{mismatch reflection coefficient})^2}$, where M is the number of data points in the preselected bandwidth.

Program Description

The impedance matching computer program is described with reference to the functional flow chart of Figure 18. A listing of the program statements is given in Appendix B. The impedance matching computer program is an iterative program which iterates in three dimensional space. The space has three coordinates of which two are of the physical dimensions of the matching element. The third dimension is the location of the matching element relative to the mismatch. A 3 x 3 x 3 array is used in dimension space forming a total of twenty-seven points.

The program begins by reading in data and storing needed constants. Nine sets of data cards are required as input for this program. The symbol corresponding to the particular data read is presented in Table 1. An explanation of the data cards read is also given by comment statements in the matching program listed in Appendix B.

Depending on the matching element chosen, an initial center point in dimension space is selected. This point is denoted as the (1,1,1) point. If the capacitive or inductive iris is selected, the I coordinate corresponds to the thickness of the iris, and the J coordinate corresponds to the height of the iris. If, however, the metal inductive post or the dielectric post is selected as matching elements, then the I coordinate corresponds to the distance from the centerline of the post to the sidewall,

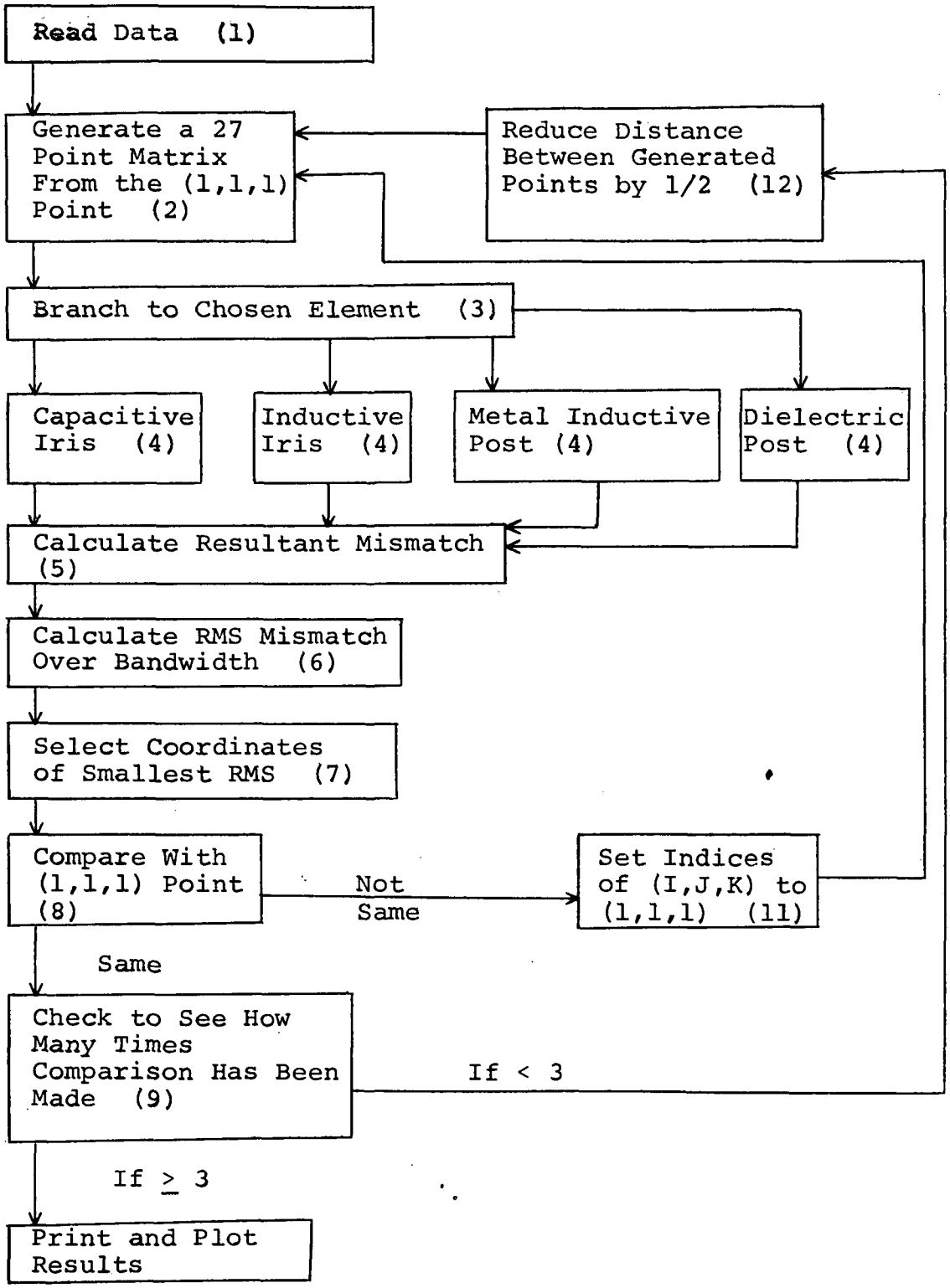

Figure 18. Impedance Matching Program Functional Flow Chart

Table 1. Impedance Matching Computer Input Data

Symbol	Corresponding Data
MACHEL	Designates matching element
EPRIM	Value of the dielectric constant of the dielectric post matching element
LE	Number of data points of the calculated mismatch reflection coefficient
FR(I)	Frequency in GHz corresponding to data points of the calculated mismatch reflection coefficient
XREL	Real part of the mismatched reflection coefficient to be impedance matched
YIMAG	Imaginary part of the mismatched reflection coefficient to be impedance matched
FRBEG, FREND	Band limits to be matched over
NOO	Number of times mismatch is to be impedance matched
ALENGH(I)	Value of the initial relative distance between the measured mismatch and the preselected matching element (the number of different ALENGH(I) equal NOO)

and the J coordinate corresponds to the diameter of the post. In all cases the K coordinate corresponds to the distance between the matching element and the mismatch. In step 2 of Figure 18, the (1,1,1) point is used to generate a set of satellite points on either side of the (1,1,1) point lying on the three axes. These points are referred to as the nearest neighbor points and are described by the coordinates (1,1,1), (3,1,1), (1,2,1), (1,1,3), (2,1,1), (1,3,1) and (1,1,2), as shown in Figure 19. The nearest neighbor points are of the greatest interest, therefore, in order to conserve computer run time calculations are made only for nearest neighbor points.

Step 2 of Figure 18, therefore consists of incrementing the (1,1,1) point to generate the 7 principal points of the 27 point array. In step 3 the matching element is selected according to the information given by the first data card. Table 2 shows the initial conditions used in the matching program.* In step 4 the reflection coefficient of the matching element chosen is calculated over the desired bandwidth (given by the last data card). This is done for

---

*The initial conditions were selected to reduce the run time of the matching program by selecting them as reasonably as possible. Large deviations of the physical dimensions of the matching elements were made and in all cases the resulting dimensions returned to the same value. Therefore, there was an absence of secondary minima as a function of matching element physical dimensions.

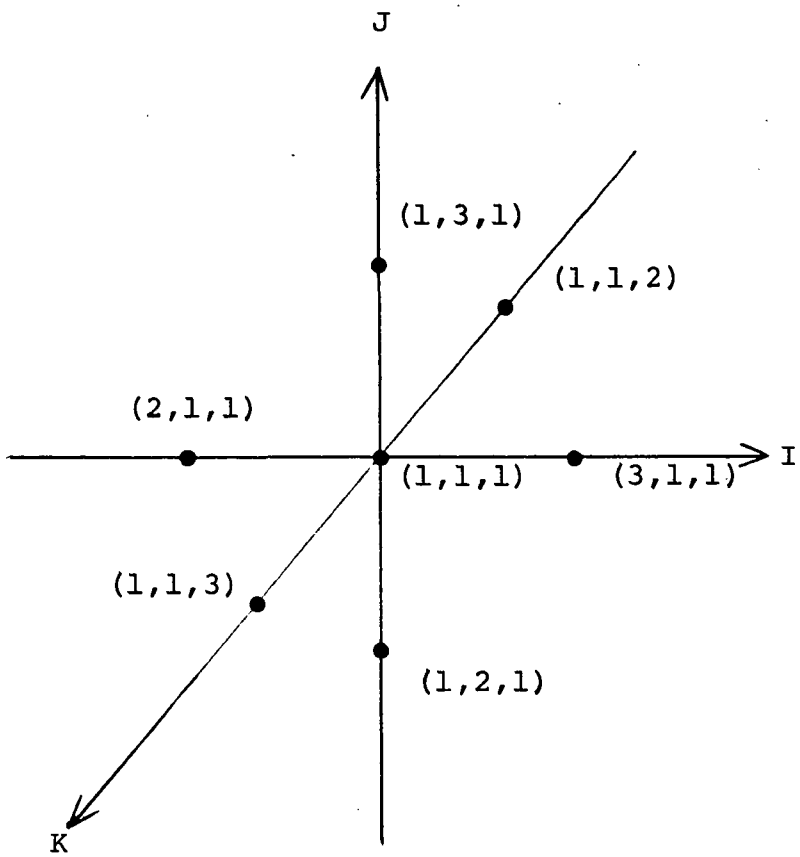

Figure 19. Dimension Space Coordinates, Showing the Seven Nearest Neighbor Points

all seven points in dimension space. Step 5 calculates the resultant mismatch between the disturbance in the waveguide (given by data) and the calculated matching element for all seven nearest neighbor points in dimension space. The equation used is referred to as the matching equation derived in Appendix C and given here as:

$$\Gamma_{It} = \frac{\Gamma_{Ia} \exp [-j2\beta L]+\Gamma_{Ib}-2 \Gamma_{Ia}\Gamma_{Ib} \exp [-j2\beta L]}{1-\Gamma_{Ia}\Gamma_{Ib} \exp [-j2\beta L]} . \qquad (49)$$

Γ_{Ia} is the current reflection coefficient of the disturbance at point A in an otherwise matched transmission line, Γ_{Ib} is the current reflection coefficient of the disturbance at point B in an otherwise matched line, and L is the distance between points A and B in Figure 20.* Equation (49) gives the total current reflection coefficient as seen by the generator as a result of two disturbances located in the line at points A and B. The equation is in terms of the individual current reflection coefficients that would be generated if each disturbance were placed individually in an otherwise matched transmission line. The program is implemented such that either Γ_{Ia} or Γ_{Ib} can play the roll of the matching element. If the disturbance is matched by placing the

---

*The complex current reflection coefficient Γ_I is equal to the negative of the complex voltage reflection coefficient Γ, i.e. $\Gamma_I = -\Gamma$.

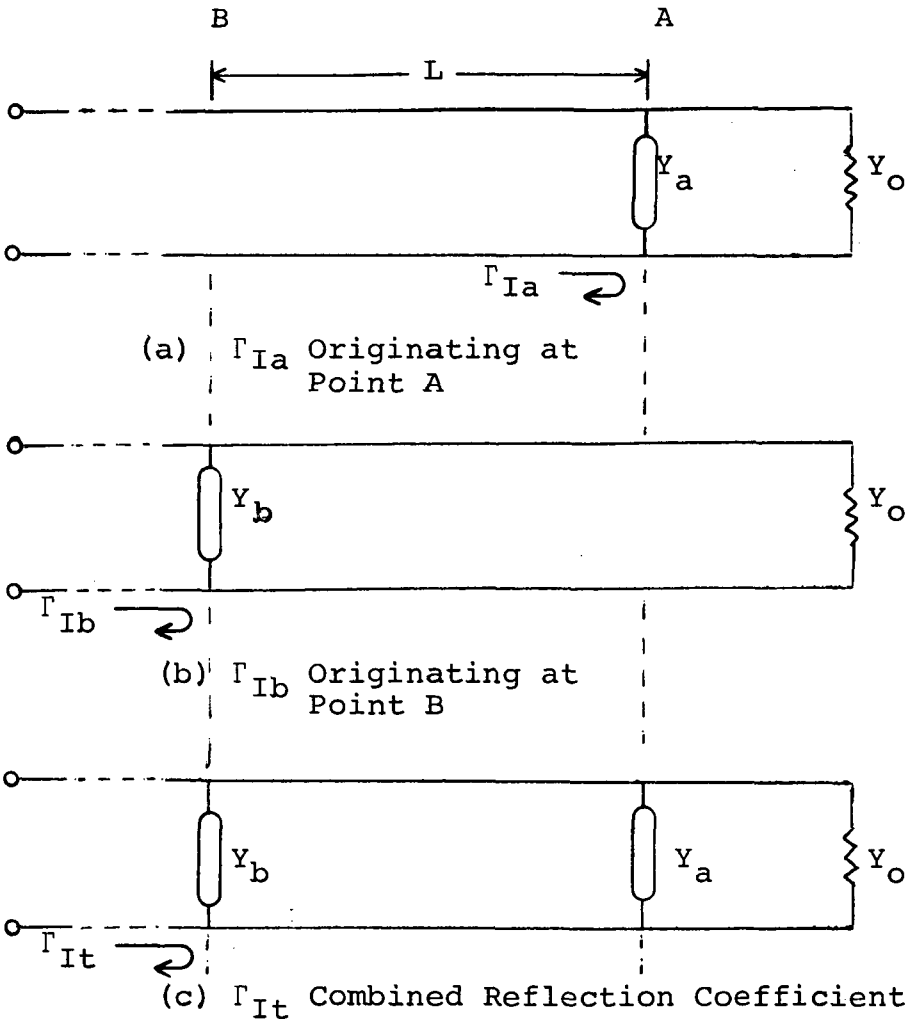

Figure 20. Current Reflection Coefficients Generated by Disturbances on an Otherwise Matched Transmission Line

matching element on the generator side, then the matching element is represented by Γ_{Ib}. If matching is accomplished on the load side of the disturbance, then the matching element is represented by Γ_{Ia}.

Table 2. Matching Element Initial Conditions on Dimensions

Element	Thickness	Height
Capacitive Iris	0.05 cm	0.32 cm
Inductive Iris	0.05 cm	0.32 cm

Element	Diameter	Sidewall Distance
Metal Inductive Post	0.16 cm	0.47 cm
Dielectric Post	0.16 cm	0.47 cm

At this point in the program the resultant mismatch as a function of frequency at intervals of approximately 100 MHz has been calculated for each point in dimension space. Step 6 of Figure 18 determines the root mean square (RMS) value of the current reflection coefficient over the frequency band of interest, i.e., the seven RMS mismatch values corresponding to the seven points in dimension space. Step 7 of Figure 18, selects the smallest of these RMS values or least root mean square (LRMS) and determines its corresponding coordinates in dimension space.

Step 8 is a branch decision. If the point selected in step 7 is not equal to the (1,1,1) point then the branch is made to step 11 and the values of the dimensions of the point (I,J,K) corresponding to the LRMS are assigned to the (1,1,1) point. In effect this moves the (1,1,1) point in dimension space. The computer returns to step 2 and calculates new nearest neighbor points around the new (1,1,1) point. If, however, the point corresponding to the LRMS in step 8 is in fact the (1,1,1) point, then a regional minimum has been determined and a check is made on the size of the increment. If the increment size has not been reduced to 1/8 the original size at the beginning of the program the computer reduces the existing increment size by a factor of 2 in step 12 and returns to step 2 to determine a better representation of the minimum mismatch. On the other hand, if the increment size has been reduced by a factor of 8 then the computer exits step 9 and prints, plots and punches results. The initial increment size used in the program is shown in Table 3 and was determined empirically to avoid large differences in reflection coefficients from neighboring points.

Program Output. The matching program output consists of printout, plots, and punched cards. A typical printout is given in Figure 21. The type of matching element, the bandwidth matched over, the physical dimensions of the matching element and the location of the matching

CAPACITIVE IRIS IS THE MATCHING ELEMENT

NUMBER OF INCREMENT = 8.

MATCHED BAND IS FROM 9.795 GHZ. TO 10.995 GHZ.

THICKNESS= .0438 IN CM HEIGHT= .1600 IN CM DISTANCE TOWARD THE GEN. FROM MISMATCH= .8375 CM

RESULTANT MISMATCH

	MATCHED		UNMATCHED	
FREQUENCY IN GHZ.	MAG. REFL. COEFF.	VSWR	MAG.REFL.COEFF.DISURB.	MEASURED
8.195	.07719	1.1673	.06696	
8.395	.07506	1.1623	.07138	
8.595	.07186	1.1549	.07563	
8.795	.06767	1.1452	.07973	
8.995	.06255	1.1334	.08373	
9.195	.05655	1.1199	.08761	
9.395	.04973	1.1047	.09140	
9.595	.04214	1.0880	.09511	
9.795	.03381	1.0700	.09875	
9.995	.02480	1.0509	.10232	
10.195	.01516	1.0308	.10584	
10.395	.00510	1.0103	.10931	
10.595	.00638	1.0128	.11272	
10.795	.01758	1.0358	.11609	
10.995	.02941	1.0606	.11942	
11.195	.04171	1.0870	.12271	
11.395	.05440	1.1150	.12596	
11.595	.06743	1.1446	.12919	
11.795	.08076	1.1757	.13238	
11.995	.09434	1.2083	.13554	
12.195	.10812	1.2424	.13868	
12.395	.12205	1.2780	.14179	

Figure 21. Printout of Matching Program Results

element from the mismatch toward the generator is given. The modulus of the reflection coefficient of both matched and unmatched discontinuity as well as the VSWR of the matched discontinuity are given.

A typical plot is given in Figure 22. The VSWR of the original discontinuity as well as the VSWR of the impedance matched discontinuity are given on the same plot as a function of frequency.

In order to add more flexibility to the impedance matching computer program, the output also consists of a set of punched cards which are punched according to the format of the data cards for the matching program. The real and imaginary parts of the resultant mismatch are punched on these cards. Therefore, if it is desirable to improve on the existing impedance match, the output cards may be used as data cards for the matching program and the type of matching element changed to provide, in many cases, an improved impedance match. The result is the original discontinuity matched by two matching elements. The location of the second matching element calculated by the matching program is referenced to the element nearest the generator, resulting from the first impedance match. This can be done as many times as may be deemed practical.

Table 3. Initial Increment Size of Physical Dimensions

Dimensions*	Capacitive and Inductive Iris	Dimensions*	Metal and Dielectric Post
Relative Distance	0.1	Relative Distance	0.1
Thickness	0.01	Sidewall Distance	0.01
Height	0.1	Diameter	0.05

*in centimeters

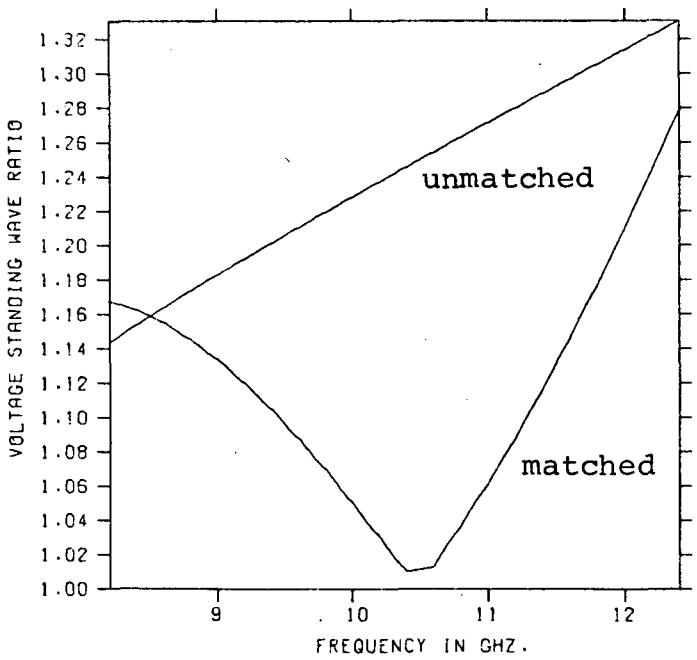

Figure 22. Typical Example of the Matching Program Output Plot of the VSWR of an Unmatched and Matched Disturbance

CHAPTER IV

EXPERIMENTAL EQUIPMENT

Introduction

The comparison reflectometer system and various test waveguide discontinuities constitute the experimental equipment. The comparison reflectometer shown in Figure 23 is comprised of various microwave components including a backward wave oscillator (BWO), a coherent synchronizer, a ratio meter, and directional couplers.

Four waveguide discontinuities were fabricated and measured to demonstrate the validity of Equations (III-34) through (III-48). A shunt slot radiator was also fabricated to demonstrate the validity of the impedance matching technique.

Comparison Reflectometer System

Functional Diagram. A block diagram of the comparison reflectometer system fabricated for this research is shown in Figure 23. A photograph of the system is given in Figure 7.

Microwave energy is generated by the backward wave oscillator (BWO) and is directed through the waveguide to the pin diode modulator. The modulator amplitude modulates the microwave energy at the audio oscillator frequency of 1 KHz. While the audio oscillator generates a sine wave,

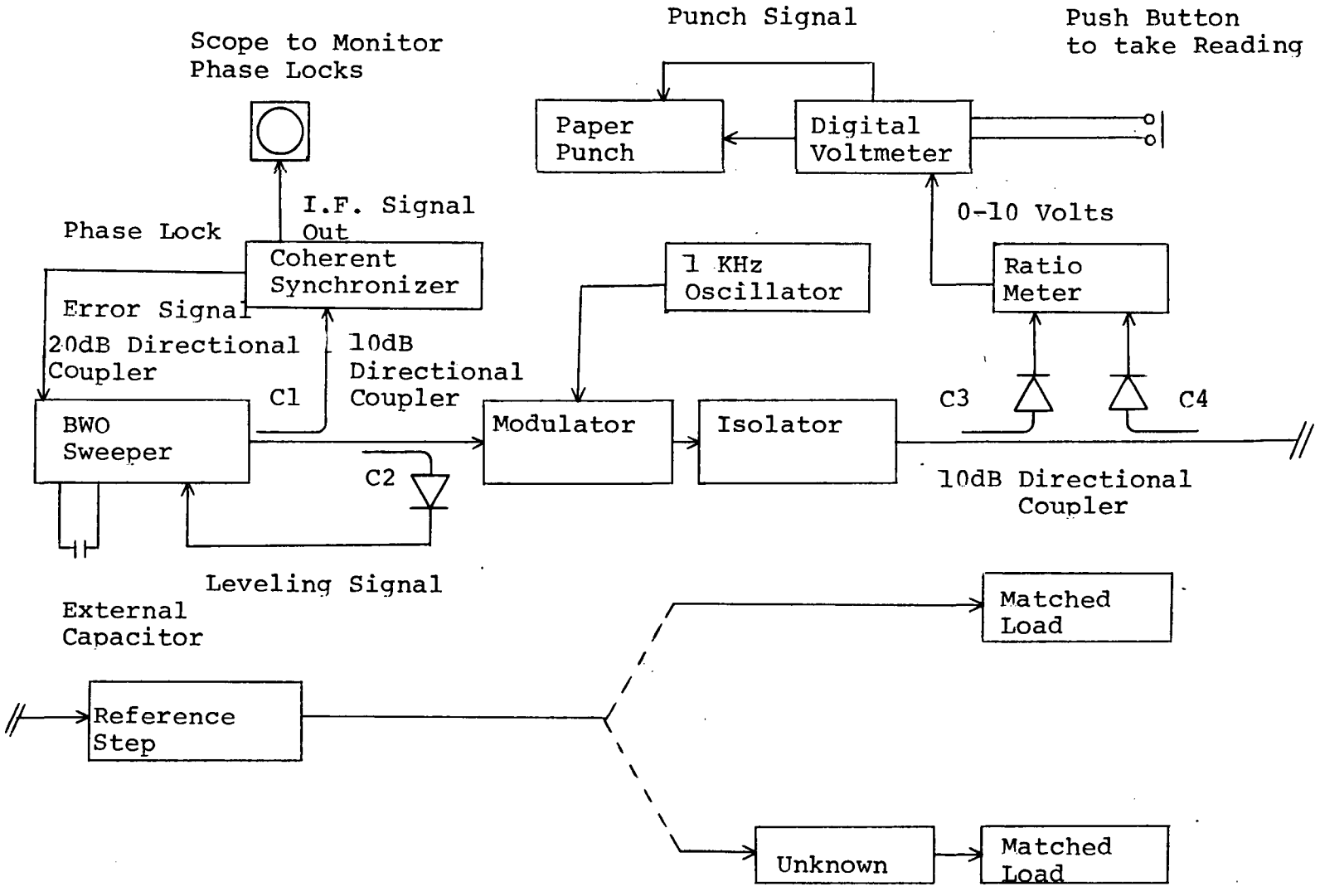

Figure 23. Comparison Reflectometer Block Diagram

the modulator is driven to the extent that the output of the modulator is an amplitude modulated square wave. The isolator serves to prevent reflected energy from pulling the BWO frequency. The wave is next partially reflected by the reference step. This step reflects a known ratio of incident energy from the reference plane. The amplitude and phase of this reflection coefficient is constant over the frequency band. Next either the matched load is attached, in which case essentially all of the remaining wave is absorbed, or the unknown is attached in which case part of the energy is reflected from the unknown and the remaining energy is absorbed in a matched load.

The two directional couplers C1 and C2 provide feedback necessary to ensure a phase locked, constant power output from the BWO. Couplers C3 and C4 are the essential elements of the reflectometer. The incident wave traveling toward the load is coupled out by C3. The reflected wave is coupled out by C4. Couplers C3 and C4 are terminated in a square law detector. The output of each detector is a square wave whose amplitude is proportional to the square of the electric field intensity incident on the respective detector. The ratio meter takes the ratio of these two input signals and provides a voltage output that is proportional to the square of the total reflection coefficient. This reflection coefficient can either be the total reflection coefficient of the reference step and the measured

device or it can be that of the reference step terminated by a matched load. This voltage output E is measured by the digital voltmeter, and the value measured is punched on paper tape at the command of the push button.

The BWO is phase locked every 50 MHz by the coherent synchronizer from 7.975 GHz to 12.425 GHz. At each of these 89 phase lock points a measurement is taken by depressing the push button, Figure 23. One complete set of measurements is made with the reference step terminated in a matched load and a second complete set is taken with the reference step terminated by the unknown device. During these measurements the gain of the ratio meter is left undisturbed. From the data collected the magnitude of the total reflection coefficient of the reference step terminated in the unknown device may be calculated by the digital computer. Detailed operating instructions for the comparison reflectometer are given in Appendix C.

Backward Wave Oscillator. The RF source used in this research is an Airborne Instruments Laboratory, Sweep Oscillator type 210. This BWO is used with the plug in unit which provides a frequency sweep from 7.975 GHz to 12.425 GHz. The oscillator frequency can be controlled by an external sweep voltage or by an internal sweep generator. The internal sweep can be set to a repetitive sweep with a variety of sweep rates or can be set up to sweep once through the band and return to the lowest

frequency, remaining there until activated by a front panel push button. The rate of this sweep is an adjustable parameter. In the reflectometer setup of Figure 23 the BWO is operated in this internal signal sweep mode. The RF signal is then blanked out while the oscillator is returning to the lowest frequency. The oscillator then remains at this starting frequency until again triggered by the front panel push button. In order to enable the coherent synchronizer to phase lock and a voltage reading to be taken, the oscillator sweep is slowed down by adding an external 200 micro-farad capacitor to the connector provided on the back panel of the unit.

When the oscillator frequency is in a capture region of the coherent synchronizer a correct error signal to the helix of the BWO will result in the phase locking of the BWO to the crystal controlled oscillator of the coherent synchronizer. The frequency is then held within 7 parts in 10^9. When the internal sweep voltage increases sufficiently to overcome the error correction signal on the helix of the BWO, the phase lock is broken. The error signal returns to zero, and the sweep signal resumes control of the RF output. The RF frequency, therefore, continues to increase until it again is within the lower bound of the 2.5 MHz capture region of the 25 MHz IF of the coherent synchronizer. In this way, the BWO is phase locked every

50 MHz from 7.975 to 12.425 GHz. This is done automatically with perfect repeatability when the system is properly set up. The entire run of 89 measurements requires 10 to 15 minutes depending on the selected sweep rate.

Coherent Synchronizer. The instrument used to obtain desired phase locks is the Sage Laboratories, Inc. model 244 coherent synchronizer. This device is generally used to phase lock a source at a single frequency. Because of this, the unit is equipped with five crystals in the basic oscillator. Depending on the frequency at which the phase lock is desired, one of the crystals operating at 5000.000 KHz, 5012.500 KHz, 5006.250 KHz, 5000.00 KHz, or 4993.750 KHz is selected. One of the 5000.000 KHz crystals is used in the fixed mode. The other four crystals are used in the variable mode. In the variable mode, by selecting the correct crystal and pulling the frequency of this crystal by a variable front panel control, any frequency from 100 MHz to 18 GHz can be phase locked. However, in the fixed mode the basic oscillator operates at a crystal controlled frequency of 5.000000 MHz. This signal is multiplied by a frequency multiplier chain to provide a 100 MHz signal, Figure 24. Functionally, the 100 MHz signal excites a varactor multiplier which in turn generates harmonics from 100 MHz to 18 GHz. Each harmonic is 100 MHz apart. This signal is then applied to the mixer which also has as an input the RF signal from the BWO oscillator to be phase

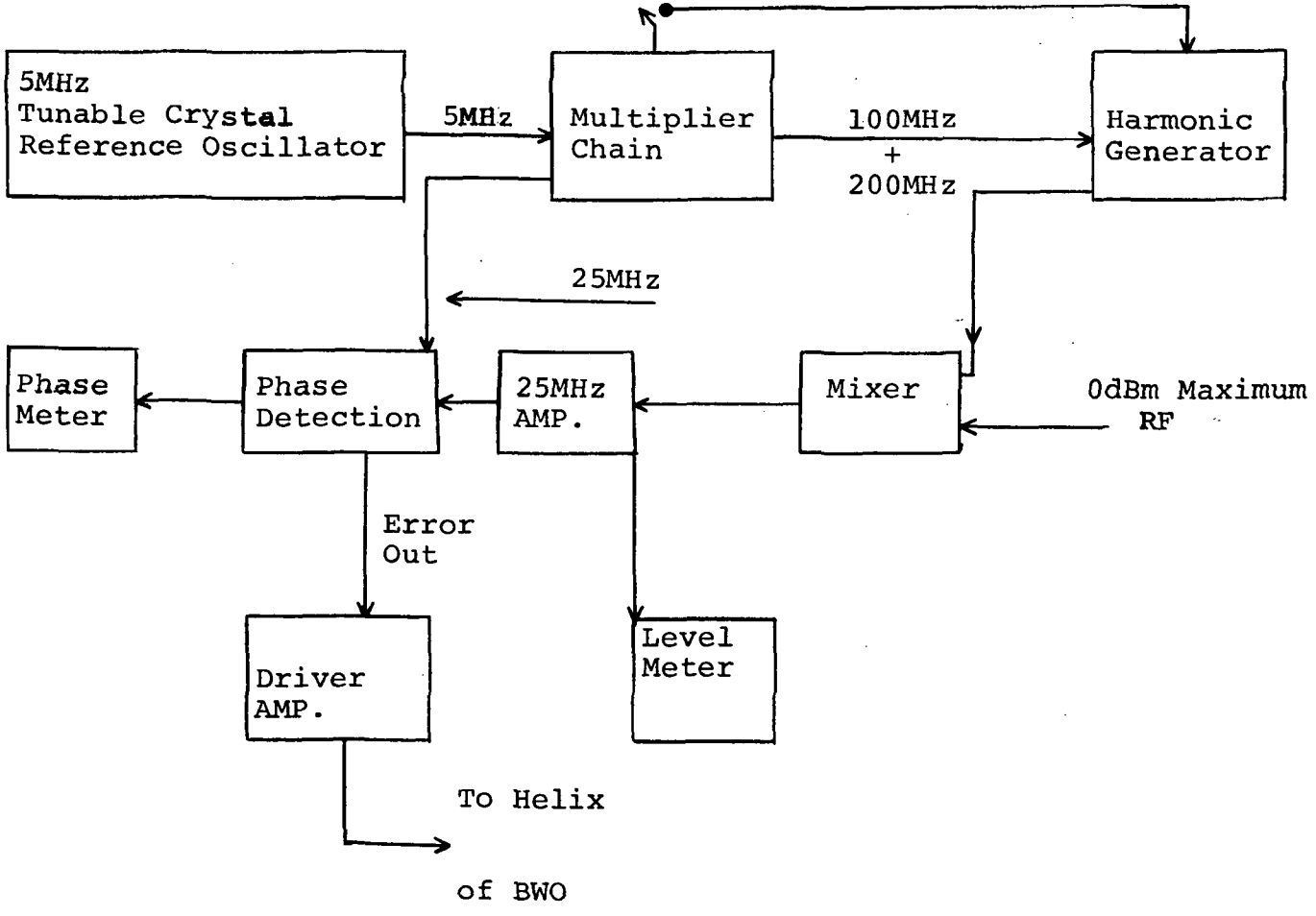

Figure 24. Simplified Block Diagram of Coherent Synchronizer

locked. The output of the mixer is the sum and difference of the two inputs. This output is the input to the 25 MHz amplifier which has a 2.5 MHz 3 dB bandwidth. If there exists a signal within approximately 1.5 MHz of 25 MHz this signal is amplified. Other signals are not amplified. The level meter gives an indication of the presence of a 25 MHz signal. Therefore, when a phase lock has occurred there is positive indication on the level meter. The output of the 25 MHz amplifier drives a phase detector which compares the phase of the 25 MHz reference signal tapped from the multiplier chain with the output of the 25 MHz amplifier. The output of the phase detector is an error signal which, after being amplified, is applied to the helix of the backward wave oscillator. This error signal can be monitored by the phase meter.

Because the comparison reflectometer phase locks at 50 MHz intervals, the reference oscillator of the coherent synchronizer is set in the fixed position. Therefore, the output of the harmonic generator is a frequency comb with harmonics at intervals of 100 MHz from 100 MHz to 18 GHz. A phase lock will occur when the RF signal input to the mixer is 25 MHz on either side of a harmonic on the comb, Figure 25, since the difference of the harmonic and the input RF from the BWO is 25 MHz at these points.

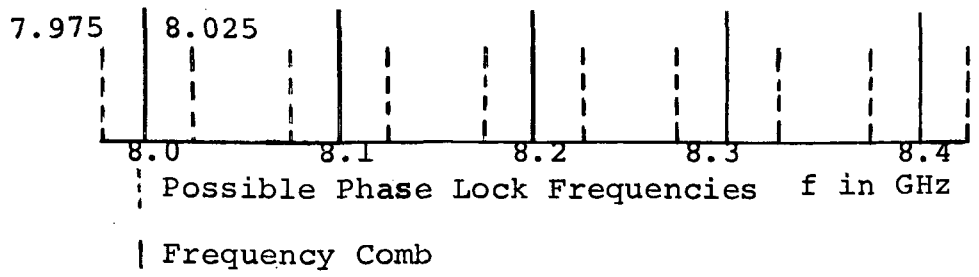

Figure 25. Partial Frequency Comb of Harmonic Generator

It was particularly important for this research to optimize conditions of the harmonic comb of the harmonic generator. In order to make a rapid set of measurements it is important to phase lock automatically from one desired frequency to the next. This requires essentially a single adjustment to the coherent synchronizer controls. It was discovered initially that this was impossible to do and in fact some of the desired phase lock points were not achievable. Further investigation pointed out that the spectrum of the harmonic comb from the harmonic generator was not at a constant level. In fact, some harmonics were apparently not present.

While it is convenient to consider the harmonic generation and the mixing as two separate operations, in the model 244 both are accomplished in one step by a single varactor. It was discovered that this varactor was not biased correctly to provide a relatively constant 25 MHz IF signal when the BWO was swept through the frequency band. This is equivalent to saying that the harmonic generator

was not providing a flat spectrum throughout the bandwidth. Adjustments were made to achieve this flat spectral behavior by observing the 25 MHz signal at the BNC connector "TP1" provided on the 25 MHz amplifier. Details of this adjustment are given in Appendix D.

A single adjustment to the error signal potentiometer enables consistent automatic phase locks as the BWO sweeps slowly through the band. Because the IF levels are relatively constant the time duration of the phase locks are also relatively constant. Further, this phase lock time can be adjusted by increasing or decreasing this maximum allowable error to the helix of the BWO. By increasing the maximum error voltage a given phase lock exists for a longer period of time.

Ratio meter. The ratio meter, Hewlett-Packard model 416B was used to determine the ratio of the incident and reflected electric field intensities, Figure 23. This ratio meter has two inputs, both are 1 KHz square wave signals whose amplitudes are proportional to the square of the incident and reflected electric field intensities of the output of the 10 dB directional couplers. Two Hewlett-Packard model 424A crystal detectors operating in the square law region were used, at the output of the two directional couplers C3 and C4, Figure 23.

The output voltage of the ratio meter is related to the reflection coefficient measured by the relation:[14]

$$|\Gamma|^2 = \xi \tan \theta \ , \tag{1}$$

where ξ is a proportionality constant depending on the reference adjustment, and the angle θ is expressed in terms of the output voltage measured:[12]

$$\theta = \gamma E / E_{max} \ , \tag{2}$$

where E is the voltage measured, E_{max} is the voltage measured when the meter reading is at the uppermost point of the scale, and γ is defined as a conduction angle. The conduction angle γ was determined by programming Equation (3) on a desk calculator. A discontinuity with a known value of $|\Gamma(f)|$ was selected and measured at two different frequencies such that,

$$\frac{|\Gamma_1|^2}{|\Gamma_2|^2} = \frac{\tan \{\gamma E_1 / E_{max}\}}{\tan \{\gamma E_2 / E_{max}\}} \tag{3}$$

E_1, E_2 and E_{max} were measured and $|\Gamma_1|$ and $|\Gamma_2|$ were known. The unknown γ was calculated by an iterative technique to satisfy Equation (3). In most cases the value of E_{max} for the particular ratio meter used is 6.928 volts, giving a value for the proportionality constant,

$$\gamma/E_{max} = (56.6\pi/180)(1/6.928)$$

$$= 0.1426 \frac{\text{radians}}{\text{volt}} \qquad (4)$$

Digital Voltmeter. The voltage recording system used is a Dymec Model DY-5552A voltage measuring and recording system. The system consists of a Model DY-2210 voltage-to-frequency converter, a Hewlett-Packard model 5211 A/E electronic frequency counter, a model DY-2540 scanner/coupler and a motorized tape punch. The voltage-to-frequency converter converts the voltage output of the ratio meter to a proportional frequency. This frequency is sampled and counted by the frequency counter. The display of this counter is the voltage accurate to the millivolt. The output of the counter is then scanned by the scanner/coupler, and the paper punch records the voltage. The counter is triggered with a remotely located push button.

Reference Step. The reference step, Figure 26, was fabricated for the comparison reflectometer according to the design given by D. L. Hollway.[12] The reference step is a gradual symmetrical E-plane taper. At the reference plane the guide suddenly resumes the standard guide dimensions resulting in a reflection at the reference plane. The magnitude and phase of the reflection coefficient of the reference step are essentially constant over the band 8.0 to

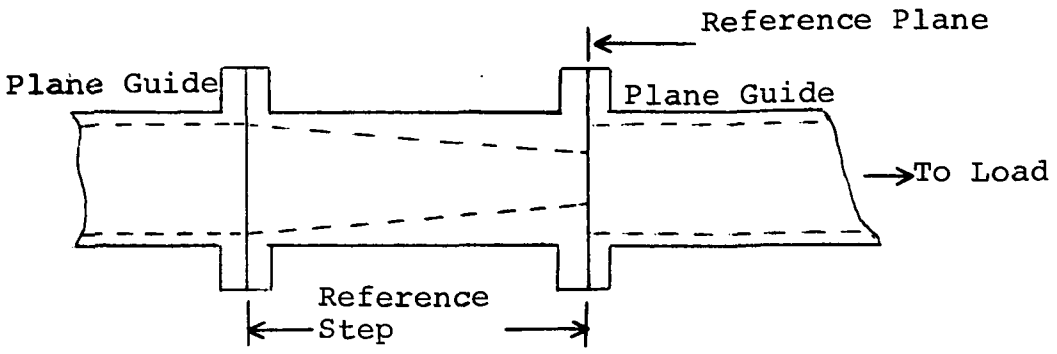

Figure 26. Reference Step

12.4 GHz. This was verified by the National Bureau of Standards over the band 8.2 GHz to 12.4 GHz, Figures 27 and 28. The reference step was measured in a line terminated in a precision matched load, the two separated by a 15 centimeter length of precision waveguide. Frequency marker pips are provided at 9, 10 and 11 GHz.

A detailed error analysis of the sweep frequency calibration results has not undergone full NBS review. However, the uncertainty in the return loss magnitude is believed to be within ± 2%. This is an uncertainty of less than 0.006 in reflection coefficient. The uncertainty in reflection coefficient angle is believed to be within ± 2.5 degrees. These uncertainties were obtained by swept frequency measurements on a calibrated sliding load by NBS.

The magnitude of the reflection coefficient for the reference step is calibrated at .2 ± .011 (VSWR = 1.5 ± .034) according to the results of Figure 27. In order to

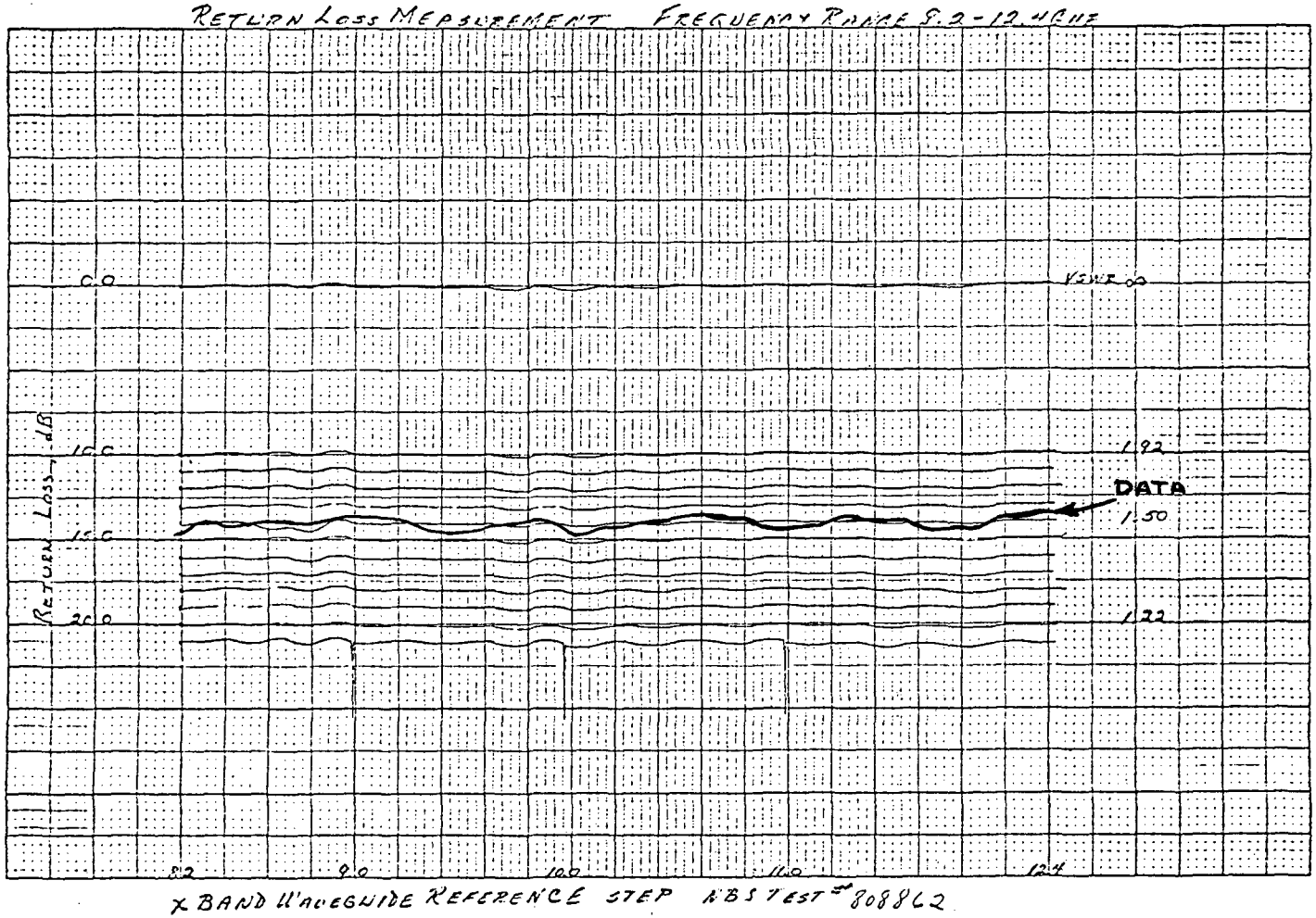

Figure 27. Reference Step, Return Loss

simplify programming a constant value (0.2) has been used for the reference step. Figure 28 shows the phase angle variation to be negligible, therefore, the angle has also been considered a constant, and the phase of the disconuity measured by the comparison reflectometer is referenced to it. The variation present in the curve of Figure 28 is due to a phase variation of $2\beta L$ where L is the separation between the NBS reference plane and the step measured.

Typical Recorded Voltages. Voltages recorded by the comparison reflectometer setup consist of two sets. The first set refered to as the reference set is taken with the reference step terminated with a matched load, Figure 29a. A second set of voltage readings is taken with the reference step terminated in the device to be measured, Figure 29b. A typical set of measurements for a symmetrical capacitive iris at 50 MHz intervals from 7.975 GHz to 12.425 GHz is given in Table 4.

The reflectometer computer program, Appendix B, uses Equation (III-31) to calculate the total magnitude reflection coefficient of the reference step and the discontinuity to be measured as shown in Figure 30. The data points of Figure 30 are connected by a continuous curve, however $|\Gamma|$ is only known at frequency points separated by 50 MHz, starting at 7.975 GHz. $|\Gamma(f)|$ of Figure 30 is the function that is Fourier transformed from the wavenumber to the distance domain using Equations (III-22, 23), where $G(\nu)$ is

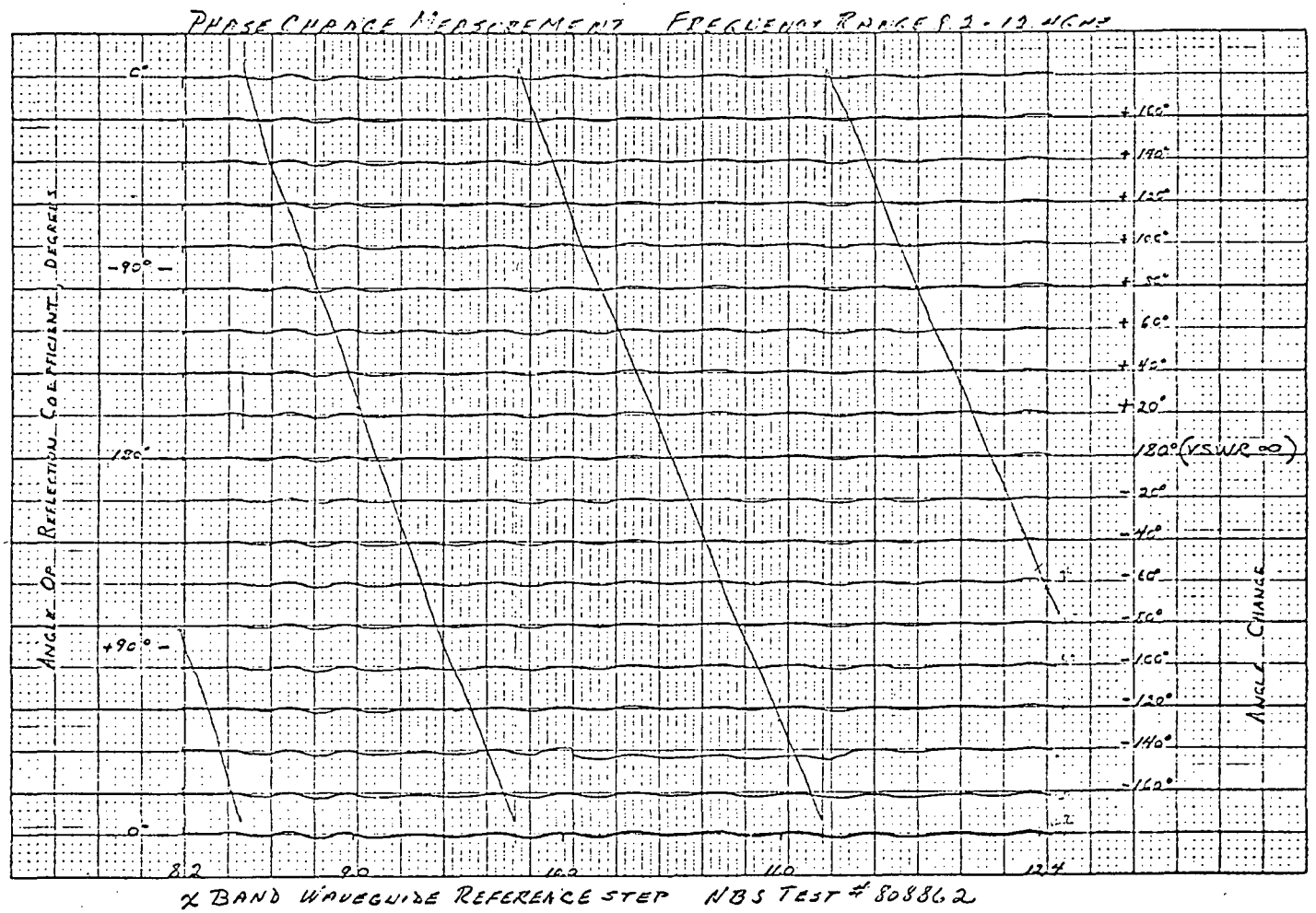

Figure 28. Reference Step, Phase Angle of the Reflection Coefficient Referenced to a Short

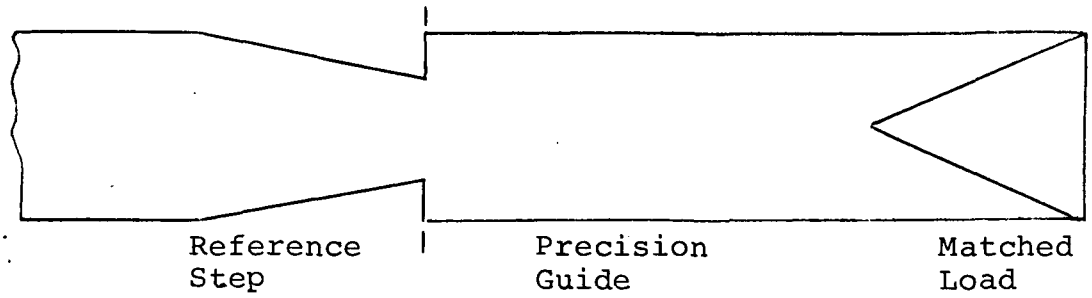

(a) Reference Step Terminated by a Matched Load

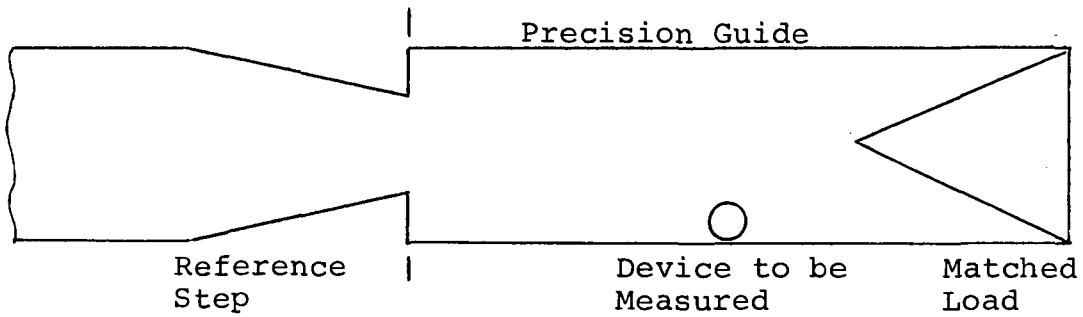

(b) Reference Step and Test Element Terminated by a Matched Load

Figure 29. Measured Setup of Reference Step

Table 4. Typical Voltage Measurements, Read from Left to Right, and Top to Bottom

REFERENCE VOLTAGE DATA														
2.839	2.061	3.171	2.776	3.691	3.176	3.140	2.830	2.277	2.719	2.310	2.916	2.885	2.713	3.157
2.561	2.875	2.998	2.737	3.377	3.286	3.161	3.463	3.017	3.010	3.161	2.856	3.064	3.180	2.982
3.130	3.092	2.979	3.138	3.027	2.996	3.103	3.004	3.050	3.171	3.128	3.252	3.352	3.205	3.253
3.277	3.088	3.144	3.191	3.112	3.302	3.388	3.296	3.418	3.442	3.268	3.279	3.292	3.090	3.108
3.159	2.999	3.041	3.200	3.135	3.180	3.358	3.306	3.247	3.350	3.314	3.264	3.338	3.315	3.192
3.187	3.132	3.025	3.028	3.035	2.976	3.069	3.194	3.183	3.219	3.371	3.335	3.244	3.289	

VOLTAGE DATA WITH UNKNOWN IN LINE														
1.105	1.870	2.328	4.400	5.359	5.706	2.080	1.155	1.112	3.107	4.627	4.821	4.294	2.701	.980
1.296	2.945	4.378	5.037	4.778	3.680	1.990	1.028	2.263	4.291	5.329	5.471	4.876	3.161	.991
.323	2.434	4.158	5.378	5.771	5.099	3.317	1.446	.729	1.553	3.758	5.591	6.167	5.685	4.339
2.350	.594	.909	3.244	5.235	6.093	6.159	5.601	4.045	1.601	.382	1.524	3.661	5.311	6.181
6.279	5.459	3.538	1.204	.281	1.510	4.002	5.880	6.617	6.516	5.646	3.899	1.519	.184	1.213
3.681	5.540	6.399	6.484	5.897	4.385	1.948	.162	.614	2.956	5.286	6.530	6.900	6.565	

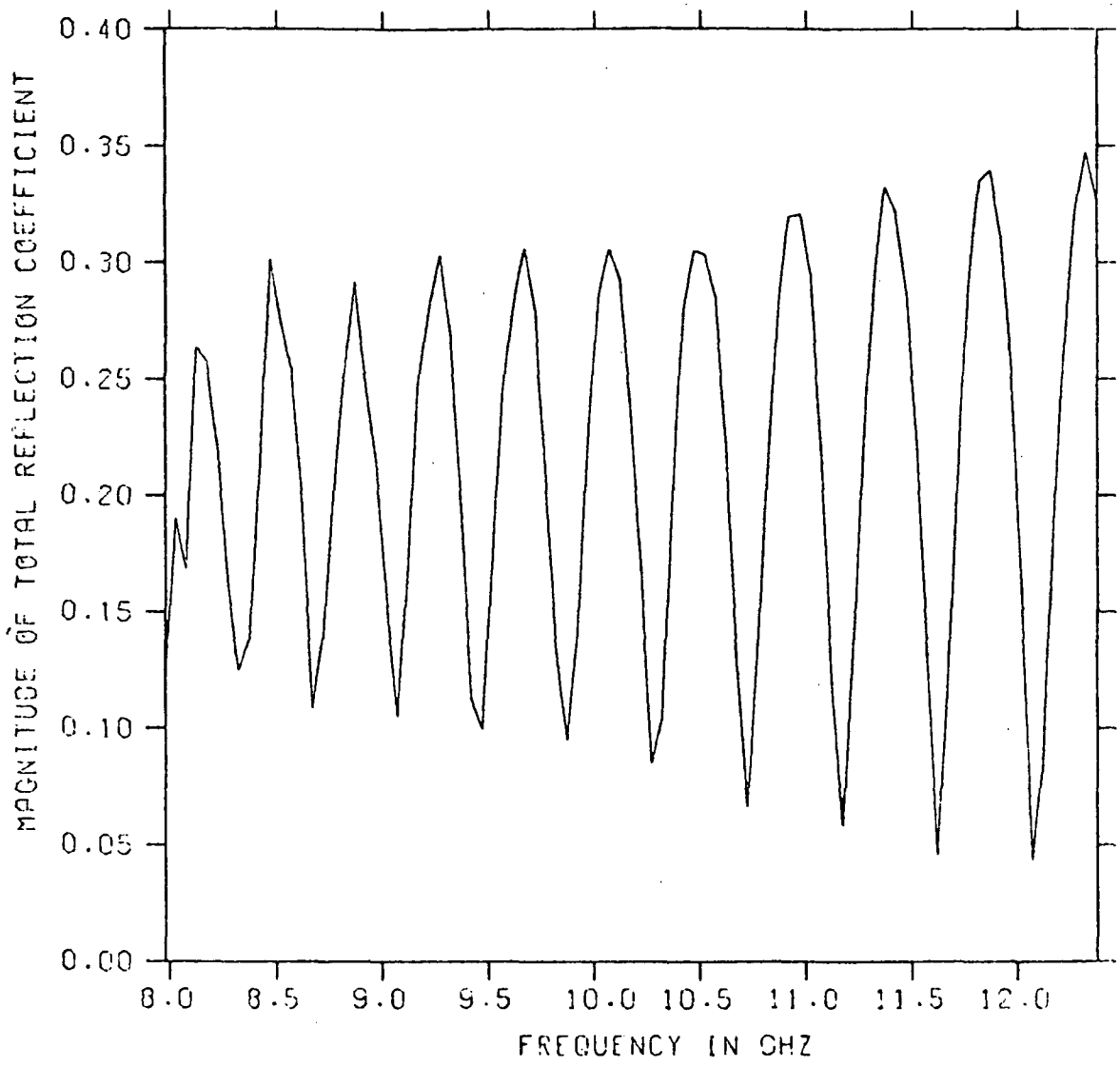

Figure 30. Total Magnitude of the Reflection Coefficient of the Reference Step and a Capacitive Iris

given by Equation (III-18).

Description of Instrumental Errors. All reflectometers suffer from small imperfections such as a lack of perfect directivity in the directional couplers and discontinuities in the couplings and imperfections in the waveguides. Generally, the two crystal detectors have different frequency responses, and these can cause changes in the output resembling those from reflections. The coupling coefficients of the directional couplers also vary slightly with frequency.

In the comparison reflectometer all measurements are made by comparison with a single known standard, the reference reflection Γ_r, and therefore, all of the instrumental defects are nearly cancelled out.

Consider a test component having no internal reflections. When the reference readings are taken, all the instrumental defects show up as a variation in E_r with frequency. However, the test readings E will be equal to E_r at every frequency and from (III-31), $G(\nu)$ is constant with frequency and a_n and b_n in (III-22, 23) are zero. Therefore, the instrumental errors have been cancelled out completely.

When a test component includes reflections, a high degree of cancellation still exists. The instrument defects correspond to a pattern of reflections spaced at different distances from the reference. Because these contribute to

both readings, only a small residue can appear in $G(\nu)$, and then only when a reflection in the test component Γ_c is in the vicinity of an instrumental reflection Γ_i. In the worse case, when the two coincide in position and phase, it has been shown by Hollway that:

$$|\Gamma_c|_{(\text{measured})} = |\Gamma_c|_{(\text{true})}(1-|\Gamma_i||\Gamma_c|)_{(\text{true})} \qquad (5)$$

Since Γ_i is small this error usually may be neglected.

A very serious error occurs should a phase lock be missed, and special care must be taken to ensure that this does not occur. If a phase lock is missed the entire set of measurements must be repeated, unless the value of the reflection coefficient can be determined at the point that was missed.

The method of taking measurements cancels out a great many errors; however, the drift with time of the ratio meter is not cancelled out. Therefore, it is important to take the two sets of measurements as quickly as possible to minimize this drift error. The effect of this drift is demonstrated in Figure 31a. Two sets of measurements were taken, each with the reference step terminated in a matched load separated by precision guide. Equation (III-22, 23, and 26) were applied to the data of Figure 31a to obtain the modulus of reflection coefficient as a function of distance given in

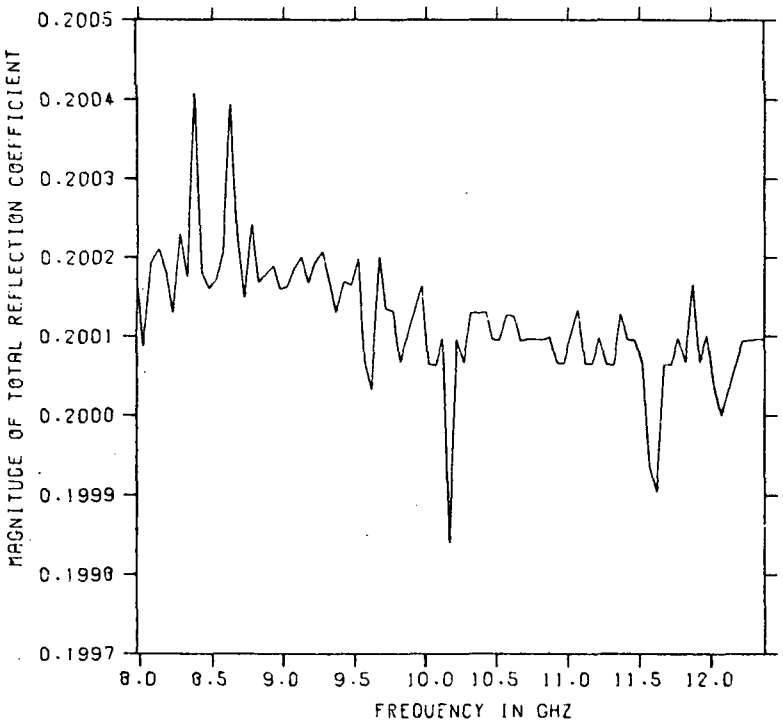

(a) Total Magnitude of Reflection Coefficient

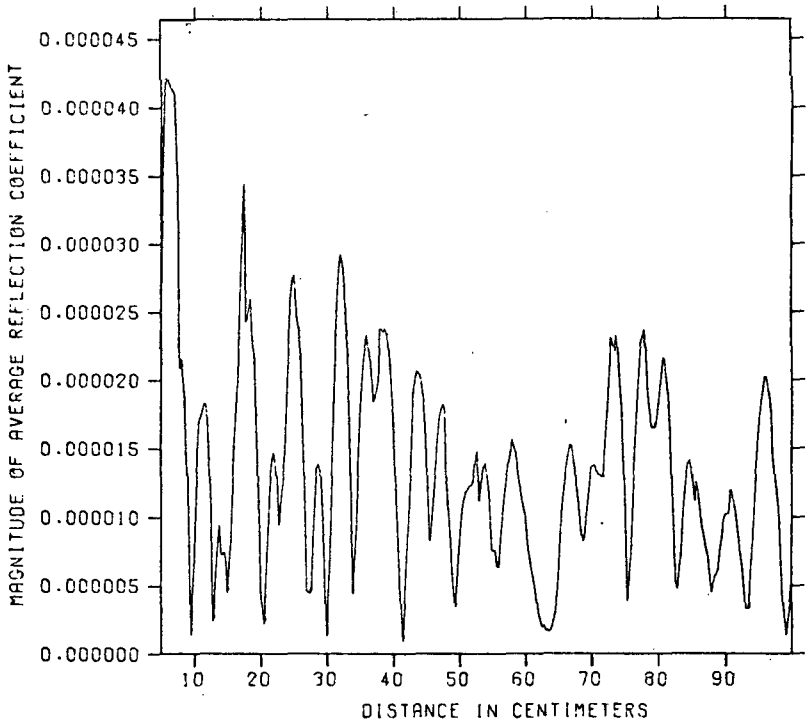

(b) Instrumental Noise

Figure 31. Magnitude of Reflection Coefficient of (a) Plain Guide and Reference Step, (b) Noise Due to Ratiometer Drift

Figure 31b. The noise level of the system was always found to correspond to a reflection coefficient variation of less than .00005 as a function of distance.

After calibration of the equipment, it was found that point reflections could be located in the waveguide within a few tenths of a millimeter and measured with an accuracy of ±3 percent in magnitude and ±5 degrees in phase angle; these results agree with those of Hollway.[1] This phase error has been verified by comparing the phase of the measured sample capacitive iris, inductive iris, metal inductive post, and dielectric post referenced to the unit conductance circle. These results are detailed in Chapter V.

CHAPTER V

EXPERIMENTAL VERIFICATION OF COMPUTED RESULTS

Introduction

A set of experiments were conducted to validate the theoretically determined values of reflection coefficient and resultant mismatch. Computed results and measured results are presented in the following pages. As a verification of the validity of the waveguide element equations given in Chapter III a symmetrical capacitive iris, asymmetrical inductive iris, metal inductive post, and a dielectric post have been fabricated and were measured using the comparison reflectometer and also using a slotted line. A standard waveguide mismatch was also measured by the comparison reflectometer and by the slotted line. In all cases the slotted line measurements, comparison reflectometer measurements and calculated results are within the uncertainty of the comparison reflectometer.

The utility of the impedance matching program was tested in two demonstrations. In the first a capacitive iris was matched with a second capacitive iris as the matching element, and the resulting impedance match agreed with the expected result for the simple combination of waveguide elements.

In order to demonstrate the power of the impedance matching technique a shunt slot radiator was fabricated, measured, and impedance matched. A comparison of predicted and measured resultant reflection coefficients is presented at selected frequencies.

Reflection Coefficient of Selected Waveguide Elements

The accuracy of the comparison reflectometer was demonstrated with corroborative measurements of several elements taken with both the comparison reflectometer and a slotted line setup. The measurements also demonstrate the validity of Equations (III-34) through (III-48) as models of the waveguide matching elements in this research.

Waveguide Standard

An X-band standard disturbance, Ga. Tech Model SR120X, with a VSWR of 1.19 was measured by the comparison reflectometer. Voltage measurements were recorded with the standard located 30.2 centimeters from the reference plane of the comparison reflectometer. Calculations of the magnitude of the reflection coefficient as a function of distance were made using Equation (III-31) and results have been plotted in Figure 32. The plot of Figure 32 appears as a continuous curve; however, only the discrete points at 50 MHz intervals from 7.975 GHz to 12.425 GHz are precisely known. This curve shows the expected periodic dependence on frequency as a result of the constructive and destructive interference of waves reflected by the reference step and by

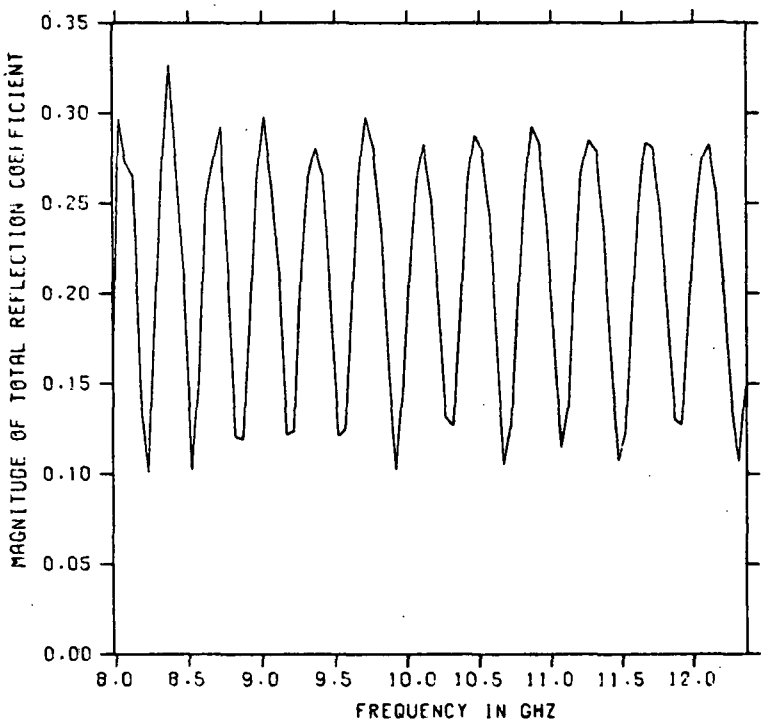

Figure 32. Magnitude of the Total Reflection Coefficient of a Waveguide Standard and Reflectometer Reference Step

the measured discontinuity.

The magnitude of the average reflection coefficient generated as a function of distance was calculated by the computer program Test 1, listed in Appendix B. These calculations were made using the results shown in Figure 32 and Equations (III-22), (III-23) and (III-26). A curve of the reflection coefficient generated as a function of distance is presented in Figure 33. An accurate electrical location was determined by measuring the distance at the 3 dB (half power points) and averaging the two distances. The

electrical location as found by this procedure was 30.16 centimeters from the reference plane of the reflectometer. The difference between this apparent electrical location and the physical location is .04 centimeters.

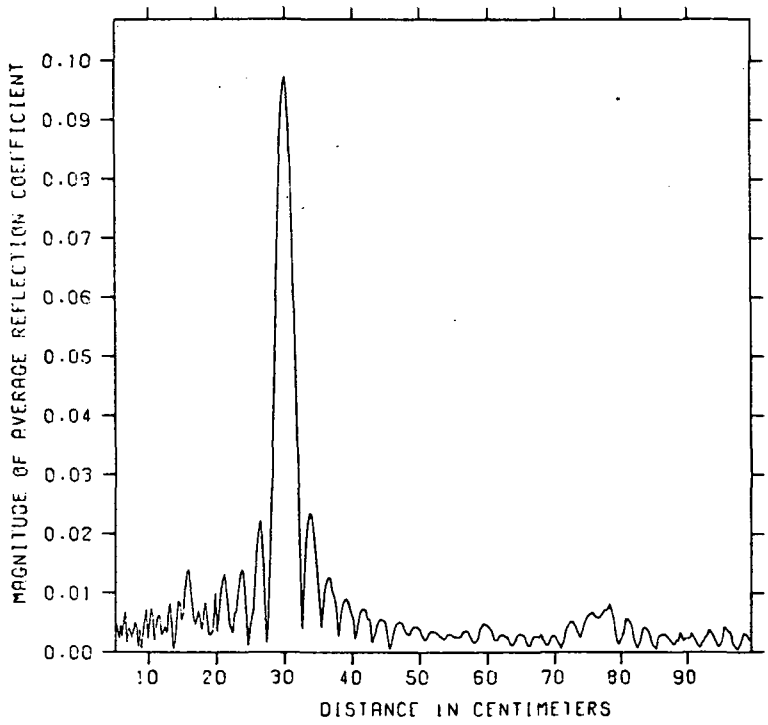

Figure 33. Electrical Location of a Waveguide Standard

The complex reflection coefficient as a function of frequency is calculated at the electrical center by Equations (III-22), (III-23) and (III-26) using overlapping intervals of integration as described in Chapter III and Appendix B. The computer program Test 2, Appendix B, implements the above equations to obtain the complex current reflection

coefficient as indicated, Figure 34. Slotted line measurements were taken at the selected frequencies of 9.0 GHz, 9.5 GHz, 10.0 GHz, 10.5 GHz, 11.0 GHz, and the maximum difference between slotted line measurements and reflectometer measurements is only 5%. This difference is within the uncertainty of the slotted line measurement. The phase of the waveguide standard is shown in Figure 34b on an expanded scale. The small variation of one to eleven degrees in phase angle as a function of frequency is characteristic of the waveguide E-plane step.

Waveguide Matching Elements

A symmetrical inguide capacitive iris, asymmetrical inguide inductive iris, solid inguide inductive post, and an inguide dielectric post were fabricated and their reflection coefficients measured. The results of these measurements were compared with the calculated reflection coefficients using Equations (III-34) through (III-48) for the respective waveguide elements.

Table 5 provides a comparison of the physically measured location and the apparent electrical location of the various elements as measured by the comparison reflectometer.

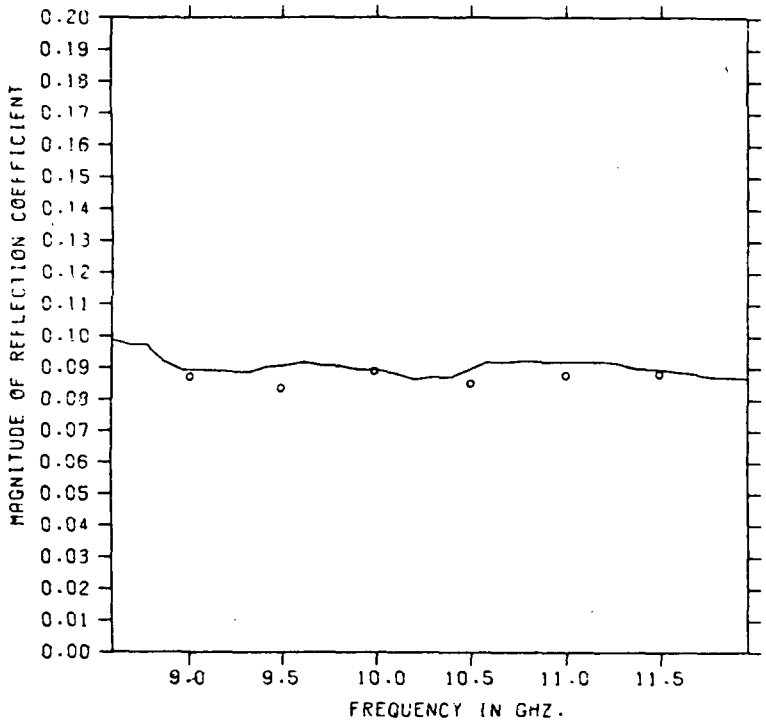

(a) Magnitude of Reflection Coefficient
o Slotted Line Measurement

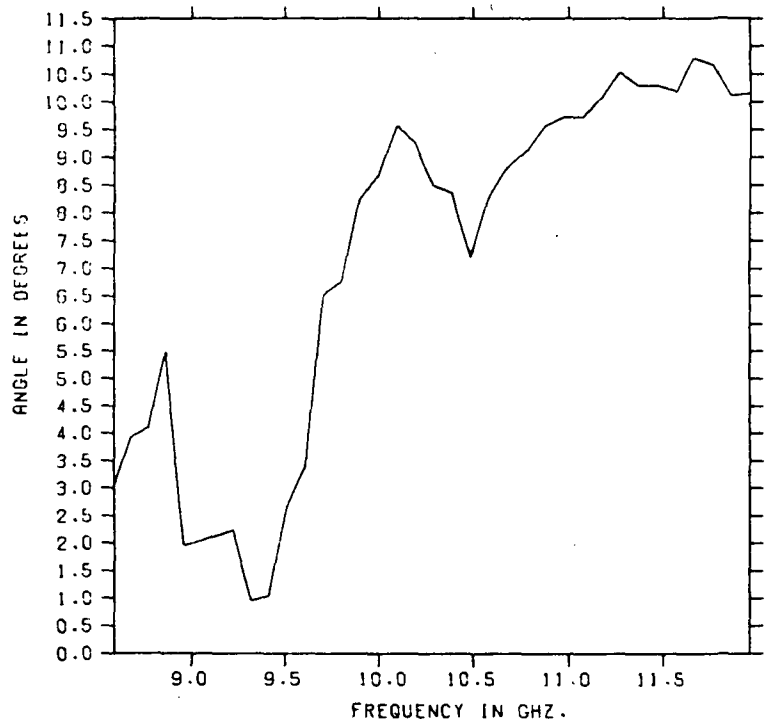

(b) Phase of Reflection Coefficient

Figure 34. Magnitude and Phase of the Reflection Coefficient of a Waveguide Standard E-Plane Step, Ga. Tech Model SR120X

Table 5. Location of Fabricated Waveguide Elements

Elements	Waveguide Location in Centimeters	Reflectometer Result Location in Centimeters	Difference
Capacitive Iris	27.0	26.94	-0.06
Inductive Iris	27.0	27.16	+0.16
Inductive Post	27.0	27.24	+0.24
Dielectric Post	27.1	27.02	-0.08
Waveguide Standard	30.2	30.16	-0.04

It is interesting to note that the electrical location of the capacitive iris appears .06 centimeters on the generator side of the geometrical location. The waveguide standard, also capacitive, is located electrically .04 centimeters on the generator side of the geometrical location. This trend is also followed by the dielectric post which appears electrically to be .08 centimeters on the generator side of its geometrical center, and is also capacitive. On the other hand, the inductive post appears to be located .16 centimeters on the load side of the geometrical location. Therefore, it could be concluded that a capacitive element appears electrically to be in front of its physical position while an inductive element appears electrically to be behind its physical location. This interesting observation

has little consequence as far as impedance matching is concerned as long as the complex reflection coefficient is computed at the electrical center.

The phase angle of the complex reflection coefficient at the apparent electrical location is different from the phase at the physical location by a factor of $2\beta L$ radians where L is the difference in the two locations. Reflectometer calculations of the complex reflection coefficient were made for the apparent electrical location of each sample element; theoretical calculations (Equations (III-34) to (III-48)) were made for the respective physical location. The results obtained by the comparison reflectometer should have the phase correction ($2\beta L$) applied before comparing with theoretically predicted results. In the following, comparisons are made between the predicted calculated phase at the physical location with that of the measured phase at the electrical location.

The fabricated symmetrical capacitive iris, Figure 14, (Chapter III) was measured by the comparison reflectometer. A plot of the average magnitude of the reflection coefficient generated as a function of distance appears as Figure 35. The complex reflection coefficient was calculated at the electrical location of 26.94 centimeters. This complex current reflection coefficient is displayed by the admittance Smith chart plot shown in Figure 36. All Smith chart plots presented in this thesis are referenced to a matched

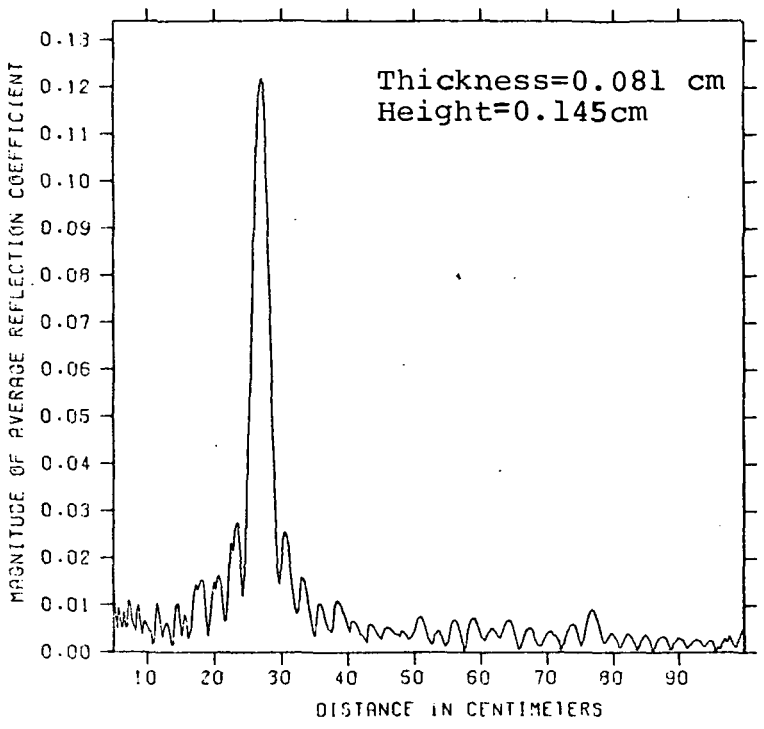

Figure 35. Distance Plot of a Symmetrical Capacitive Iris

load termination. As the observer moves away from the location of the disturbance the phase of the complex reflection coefficient varies according to exp (-j2βL) where β is given by Equation (I-1) and L is the distance between the location of the disturbance and the observer. For a frequency of 10.0 GHz the phase sensitivity is 182.88 degrees per centimeter distance. The departure of the measured points in Figure 36 from the unit conductance circle can be attributed to the 0.06 centimeter difference between the physical center and the electrical center. This difference in distance results in a phase angle difference of approximately 11

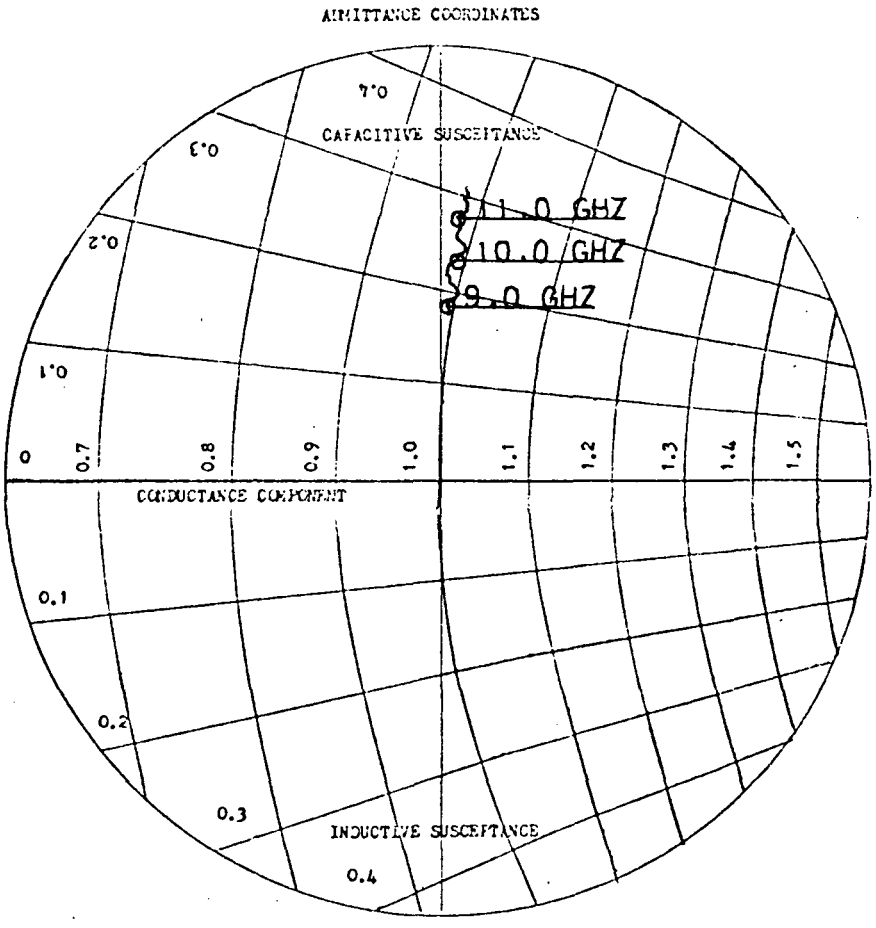

(a) Smith Chart Display of Current Reflection Coefficient

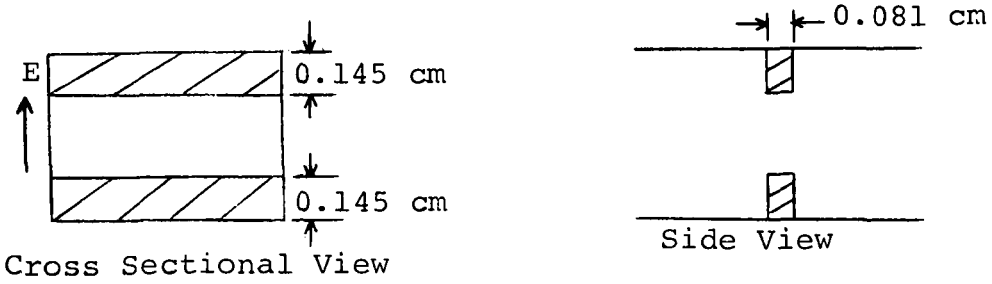

(b) Symmetrical Capacitive Iris

Figure 36. Complex Current Reflection Coefficient of the Fabricated Capacitive Iris on Expanded Admittance Plot at the Electrical Location

degrees at 10.0 GHz. The actual phase difference measured from Figure 36 is approximately 5 degrees. This difference in phase is within the predicted accuracy of the comparison reflectometer.[1]

A comparison of the measurements taken of the fabricated capacitive iris and the calculated results are shown in Figure 37. In Figure 37, a curve of magnitude of reflection coefficient is given as a function of frequency. Superimposed on this curve are the theoretical points and the slotted line measurements, both at selected frequencies. There is good agreement between the three sets of results. The phase, in Figure 37b, is compared with the calculated phase at selected frequencies. The measured results are in good agreement with the predicted characteristics and it can be concluded that the capacitive iris is adequately modeled by Equations (III-34) through (III-37) in the impedance matching computer program listed in Appendix B.

The fabricated asymmetrical inductive iris of Figure 15 was also measured by the comparison reflectometer. A plot of the average magnitude of the reflection coefficient as a function of distance is given in Figure 38.

The complex reflection coefficient was calculated at the apparent electrical location of 27.16 centimeters with respect to the reflectometer reference plane. This complex reflection coefficient is given by the admittance Smith chart plot of Figure 39. The results of Figure 39 are

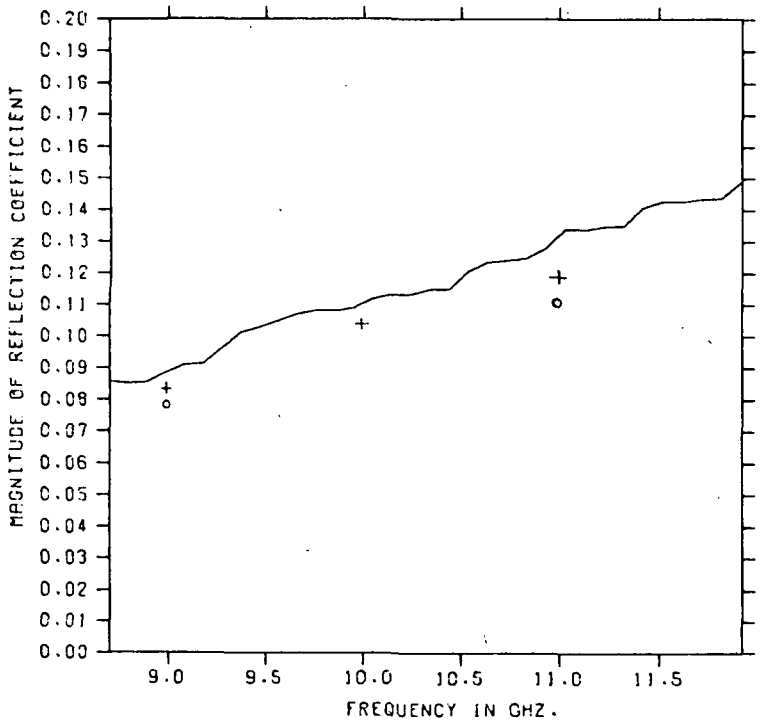

(a) -Reflectometer Measurement
+Calculated Result
o Slotted Line Measurement

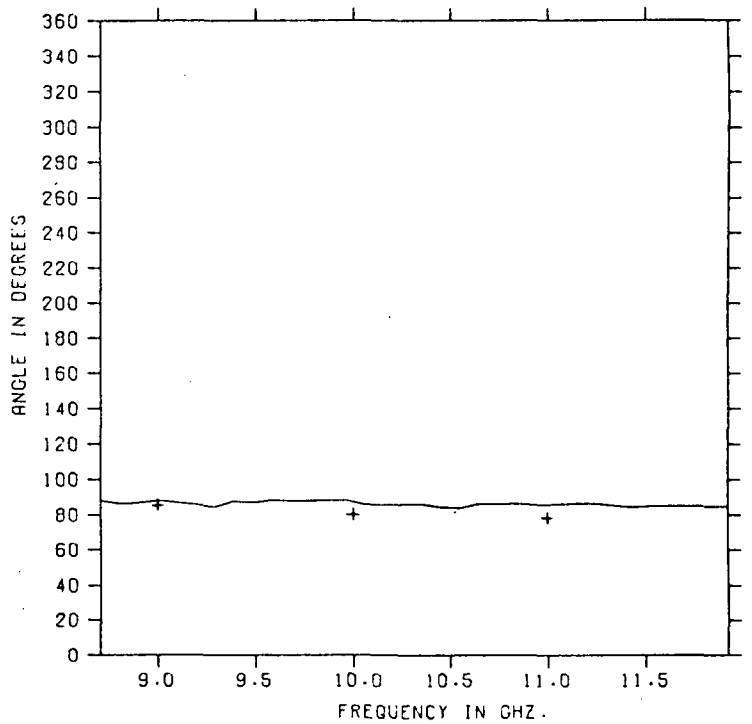

(b) -Reflectometer Measurement
+Calculated Result

Figure 37. Reflection Coefficient of a Fabricated Capacitive Iris with Iris Thickness 0.081 cm and Iris Height = 0.145 cm

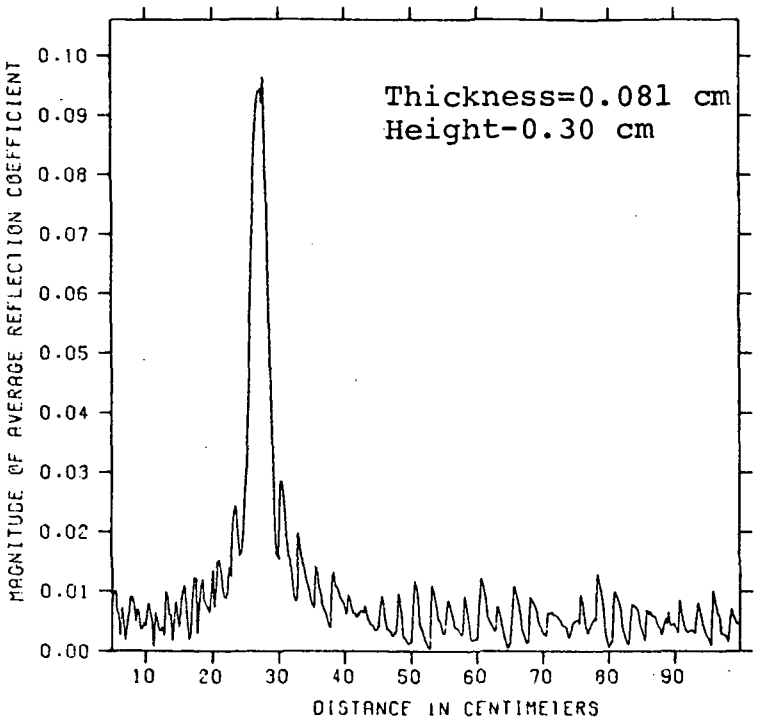

Figure 38. Distance Plot of an Asymmetrical Inductive Iris

within the uncertainty of the comparison reflectometer when electrical and physical center separation are taken into account. A comparison of the measurements taken of the fabricated inductive iris and the calculated results are shown in Figure 40. The measured magnitude of the reflection coefficient is plotted as a function of frequency in Figure 40a, and compared to theoretical points and slotted line measurements, both at selected frequencies. There is good agreement between the three sets of data.

The phase in Figure 40b, is compared with the calculated phase at selected frequencies. The 29 degree difference in phase between the measured and calculated results

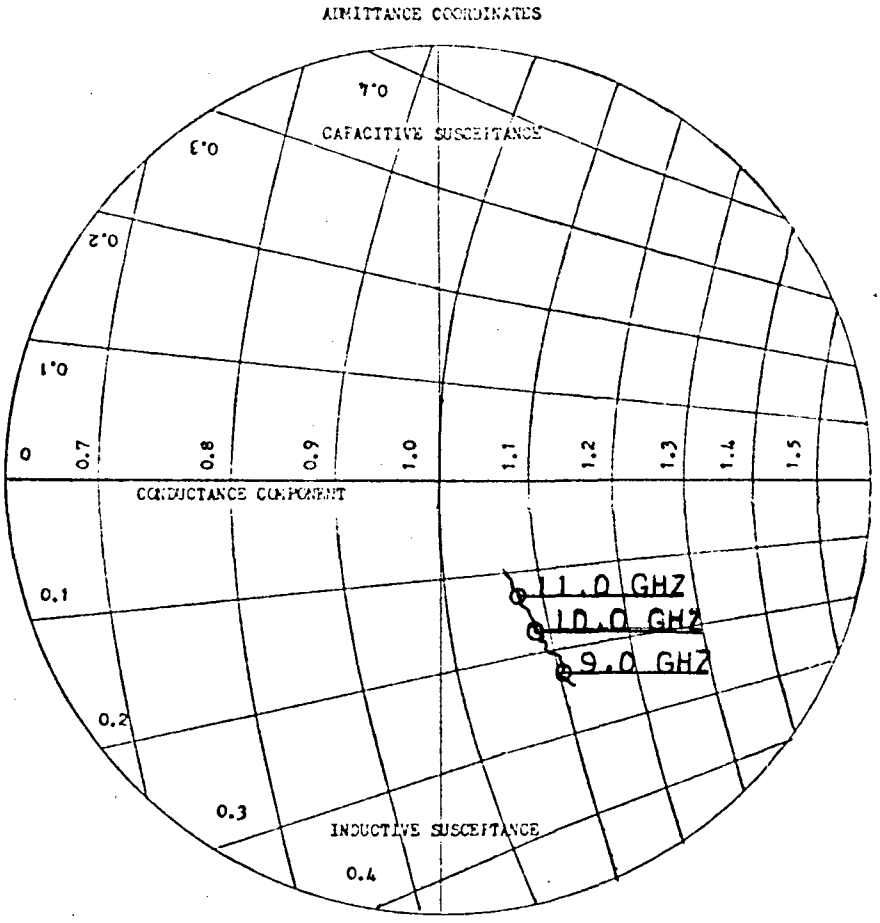

(a) Smith Chart Display of Current Reflection Coefficient

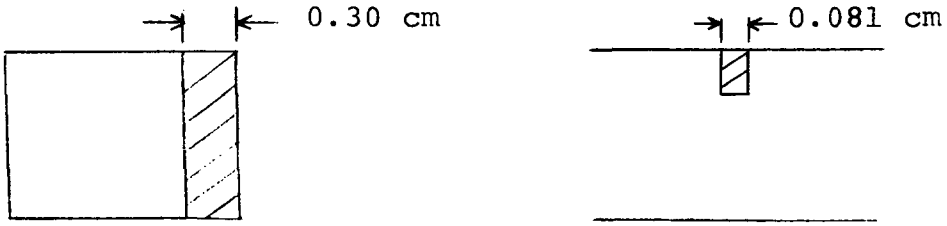

(b) Asymmetrical Inductive Iris

Figure 39. Complex Current Reflection Coefficient of the Fabricated Inductive Iris at the Electrical Location on Expanded Admittance Plot

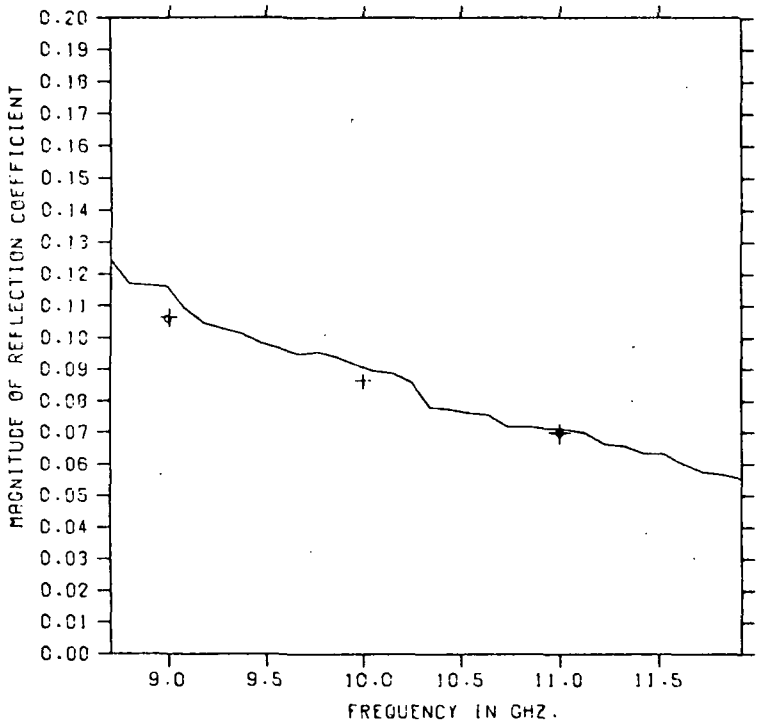

(a) -Reflectometer Measurement
+Calculated Result
o Slotted Line Measurement

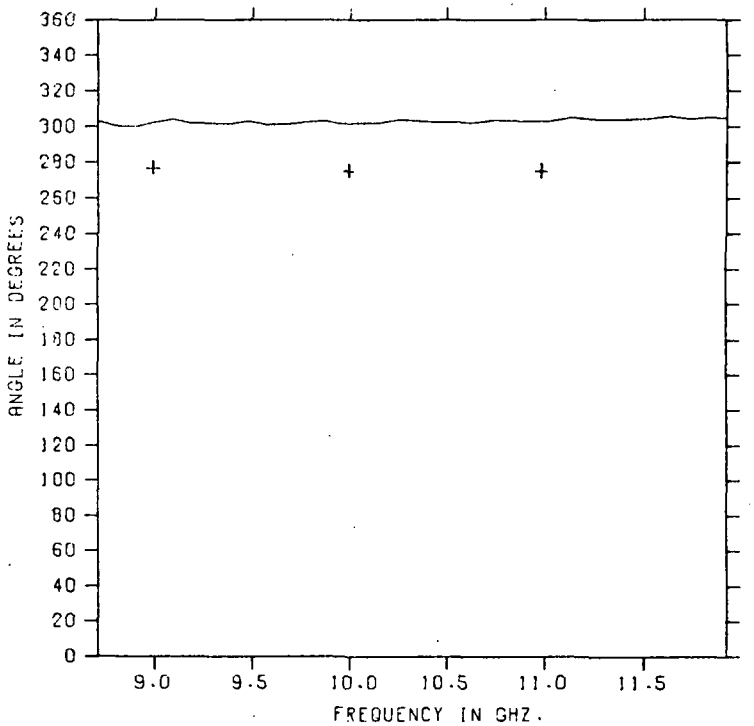

(b) -Reflectometer Measurement
+Calculated Result

Figure 40. Reflection Coefficient of a Fabricated Inductive Iris with Iris Thickness = 0.081 cm and Iris Height = 0.30 cm

is largely due to the difference of 0.16 centimeters (equivalent to 29.8 degrees at 10 GHz) between the electrical and geometrical locations. Therefore, it can be concluded that the measured result is in good agreement with the predicted characteristics.

A sample of the metal inductive post of Figure 16, was given a similar experimental check. A plot of the average magnitude of the reflection coefficient as a function of distance is given in Figure 41.

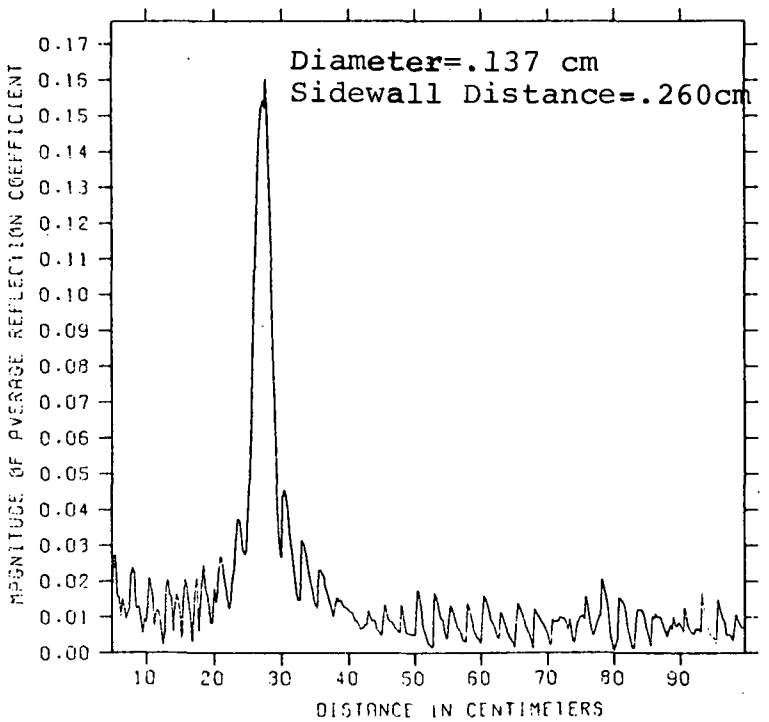

Figure 41. Distance Plot of a Metal Inductive Post

The complex reflection coefficient was calculated at the apparent electrical location of 27.24 centimeters. This complex reflection coefficient is displayed, Figure 42, by the admittance Smith chart plot. While the difference in phase between the calculated and measured results is 44 degrees at 10. GHz, the difference in phase between the geometrical location and the electrical location is 43.89 degrees corresponding to the 0.24 centimeters of Table 5. Therefore, there is a difference of only 0.11 degrees which is well within the accuracy of the reflectometer.

A comparison of the experimental and theoretical data for the fabricated inductive post is shown in Figure 43. In Figure 43a, a curve of magnitude of reflection is given as a function of frequency. Superimposed on this curve are the theoretical points and the slotted line measurements, both at selected frequencies. Again good agreement is found among the three sets of results.

The dielectric post sample was fabricated from hot-pressed boron nitride, HD-0092. Boron nitride has a relative dielectric constant of 4.07 and a loss tangent of 0.0003.

The locating plot of the average magnitude of the reflection coefficient as a function distance is given in Figure 44.

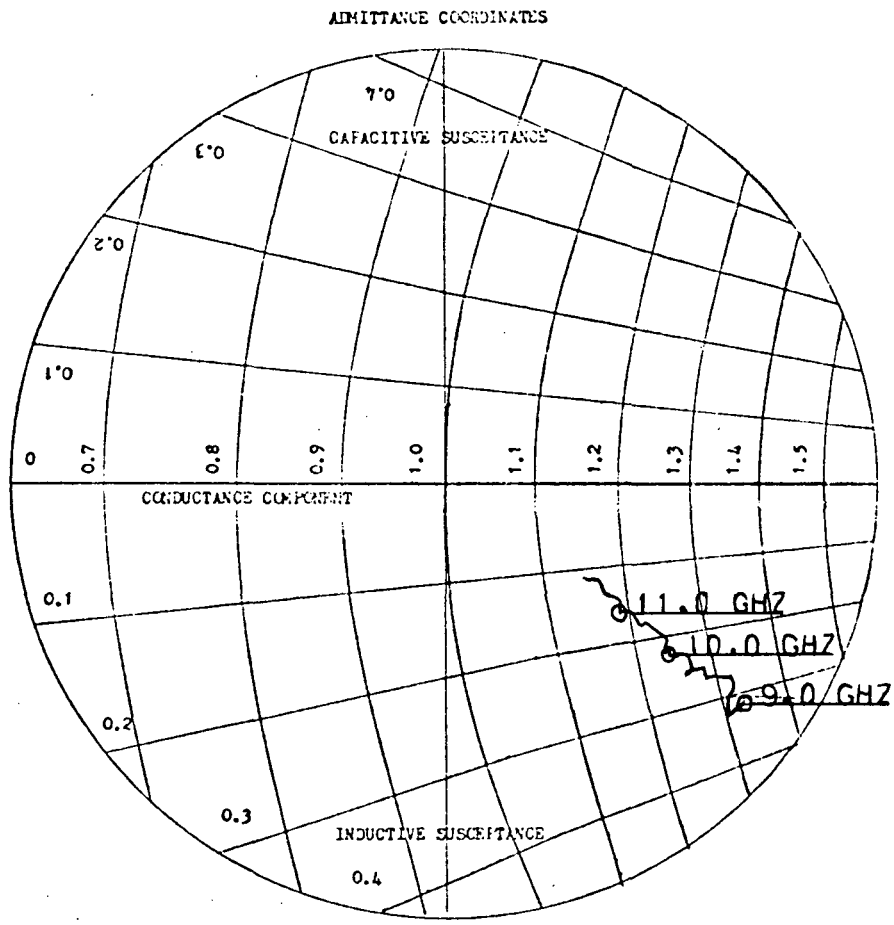

(a) Smith Chart Display of Current Reflection Coefficient

(b) Metal Inductive Post

Figure 42. Complex Current Reflection Coefficient of the Fabricated Metal Inductive Post at the Electrical Location on Expanded Admittance Plot

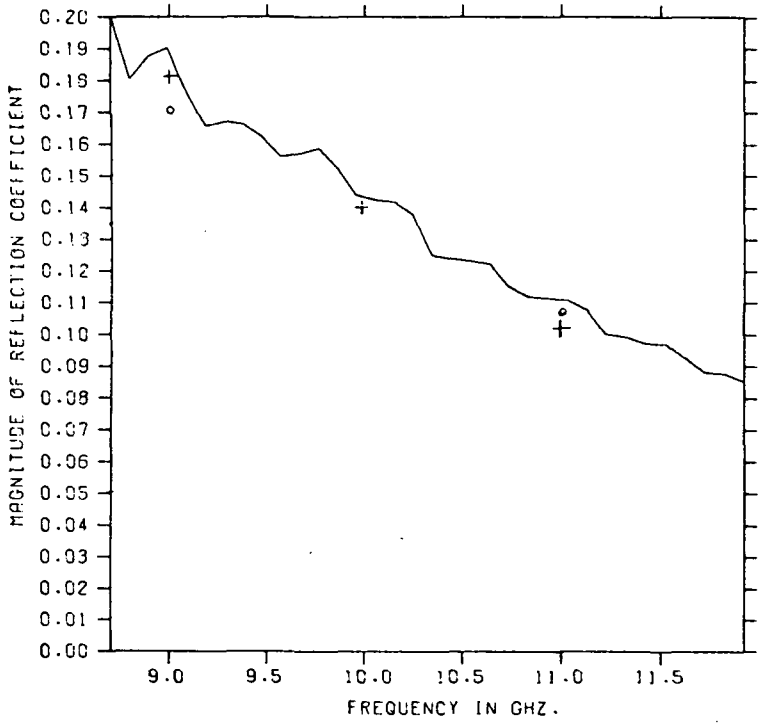

(a) -Reflectometer
+Calculated Resule
o Slotted Line Measurement

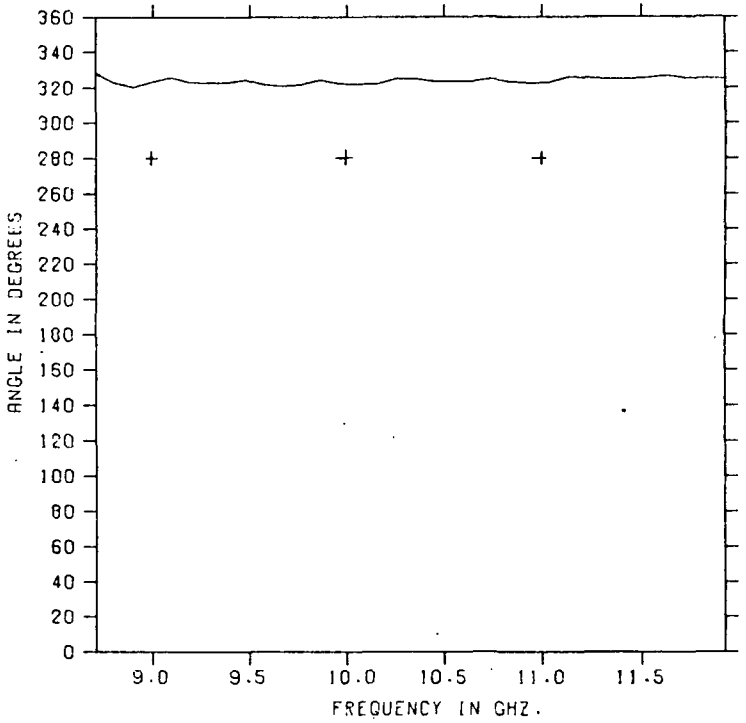

(b) -Reflectometer Measurement
+Calculated Result

Figure 43. Reflection Coefficient of a Fabricated Inductive Post with Diameter = 0.137 cm and Sidewall Distance = 0.260 cm

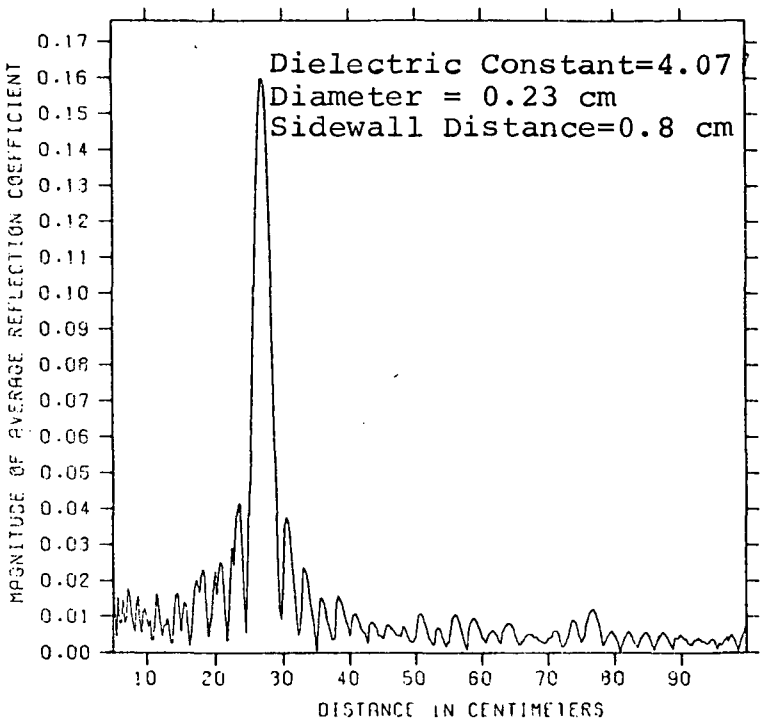

Figure 44. Distance Plot of an Inguide Dielectric Post

The complex reflection coefficient was calculated at the electrical location of 27.02 centimeters. For this element, the expected difference in phase resulting from the lack of coincidence of geometrical and electrical centers is 14.6 degrees. The actual phase difference between the measured response and the unit conductance circle is 16 degrees, shown in Figure 45. Therefore, the difference in predicted and measured phase is only 1.4 degrees.

In a test of resolution of the technique a fabricated capacitive iris and an inductive iris were measured at the same time by the comparison reflectometer. The capacitive

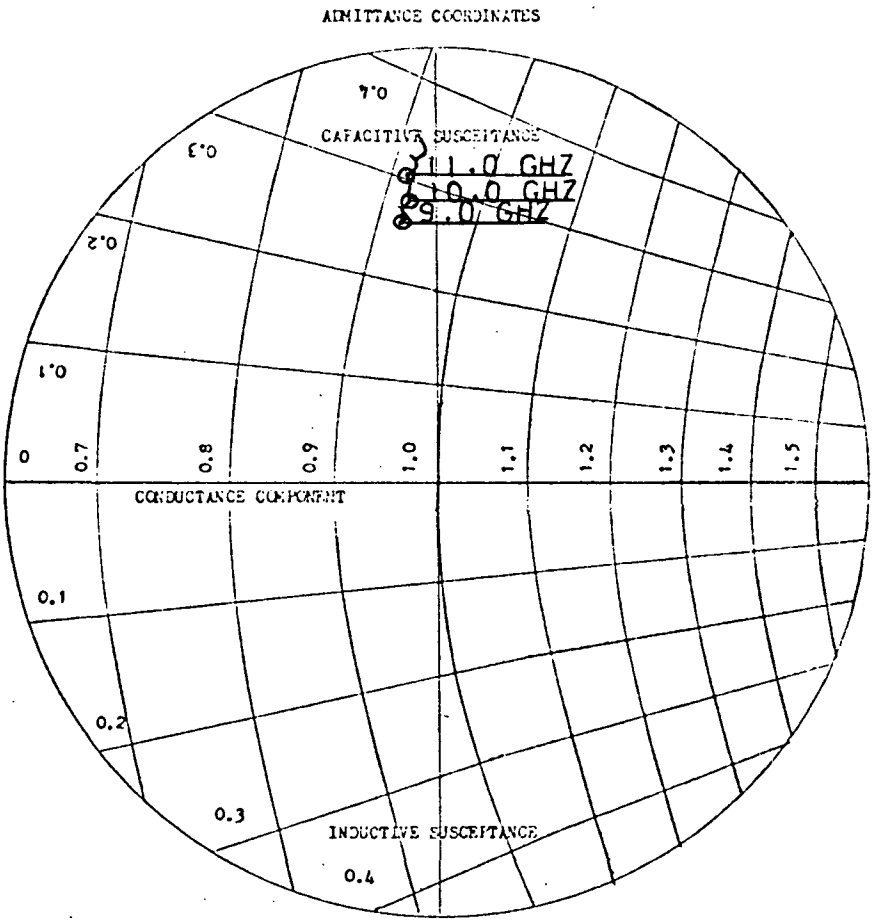

(a) Smith Chart Display of Current Reflection Coefficient

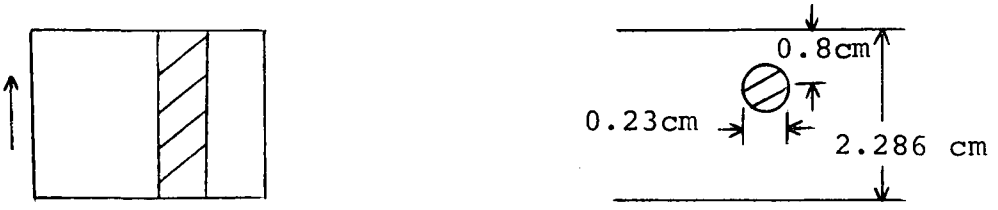

(b) Dielectric Post with Dielectric Constant $\varepsilon' = 4.07$

Figure 45. Complex Current Reflection Coefficient of the Fabricated Dielectric Post at the Electrical Location on Expanded Admittance Chart

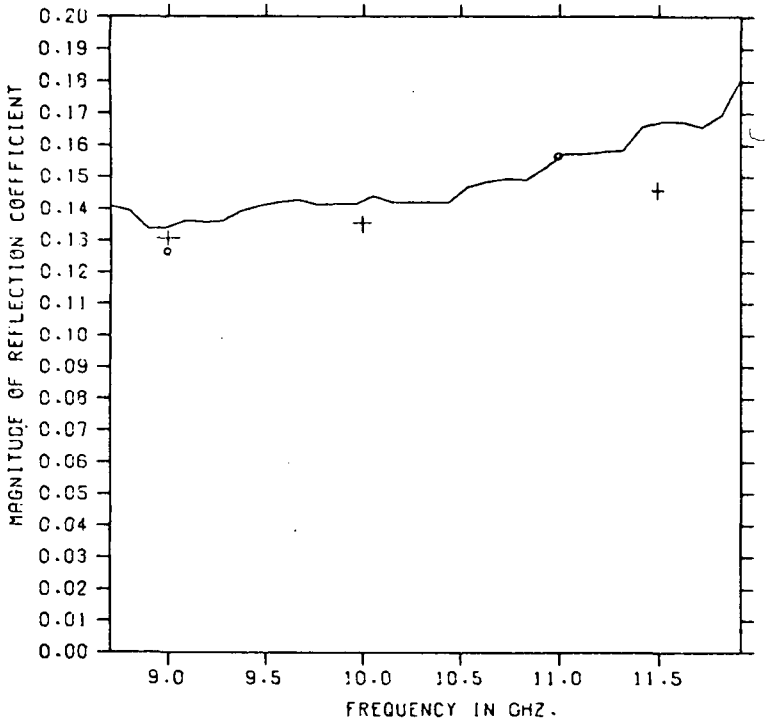

(a) -Reflectometer Measurement
+Calculated Result
o Slotted Line Measurement

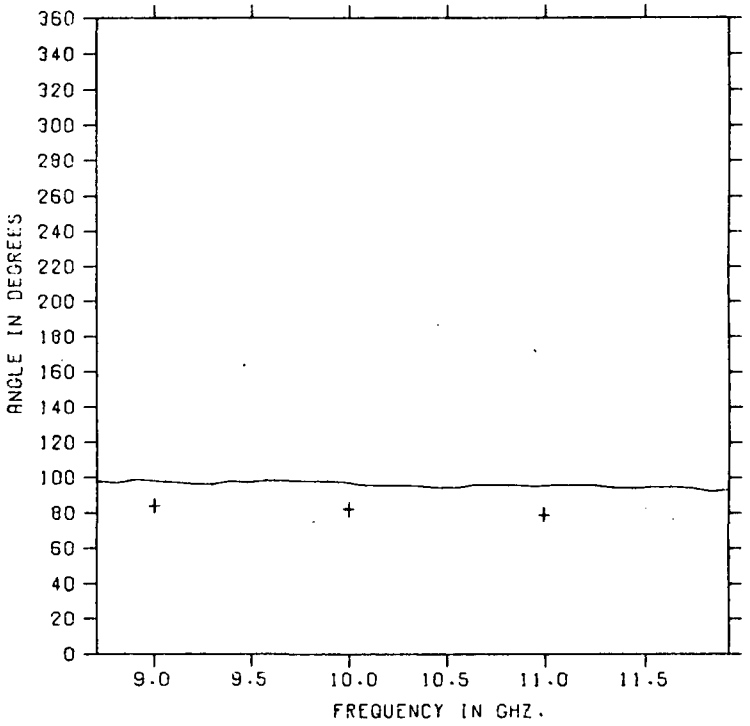

(b) -Reflectometer Measurement
+Calculated Result

Figure 46. Reflection Coefficient of a Fabricated Dielectric Post with Diameter = 0.23 cm, Sidewall Distance = 0.80 cm, and Dielectric Constant = 4.07

iris was located 27.00 centimeters from the reference plane and the inductive iris 51.00 centimeters from the reference plane. A curve of the total magnitude of the reflection coefficient of the reference step, capacitive iris, and inductive iris is given by Figure 47a. From this information the average magnitude of the reflection coefficient generated as a function of distance is calculated, Figure 47b. The electrical location for the capacitive iris is calculated to be 26.98 centimeters, and that of the inductive iris 51.16 centimeters. The difference in the geometrical and electrical location of the capacitive iris is .01 centimeters. In Table 5, for a single capacitive iris in the guide the difference is 0.06 centimeters.

The distance between the electrical and geometrical locations for the inductive iris is 0.16 centimeters and compares with the 0.16 cm difference of Table 5. This good agreement between the single disturbances and multiple disturbance tests made by the reflectometer tends to justify the approximations made in Chapter III, Equation (14).

Impedance Matching

Impedance Matching a Capacitive Iris

In a trial test of the impedance matching program a single capacitive iris was used as the waveguide disturbance. A second capacitive iris was selected as the matching element. The disturbance was impedance matched over three different bandwidths to demonstrate the adaptability of the im-

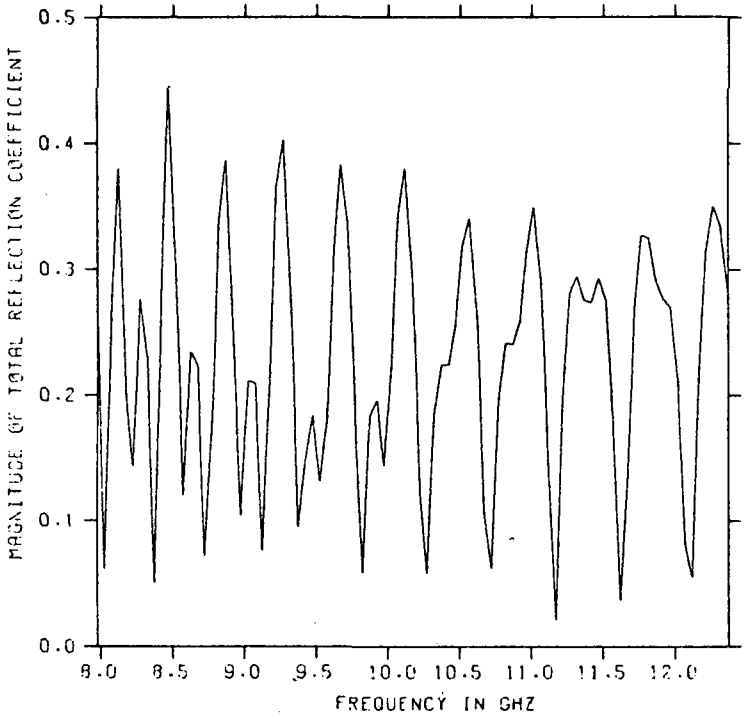

(a) Total Magnitude of Reflection Coefficient

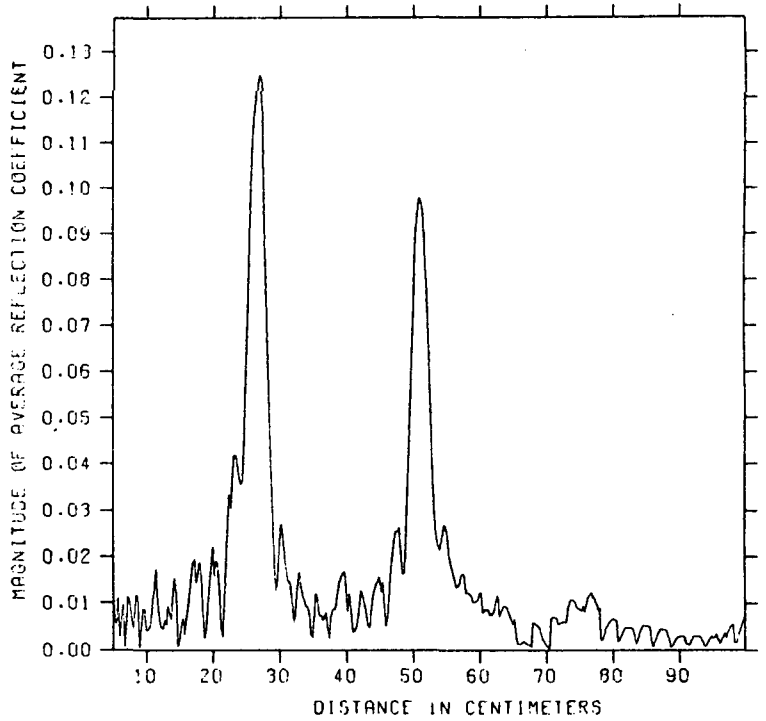

(b) Average Magnitude as a Function of Distance

Figure 47. Measurement of the Capacitive Iris and Inductive Iris in the Test Waveguide

pedance matching program. The iris selected as the mismatch has a thickness of 0.081 centimeters and an iris height of 0.145 centimeters.

If an impedance match were calculated using a Smith chart as a tool, generally, a capacitive iris of the same dimensions would be placed a quarter wavelength from the first iris, where the wavelength corresponds to the center frequency of the matched bandwidth. Using this procedure there would be no control of the resulting mismatch over the rest of the band. The impedance matching computer program, Appendix B, calculates the combination of physical dimensions and relative distance between elements which results in the least root mean square mismatch over the bandwidth to be matched. Therefore, the technique developed in this thesis provides some control over the resulting mismatch over the entire bandwidth. This can be seen by considering Figure 48. In Figure 48 the VSWR of the initial mismatched capacitive iris is given together with three other curves of VSWR, one for each match band.

The narrowest band provides the smallest mismatch at the center of the band, but the mismatch increases more rapidly than that of the broader band impedance match. The narrowest band match is from 10.195 to 10.595 GHz, with a center frequency of 10.395 GHz. At the center frequency the VSWR is equal to 1.0006. The next broader bandwidth is from 9.795 GHz to 10.995 GHz, also with a center frequency of

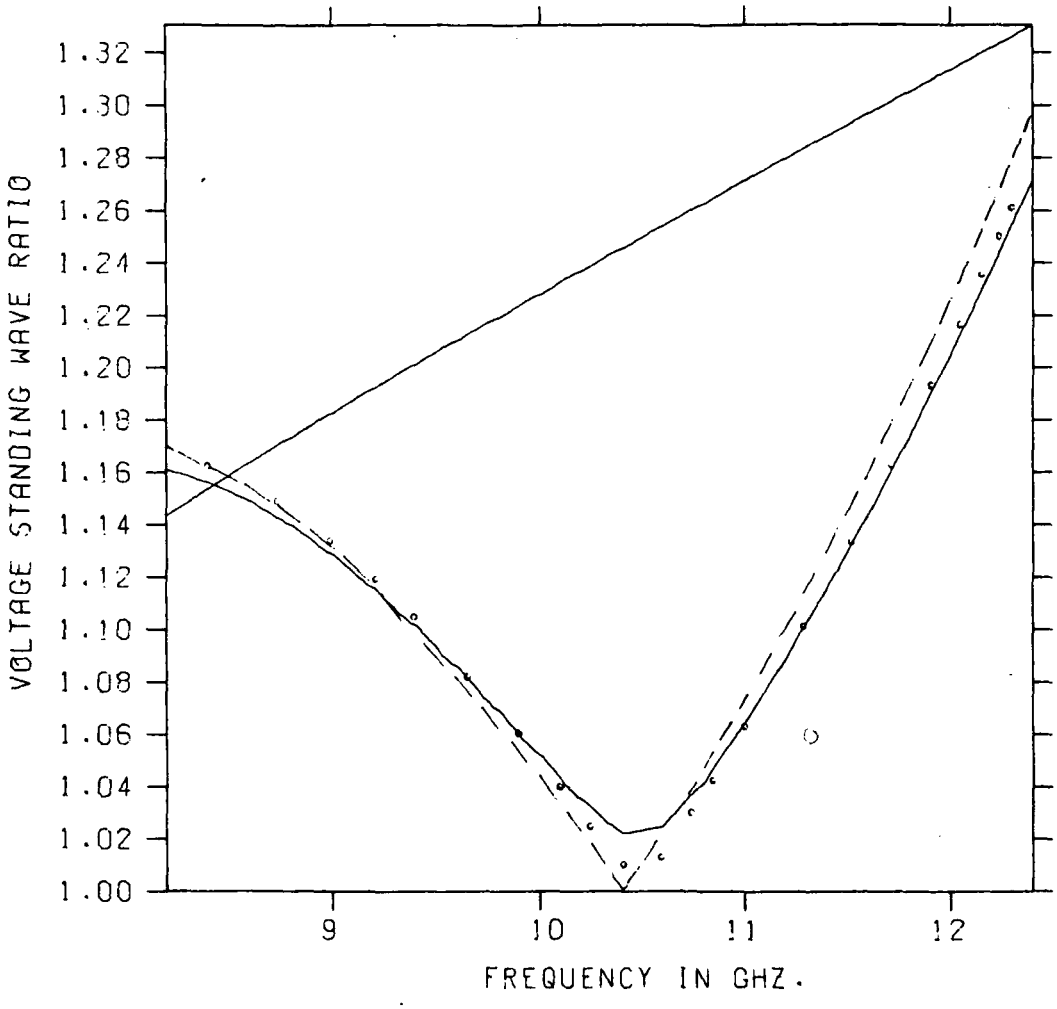

(1) Bandwidth 10.195 - 10.595 GHz ----
(2) Bandwidth 9.795 - 10.995 GHz ....
(3) Bandwidth 8.595 - 11.595 GHz ——

Figure 48. Characteristics of a Capacitive Iris Impedance Matched Over Three Bandwidths

10.395 GHz. At the center frequency the VSWR is equal to 1.022.

While the effectiveness of the broad band impedance matching program is demonstrated in these test runs, the restriction of the matching element to a second capacitive iris makes the change in resultant mismatch small.

Shunt Slot Radiator

The shunt slot radiator has been selected to demonstrate the power of this computer aided impedance matching technique. Interest in the slot was primarily motivated by by the need to broadband impedance match this element when it is used in a broad side steerable array. While this research is concerned primarily with inguide disturbances, the radiating slot provides an interesting application of this matching technique.

The reflectometer measured the slot apparent electrical location as 28.68 centimeters from the reference step as shown in Figure 29. The geometrical center of the slot is located 27.0 centimeters from the reflectometer reference step. Therefore the electrical center is located 1.68 centimeters on the load side of the physical center of the slot.

The shunt slot is a radiating device, and there are surface currents on the outer surface of the waveguide in the vicinity of the slot. These surface currents together with the disturbed surface currents on the inside wall of

the slot, determine the electrical location of the slot as measured by the comparison reflectometer.

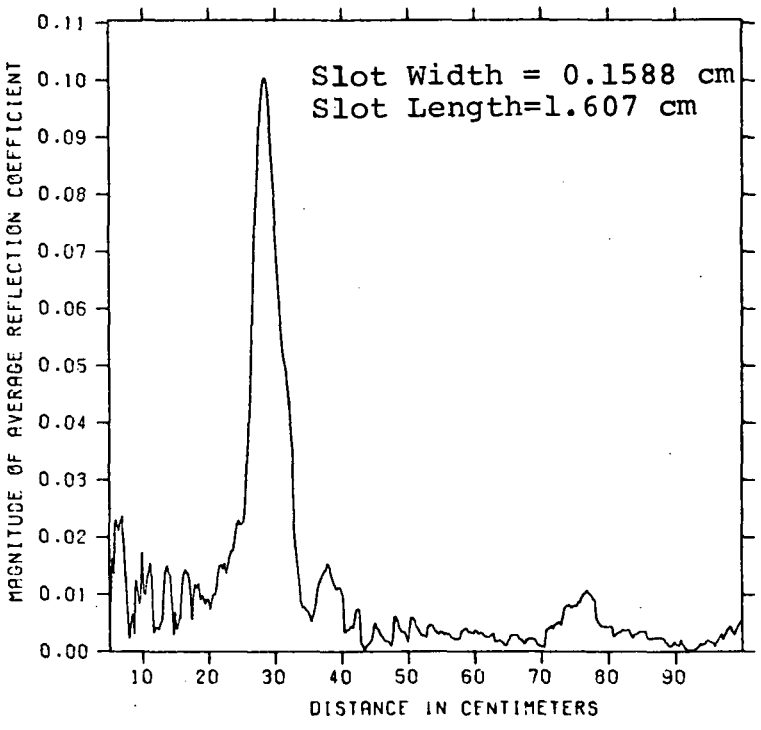

Figure 49. Distance Plot of the Shunt Slot Radiator

Unlike the nonradiating elements, the shunt slot radiator showed a marked separation between the electrical location and the geometrical location.

In Figure 50a, and 50b the magnitude and phase of the complex reflection coefficient at the apparent electrical location are given. These results were calculated by the comparison reflectometer programs, Test 1 and 2. It is possible to calculate the complex reflection coeffi-

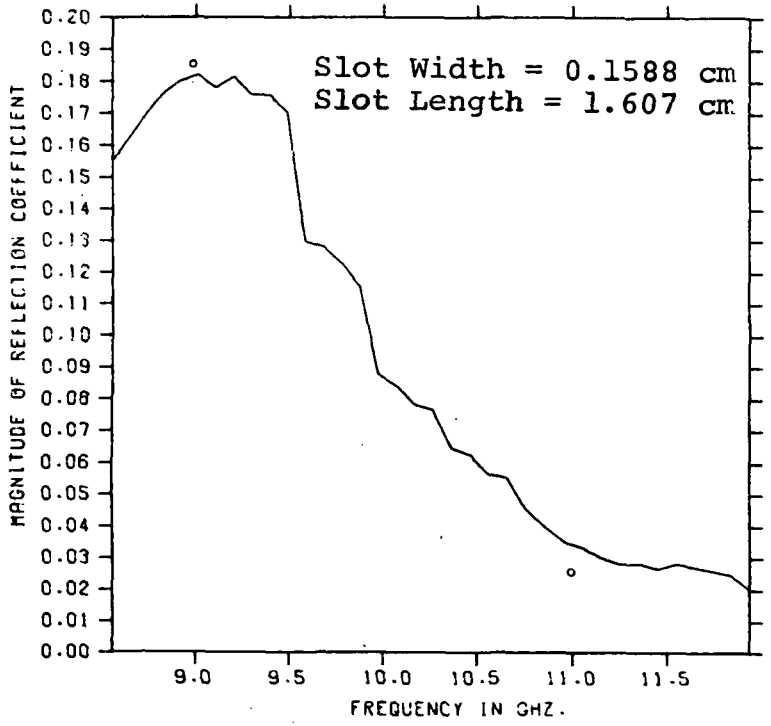

(a) Magnitude Reflection Coefficient
o Slotted Line Measurement

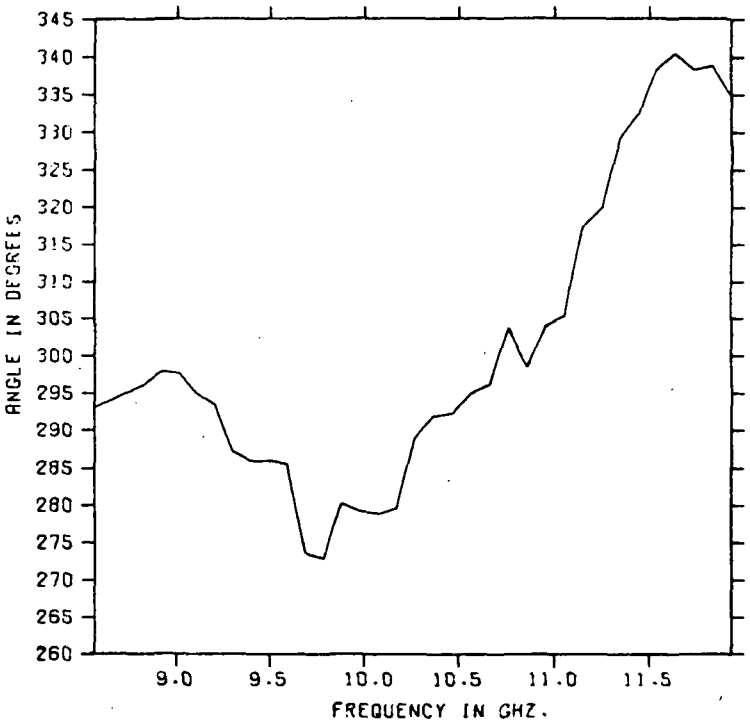

(b) Phase at Electrical Location

Figure 50. Magnitude and Phase of the Reflection Coefficient of a Shunt Slot Radiator at the Apparent Electrical Location

cient two ways at the physical location. The complex reflection coefficient can be calculated at the apparent electrical location and multiplied by exp (-j2β(1.68 cm)) resulting in the correct magnitude and phase at the physical center of the slot. On the other hand, the complex reflection coefficient can be calculated directly at the physical location by the program Test 2. This calculation at the geometrical location results in an erroneous result. The error stems from the fact that the locating nature of the transforms of Equation (III-22) and (III-23) attenuate the magnitude of the reflection coefficient at distance points not equal to the electrical location, shown in Figure 49.

To test for the existance of secondary regional matching minima the slot radiator was matched by a capacitive iris using several different initial positions for the matching iris. Ideally, the matching program should find the same match point (location, iris dimension and RMS mismatch) independent of the starting point, in the absence of secondary minima. These results are tabulated in Table 6. The relative starting locations are the electrical center, (0,0), and ±0.5566, ±1.1133, ±1.6699 and ±2.2265 centimenters from the electrical center. These distances correspond to 1/8 wavelength, 1/4 wavelength, 3/8 wavelength, and 1/2 wavelength magnitudes respectively at the frequency of 9.395 GHz. The frequency of 9.395 GHz was chosen for convenience.

Table 6. Capacitive Iris Matching of the Slot Radiator Referenced to the Slot Electrical Center

Initial Distance From Electrical Center of Slot*	RMS Mismatch	Iris Thickness*	Iris Height*	Iris Distance From Electrical Center of Slot*
2.2265	0.105	0.054	0.154	2.177
1.6699	0.105	0.041	0.160	2.182
1.1133	0.064	0.044	0.185	0.013
0.5566	0.063	0.095	0.160	0.032
0.0000	0.063	0.095	0.160	0.025
-0.5566	0.063	0.095	0.160	0.031
-1.1133	0.064	0.044	0.185	0.012
-1.6699	0.098	0.050	0.160	-2.182
-2.2265	0.098	0.050	0.160	-2.176

*In centimeters

At any selected frequency point the complex reflection coefficient varies in phase as a function of distance from the generating disturbance. This variation can be expressed in the form of Equation (1):

$$\Gamma(f,L) = \Gamma_c(f)\exp[-j2\beta L], \qquad (1)$$

where β is the propagation constant and $\Gamma_c(f)$ is the complex reflection coefficient of the disturbance when L = 0. The greater the distance L between the matching element and disturbance the more rapid the change in phase with frequency.

As a result of this variation in phase of the complex reflection coefficieint as a function of distance, it is reasonable to expect a least root mean square mismatch (LRMS) to occur for matching iris placements at intervals of $\lambda_g/2$ distance as shown in Figure 51, where λ_g is the guide wavelength of the center frequency of the matching bandwidth. However, because the RMS is taken over the entire bandwidth of interest, this distance is not expected to be exact. As the magnitude of the distance L increases so does the phase change with frequency. Therefore, the quality of the impedance match is expected to change as the matching element is located at distances that are integral multiples of $\lambda_g/2$. It is important to notice the absence of large secondary minima when initiating calculations from different relative separation distances L between the disturbance and the matching element. All five points of Table 6 that are 1/4 wavelength or less from the electrical center resulted in virtually the same match point. At each end the two most distant starting points again resulted in essentially identical match points each located approximately $\lambda_g/2$ from the central point.

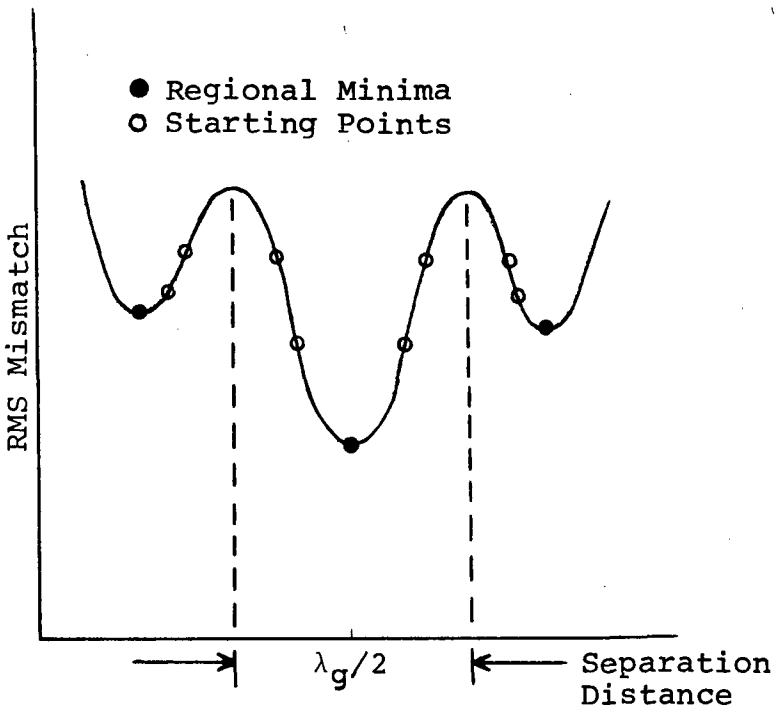

Figure 51. Schematic Plot of RMS Mismatch as a Function of Separation Distance L, Showing the Absence of Secondary Minima Within $\lambda_g/2$ Intervals Centered at Regional Minima, Initial Starting Position of Table 6 Are Sketched

Better RMS impedance matches are accomplished by placing the capacitive iris on the load side of the geometrical center of the slot. In fact, the lowest RMS impedance match is achieved by placing the capacitive iris approximately 0.03 centimeters on the generator side of the apparent electrical center of the slot.

In all of the broad band impedance matching done in this research, the best broad band matches were achieved with the matching element placed in the immediate vicinity of the

electrical center. This result is to be expected, since a large separation distance L between disturbance and matching element results in an interference pattern which is generally dominated by the exp(-j2βL) phase factor of Equation (III-49), and is narrow band in nature.

In Table 6 the starting positions of 0.5566, 0.0000, and -0.5566 centimeters results in an impedance match which places a capacitive iris of equivalent dimensions at practically the same location. The slight variation in the final location is due to the final increment size of the relative distance, ALENGH in the impedance matching program described in Appendix B. Starting positions of 1.6699 and 2.2265 centimeters in Table 6 result in the placing of an iris at the same location of approximately 2.18 centimeters resulting in an RMS mismatch of 0.105. This is not physically realizable, however, since the iris would be located in the slot. All other entries in Table 6 are physically realizable because they are either located at the apparent electrical location or 2.18 centimeters on the load side of the apparent electrical location. From Table 6 it is easily recognized that when impedance matching the slot by a capacitive iris, superior results are achieved by impedance matching in the vicinity of the electrical center. Table 6 agrees with Figure 51 and demonstrates the absence of large secondary minima within relative distances which are

multiples of $\lambda_g/2$.

Impedance Matching the Slot Radiator

For completeness the characteristics of the shunt slot radiator were impedance matched by each of the four matching elements at the apparent electrical location. Table 7 provides a tabulation of the calculated results of the slot relative to the apparent electrical location. The relative quality of the impedance match is indicated by the RMS mismatch achieved using each matching element. The physical dimensions of each matching element are given, and the placements toward the generator are given. The two best matches occur with the inductive metal post and the dielectric post with a dielectric constant of 4.07. The metal post located 1.175 centimeters toward the load matches the slot to an RMS mismatch of 0.056, Figure 52a. The dielectric post located 0.012 centimeters toward the load matches the slot to an RMS mismatch of 0.058, Figure 52b. From Figure 52a the resultant VSWR at 8.551 GHz is 1.177, and at the upper limit of the matching band, 10.560 GHz, it is 1.184. In all cases the slot radiator has been impedance matched over 2 GHz bandwidth, 8.551 GHz to 10.560 GHz. From Figure 52b the VSWR at 8.551 GHz is 1.09 and at the upper limit of the band, 10.560 GHz, it is 1.188. Both the metal inductive post and the dielectric post provide good impedance matches, less than 1.2 VSWR over the chosen 2 GHz bandwidth. It is interesting to note that the metal

inductive post matches the slot radiator to less than 1.23 VSWR over the entire band from 8.551 GHz to 11.934 GHz.

Table 7. Slot Radiator Impedance Matched by a Single Matching Element Referenced to the Apparent Electrical Center

Matching Element	RMS Mismatch	Physical Dimension	Physical Dimension	Distance Toward Generator in Centimeters
Capacitive Iris	0.063	0.095*	0.160**	0.025
Inductive Iris	0.072	0.051*	0.335**	1.187
Inductive Post	0.056	0.010+	0.315++	-1.175
Dielectric	0.058	0.297+	0.477++	-0.025

* Thickness in Centimeters
** Height in Centimeters
\+ Diameters in Centimeters
++ Sidewall Distance in Centimeters

The above results can be improved by use of the impedance matching program to successively match the slot with two elements. The slot is first matched with a single matching element, and the results of this impedance match are then recorded on data cards in the form of the complex reflection coefficient of the resulting mismatch. If the matching element is located on the load side of the distur-

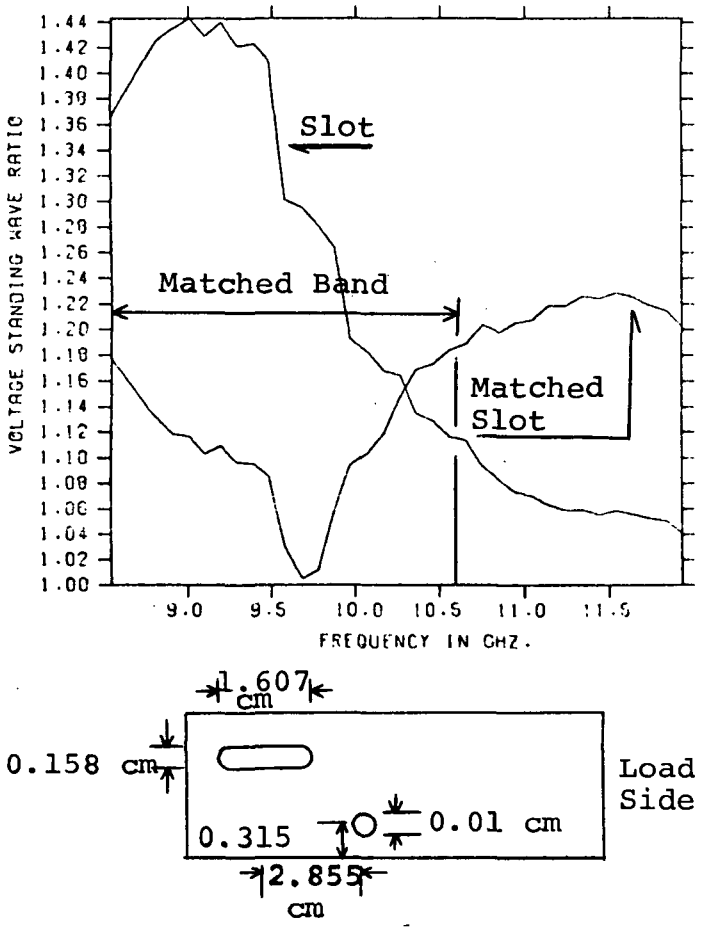

(a) Slot Matched by Metal Inductive Post

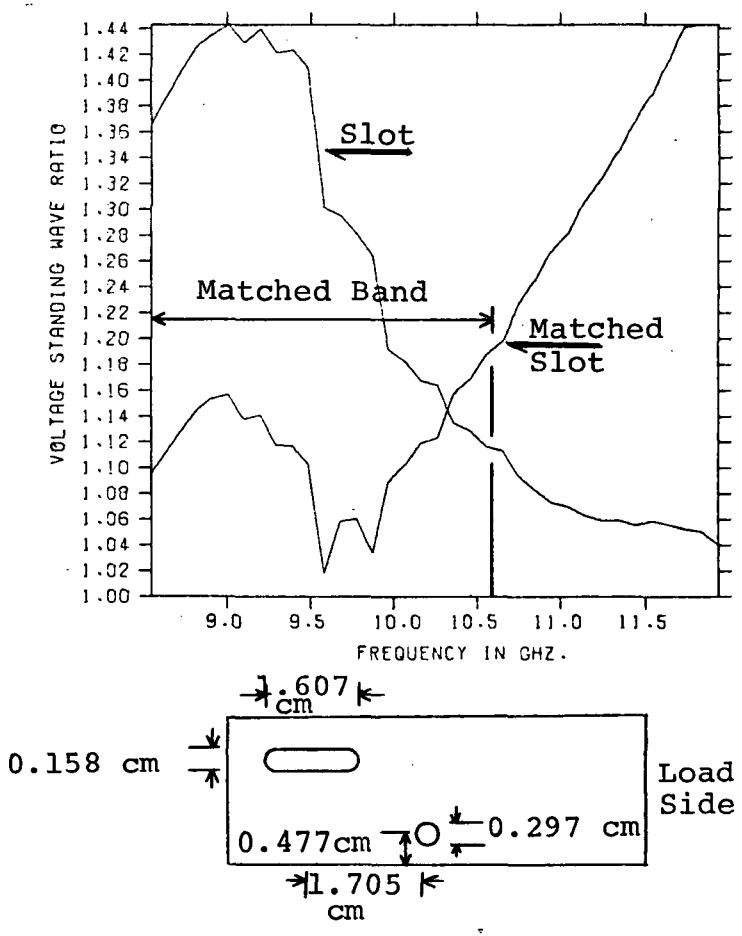

(b) Slot Matched by Dielectric Post

Figure 52. Slot Radiator Impedance Matched by (a) Metal Inductive Post (b) Dielectric Post

bance then the reference plane of the reflection coefficient of the resultant match is that of the original disturbance. When the matching element is located on the generator side of the disturbance, the reference plane of the resultant mismatch is that of the matching element.

The results of the first match are then used as data cards, i.e., the disturbance to be matched, and an additional matching element is calculated by the impedance matching program. Following this strategy, the results of the four impedance matches of Table 7 were matched with an additional element. The results of this impedance match are tabulated in Table 8 as the RMS mismatch over the 2.GHz bandwidth of interest. The element used to match the slot the first time is listed in the first column. The second matching element used is listed by the first row. For example the first number in the second column of numbers, 0.063 is the RMS mismatch resulting from matching the slot with both a capacitive iris and an inductive iris located in the guide. The first matching element is the capacitive iris and the second is the inductive iris. There are four combinations which produce good matches as seen in Table 8. These combinations are the inductive post-capacitive iris combination with an RMS value of 0.047, inductive post-inductive iris combination with an RMS of 0.056, inductive post-dielectric post combination with an RMS of 0.049 and dielectric post-capacitive iris combination with an RMS of

0.056.

Table 8. Slot Radiator Impedance Matched by Two Matching Elements

First Match \ Second Match	Capacitive Iris	Inductive Iris	Inductive Post	Dielectric Post
Capacitive Iris	xxxxx	0.063	0.093	0.061
Inductive Iris	0.071	xxxxx	0.078	0.072
Inductive Post	0.047	0.056	xxxxx	0.049
Dielectric Post	0.056	0.058	0.088	xxxxx

The curves of VSWR as a function of frequency are given for the above combinations in Figures 53, 54, 55 and 56, respectively. The relative location of the matching elements with respect to the slot is given by the (a) part of the respective figures, and the VSWR is given by the (b) part of the respective figures.

The dielectric post-capacitive iris matching combination was fabricated to compare the computer predicted resultant mismatch with an experimentally measured resultant mismatch. The boron nitride was machined into a post with a

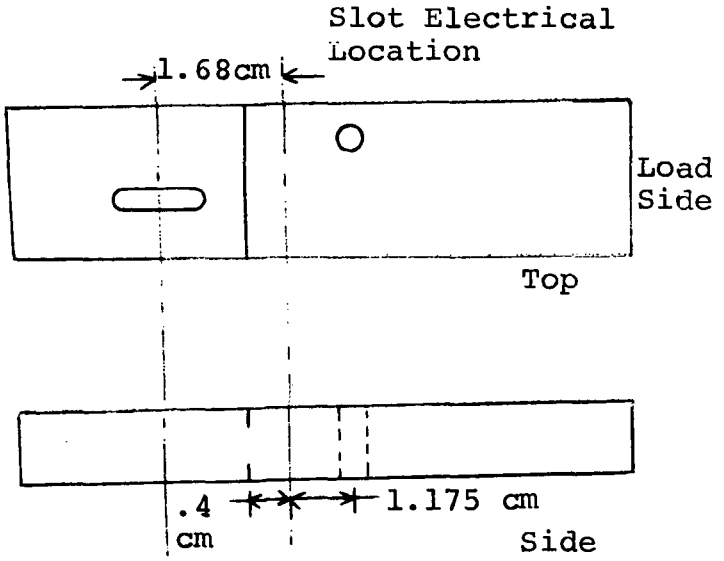

(a) Location of Matching Elements
Post Diameter = 0.01 cm
Post Sidewall Distance = 0.3150 cm
Iris Thickness = 0.120 cm
Iris Height = 0.060 cm

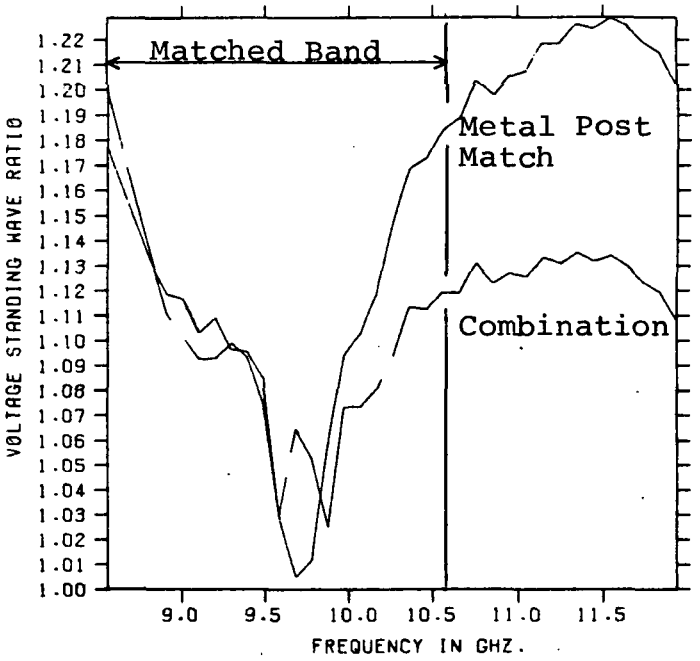

(b) Response of a Slot Matched by a Metal Post and by a Metal Post Capacitive Iris Combination

Figure 53. Shunt Slot Radiator Impedance Matched by a Metal Post and by a Metal Post-Capacitive Iris Combination

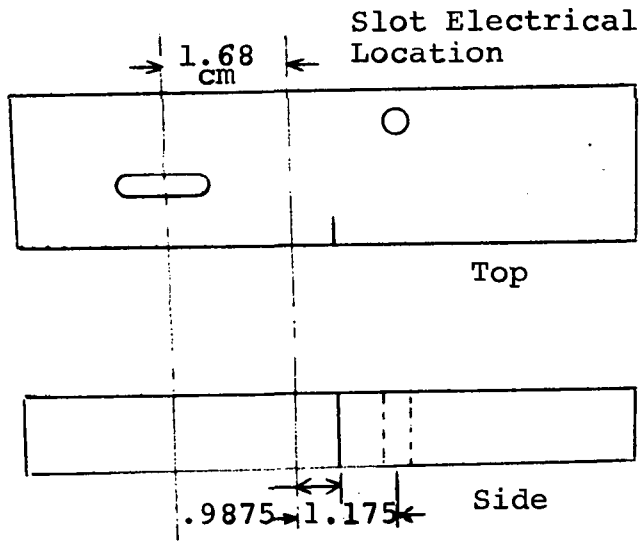

(a) Location of Matching Elements
Post Diameter = 0.01 cm
Post Sidewall Distance = 0.3150 cm
Iris Thickness = 0.0375 cm
Iris Height = 0.060 cm

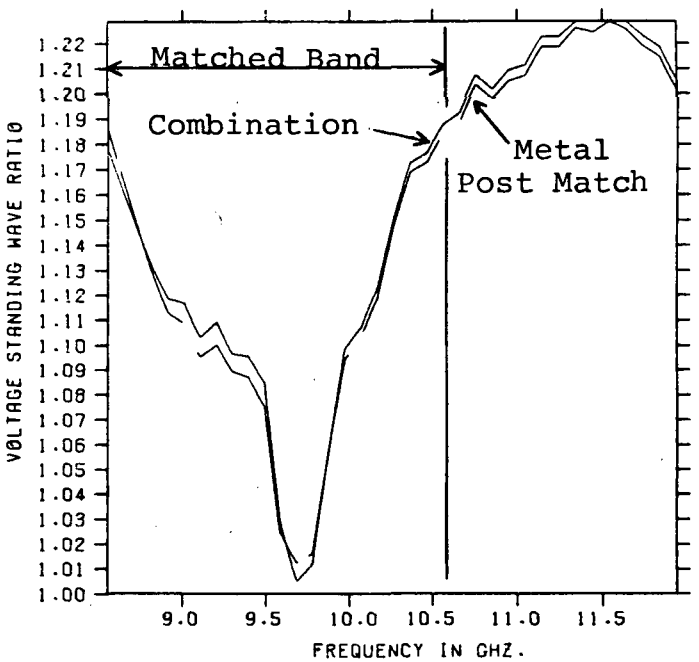

(b) Response of a Slot Matched by a Metal Post and by a Metal Post-Capacitive Iris Combination

Figure 54. Shunt Slot Radiator Impedance Matched by a Metal Post and by a Metal Post-Capacitive Iris Combination

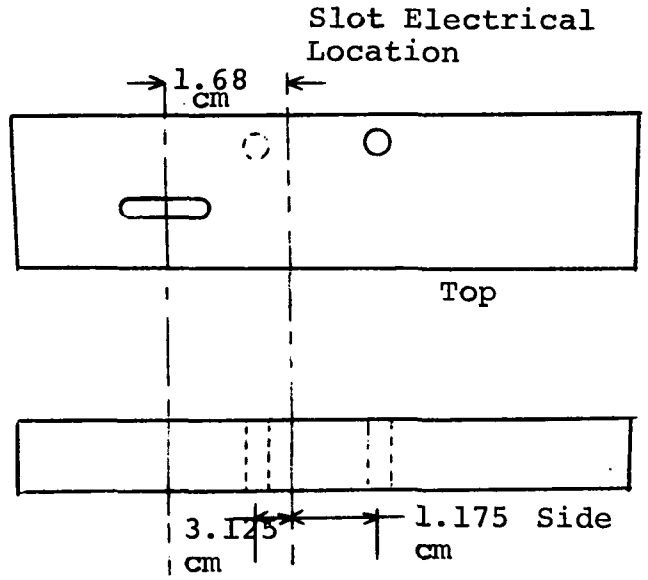

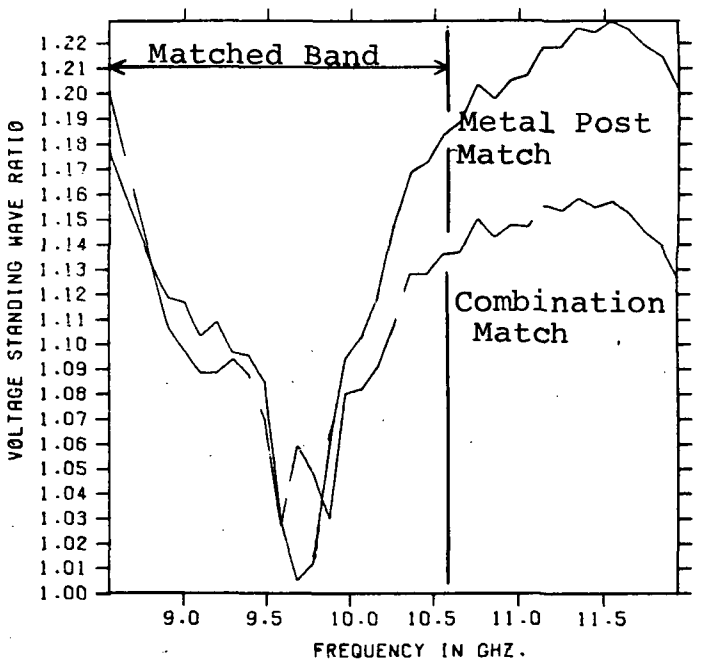

(a) Location of Matching Elements
Metal Post Diameter .01 cm
Dielectric Post Diameter .1538 cm
Metal Post Sidewall Distance .3150 cm
Dielectric Post Sidewall Distance .4637 cm

(b) Response of Slot Matched by a Metal Post and by a Metal Post-Dielectric Post Combination

Figure 55. Shunt Slot Radiator Impedance Matched by a Metal Post and by a Metal Post-Dielectric Post Combination

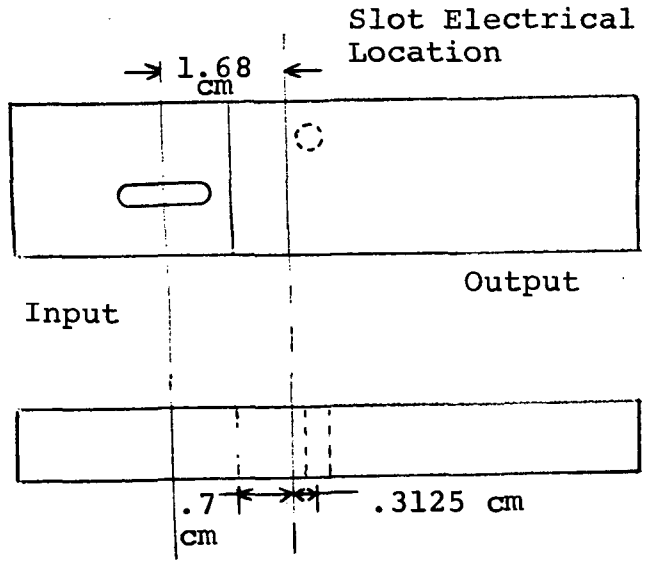

(a) Location of Matching Element
Dielectric Post Diameter .2975 cm
Dielectric Post Sidewall Distance = .4775 cm
Capacitive Iris Thickness .035 cm
Capacitive Iris Height .060 cm

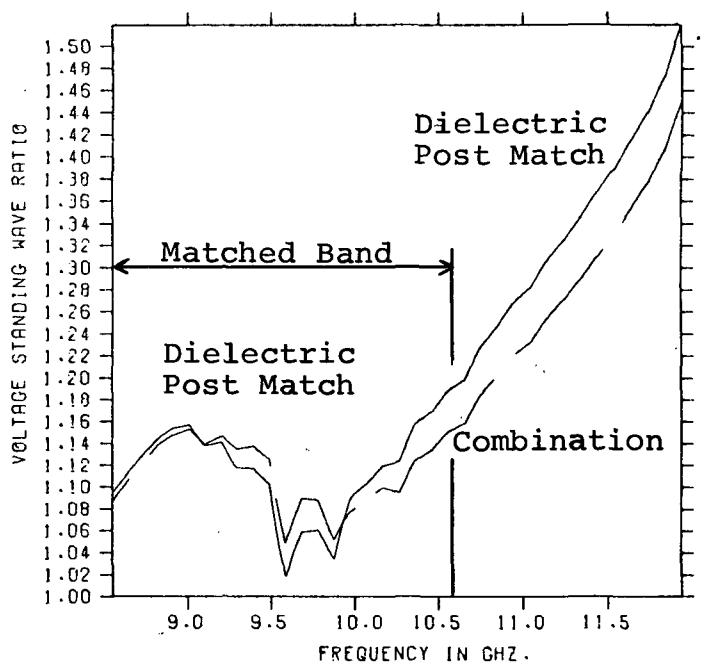

(b) Response of a Slot Matched by a Dielectric Post and by a Dielectric Post-Capacitive Iris Combination

Figure 56. Shunt Slot Radiator Impedance Matched by a Dielectric Post and by a Dielectric Post-Capacitive Iris Combination

diameter of 0.117 ± .002 inches and inserted between the walls of the waveguide to the position given in Figure 56. While the tolerance on the post location was difficult to measure, it is estimated to be within 0.002 inches of the desired location. The symmetrical capacitive iris was machined to fit two slots sawed through the broad side of the waveguide. The slots are 0.014 ±.002 inches wide and 0.074 ± .002 inches deep. The dielectric post was positioned in the guide, and the capacitive irises were fitted into the respective slots. A silver based conductive paint was painted on the outside wall of the waveguide over the ends of the irises and on the intersection of the iris and the inside waveguide walls.

The impedance matched shunt slot was then measured by the slotted line at 100 MHz intervals starting at 8.575 GHz through 10.875 GHz. The results of these measurements are tabulated in Table 9. The results are also given in Figure 57 where the calculated impedance match is plotted as a function of frequency and the measured results are plotted at discrete points. The excellent agreement displayed between the computer calculated VSWR and the experimentally measured VSWR, validate the impedance matching computer program and in turn the entire computer aided broad band impedance matching technique.

The Effect of Fabrication Tolerances

While mechanical tolerance is of little importance in

Table 9. VSWR Measurements of the Fabricated Impedance Matched Shunt Slot Radiator

Frequency in GHz	Measured VSWR
8.575	1.07
8.675	1.08
8.775	1.07
8.875	1.12
8.975	1.14
9.075	1.155
9.175	1.16
9.275	1.14
9.375	1.145
9.475	1.115
9.575	1.07
9.675	1.04
9.775	1.02
9.875	1.015
9.975	1.02
10.075	1.04
10.175	1.07
10.275	1.08
10.375	1.12
10.475	1.13
10.575	1.13
10.675	1.15
10.775	1.17
10.875	1.19

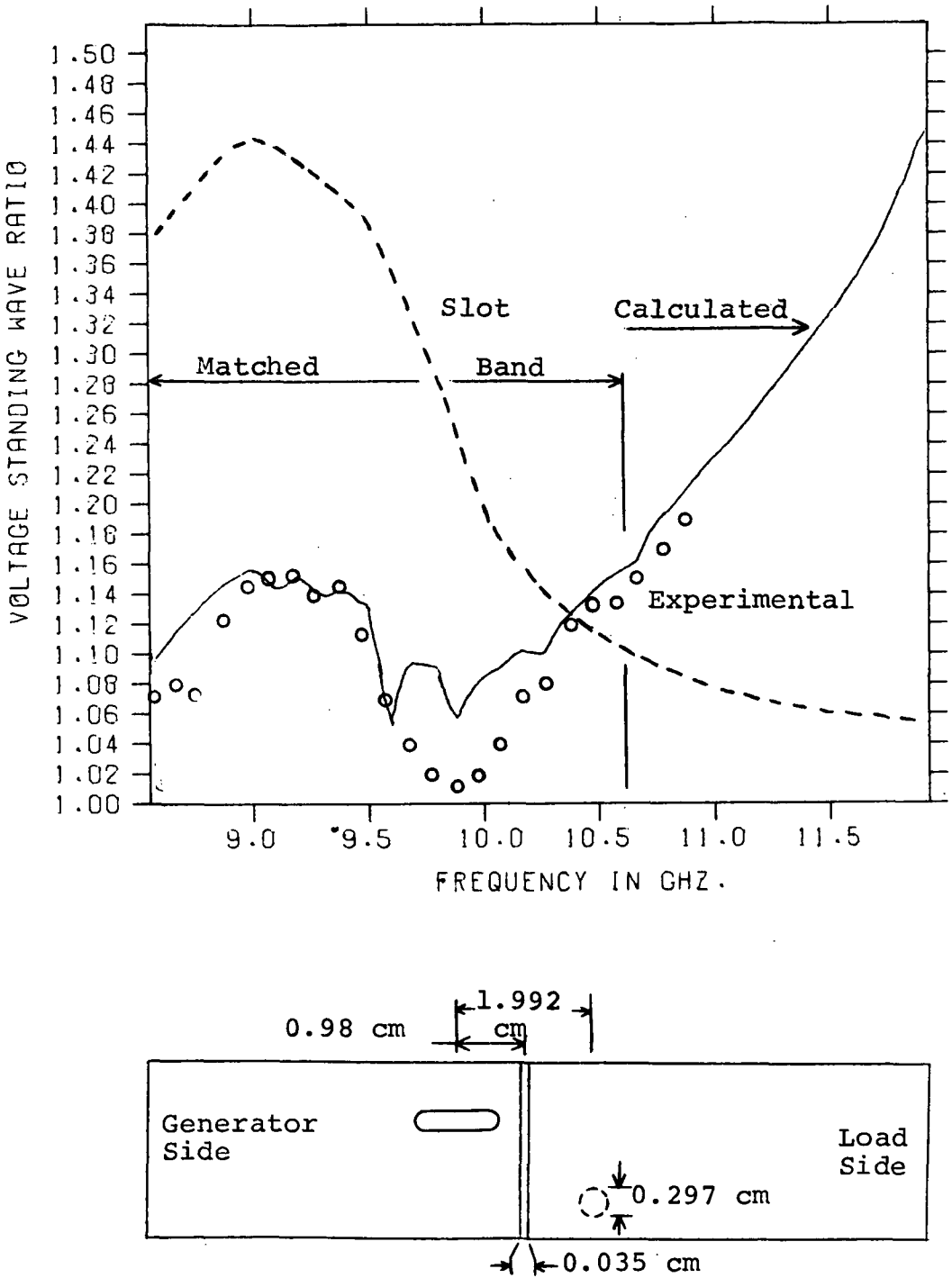

Figure 57. Comparison of Calculated Mismatch and Measured Mismatch

theoretical studies, the allowable tolerance greatly influences the cost of a practical device. Certainly the specified tolerances should depend on the effect of the dimensional variations on the resultant mismatch. This is true because generally closer tolerances increase the expense of fabrication.

In Table 10 the RMS mismatch values for the final nearest neighbor points for the slot impedance matched by a dielectric post are given. The final increment size for the sidewall distance of the dielectric post is 0.00125 centimeters, for the post diameter it is 0.00625 centimeters, and for the relative separation distance it is 0.0125 centimeters. Table 10 shows the variation in the RMS mismatch as a result of a change in a single dimension holding the remaining two dimensions equivalent to the LRMS or (1,1,1) point dimensions. Since the unequal increment sizes were selected so as to produce equivalent changes in RMS mismatch, it is difficult to determine the relative sensitivity of this mismatch to changes in a single parameter. Therefore, it is of further interest to examine the sensitivity of the LRMS mismatch as a function of equal increment variations of each physical dimension, since this sensitivity determines the importance of machining tolerances.

An examination of the effect of machining tolerances on the resultant mismatch was conducted in two steps. First the slot was theoretically impedance matched by a dielectric

Table 10. Final RMS Mismatch Values for the Nearest Neighbor Points of the Dimensional Space Array for the Case of the Slot Matched by a Dielectric Post

Coordinates* (I,J,K)	Sidewall Distance	Diameter	Separation Distance	RMS Mismatch
(1,1,1)	0.47750	0.29750	-0.0125	0.058713
(1,1,2)	0.47750	0.29750	-0.025	0.058813
(1,1,3)	0.47750	0.29750	+0.000	0.058982
(1,2,1)	0.47750	0.29125	-0.0125	0.058790
(1,3,1)	0.47750	0.30375	-0.0125	0.059385
(2,1,1)	0.47625	0.29750	-0.0125	0.058715
(3,1,1)	0.47875	0.29750	-0.0125	0.058717

* I Corresponds to sidewall distance of the dielectric post.

J Corresponds to diameter of the dielectric post.

K Corresponds to relative separation distance.

post with various dimensions. The dimensions consisting of the optimum dimensions determined by the impedance matching program and variations of these dimensions by four thousands of an inch. Because the diameter of the post is the easiest dimension to machine to ± 0.001 inches, the diameter was held constant and the sidewall distance and relative distance between disturbances was varied. The dielectric post material used is boron nitride grade HD-0092 hot pressed. The average reflection coefficient over the 2.GHz bandwidth from 8.551 to 10.560 GHz was used to compare the quality of the resulting matches obtained. Table 11 gives a tabulation of the dimensional combinations used and the average theoretical reflection coefficient obtained. From Table 11 the largest average matched reflection coefficient 0.0544 has a corresponding diameter of 0.2975 centimeters, sidewall distance of 0.4673 centimeters, and a relative displacement of 0.0023 centimeters. This combination will be retained and used in the next step of the perturbation examination, since the strategy is to obtain an indication of the worst effect of tolerances.

The second phase of this examination consists of using the combination of dimensions which produce the largest average matched reflection coefficient and performing a second match on this result using a capacitive iris as the matching element. The effect of tolerances is studied by varying the capacitive iris height and relative distance

from the first match determined in the first step of this study. The thickness of the capacitive iris is held constant in this study since this is generally determined by a commercially available shim stock and the match is relatively insensitive to ± 0.002 inch variation. The physical dimensions used for the capacitive iris are iris thickness 0.0350 centimeters, iris height 0.060 ± .01016 centimeters and iris distance from electrical location of slot 0.70 ± .01016 centimeters. Table 12 illustrates the average total matched reflection coefficient and the respective physical dimensions.

Table 11. Average RMS Mismatch Over the Band of 8.55 GHz to 10.56 GHz Resulting from the First Phase of the Machining Tolerance Study, Dielectric Post Diameter = 0.2975 Centimeters, $\varepsilon' = 4.07$

Relative Displacement* / Sidewall Distance*	-0.0023	-0.0125	-0.0227
0.4673	0.0544	0.0537	0.0533
0.4775	0.0542	0.0536	0.0532
0.4877	0.0542	0.0535	0.0532

*In Centimeters

Table 12. Average RMS Mismatch Over the Band of 8.55 GHz to 10.56 GHz Resulting from the Second Phase of the Machining Tolerance Study, Capacitive Iris Thickness = 0.0350 Centimeters

Iris Height* \ Relative Displacement*	0.6898	0.7000	0.7101
0.0498	0.058	0.057	0.054
0.0600	0.055	0.054	0.054
0.0701	0.055	0.055	0.055

*In Centimeters

The largest mismatch listed in Table 12 results from the capacitive iris dimensions of iris thickness 0.0350 centimeters, iris height 0.0498 centimeters and relative displacement 0.6898 centimeters. Figure 58 gives curves of the first impedance match by the dielectric post resulting in an average mismatch reflection coefficient of 0.054 and the results of matching the first match by a capacitive iris giving an average reflection coefficient of 0.058.

It is interesting to note that while the dielectric post-capacitive iris combination match has a higher average reflection coefficient than the dielectric post match, the combination match is a better broad band match over a larger bandwidth of interest.

From Table 11 the most sensitive dimension to change

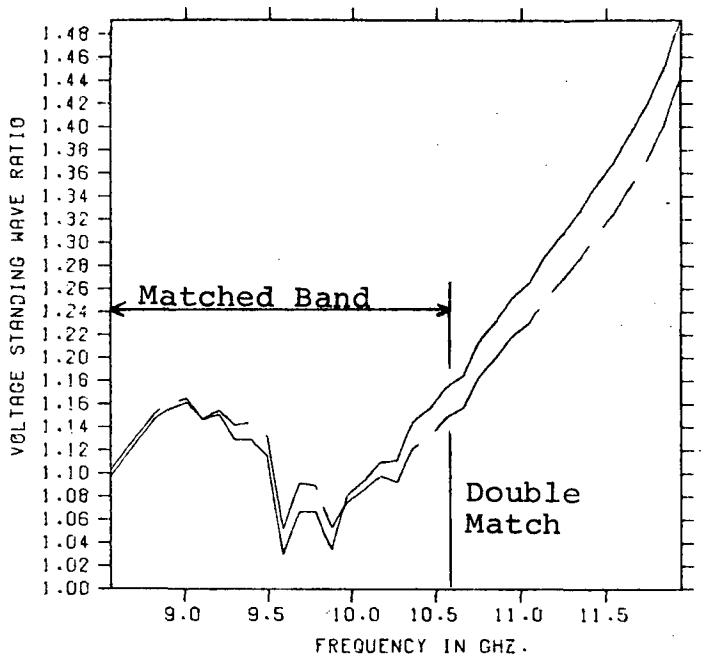

Figure 58. Comparison of the VSWR of a Slot Radiator Impedance Matched by a Dielectric Post and by a Dielectric Post-Capacitive Iris Combination

is the relative distance along the waveguide. In the second row first column of numbers in Table 11 the relative displacement is -0.0023 centimeters, that is, 0.0023 centimeters toward the load from the electrical location of the slot radiator. The average reflection coefficient is 0.054. From Table 12 the most sensitive parameter is the iris height. In the second row of numbers, reducing the iris height to 0.0498 centimeters increases the average reflection coefficient to 0.0579. Therefore, close tolerances are indicated for the relative distance between the dielectric post and the electrical location of the slot radiator.

Close tolerances are also indicated for the capacitive iris height. However, the overall results indicate that the entire matching process is relatively insensitive to machining tolerances of ± 4 thousanth of an inch or ± 0.01016 centimeters.

CHAPTER VI

CONCLUSIONS AND RECOMMENDATIONS

Introduction

Several important conclusions can be drawn as a result of this study. They deal with the experimental equipment and with the computer aided matching program. The following paragraphs highlight these conclusions

Conclusions

As a result of this research, an economical, fast, and reliable impedance matching technique has been established which can provide broad band impedance matches.

The measured results of the comparison reflectometer in resolving waveguide disturbances and in the determination of their complex reflection coefficients have been excellent. Reflectometer measurements have been compared with both theoretical calculations and slotted line measurements.

Measurements of the sample waveguide discontinuities have pointed out the difference in the apparent electrical location and the geometrical location. While the two locations were closely spaced for the inguide disturbances, measured as described in Chapter V, there was a considerable difference in the locations for the shunt slot radiator. The shunt slot radiator was impedance matched relative to

the apparent electrical location both theoretically and experimentally over a 2 GHz bandwidth as shown in Figure 56. The excellent agreement between the theoretical and experimental impedance matches demonstrates the validity of this research.

The impedance matching computer program demonstrated an ability to calculate the physical dimensions of a predetermined matching element in order to achieve an impedance match which is best over a specified bandwidth in the RMS mismatch sense, Chapter III.

It has been shown that the computer matched solutions are relatively free of secondary RMS minima. Regional minima are found at intervals of approximately half guide wavelength separations between the measured disturbance and the matching element, described in Chapter V, Table 6.

For the cases investigated the impedance match improved in the vicinity of the apparent electrical center of the test disturbance. The shunt slot radiator was impedance matched to a VSWR of 1.16 to 1.0 over a 2 GHz bandwidth. This match was fabricated to demonstrate the validity of the impedance matching program. The agreement between the predicted and measured results for the matched slot was very good.

It was found that while machining tolerances affect the calculated impedance match, for a reasonably good

matching tolerance of ± 0.002 of an inch the results are relatively insensitive. This conclusion increases the practical significance of this research, by providing a technique that is practically realizable.

Recommendations

There are several areas in which this research can be extended. Extension of the theory of the comparison reflectometer, to enable it to measure larger disturbances, both in magnitude of reflection coefficient and in physical length, can be made. The impedance matching computer program can be extended by both adding additional matching elements and enabling the program to calculate the location and physical parameters of more than one matching element simultaneously. A modification of the matching criterion could be implemented. The program could also be extended to select the most favorable type of matching element.

Extending the Comparison Reflectometer

The comparison reflectometer fabricated for this research is capable of locating disturbances resulting in reflection coefficients less than or equal to 0.2. This limitation is in part due to the approximations made in the development of the theory and in part due to the reference step fabricated, since the development assumes that the tested reflection coefficient does not exceed the reference reflection coefficient. Secondly an equipment limitation is present in the

ratio meter used. The combined magnitude of the reflection coefficient of the reference step and the test disturbance of 0.2 reflection coefficient results in a full scale deflection of the ratio meter. Measuring reflection coefficients greater than 0.2 would result in off scale deflections. For single frequency measurements the range of the ratio meter may be adjusted to prevent overdriving the unit. This is not possible in the comparison reflectometer system, however, since the two sets of measurements taken are compared to reduce instrumental errors.

The length of line which can be measured is dependent on the sample intervals. At present the comparison reflectometer is phased locked, and a sample is taken every 50 MHZ. As such, the approximate limit on the line length measured is one meter. This can be increased to 5 meters by phase locking and taking a reading every 10 MHz. The closer the samples are taken in the wavenumber domain the greater the relative allowable distance between the reference step and test element.

The Impedance Matching Program

The impedance matching program was developed to match an arbitrary waveguide element as measured by the comparison reflectometer. The impedance match is performed by calculating the physical dimensions of a single preselected matching element. The criterion used by the matching program is the LRMS reflection coefficient resulting from the combined

wave reflected by the disturbance and the matching element.

It may be desirable in some applications to use a maximum point VSWR criterion. That is, the matching program determines the maximum VSWR over the matching bandwidth for each of the dimensional space nearest neighbor points. The point selected as the (1,1,1) point would be that nearest neighbor point which has the smallest maximum VSWR.

The matching program could also be extended to automatically select an element among the programmed matching elements which would provide the best broad band impedance match. This could be accomplished by assuming a broad band match and solving Equation (III-49) for the complex reflection coefficient of the required matching element. The prospective matching element that compares most favorably with the required complex reflection coefficient could then be selected. This selection could be made by loosely comparing the slope and phase of each available matching element with the necessary characteristics calculated from Equation (III-49).

The function of the matching program implemented in this work is to minimize the VSWR resulting from the test element and a single matching element using the RMS criterion. To this end the program functions properly. In some cases it is important to achieve a lower VSWR mismatch than is obtainable with the programmed matching ele-

ments. For these cases it is desirable to use two or more matching elements to achieve the desired impedance match. This, in fact, has been demonstrated in Chapter V when matching the shunt slot radiator.

It is important to recognize that the first impedance match using a dielectric post was calculated as the LRMS over the selected 2 GHz bandwidth, subject to increment size. The result of the procedure was then improved upon by the capacitive iris by again impedance matching this initial result using the LRMS criterion. The slot and two matching elements are not a true optimum, however, since the two matching elements were not determined simultaneously.

To demonstrate that a lower overall reflection coefficient is possible, the mismatch resulting from the dimensional combinations of Table 11 were used as the input data to the impedance matching program. A capacitive iris was sized for each case providing an LRMS mismatch. The results of this study are given in Table 13. The first row listed in Table 13 corresponds to the original combination of Figure 55a. This is also the combination of elements which has been fabricated, and a comparison of theoretical and experimental results are shown in Figure 56. There are six combinations in Table 13, resulting from perturbations of the dielectric post, which provide a lower RMS mismatch than that originally obtained. A comparison of the response of the initial combination and the combina-

tion of matching elements resulting in an RMS mismatch of 0.054 is given in Figure 59.

While the improvement observed is small it must be remembered the dimensional changes were constrained to be small. The results do indicate clearly that if more than one element is needed to provide a desired broad band impedance match an extension of the program to simultaneously adjust more than one element would be desirable.

Table 13. RMS Mismatch Using a Capacitive Iris as the Second Matching Element

RMS Mismatch	Iris Thickness	Iris Height	Relative Distance from Electrical Center
0.056	0.0350	0.0600	0.7000
0.055	0.0575	0.0600	0.6875
0.056	0.0300	0.0600	-0.6275
0.055	0.0512	0.0600	0.7625
0.057	0.0412	0.0538	0.6375
0.054	0.0737	0.0600	0.7375
0.056	0.0400	0.0600	-0.6875
0.056	0.0450	0.0600	0.6125
0.057	0.0300	0.0600	-0.5625

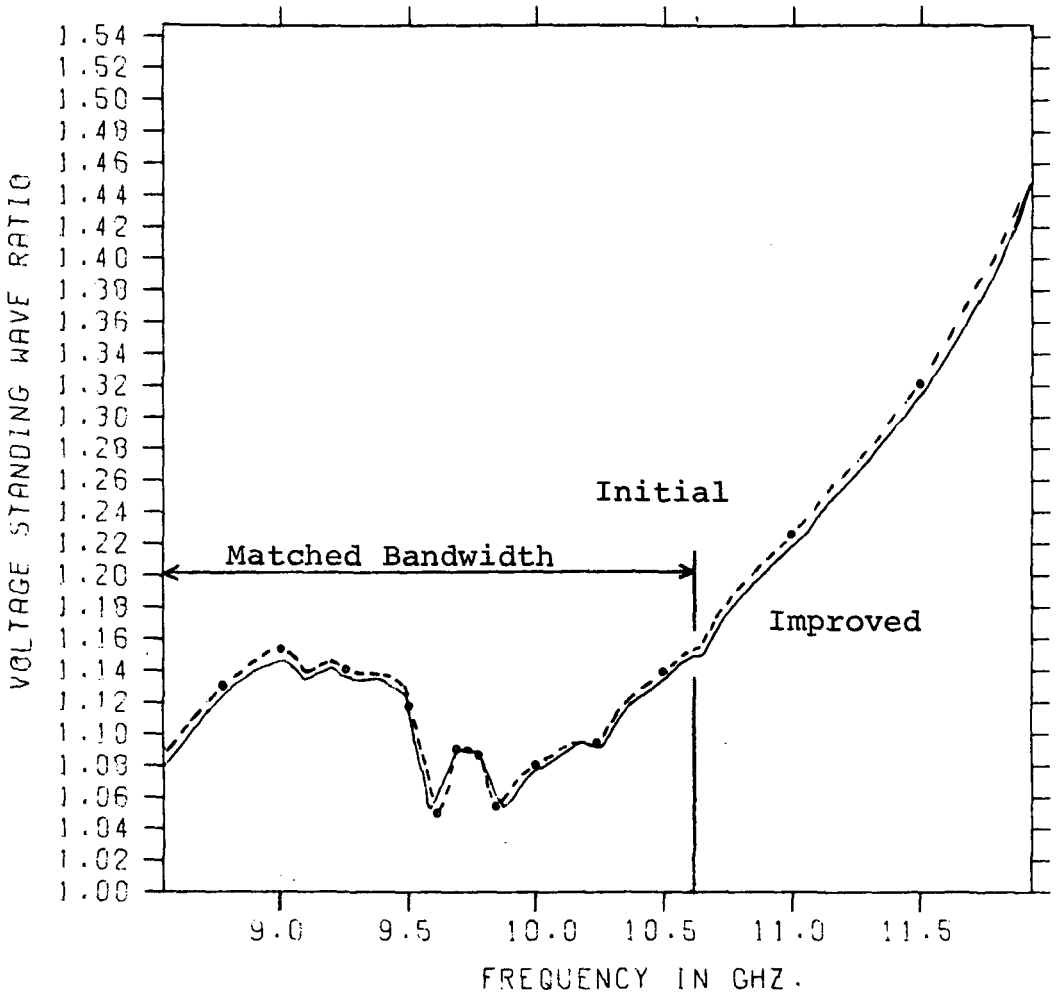

Figure 59. Comparison of Initial and Improved VSWR

APPENDICES

APPENDIX A

LIBRARY OF THE CHARACTERISTICS OF SELECTED MATCHING ELEMENTS

The following families of curves are included to provide engineering insight into the type of response associated with each element. Curves also indicate the dependence on parameters of the discontinuity.

The families of curves provide the current reflection coefficient and the normalized shunt admittance as a function of physical dimensions and frequency, for the capacitive iris, the inductive iris, the solid metal inductive post and the dielectric post located in an otherwise matched waveguide. A waveguide description and an equivalent circuit are given for each type of discontinuity.

The following results are based on an evaluation of the respective equations given by N. Marcuvitz,[13] and reproduced in Chapter III, Equations (34) to (48). The following curves were calculated for propagation in rectangular waveguide with a width a = .9 inches and height b= .4 inches.

A typical discontinuity of each type was fabricated and its characteristics measured. A comparison of the evaluation of Equations (III-34) to (III-48) for the respective physical parameters, Chapter V, Table 2, shows good agreement with the results measured by the compari-

son reflectometer, as described in Chapter V. All curves given apply to the admittance Smith chart plot.

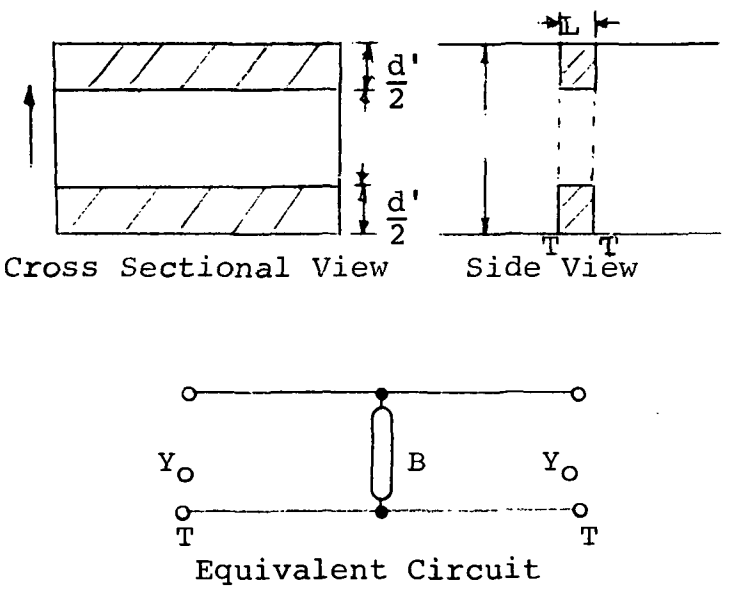

(a) Capacitive Iris

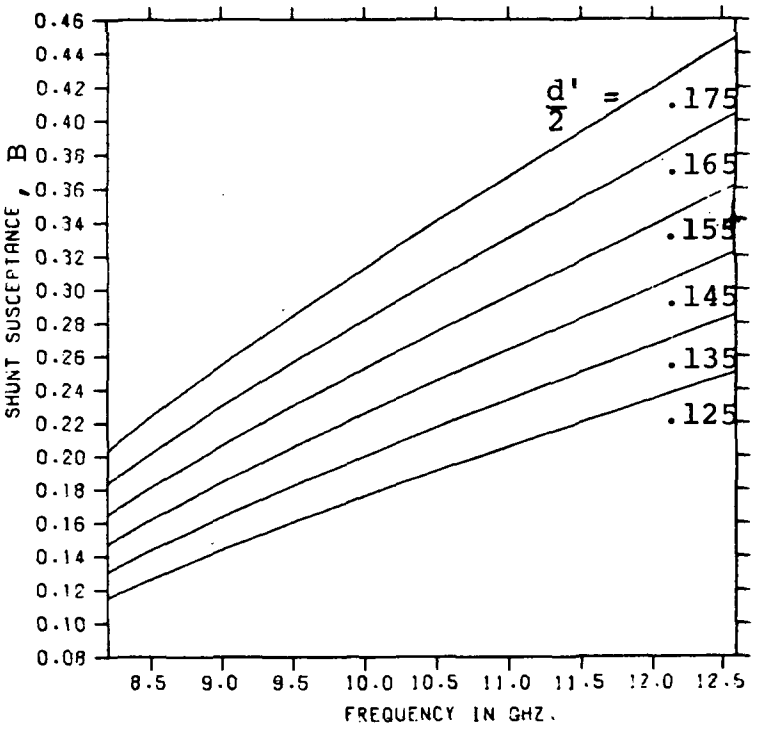

(b) L = .1 cm

Figure 60. Capacitive Obstacle of Finite Thickness, Shunt Susceptance with a Fixed Thickness = .1 cm, Varying Iris Height $\frac{d'}{2}$ in cm

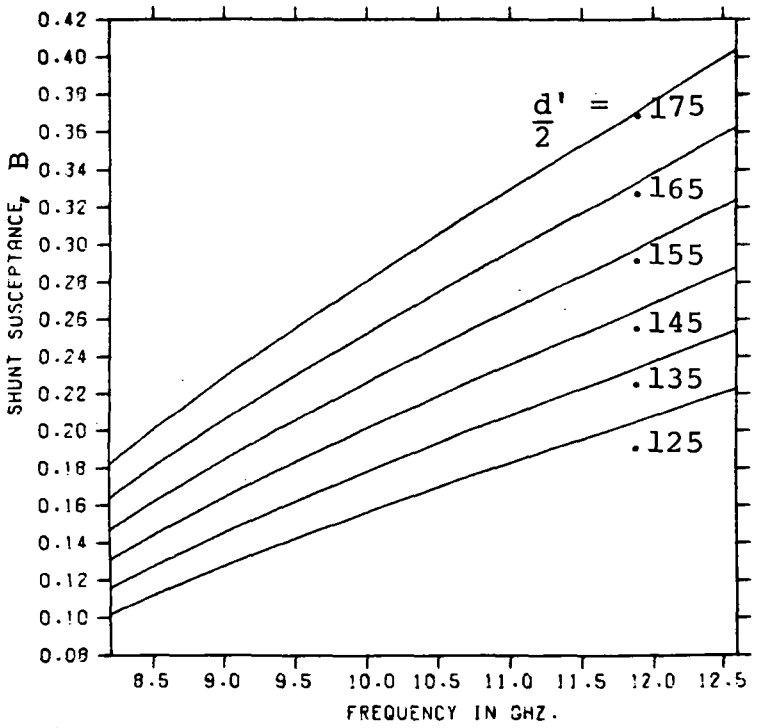

(a) L = .075 cm

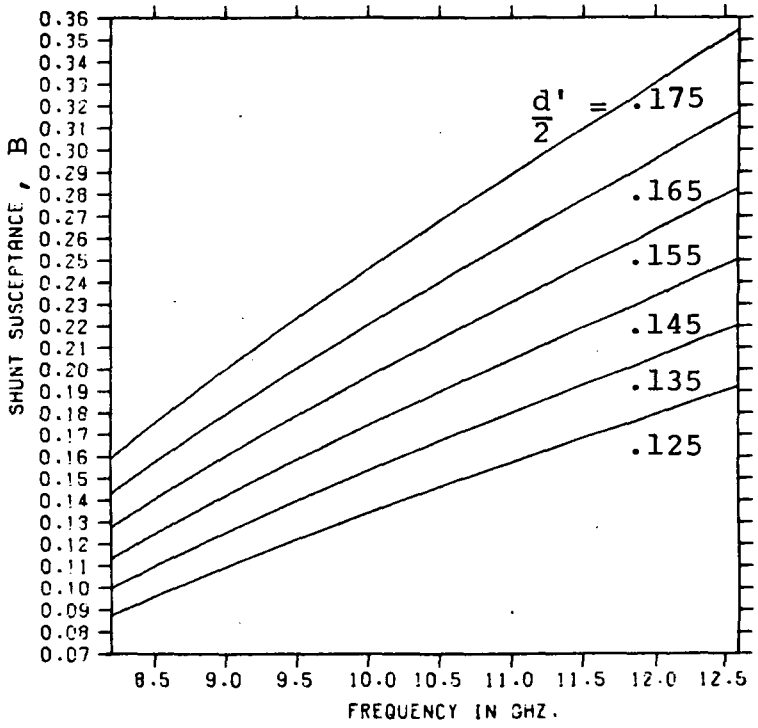

(b) L = .05 cm

Figure 61. Capacitive Obstacle of Finite Thickness, Shunt Susceptance with a Fixed Thickness L, Varying Iris Height $\frac{d'}{2}$ Centimeters

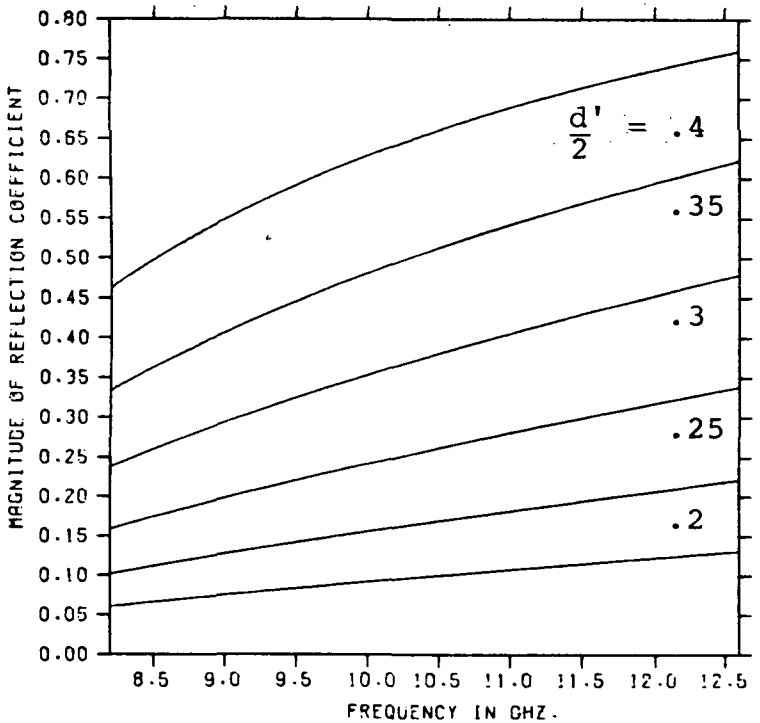

(a) Magnitude
L = .05 cm

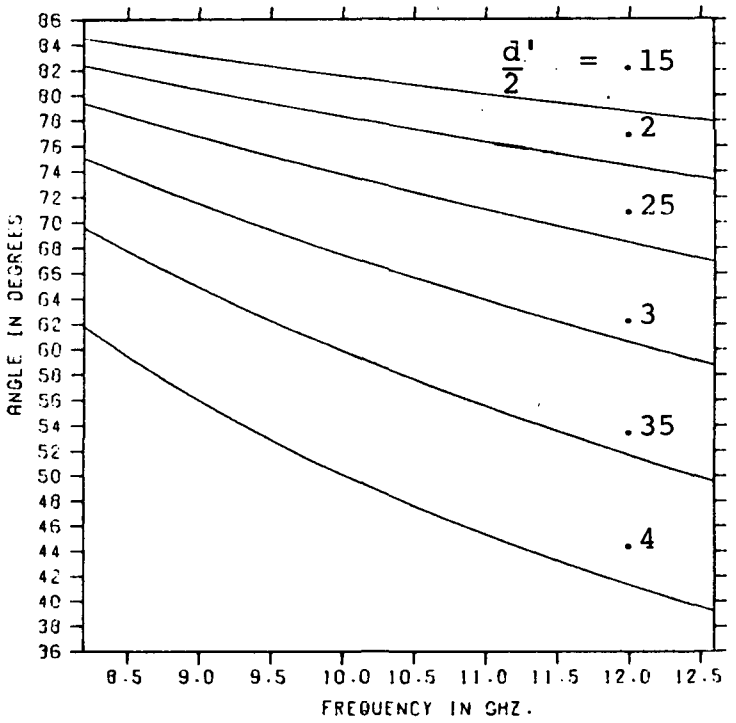

(b) Phase
L = .05 cm

Figure 62. Magnitude and Phase of the Current Reflection Coefficient of a Capacitive Iris, Thickness of .05 cm Varying Height in Centimeters

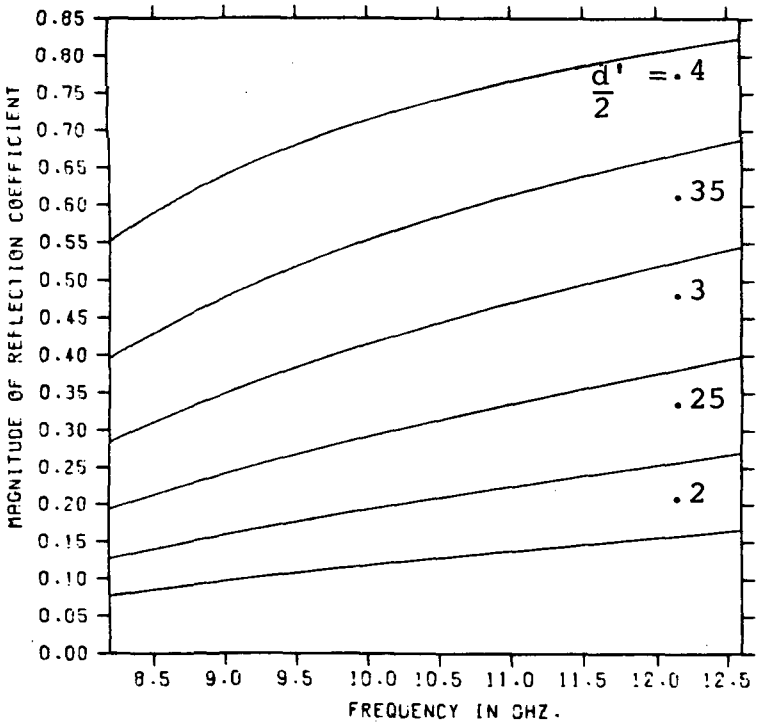

(a) Magnitude
L = .1 cm

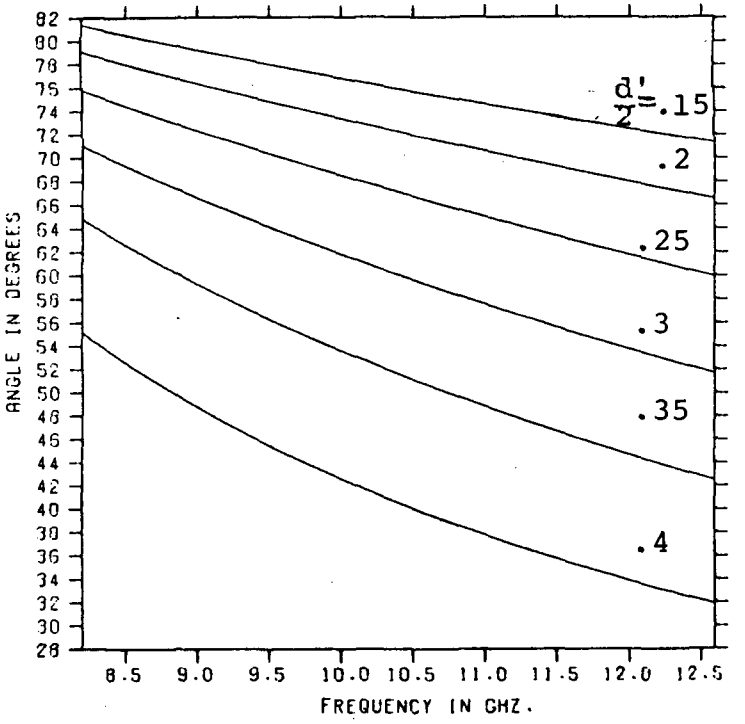

(b) Phase
L = .1 cm

Figure 63. Magnitude and Phase of the Current Reflection Coefficient of a Capacitive Iris, Thickness of .1 cm Varying Height in Centimeters

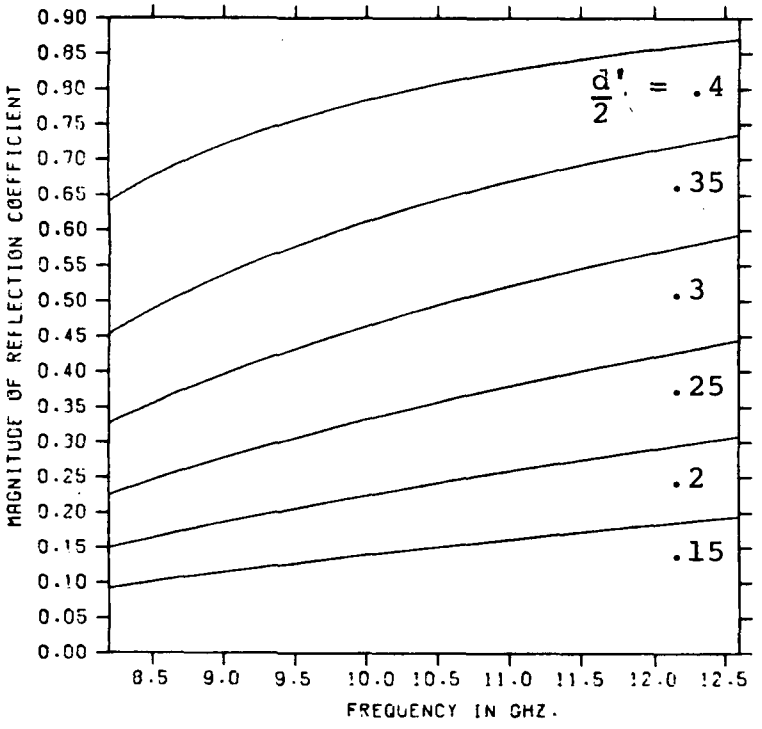

(a) Magnitude
L = .15 cm

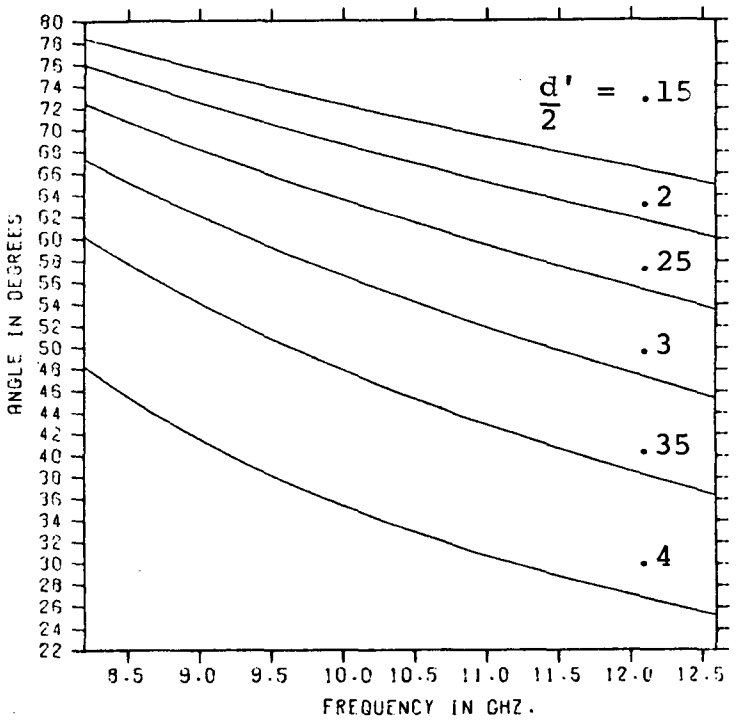

(b) Phase
L = .15 cm

Figure 64. Magnitude and Phase of the Current Reflection Coefficient of a Capacitive Iris, Thickness of .15 cm Varying Height in Centimeters

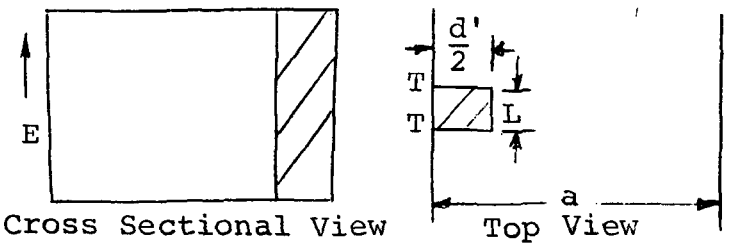

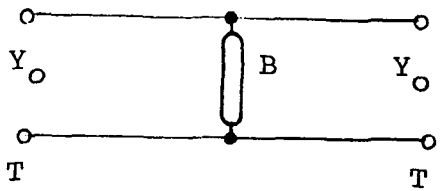

Equivalent Circuit

(a) Asymmetrical Inductive Iris

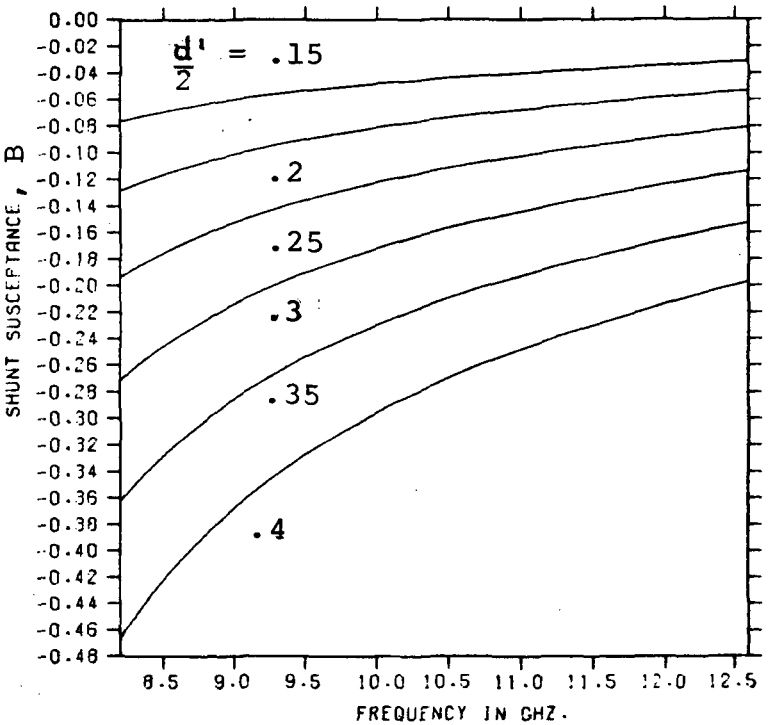

(b) L = .05 cm

Figure 65. Inductive Iris of Finite Thickness, Shunt Suspectance with Fixed Thickness L. Varying Height $\frac{d'}{2}$ in Centimeters

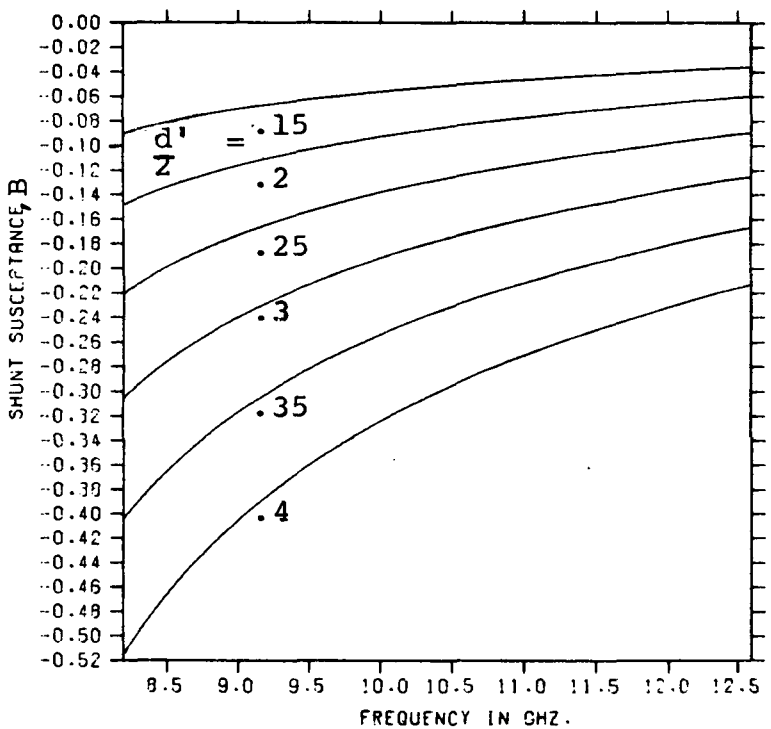

(a) L = .15 cm

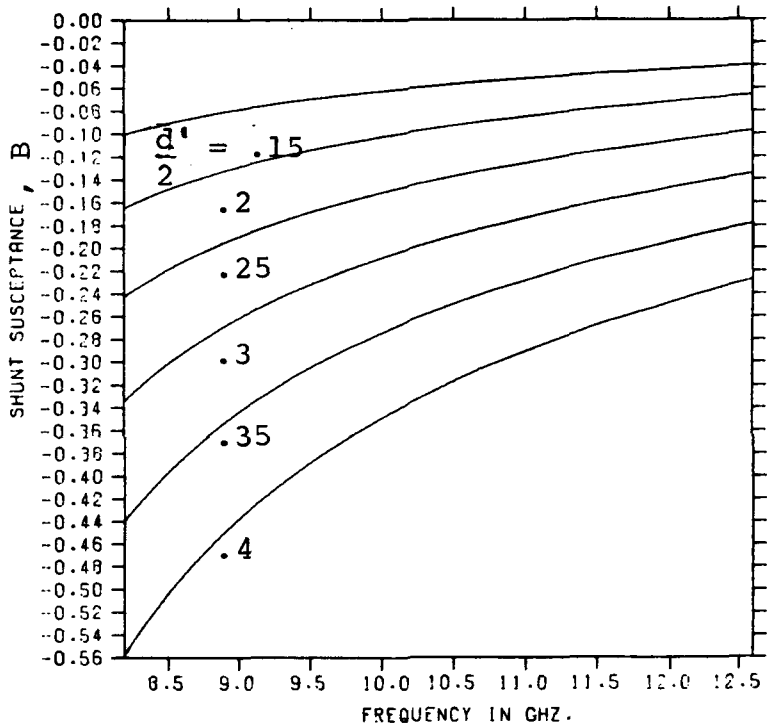

(b) L = .15 cm

Figure 66. Inductive Iris of Finite Thickness, Shunt Susceptance with Fixed Thickness L. Varying Height d'/2 in Centimeters

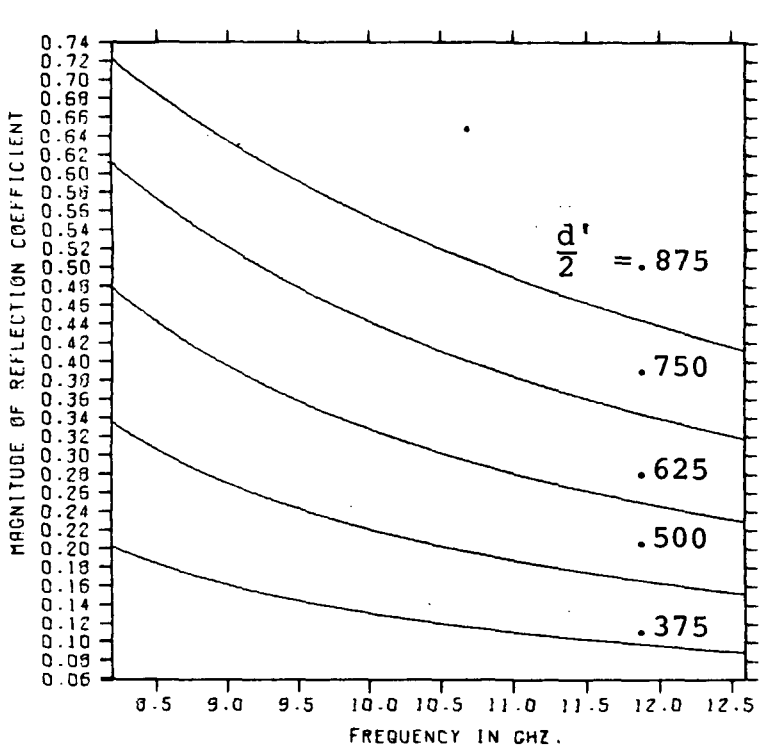

(a) Magnitude
L = .05 cm

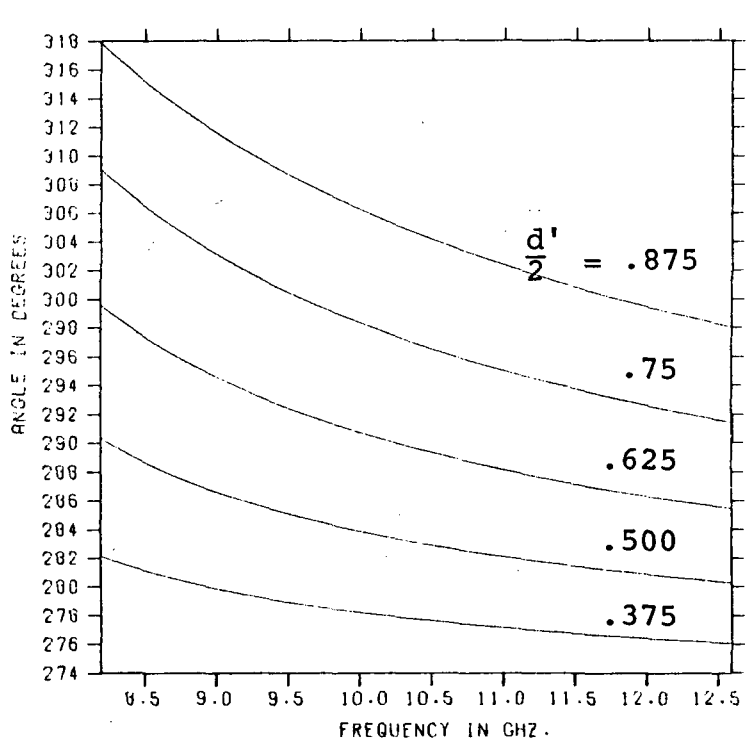

(b) Phase
L = .05 cm

Figure 67. Magnitude and Phase of the Current Reflection Coefficient of a Inductive Iris, Thickness of .05 cm, Varying Height in Centimeters

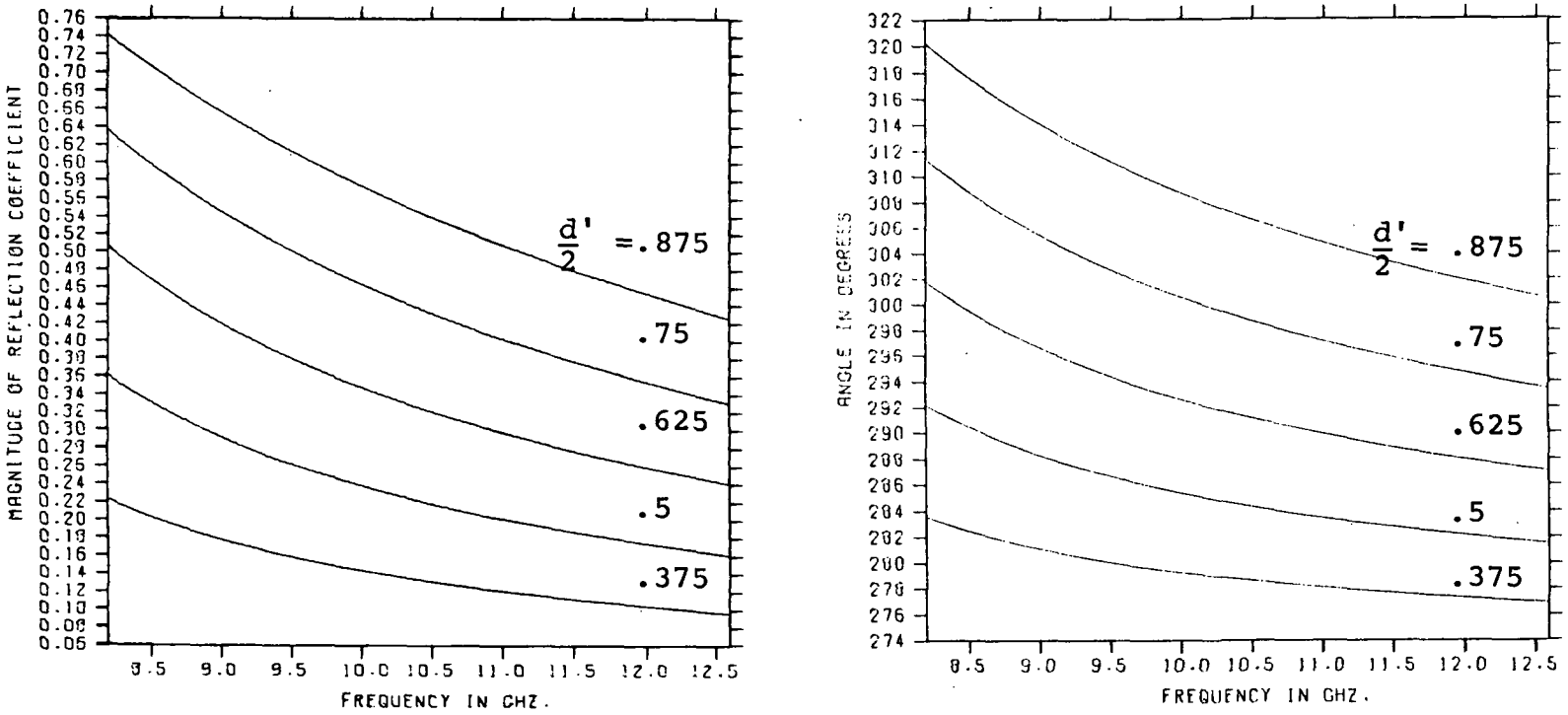

(a) Magnitude
L = .1 cm

(b) Phase
L = .1 cm

Figure 68. Magnitude and Phase of the Current Reflection Coefficient of an Inductive Iris, Thickness of .1 cm, Varying Height in Centimeters

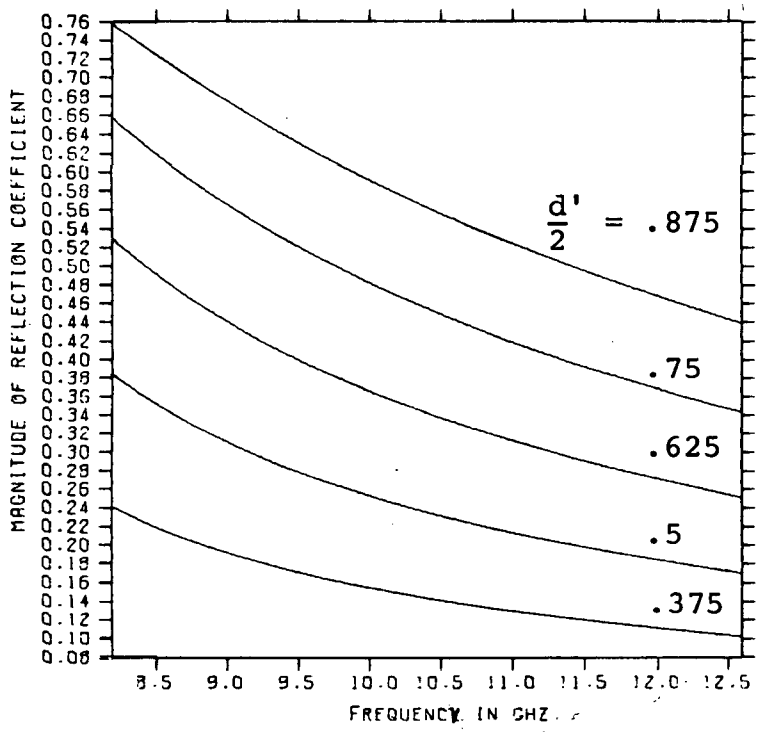

(a) Magnitude
L = .15 cm

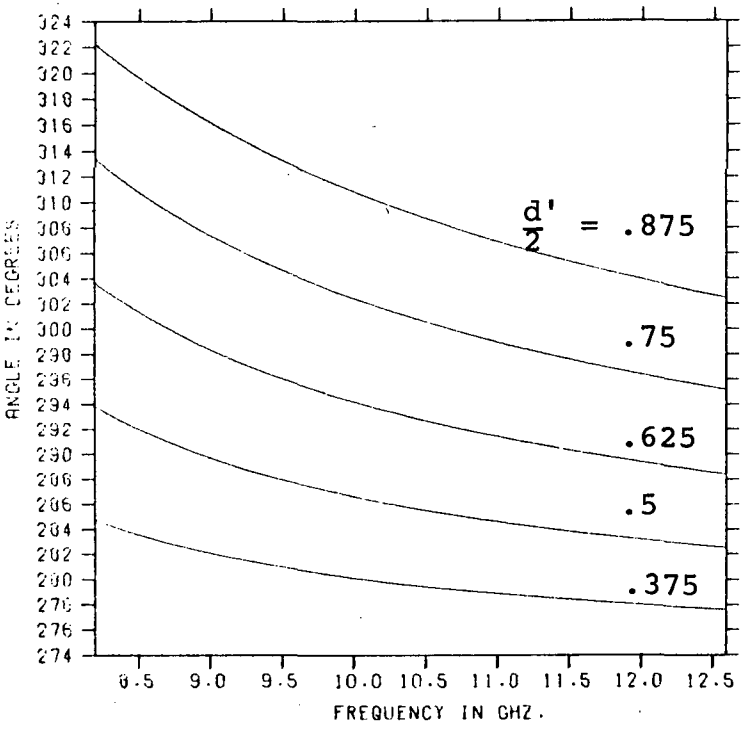

(b) Phase
L = .15 cm

Figure 69. Magnitude and Phase of the Current Reflection Coefficient of an Inductive Iris, Thickness = .15 cm, Varying Height in Centimeters

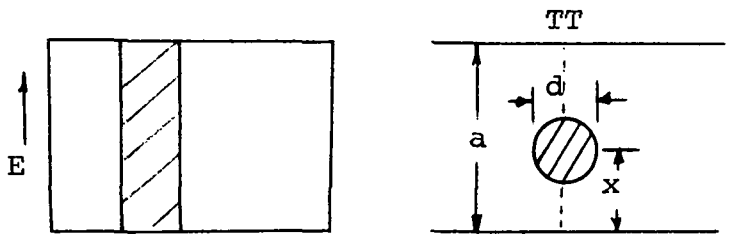

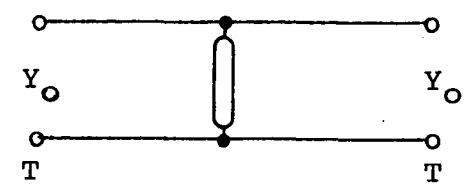

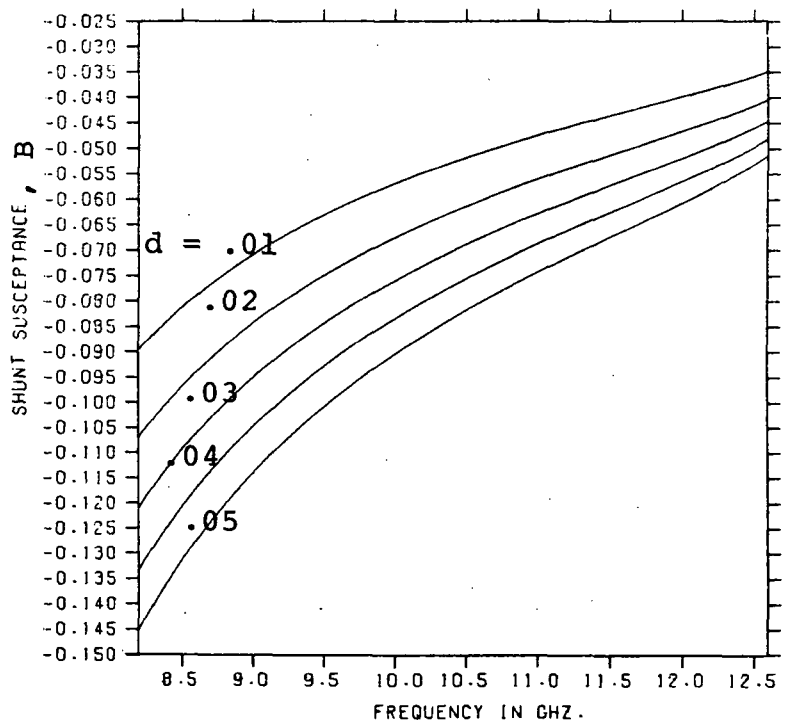

(a) Metal Inductive Post

(b) x = .20 cm

Figure 70. Metal Inductive Post, Shunt Susceptance with a Fixed Sidewall Distance, Varying Diameter of the Post

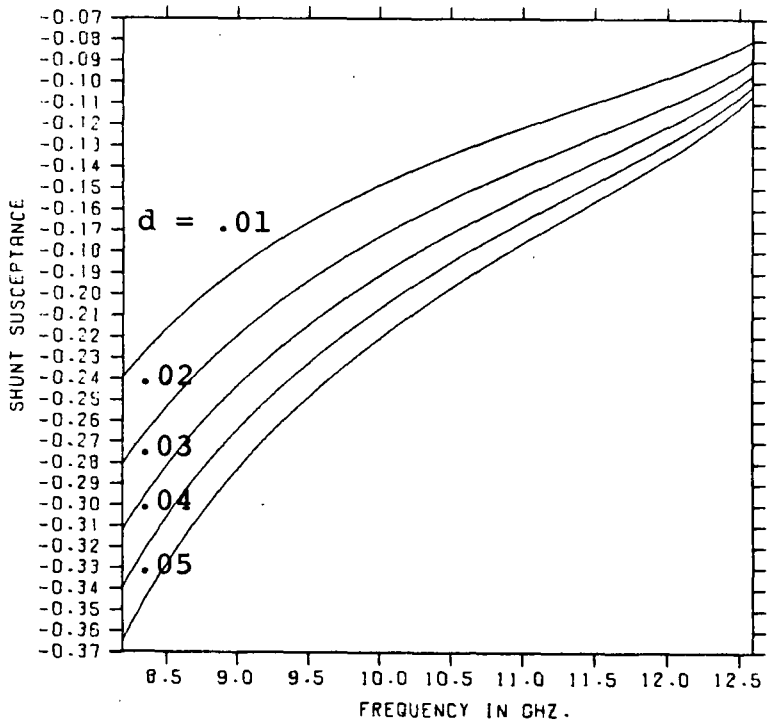

(a) x = .350 cm

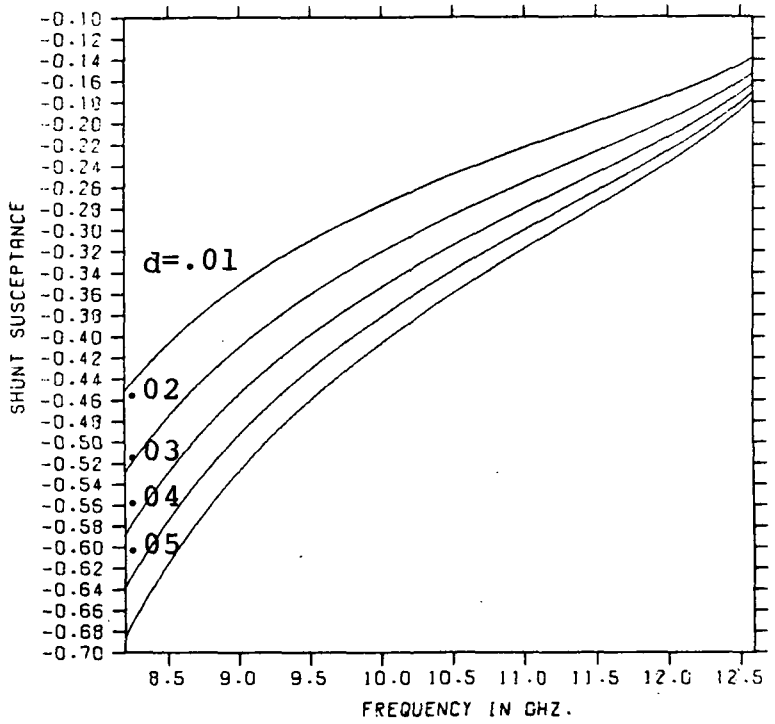

(b) x = .50 cm

Figure 71. Metal Inductive Post, Shunt Susceptance with a Fixed Sidewall Distance, Varying Diameter of Post

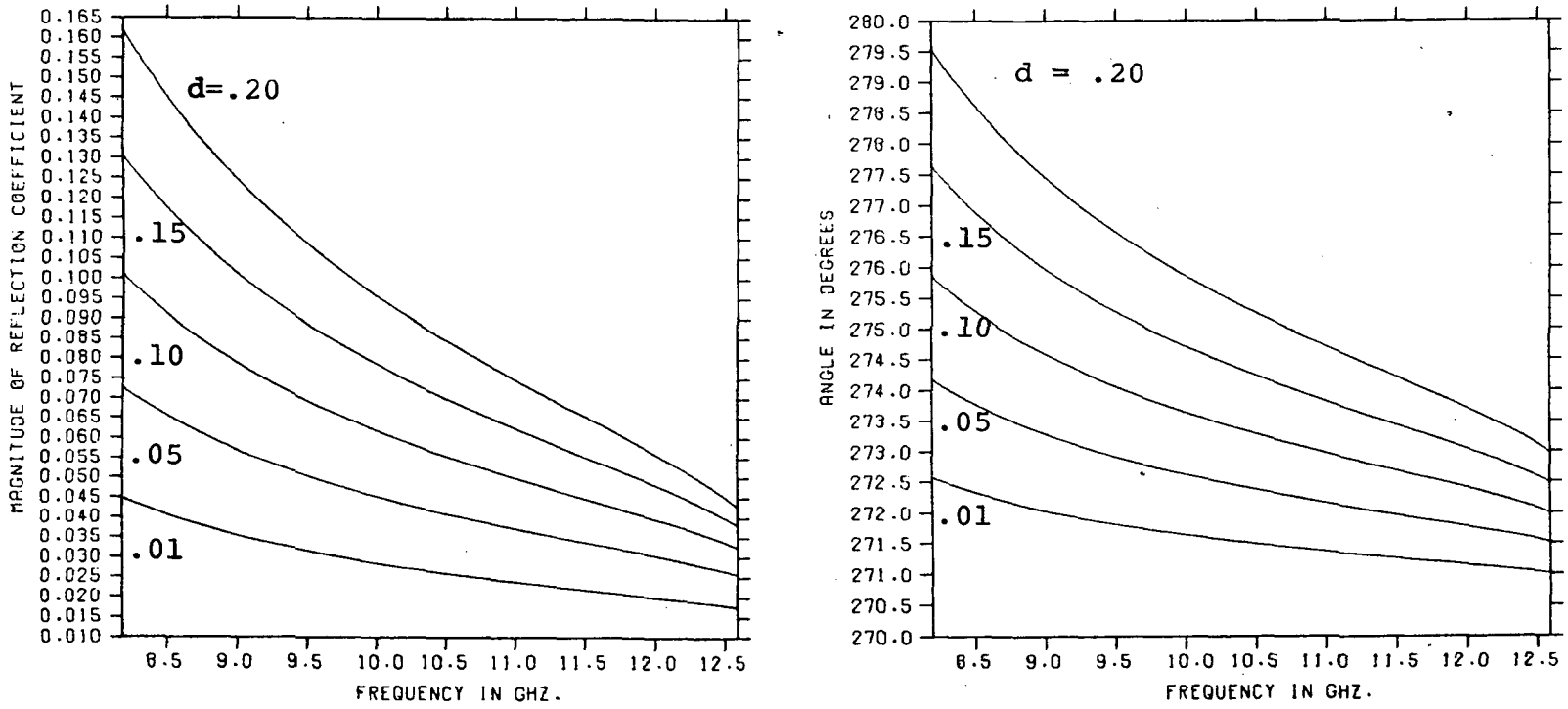

(a) Magnitude
x = .20

(b) Phase
x = .20

Figure 72. Magnitude and Phase of the Current Reflection Coefficient of a Metal Inductive Post, Sidewall Distance x = .20 cm, Diameter Varies in Centimeters

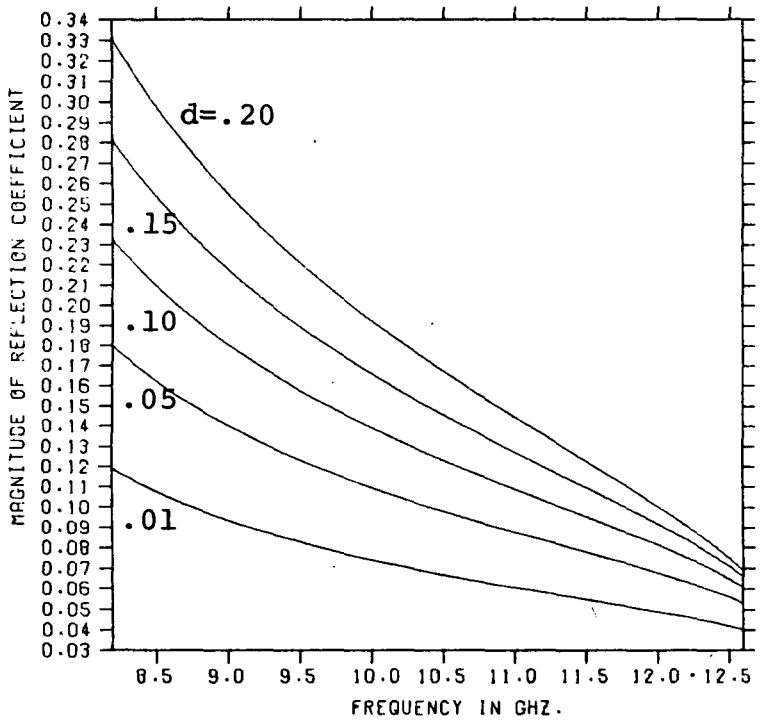

(a) Magnitude
x = .350 cm

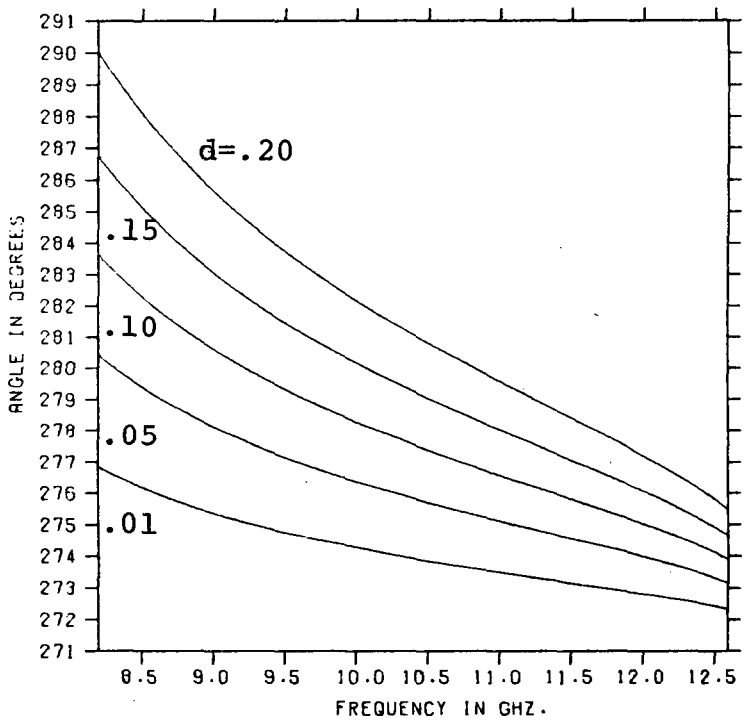

(b) Phase
x = .350 cm

Figure 73. Magnitude and Phase of the Current Reflection Coefficient of a Metal Inductive Post, Sidewall Distance x = .350 cm, Diameter Varies in Centimeters

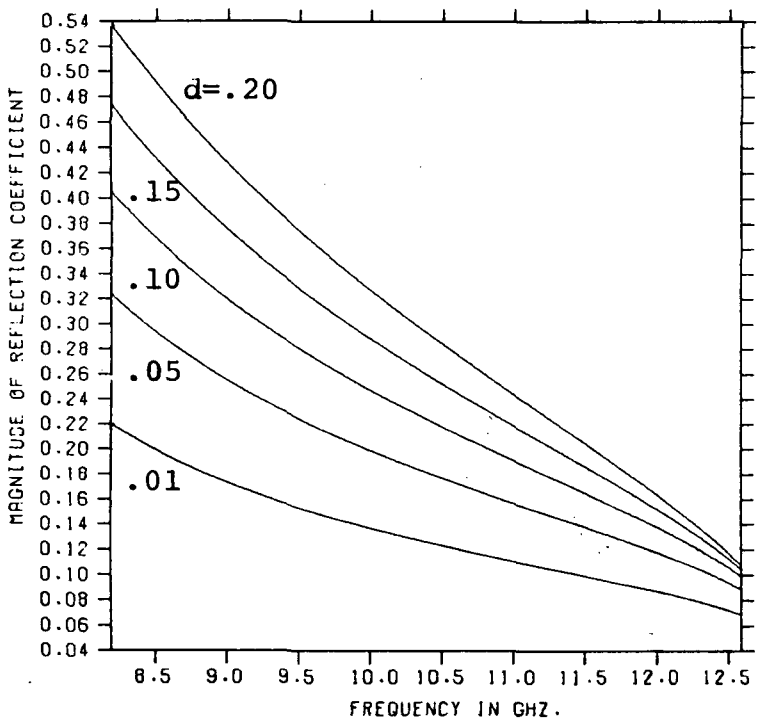

(a) Magnitude
x = .50 cm

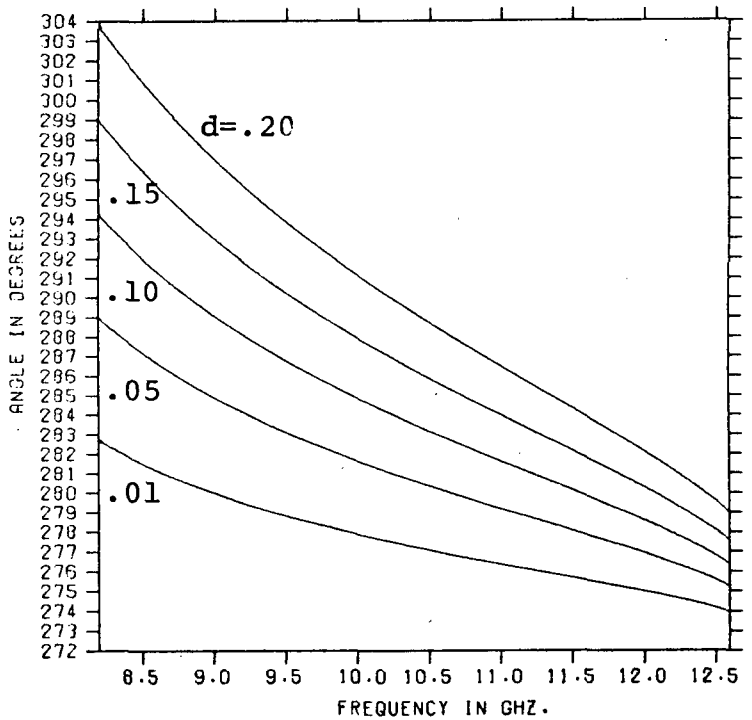

(b) Phase
x = .50 cm

Figure 74. Magnitude and Phase of the Current Reflection Coefficient of a Metal Inductive Post, Sidewall Distance x = .50 cm, Diameter Varies in Centimeters

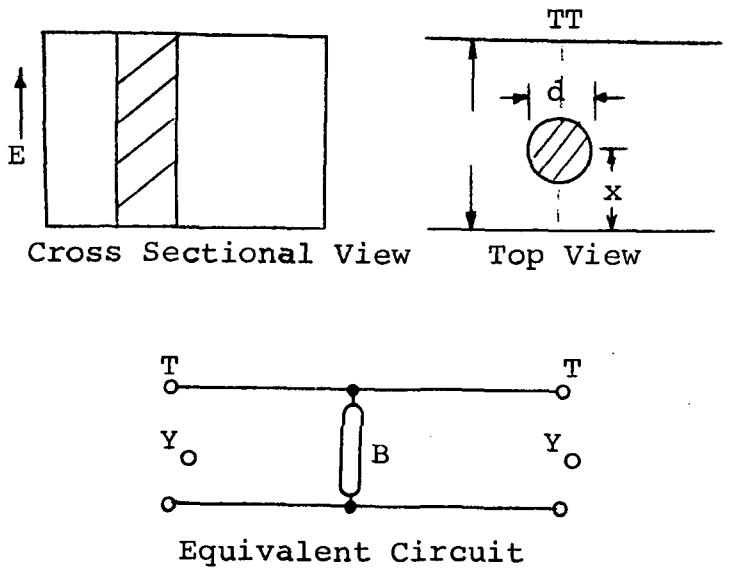

(a) Dielectric Post

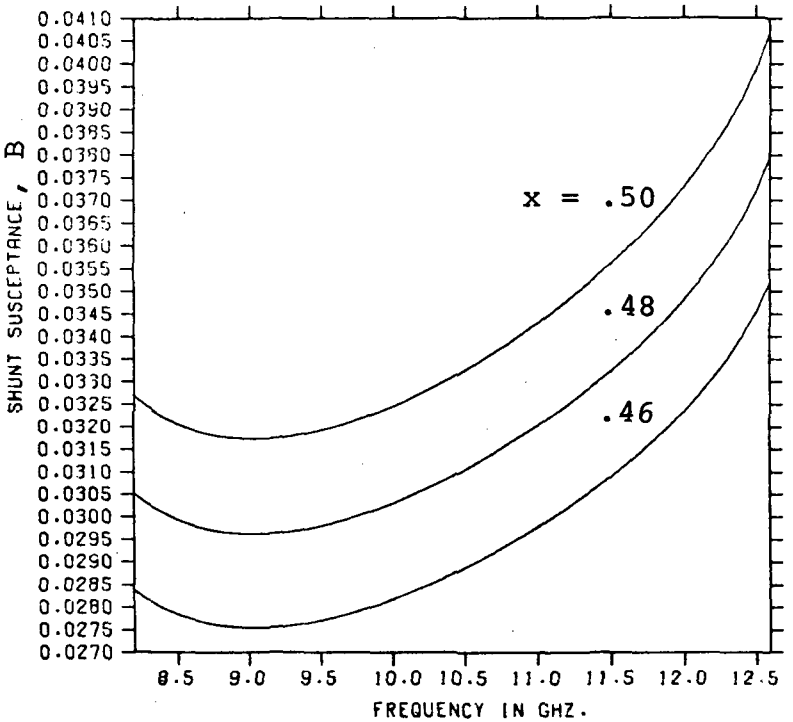

(b) Dielectric Constant = 4.07
Diameter = .114cm

Figure 75. Shunt Susceptance of a Dielectric Post with a Fixed Dielectric Constant, Fixed Diameter, Varying Sidewall Distance

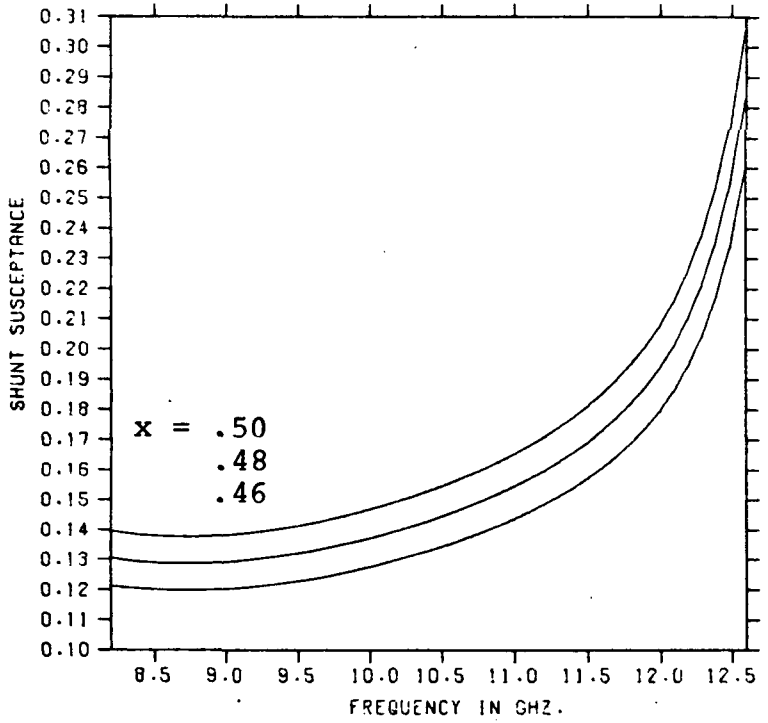

(a) Dielectric Constant = 4.07
Diameter = .228 cm

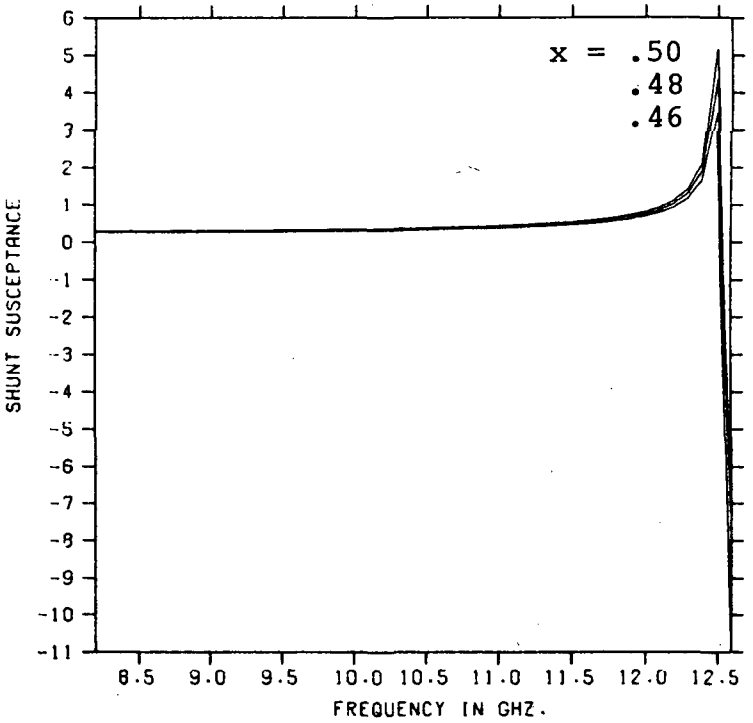

(b) Dielectric Constant = 4.07
Diameter = .328 cm

Figure 76. Shunt Susceptance of a Dielectric Post with a Fixed Dielectric Constant, Fixed Diameter, Varying Sidewall Distance

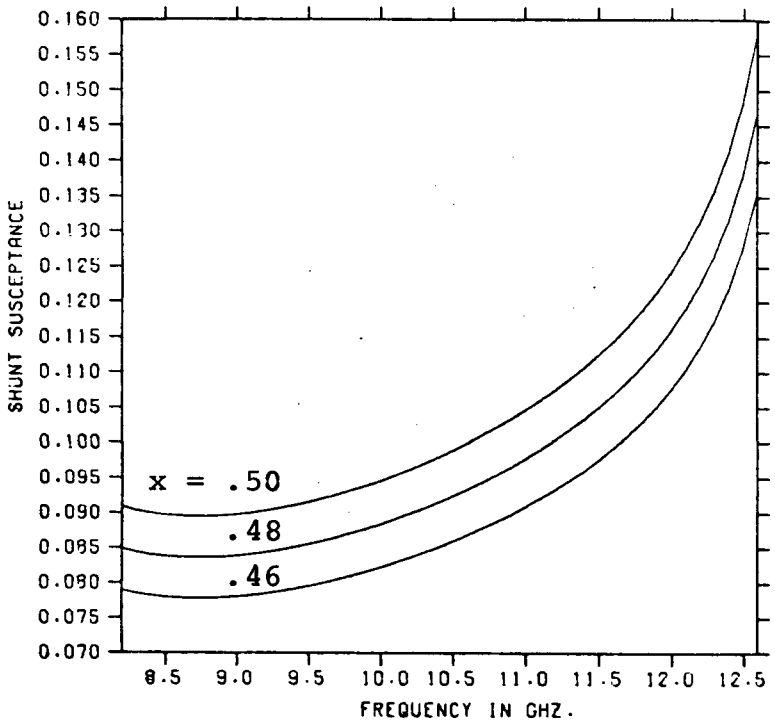

(a) Dielectric Constant = 9.0
Diameter = .114 cm

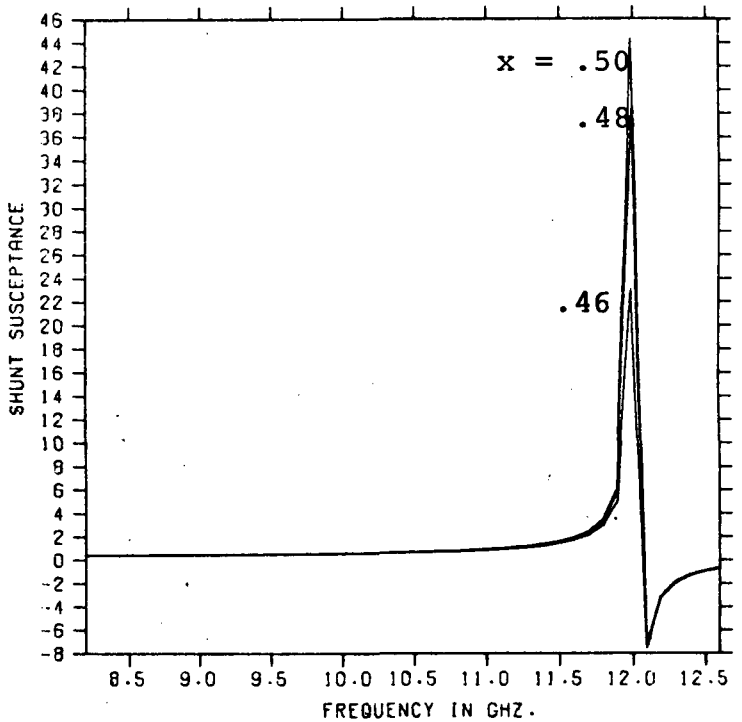

(b) Dielectric Constant = 9.0
Diameter = .228 cm

Figure 77. Shunt Susceptance of a Dielectric Post with a Fixed Dielectric Constant, Fixed Diameter, Varying Sidewall Distance

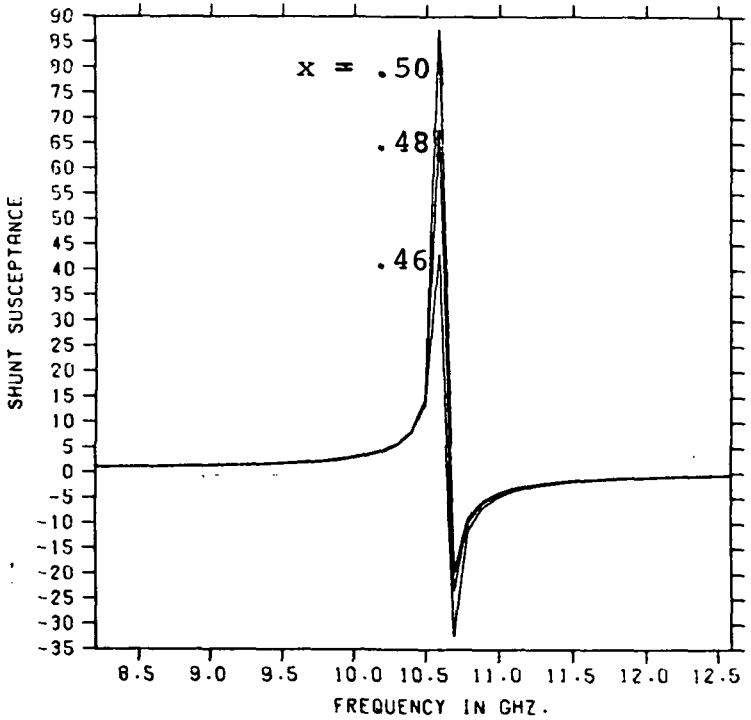

(a) Dielectric Constant = .9
Diameter = .328 cm

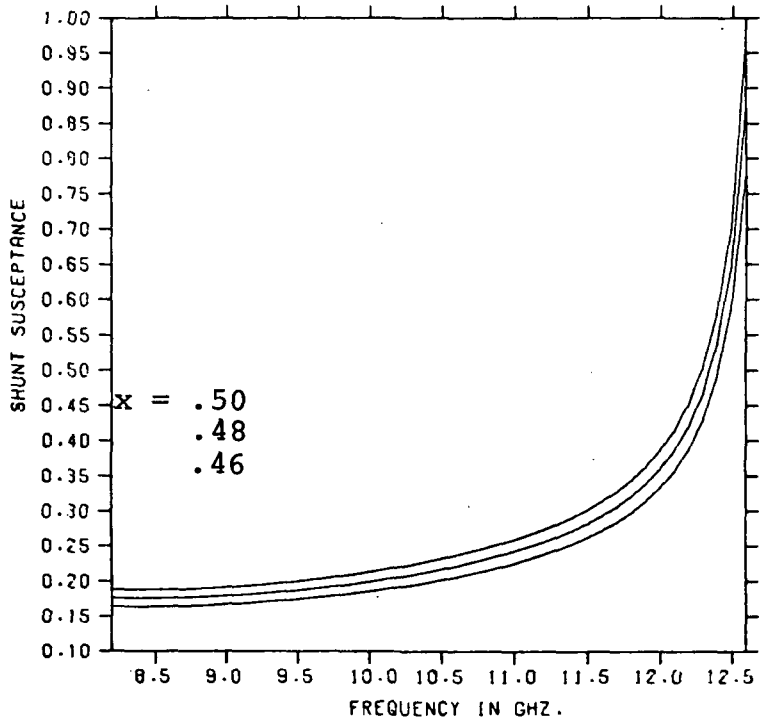

(b) Dielectric Constant = 16.0
Diameter = .114 cm

Figure 78. Shunt Susceptance of a Dielectric Post with a Fixed Dielectric Constant, Fixed Diameter, Varying Sidewall Distance

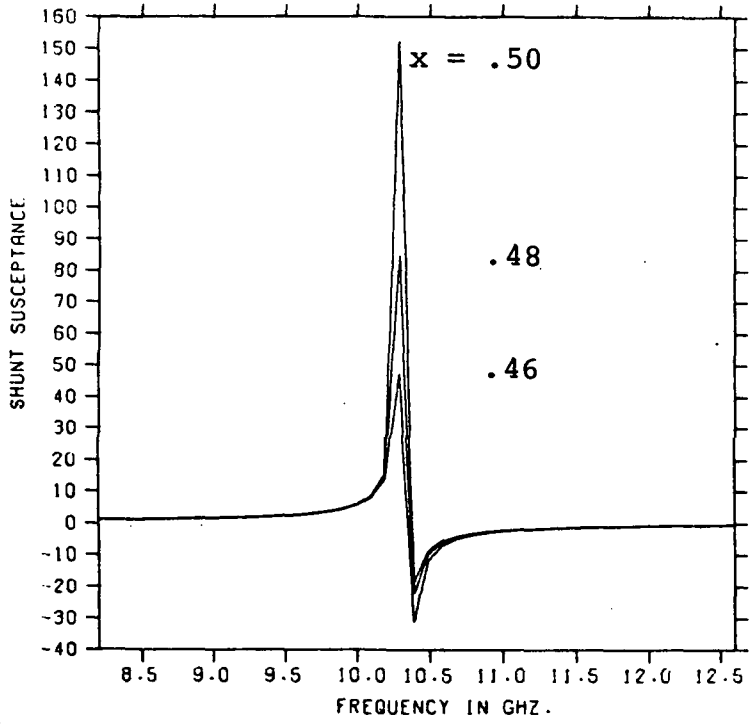

(a) Dielectric Constant = 16.0
Diameter =.228 cm

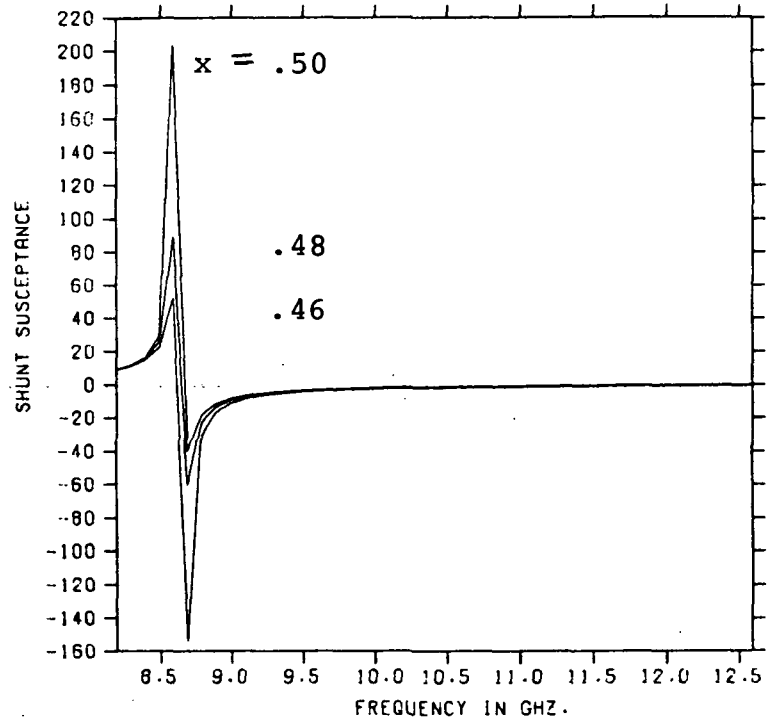

(b) Dielectric Constant = 16.0
Diameter = .328 cm

Figure 79. Shunt Susceptance of a Dielectric Post with a Fixed Dielectric Constant, Fixed Diameter, Varying Sidewall Distance

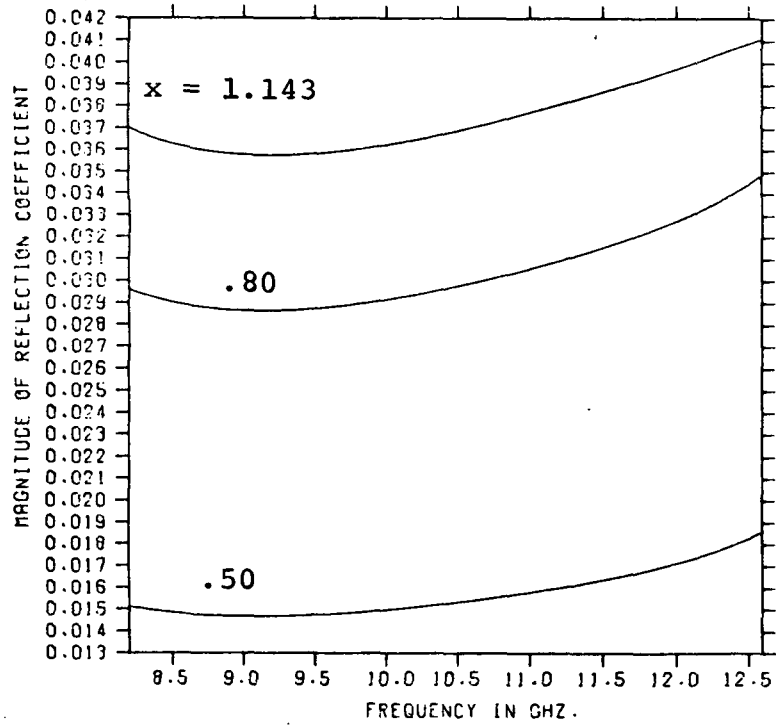

(a) Magnitude
d = .114 cm

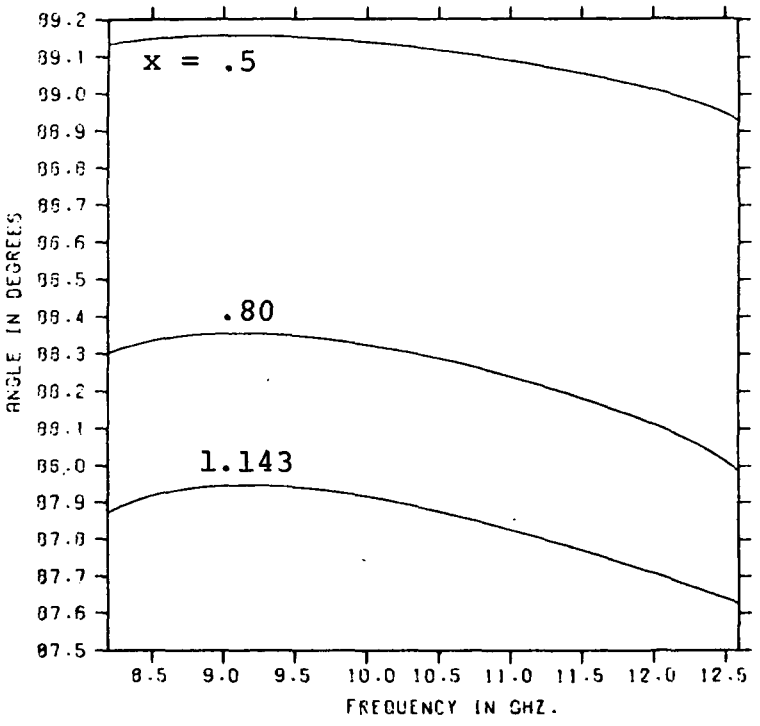

(b) Phase
d = .114 cm

Figure 80. Magnitude and Phase of the Current Reflection Coefficient of a Dielectric Post with 3.85 Dielectric Constant, .114 cm Diameter, and Varied Sidewall Distances in Centimeters

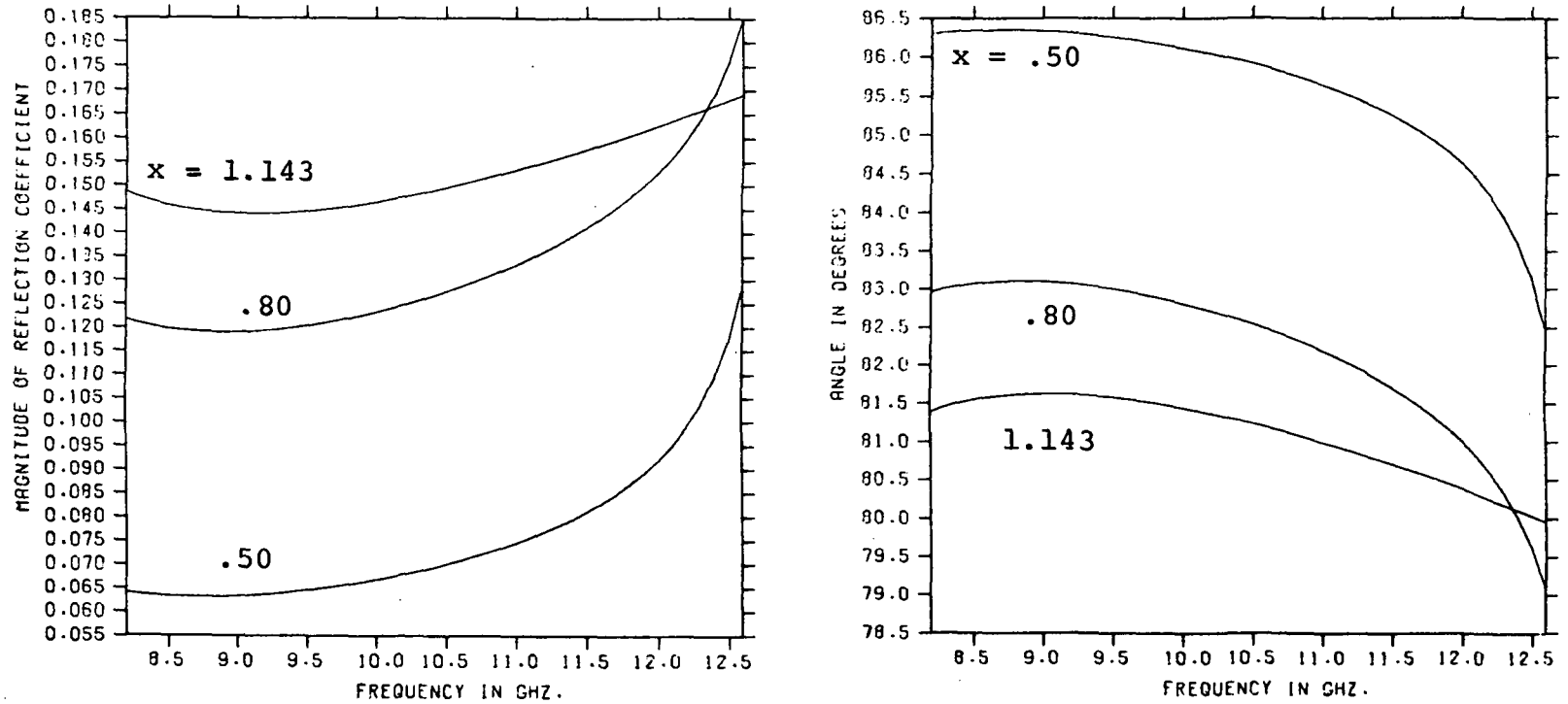

(a) Magnitude
d = .228 cm

(b) Phase
d = .228 cm

Figure 81. Magnitude and Phase of the Current Reflection Coefficient of a Dielectric Post with 3.85 Dielectric Constant, .228 cm Diameter, and Varied Sidewall Distance in Centimeters

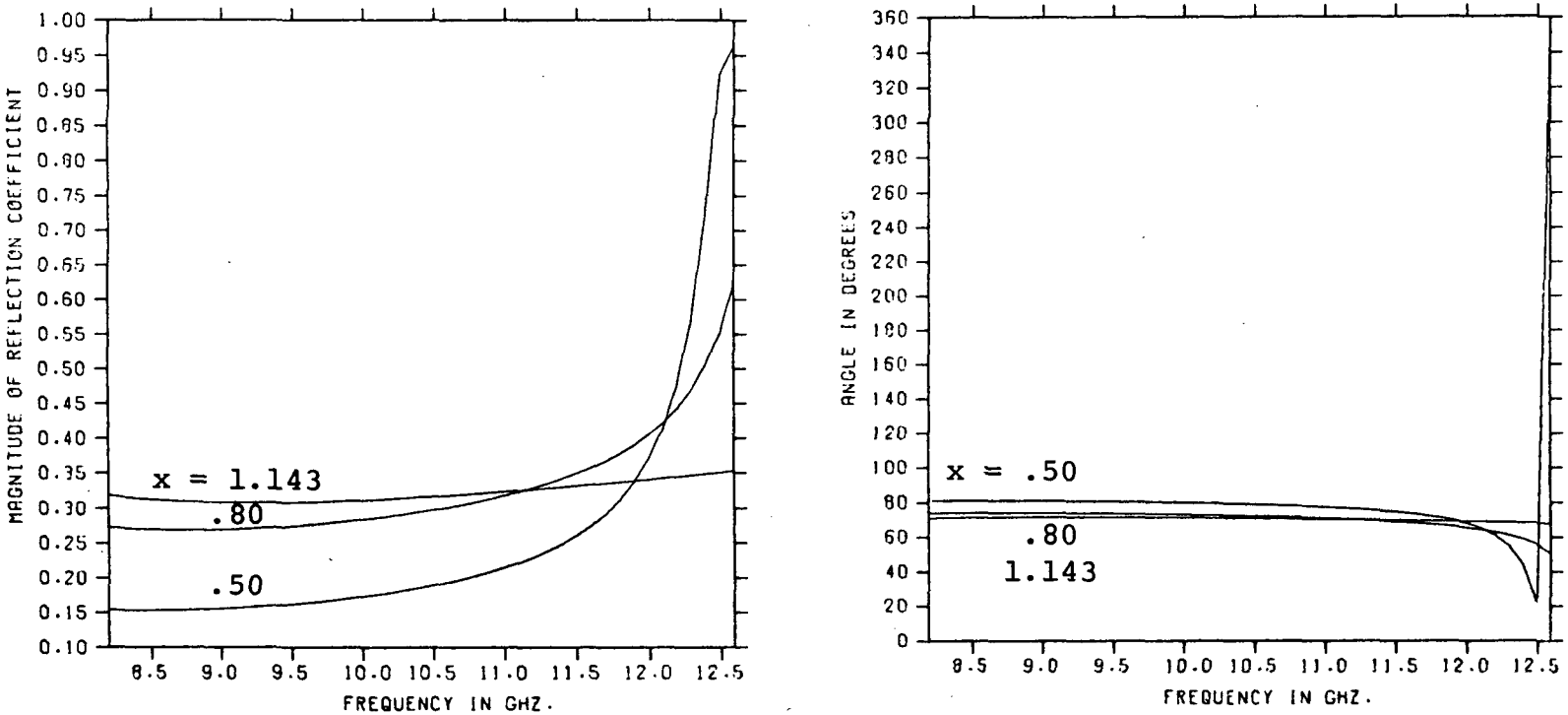

(a) Magnitude
d = .343

(b) Phase
d = .343

Figure 82. Magnitude and Phase of the Current Reflection Coefficient of a Dielectric Post with 3.85 Dielectric Constant, .343 cm Diameter, and Varied Sidewall Distances in Centimeters

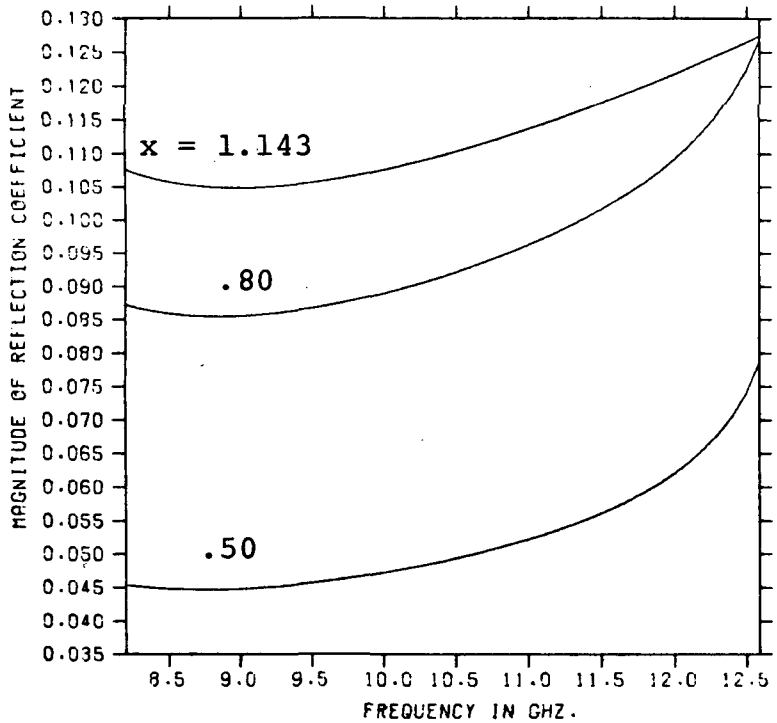

(a) Magnitude
d = .114 cm

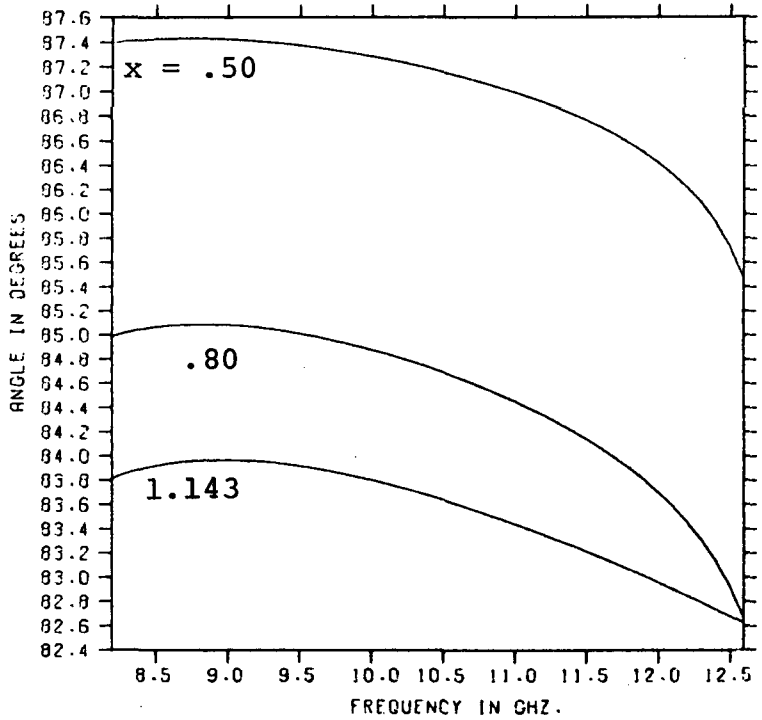

(b) Phase
d = .114 cm

Figure 83. Magnitude and Phase of the Current Reflection Coefficient of a Dielectric Post with 9.0 Dielectric Constant, .114 cm Diameter and Varied Sidewall Distances in Centimeters

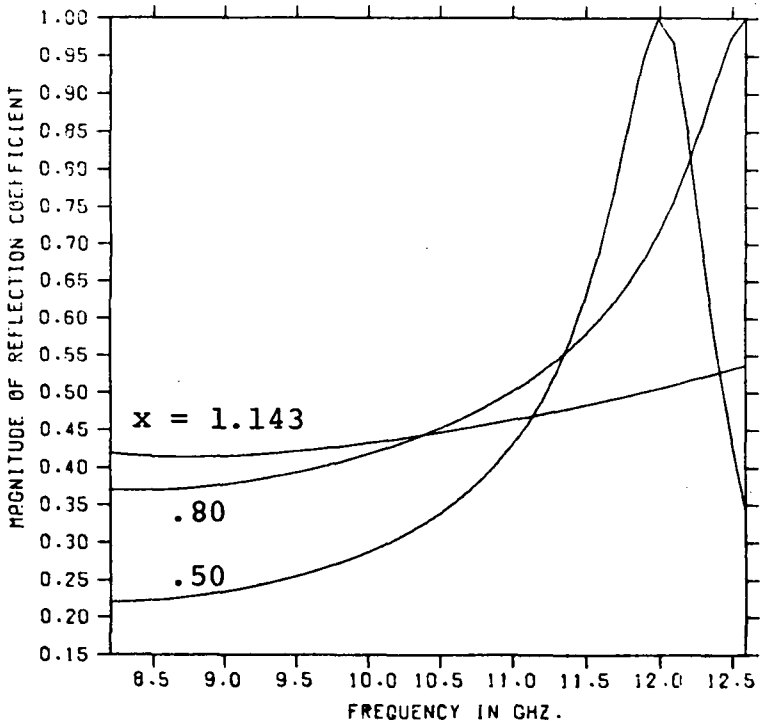

(a) Magnitude
d = .228 cm

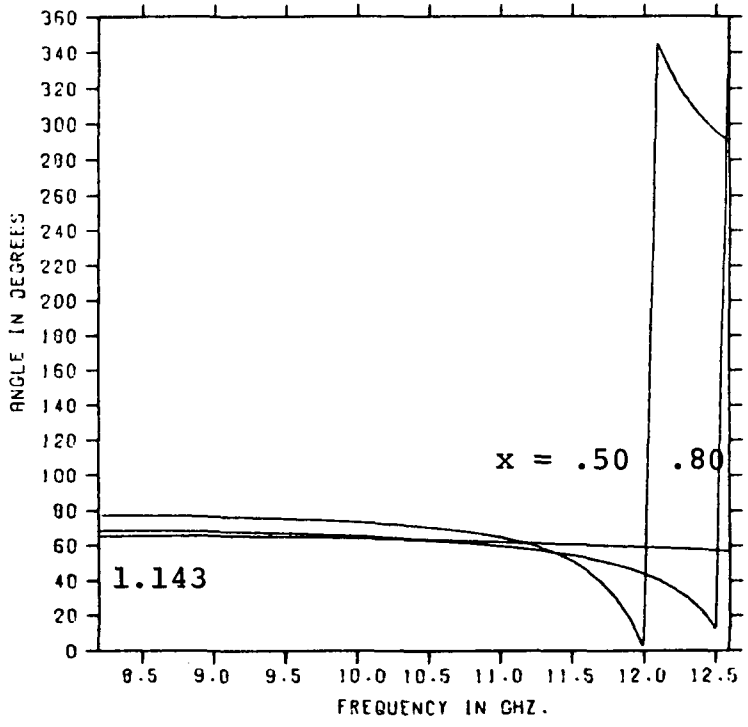

(b) Phase
d = .228 cm

Figure 84. Magnitude and Phase of the Current Reflection Coefficient of a Dielectric Post with 9.0 Dielectric Constant, .228 cm Diameter, and Varied Sidewall Distances in Centimeters

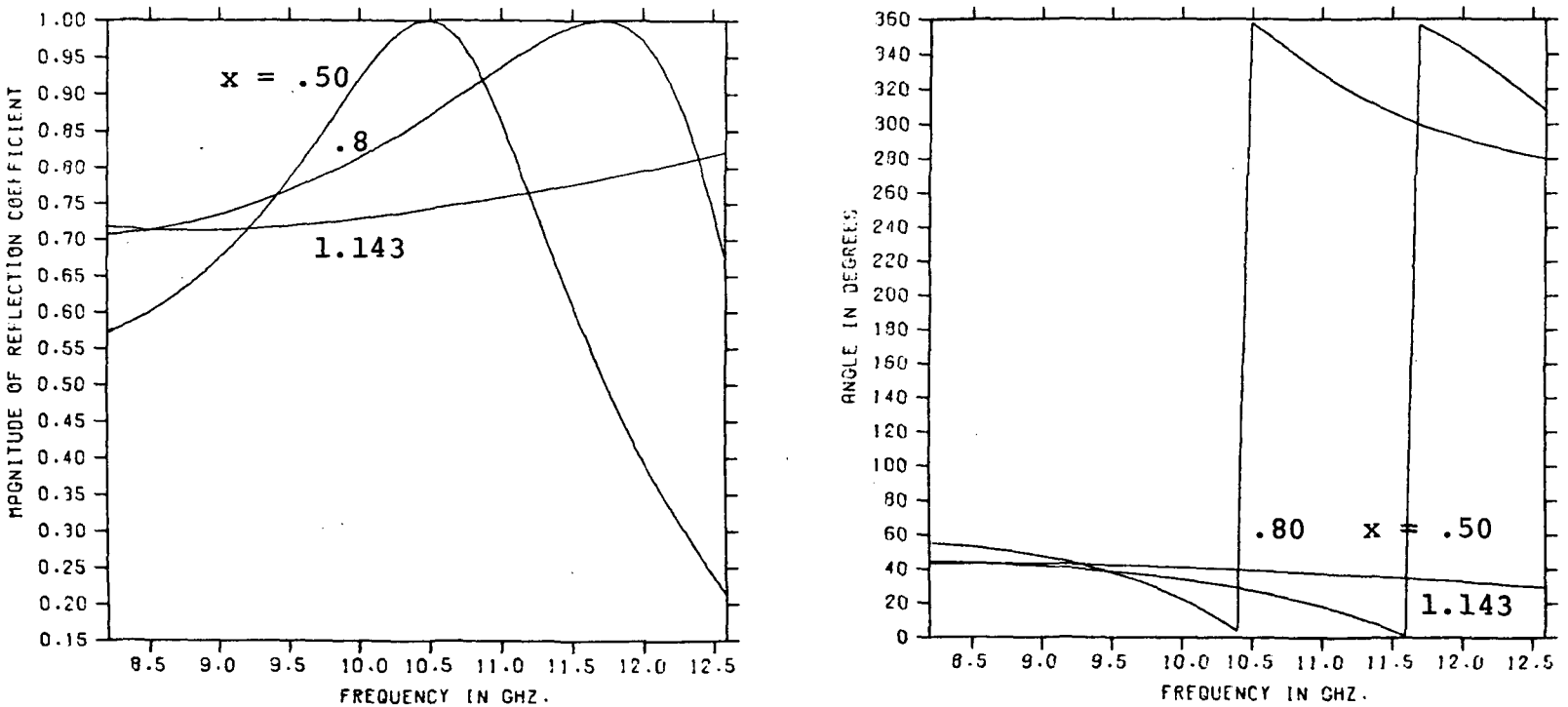

(a) Magnitude
d = .343 cm

(b) Phase
d = .343 cm

Figure 85. Magnitude and Phase of the Current Reflection Coefficient of a Dielectric Post with 9.0 Dielectric Constant, .343 cm Diameter, and Varied Sidewall Distances in Centimeters

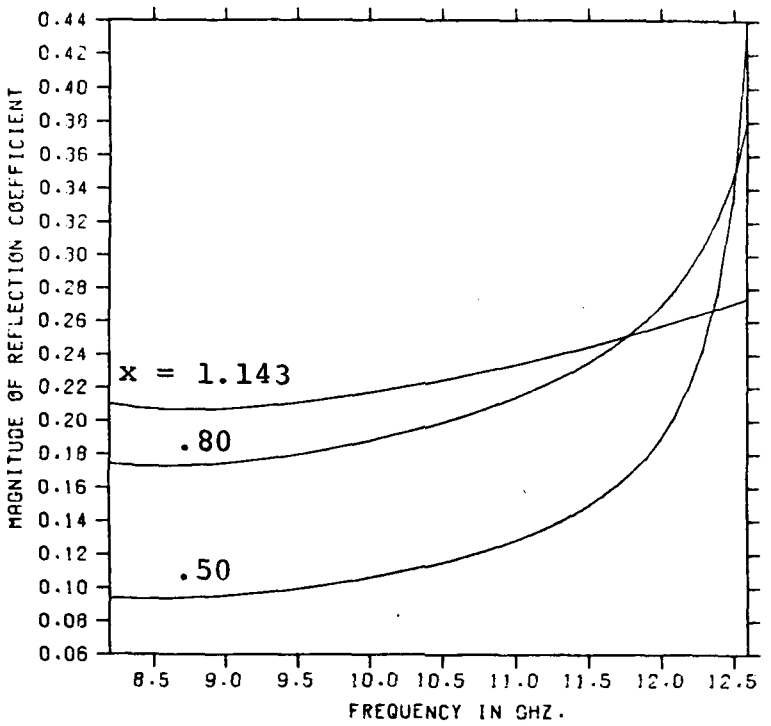

(a) Magnitude
d = .114 cm

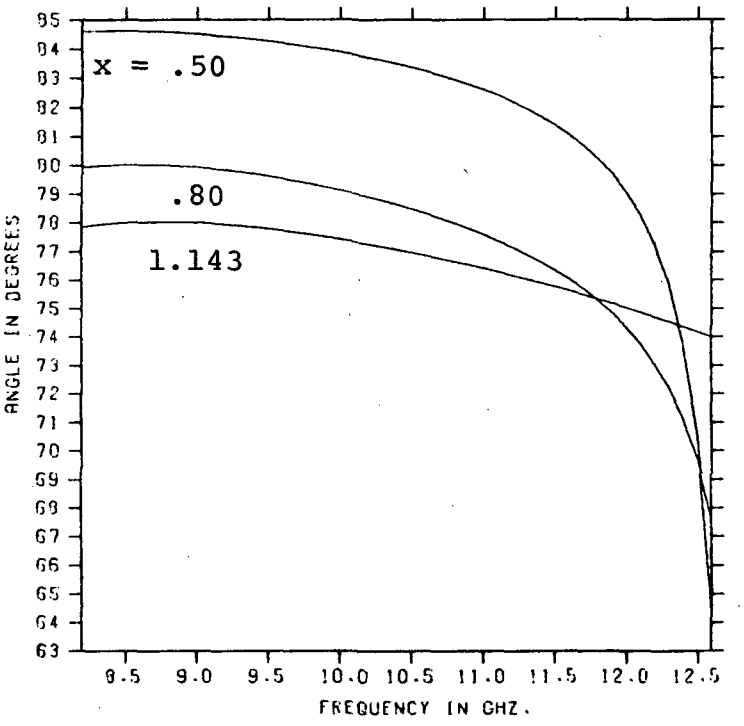

(b) Phase
d = .114 cm

Figure 86. Magnitude and Phase of the Current Reflection Coefficient of a Dielectric Post with 16.0 Dielectric Constant, .114 cm Diameter, and Varied Sidewall Distances in Centimeters

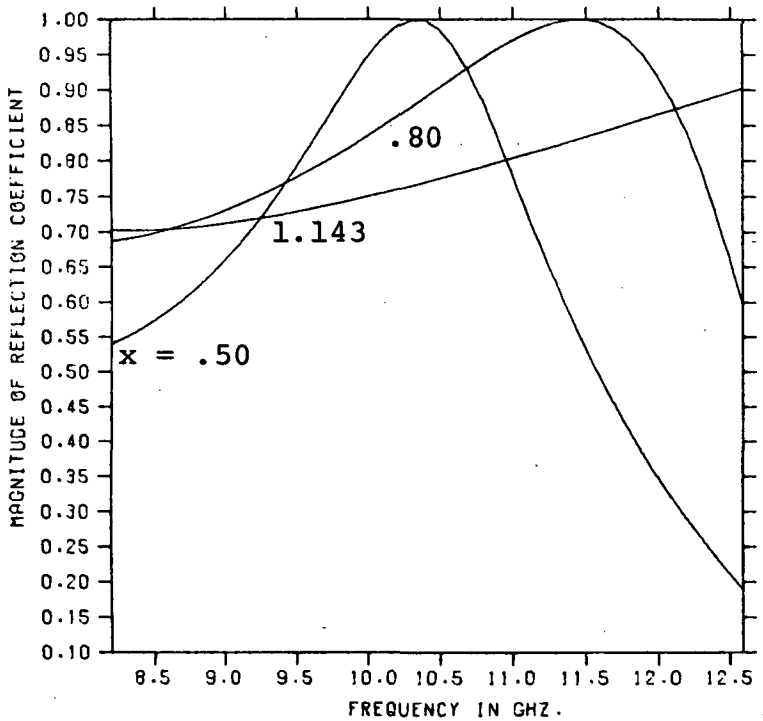

(a) Magnitude
d = .228 cm

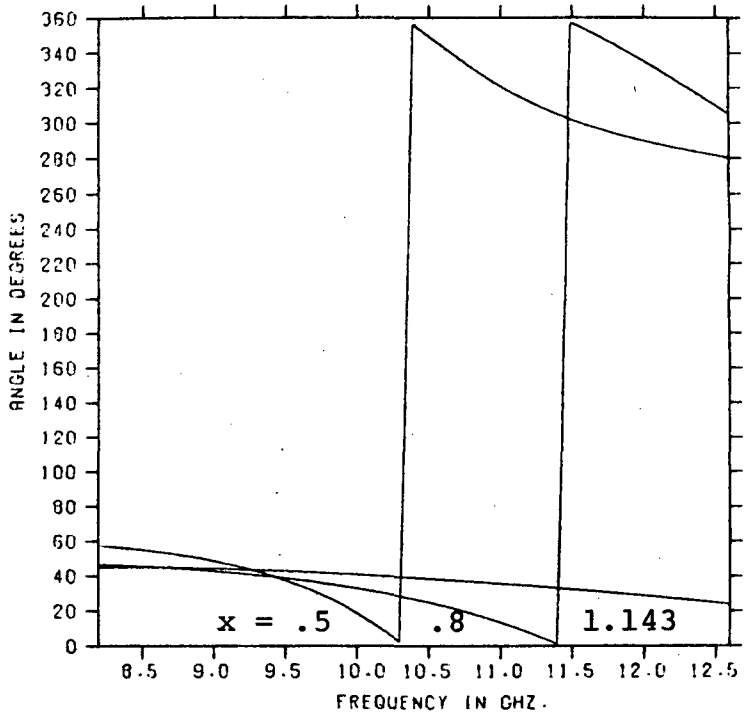

(b) Phase
d = .228 cm

Figure 87. Magnitude and Phase of the Current Reflection Coefficient of a Dielectric Post with 16.0 Dielectric Constant, .228 cm Diameter, and Varied Sidewall Distances in Centimeters

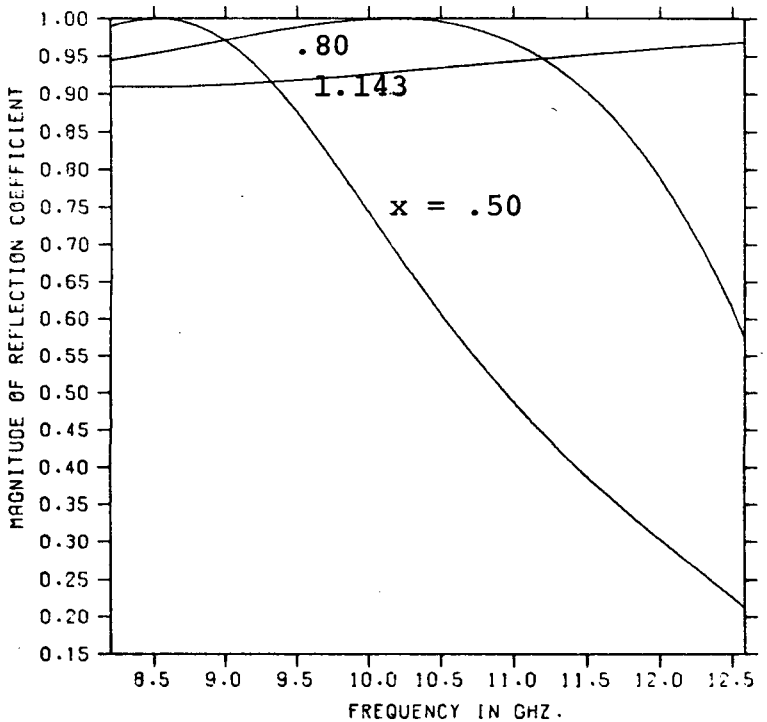

(a) Magnitude
d = .343 cm

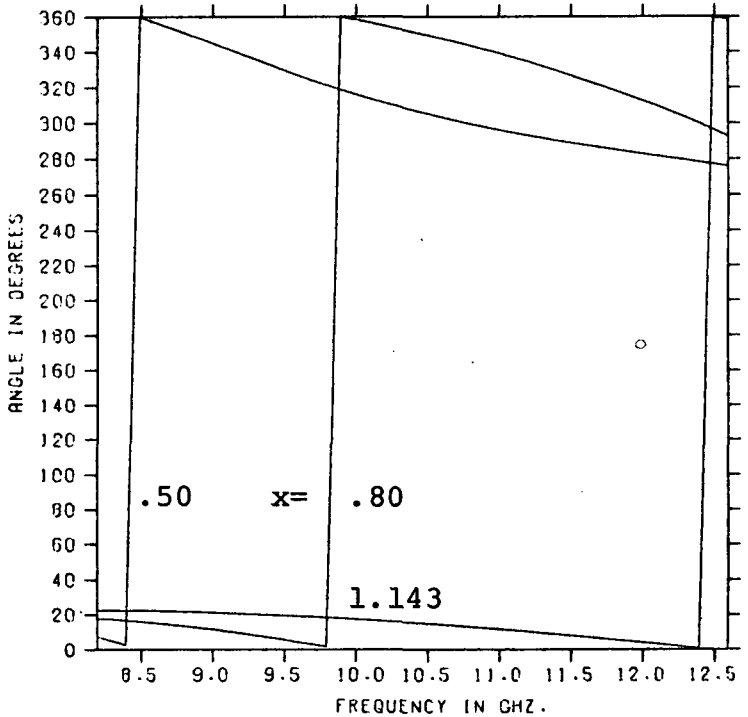

(b) Phase
d = .343 cm

Figure 88. Magnitude and Phase of the Current Reflection Coefficient of a Dielectric Post with 16.0 Dielectric Constant, .343 cm Diameter, and Varied Sidewall Distances in Centimeters

APPENDIX B

COMPUTER PROGRAM LISTING

Three computer programs are described on the following pages. The programs are written in Fortran V computer language for the Univac 1108 compiler. The first program described is referred to as Test 1. This program calculates the mean reflection coefficient generated as a function of distance.[12] That is, it determines the electrical location of discontinuities in a waveguide. A functional block diagram of Test 1 and Test 2 are shown in Figures 89 and 90 respectively. The second program, Test 2 calculates the complex reflection coefficient as a function of frequency at a predetermined position in the waveguide.[12] The above two programs utilize voltage measurements taken by the comparison reflectometer.

The third program listed is the impedance matching program. This program uses data generated by Test 2, as the disturbance to be impedance matched, Chapter III. The matching program then calculates the physical dimensions and location of a predetermined matching element. The location is relative to the original disturbance. Generally, this program requires five seconds run time on the Univac 1108 to realize an impedance match.

Comment statements have been provided throughout the program listing to partially explain the meaning of para-

meters used.

Test 1 begins with a listing of constants to be used. Statement (9) and (10) give values to XMAX and XMIN, the range in distance along the waveguide relative to the reference step. A table of sines and cosines are generated by statements (27) to (33). The use of this table reduces computer run time, since it requires less time to obtain this information from memory than to calculate the sine and cosine when needed. An envelope shaping function,[1] when used, reduces side lobe levels at the expense of broadening the main peak of the locating curve. This part of the program has no direct application to this research, therefore, statement (38) prevents it from entering the following calculations. The constant NO read in at statement (43) is the number of sets of data to be read by the computer. The constant NF is the number of data points measured. REFPT the magnitude of the reflection coefficient of the reference step used.

Data is read in without a decimal point present. Therefore, statements (57) through (60) place the decimal point in the proper location. Statements (69) through (72) calculate Equation (III-31). Statements (72) and (78) determine the wavenumber and the wavelength for each frequency corresponding to a voltage measurement by the comparison reflectometer. Equation (III-31) is normalized to the average value of $|\Gamma|^2$ (YRS(N)), for purposes of the computer

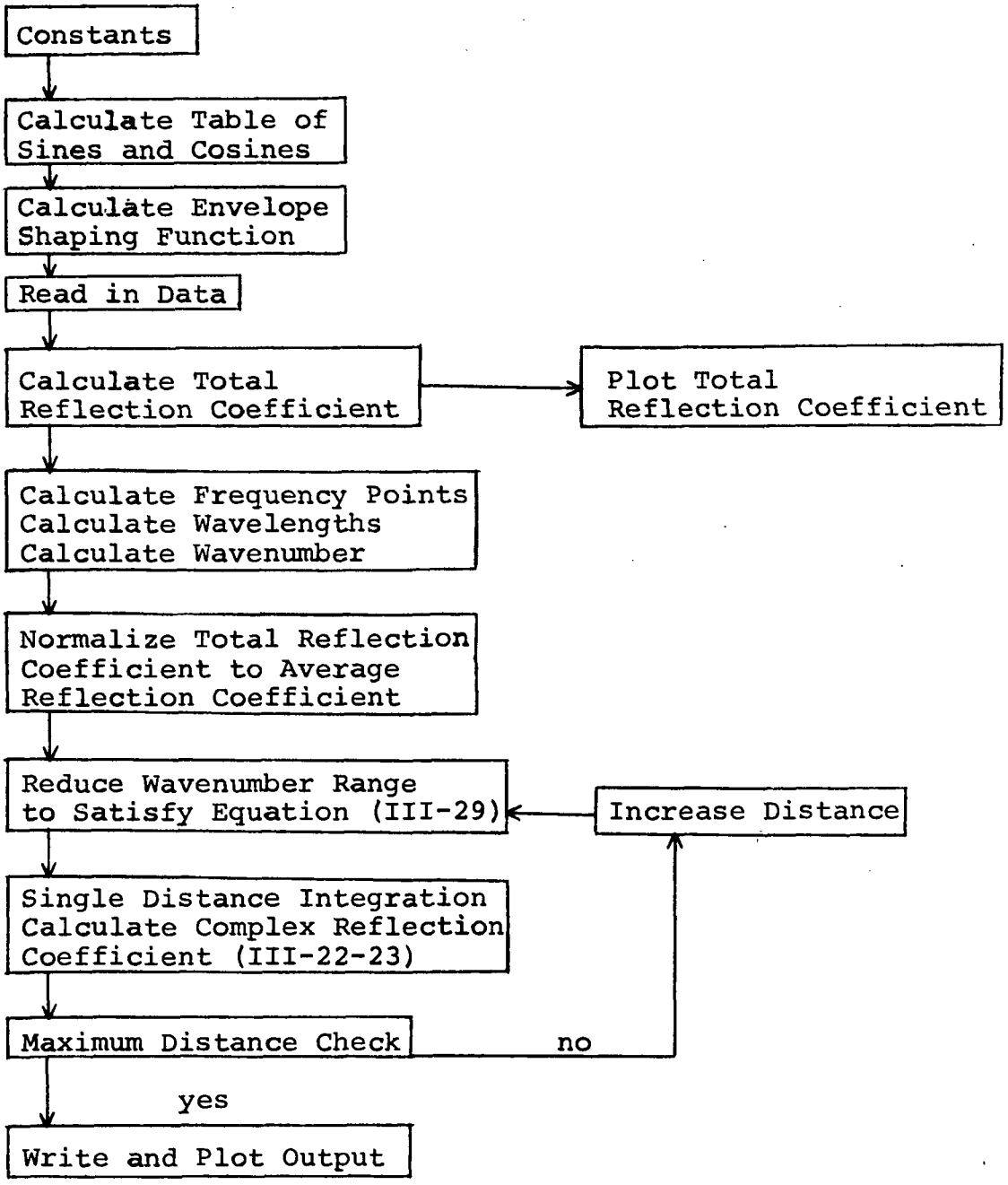

Figure 89. Functional Flow Chart of Test 1 Computer Program

calculation, by statements (80) to (90). The total magnitude of the reflection coefficient measured is plotted out by statements (91) and (120) using a plot subroutine not given here. The wavenumber range is adjusted by statements (121) to (159) in order to satisfy Equation (III-29).

A single distance integration is performed by statements (162) to (178). It has been found by D.L. Hollway[12] that linear interpolation between values of YRS(N) cannot be used without loss of accuracy, therefore, integration is performed by considering each value of YRS(N) to apply over the internal from (WN(NN-1) + (WN(NN))/2 to (WN(NN) + (WN(NN+1))/2. The range of integration WNRR extends from WNT (top) to WNB (bottom).

The discrete Fourier transform, or the fast Fourier transform, was not used in this program because the discrete Fourier transform requires that data samples be taken at equal increments of the argument. While samples are taken at equal intervals of frequency (50 MHz), the transformation is from wavenumber to distance. The wavelength of the energy in the waveguide deviates from the free space wavelength due to the dispersion of energy within the waveguide, therefore, the wavenumber intervals are not equal in increments. The wavenumber intervals corresponding to equal frequency intervals, increases as the frequency is increased.

H(L,1) and H(L,2) are the real and imaginary parts

of the reflection coefficient generated at the distance Y(L), statements (185) and (186). Depending on the slope of the magnitude of this reflection coefficient the distance Y(L) is increased by .5 or .25 by statements (197) to (202). If Y(L) is equal to or greater than XMAX in statement (204) the calculations are completed and the remaining plots and printout are executed.

Test 2 is very similar to Test 1, the difference being in the size in the internal WNRR. In Test 1 the entire spectrum measured was used for each distance calculation. The result is a magnitude and phase of an average reflection coefficient generated at the distance of interest. In Test 2, however, a single distance or location is of interest and this is read into the program by XSET. For this particular distance XSET, the reflection coefficient is calculated over overlapping subintervals of 500 MHz. Each subinterval overlapping by 100 MHz, Figure 13. The value of the reflection coefficient calculated over any particular subinterval is assigned to the center frequency of that subinterval. The result is that at approximately 100 MHz intervals the reflection coefficient is known. Since each adjusted subinterval WNRR must satisfy Equation (III-29), where the distance L_n is the predetermined location of the discontinuity, the resulting reflection coefficient is known at unequal subintervals of frequency.

Calculations are actually made at ten locations along

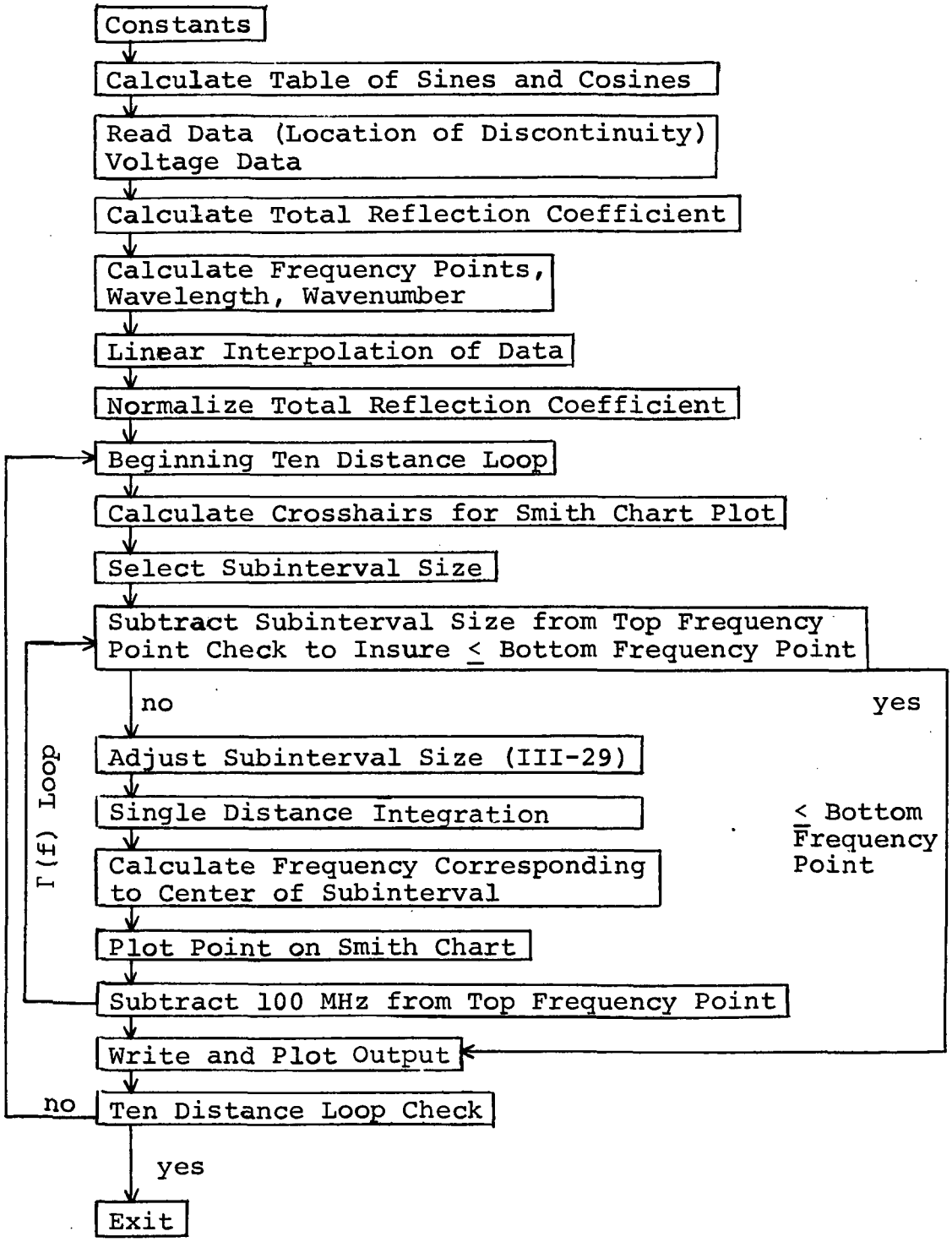

Figure 90. Functional Flow Chart of Test 2 Computer Program

the waveguide at intervals XINCR centered around the location, of the discontinuity, XSET. This is done to provide insight as to the effects of dispersion, on the reflection coefficient of the disturbance measured, as the energy travels through the waveguide.

In order to provide a smoother, more accurate curve, a linear interpolation is made between the 50 MHz points, resulting in data at 10 MHz intervals. This does not add any information about the total reflection coefficient, but it reduces the ripple in the resulting waveform, inherent in the algorithm used to perform the integration.

The upper bound of the first subinterval is the upper bound of the measured spectrum, point NF. The lower bound of this subinterval is given by the statement (109) and is referred to as the NS point. The remaining calculations through statement (184) are duplicated from Test 1. The subinterval is shifted down the spectrum 100 MHz by the statement (216), and the program returns to statement Table (302) to determine the reflection coefficient from this new subinterval. When subscript NS is less than or equal to NSS, the subscript corresponding to the lowest data point taken, the program then exists from statement (110) to statement (220). The program prints and plots results and ends.

The impedance matching program calculates the physical dimensions of a predetermined matching element and the

location of the element in the waveguide relative to the location of the disturbance as calculated by Test 1. The results of Test 2 on punched data cards are the input data for this matching program.

The program begins with a list of constants. Comment statements have been provided in the program listing to identify selected parameters. The matching element to be used is identified by the constant MACHEL, the number of data points by LE. Since the data points are not known at equal frequency increments, the frequency points are read in at statement number (60). The real and imaginary part of the reflection coefficient is read in corresponding to the highest frequency point first, by statements (62) and (63). The complex reflection coefficient of the test element is referred to as GAM(N), where N varies from 1 to LE.

This program is equipped to begin calculations from any position along the waveguide, the starting position being denoted by ALENGH(1). The constant NOO read in at statement (108) denotes the number of times the results will be recalculated at corresponding starting points read in by statement (111). This is a particularly interesting feature, since the set of physical parameters and the quality of the impedance match is a function of $\lambda_g/2$ changes in the ALENGH(1) starting point, Chapter V. Generally, the best impedance match will be achieved by setting the starting ALENGH to zero, i.e. the electrical location of the test ele-

ment.

Depending on the matching element selected, various appropriate starting points are programmed in statements (116) to (119) and described in Table 2. The three dimensional array is generated by statements (128) to (139). A description of this dimensional space array is given in Chapter III. There are two cases possible, the matching element may be located on the generator side of the measured mismatch or the matching element may be located on the load side of the measured mismatch. The results of Appendix C are used accordingly.

Statement (149) branches the program to the appropriate section of the program pertaining to the matching element designated by the value of MACHEL. The reflection coefficient for this chosen matching element is then calculated for the seven points of interest in dimension space, see Figure 19. The value of the complex reflection coefficient is carried by the variable four dimensional array GGAN (I, J, KK, N), where the first, second and fourth index correspond to the axis of the dimensional space array of Figure 19. The third index corresponding to frequency. When the array GGAM is completed, control is transferred to statement (375). Statement (378) to (400) calculate the RMS of the mismatch, resulting from the measured discontinuity and the matching element, for each point in dimension space. Statements (405) to (418) determine the smallest

RMS value, while statements (419) to (432) determine the value of the I, J, K indices that correspond to this smallest value. Statement (436) tests for termination. If the indices corresponding to the least RMS are the I=1, J=1, K=1, then a minimum value has been determined, if not, control is shifted to statement (439). If a minimum value has been determined, a check is made to determine whether the increment size has been reduced to 1/8 of the original size, if not, control is shifted to label 350 where the present increment size is divided by two. If on the other hand the increment size is 1/8 of the original value, control is shifted to statement (447) or label 200, and the program begins to write output. If a minimum was not determined at statement (436) control if shifted to statement (439) or label 108 and the physical parameters of the dimension space (1, 1, 1) point are set equal to the physical dimensions of the point corresponding to the LRMS mismatch. Control is then shifted to lable 250 and calculations are again performed for the seven points in dimension space centered around the new (1, 1, 1) point.

Calculations to determine the physical parameters of the matching element are performed over the bandwidth of interest having the index points JBEG and JEND. When the matching element size has been determined the results of the mismatch are calculated over the entire known spectrum originally read in. Therefore, the characteristics of the chosen

matching element must again be calculated as determined by statement (468), and the resulting mismatch again calculated.

The output consists of printout of RMS mismatch over the band of interest, size and location of the matching element, and a listing of the reflection coefficient and the VSWR of the mismatch over the full band. A plot is made of the VSWR of the original disturbance and the matched disturbance over the full band. Also, data cards are punched, recording the real and imaginary parts of the resultant mismatch. Some typical results of this program are given in Chapter III.

Test 1

Statement Number	Label Number	Statement
1*		DIMENSION ISUF(20000)
2*		DIMENSION PTITLE(12),RTITLE(12),MTITLE(12)
3*		DIMENSION X(400),VTITLE(12),HTITLE(12)
4*		DIMENSION P(200),S(1260),CKS(100),YREF(90),YU(90)
5*		DIMENSION YR(100),WN(100),WL(100),H(400,4),Y(400),ER(100),YRS(100)
6*		DIMENSION NREF(100),NYU(100)
7*	C	PRESET CONSTANTS AND TABLES OF FUNCTIONS.
8*	C	XMAX IS THE MAXIMUM DISTANCE IN CMS FROM THE REF. REFLECTION
9*		XMAX=100.
10*		XMIN=5.
11*	C	WGW IS THE WIDTH OF THE WAVEGUIDE IN INCHES.
12*		WGW=0.9
13*		PLRF=-1
14*		PLRF=1.0
15*	C	PLPX PHASE ANGLE OF THE REFLECTION COEFFICIENT AGAINST DISTANCE.
16*		PLPX=1.
17*		PLPX=-1.
18*		NS=1
19*		PI=3.1415926536
20*	C	RPV,RADIANS PER VOLT,IS A CONSTANT OF THE RATIOMETER. IT IS THE
21*	C	CONDUCTION ANGLE AT FULL SCALE DIVIDED BY THE CORRESPONDING
22*	C	VOLTAGE OUTPUT.
23*		RPV=56.6*PI/(6.928*180.)
24*	C	ATTEN CORRECTS FOR A WAVEGUIDE ATTENUATION OF 0.036 DB/FOOT.
25*		ATTEN=0.036*2.3026/(10.**12.**2.54)
26*	C	TABLES OF SINES AND COSINES
27*		DO6N=1,500
28*		S(N)=SIN(N*PI/500.)
29*		S(N+500)=-S(N)
30*	6	CONTINUE
31*		DO8N=1,260
32*		S(N+1000)=S(N)
33*	8	CONTINUE
34*	C	ENVELOPE SHAPING FUNCTION
35*		DO35N=1,200
36*		PANGLE=2.*PI*N/200.
37*		P(N)=1.-0.889*COS(PANGLE)+0.0112*COS(2.*PANGLE)
38*		P(N)=1.
39*	35	CONTINUE
40*	C	2
41*	C	NO IS THE NUMBER OF UNKNOWN COMPONENTS TO BE MEASURED.
42*	C	NO IS THE FIRST DATA CARD.
43*		READ(5,601)NO
44*	601	FORMAT(I3)
45*		READ(5,400)NF
46*	400	FORMAT(I3)
47*		READ(5,12)REFPT
48*	12	FORMAT(F10.5)
49*		REFPTS=REFPT*REFPT
50*		DO600K=1,NO
51*		READ(5,200)(NREF(N),N=1,NF)
52*		READ(5,201)(NYU(N),N=1,NF)
53*	200	FORMAT(4X,I4,1X,I4,1X,I4,1X,I4,1X,I4,1X,I4,1X,I4,1X,I4,1X,I4,1X,I4,1X,I4
54*		1,1X,I4,1X,I4,1X,I4,1X,I4,1X,I4,1X,I4,2X)
55*	201	FORMAT(4X,I4,1X,I4,1X,I4,1X,I4,1X,I4,1X,I4,1X,I4,1X,I4,1X,I4,1X,I4,1X,I4
56*		1,1X,I4,1X,I4,1X,I4,1X,I4,1X,I4,1X,I4,2X)

```
      DO500N=1,NF
      YREF(N)=NREF(N)/1000.
      YU(N)=NYU(N)/1000.
  500 CONTINUE
      WRITE(6,502)
  502 FORMAT(1H1,30X,'REFERENCE VOLTAGE DATA',///)
      WRITE(6,501)(YREF(N),N=1,NF)
      WRITE(6,503)
  503 FORMAT(////,30X,'VOLTAGE DATA WITH UNKNOWN IN LINE',///)
      WRITE(6,501)(YU(N),N=1,NF)
  501 FORMAT(15(3X,F5.3))
      FR(1)=7.975
      DO202N=1,NF
      CKS(N)=(REFPT**2*COS(YREF(N)*RPV))/SIN(YREF(N)*RPV)
      YRS(N)=(CKS(N)*SIN(YU(N)*RPV))/COS(YU(N)*RPV)
      YR(N)=SQRT(YRS(N))
      FR(N+1)=FR(N)+.050
  202 CONTINUE
      NFP=NF+1
      DO56N=1,NFP
      WN(N)=SQRT((FR(N)/29.9695)**2-(1./(2.*2.54*WGW))**2)
      WL(N)=1./WN(N)
   56 CONTINUE
      YRW=0.
      YRSW=0.
      DO49N=1,NF
      YRW=YRW+YR(N)*(WN(N+1)-WN(N))
      YRSW=YRSW+YRS(N)*(WN(N+1)-WN(N))
   49 CONTINUE
      YRSM=YRSW/(WN(NF+1)-WN(NS))
      YM=YRW/(WN(NF+1)-WN(NS))
      DO50N=1,NF
      YRS(N)=YRS(N)-YRSM
   50 CONTINUE
      IF(PLRF)16,16,51
   51 CONTINUE
      REAL LTRSZ,LENGTH
      LOGICAL BOX,FIXLIM,USELIM
      DATA HTITLE/'FREQUENCY IN GHZ
     2                    '/
      DATA VTITLE/'MAGNITUDE OF TOTAL REFLECTION COEFFICIENT
     2                    '/
      CALL PLOTS(IBUF(1),20000,2)
      DO401N=1,NF
      X(N)=YR(N)
  401 CONTINUE
      CALL PLOT(10.,-3.,-3)
      MODE=1
      LTRSZ=.1
      UP=2.5
      OVER=0.
      HEIGHT=5.
      LENGTH=5.
      PERCNT=.9
      NUMINT=6
      HLBND=FR(1)
      HUBND=FR(39)
```

```
114*            ICOUNT=89
115*            BOX=.TRUE.
116*            FIXLIM=.FALSE.
117*            USELIM=.FALSE.
118*         403 CALL PLOTX(MODE,X,ICOUNT,UP,OVER,HEIGHT,LENGTH,BOX,FIXLIM,USELIM,
119*           1 NUMINT,YTITLE,HTITLE,LTRSZ,VLBND,VUBND,HLBND,HUBND,PERCNT)
120*          16 CONTINUE
121*       C    FUNCTION OF DISTANCE.
122*            WNR=WN(NF)-WN(NS)
123*            ELDASH=0.5/WNR
124*            IST=ELDASH+1.
125*            L=1
126*            YRS(NF+1)=YRS(NF)
127*            IF(XMIN-IST)86,86,84
128*         84 Y(L)=XMIN
129*            GO TO 88
130*         86 Y(L)=IST
131*       C DISTANCE LOOP BEGINS
132*         88 CONTINUE
133*            NN=NS
134*            RM=(Y(L)-0.04)/ELDASH
135*            M=RM
136*            XA=0.
137*            XB=0.
138*            WNT=(WN(NF+1)+WN(NF))/2.
139*            WNRR=WNR*M/RM
140*       C WNR=TOTAL WAVE NUMBER RANGE.
141*       C WNRR=A FUNCTION OF DISTANCE,IS THE RANGE REDUCED TO MAKE THE ANGLE AN INTEGER
142*       C *2*PI
143*            WNB=WNT-WNRR
144*            ATTER=1.+ATTEN*Y(L)
145*         85 IF(WN(NN+1)+WN(NN)-2.*WNB)81,91,95
146*         81 NN=NN+1
147*            GO TO 85
148*         95 IF(NN-1)301,301,89
149*        301 NN=NN+1
150*            GO TO 91
151*         89 IF (WN(NN)+WN(NN-1)-2.*WNB) 91,91,93
152*         93 NN=NN-1
153*            GO TO 95
154*         91 CONTINUE
155*            WNA=(WN(NN)+WN(NN+1))/2.-WNB
156*            WNSO=WN(NN-1)
157*            WNST=WN(NN)
158*            WN(NN)=WNB+WNA/2.
159*            WN(NN-1)=WNB-WNA/2.
160*       C       6
161*       C SINGLE DISTANCE INTEGRATION
162*            DO94N=NN,NF
163*            ALP=2.*(Y(L)-0.04)*WN(N)
164*       C ALPHA=4.*PI*Y(L)*WN(N) , NALP IS THE MULTIPLE OF 2.*PI REMOVED.
165*            NALP=ALP
166*            AA=1000.*(ALP-NALP)
167*            IF (AA) 90,90,92
168*         90 AA=AA+1000.
169*         92 NA=AA
170*            AANA=(AA-NA)
```

```
171*            SALP=S(NA)+(S(NA+1)-S(NA))*AANA
172*            NA=NA+250
173*            CALP=S(NA)+(S(NA+1)-S(NA))*AANA
174*            IP=1.+(WN(N)-WN(NN))*199./(WN(NF)-WN(NN))
175*            YRSPI=YRS(N)*P(IP)*(WN(N+1)-WN(N-1))
176*            XA=XA+YRSPI*CALP
177*            XB=XB+YRSPI*SALP
178*         94 CONTINUE
179*            WN(NN)=WNST
180*            WN(NN-1)=WNSO
181*            HL1=XA/(REFPT*WNRR*2.)
182*            HL2=XB/(REFPT*WNRR*2.)
183*            HLSO=HL1*HL1+HL2*HL2
184*            CORRN=ATTER/(1.-HLSO-REFPTS+HLSO*REFPTS)
185*            H(L,1)=HL1*CORRN
186*            H(L,2)=HL2*CORRN
187*            H(L,3)=SQRT(H(L,1)**2.+H(L,2)**2.)
188*            ANG=57.29578*ATAN(H(L,2)/H(L,1))
189*            IF (H(L,1)) 96,102,102
190*         96 IF (H(L,2)) 100,98,98
191*         98 H(L,4)=ANG+180.
192*            GO TO 104
193*        100 H(L,4)=ANG-180.
194*            GO TO 104
195*        102 H(L,4)=ANG
196*        104 CONTINUE
197*            NXL=Y(L)
198*            IF (Y(L)-NXL-0.01) 112,112,116
199*        112 IF (H(L,3)-0.005) 114,114,116
200*        114 Y(L+1)=Y(L)+0.5
201*            GO TO 118
202*        116 Y(L+1)=Y(L)+0.25
203*        118 L=L+1
204*            IF (XMAX-Y(L)) 122,122,88
205*      C        7
206*      C DISTANCE=LOOP ENDS
207*        122 CONTINUE
208*            LE=L-1
209*            WRITE(6,109)
210*        109 FORMAT(1H1,'Y(L)',6X,'A(N)',6X,'B(N)',3X,'MAG. REFPT. COEFF.',3X,
211*           1'PHASE ANG.',///)
212*        106 WRITE(6,108)(Y(L),(H(L,J),J=1,4),L=1,LE)
213*        108 FORMAT(F10.2,3F10.5,F10.1)
214*        110 CONTINUE
215*            IF (PLRF) 411,411,412
216*        412 CONTINUE
217*            DATA RTITLE/'DISTANCE IN CENTIMETERS
218*           2                                    '/
219*            DATA PTITLE/'MAGNITUDE OF AVERAGE REFLECTION COEFFICIENT
220*           2                                    '/
221*            DO404N=1,LE
222*            X(N)=H(N,3)
223*        404 CONTINUE
224*            AR=X(1)
225*            DO1000N=1,LE
226*            IF(X(N).GT.AR)AR=X(N)
227*       1000 CONTINUE
```

```
      VLBND=0.0
      VUBND=AR+.1*AR
      CALL PLOT(10.,-3.,-3)
      MODE=1
      LTRSZ=.1
      UP=3.
      OVER=0.
      LENGTH=5.
      HEIGHT=5.0
      HLBND=Y(1)
      HUBND=Y(LE)
      NUMINT=12
      ICOUNT=LE
      BOX=.TRUE.
      FIXLIM=.FALSE.
      USELIM=.FALSE.
      FIXLIM=.TRUE.
      USELIM=.TRUE.
      PERCNT=.99
      CALL PLOTY(MODE,X,Y,ICOUNT,UP,OVER,HEIGHT,LENGTH,BOX,FIXLIM,USELIM
     1 ,NUMINT,PTITLE,RTITLE,LTRSZ,VLBND,VUBND,HLBND,HUBND,PERCNT)
  411 CONTINUE
      IF (PLPX) 408,408,410
  410 CONTINUE
      DATA MTITLE/'PHASE ANGLE
     2                    '/
      DO406N=1,LE
      X(N)=H(N,4)
  406 CONTINUE
      MODE=1
      CALL PLOT(10.,-3.,-3)
      HEIGHT=5.
      LENGTH=5.
      LTRSZ=.1
      UP=3.
      OVER=0.
      HLBND=XMIN
      HUBND=Y(LE)
      ICOUNT=L
      BOX=.TRUE.
      FIXLIM=.TRUE.
      USELIM=.TRUE.
      VUBND=180.
      VLBND=-180.
      PERCNT=.99
      CALL PLOTY(MODE,X,Y,ICOUNT,UP,OVER,HEIGHT,LENGTH,BOX,FIXLIM,USELIM
     1 ,NUMINT,MTITLE,RTITLE,LTRSZ,VLBND,VUBND,HLBND,HUBND,PERCNT)
  408 CONTINUE
  600 CONTINUE
      CALL PLOT(0.0,0.0,999)
      END

END OF COMPILATION:        NO  DIAGNOSTICS.
```

Test 2

Statement Number	Label Number	Statement
1*		DIMENSION PTITLE(12)
2*		DIMENSION YL(20),B(10,50,4),P(200),ENN(6)
3*		DIMENSION FN(100)
4*		DIMENSION Y(100)
5*		DIMENSION IBUF(20000),NREF(100),NYU(100),YREF(100),YU(100),S(1260)
6*		1,CKS(100),FR(500),YRS(500),YR(100),WN(500),WL(500),H(100,4),X(100)
7*		2,HTITLE(12),VTITLE(12),RTITLE(12)
8*		DIMENSION ARYR(500)
9*		CALL PLOTS(IBUF(1),20000,2)
10*		WGW=0.9
11*		NS=1
12*		PI=3.1415926536
13*		RPV=56.6*PI/(6.928*180.)
14*		ATTEN=0.036*2.3026/(10.**12.*2.54)
15*		DO6N=1,500
16*		S(N)=SIN(N*PI/500.)
17*		S(N+500)=-S(N)
18*	6	CONTINUE
19*		DO8N=1,260
20*		S(N+1000)=S(N)
21*	8	CONTINUE
22*		READ(5,2000)NO
23*	2000	FORMAT(I2)
24*		READ(5,12)REFPT
25*	12	FORMAT(F10.5)
26*	C	XINCR IS THE INCREMENT IN CM. FROM THE LOCATION OF THE MISMATCH.
27*		READ(5,601)XINCR
28*	601	FORMAT(F10.5)
29*		REFPTS=REFPT*REFPT
30*		DO2001IJ=1,NO
31*	C	NF IS THE UPPER FREQUENCY LIMIT.
32*		READ(5,9)NF
33*	9	FORMAT(I3)
34*	C	XSET IS THE LOCATION IN CM. OF THE MISMATCH FROM THE REFERENCE.
35*		READ(5,602)XSET
36*	602	FORMAT(F10.5)
37*		READ(5,200)(NREF(N),N=1,NF)
38*		READ(5,201)(NYU(N),N=1,NF)
39*	200	FORMAT(4X,I4,1X,I4,1X,I4,1X,I4,1X,I4,1X,I4,1X,I4,1X,I4,1X,I4,1X,I4,1X,I4,1X,I4
40*		1,1X,I4,1X,I4,1X,I4,1X,I4,1X,I4,1X,I4,2X)
41*	201	FORMAT(4X,I4,1X,I4,1X,I4,1X,I4,1X,I4,1X,I4,1X,I4,1X,I4,1X,I4,1X,I4,1X,I4,1X,I4
42*		1,1X,I4,1X,I4,1X,I4,1X,I4,1X,I4,1X,I4,2X)
43*		DO500N=1,NF
44*		YREF(N)=NREF(N)/1000.
45*		YU(N)=NYU(N)/1000.
46*	500	CONTINUE
47*		FR(1)=7.975
48*		DO55N=1,200

```
      PANGLE=2.*PI*N/200
      P(N)=1.-0.889*COS(PANGLE)+0.0112*COS(2.*PANGLE)
      P(N)=1.
   55 CONTINUE
      DO202N=1,NF
      CKS(N)=(REFPT**2*COS(YREF(N)*RPV))/SIN(YREF(N)*RPV)
      YRS(N)=(CKS(N)*SIN(YU(N)*RPV))/COS(YU(N)*RPV)
      YR(N)=SQRT(YRS(N))
  202 CONTINUE
      NFP=NF+1
      DO1002N=1,461
      FR(N+1)=FR(N)+.010
      WN(N)=SQRT((FR(N)/29.9695)**2-(1./(2.*2.54*WGW))**2)
      WL(N)=1./WN(N)
 1002 CONTINUE
      J=1
      DO1000N=1,88
      DELY=YRS(N+1)-YRS(N)
      DO1001I=1,5
      ARYR(J)=YRS(N)+DELY*.2*(I-1)
      J=J+1
 1001 CONTINUE
 1000 CONTINUE
      ARYR(J)=YRS(89)
      NFF=J
      NF=NFF
      NFP=NFF+1
      DO1004N=1,NFP
      YRS(N)=ARYR(N)
 1004 CONTINUE
      YRSW=0.
      DO49N=NS,NF
      YRSW=YRSW+YRS(N)*(WL(N+1)-WL(N))
   49 CONTINUE
      YRSM=YRSW/(WL(NF+1)-WL(NS))
      DO50N=NS,NF
      YRS(N)=YRS(N)-YRSM
   50 CONTINUE
      YRS(NF+1)=YRS(NF)
      YL(1)=XSET-4.*XINCR
      NFF=NF
      NSS=NS
      CALL PLOT(0.0,3.0,-3)
      DO5000LL=1,10
C     PLOT AXIS.
      CALL PLOT(10.0,0.0,-3)
      CALL PLOT(0.0,2.203,3)
      CALL PLOT(4.406,2.203,2)
      CALL PLOT(2.203,0.0,3)
      CALL PLOT(2.203,4.406,2)
      CALL PLOT(0.0,0.0,3)
      YL(LL+1)=YL(LL)+XINCR
      WRITE(6,84)YL(LL)
   84 FORMAT(1H0,10X,'DISTANCE',F6.2,'  CM.')
      ATTFR=1.+ATTEN*YL(LL)
      XINT=100.
      IF(YL(LL).GT.21.) XINT=50.
```

```
106*            NF=NFF
107*            L=1
108*      C  BEGINNING OF NEW WAVENUMBER RANGE IDENTIFIED BY (L)
109*        302 NS=NF-XINT
110*            IF(NSS+1-NS)303,301,301
111*        303 CONTINUE
112*            NN=NS
113*            WNR=(WN(NF+1)+WN(NF)-WN(NS)-WN(NS-1))/2.
114*            ELDASH=0.5/WNR
115*            RM=(YL(LL)-0.04)/ELDASH
116*            M=RM
117*            IF(M)301,301,86
118*         86 XA=0.
119*            XB=0.
120*            WNRR=WNR*M/RM
121*            WNT=(WN(NF+1)+WN(NF))/2.
122*      C WNR=TOTAL WAVE NUMBER RANGE.
123*      C WNRR=A FUNCTION OF DISTANCE,IS THE RANGE REDUCED TO MAKE THE ANGLE AN INTEGER
124*      C *2*PI
125*            WNB=WNT-WNRR
126*         85 IF(WN(NN+1)+WN(NN)-2.*WNB)81,91,95
127*         81 NN=NN+1
128*            GO TO 85
129*         95 IF(NN-1)301,301,89
130*         89 IF (WN(NN)+WN(NN-1)-2.*WNB) 91,91,93
131*         93 NN=NN-1
132*            GO TO 95
133*         91 CONTINUE
134*            WNA=(WN(NN)+WN(NN+1))/2.-WNB
135*            WNSO=WN(NN-1)
136*            WNST=WN(NN)
137*            WN(NN)=WNB+WNA/2.
138*            WN(NN-1)=WNB-WNA/2.
139*            ENN(1)=WNT
140*            ENN(2)=WNB
141*            ENN(3)=WNA
142*      C        6
143*            DO94N=NN,NF
144*            ALP=2.*(YL(LL)-0.04)*WN(N)
145*            NALP=ALP
146*            AA=1000.*(ALP-NALP)
147*            IF(AA)222,222,223
148*        222 AA=AA+1000.
149*        223 NA=AA
150*            AANA=(AA-NA)
151*            SALP=S(NA)+(S(NA+1)-S(NA))*AANA
152*            NA=NA+250
153*            CALP=S(NA)+(S(NA+1)-S(NA))*AANA
154*            IP=1.+(WN(N)-WN(NN))*199./(WN(NF)-WN(NN))
155*            YRSPI=YRS(N)*P(IP)*(WN(N+1)-WN(N-1))
156*            ENN(4)=XA
157*            ENN(5)=XB
158*            XA=XA+YRSPI*CALP
159*            XB=XB+YRSPI*SALP
160*         94 CONTINUE
161*            WN(NN)=WNST
162*            WN(NN-1)=WNSO
```

```
163*            HL1=XA/(REFPT*WNRR*2.)
164*            HL2=XB/(REFPT*WNRR*2.)
165*            HLSQ=HL1**2+HL2**2
166*            CORRN=ATTFR/(1.-HLSQ-REFPTS+HLSQ*REFPTS)
167*       C  THE FOLLOWING NEG. SIGN CONVERTS FROM IMPEDANCE SMITH CHART TO
168*       C  ADMITTANCE SMITH CHART.
169*            H(L,1)=-HL1*CORRN
170*            H(L,2)=-HL2*CORRN
171*            B(LL,L,3)=SQRT(H(L,1)**2+H(L,2)**2)
172*       C    PREPARATION FOR THE SMITH CHART PLOT.
173*            ANG=ABS(ATAN(H(L,2)/H(L,1)))
174*            IF(H(L,2))700,701,701
175*        701 IF(H(L,1))703,702,702
176*        702 ANG=ANG
177*            GO TO 710
178*        703 ANG=PI-ANG
179*            GO TO 710
180*        700 IF(H(L,1))704,705,705
181*        704 ANG=ANG+PI
182*            GO TO 710
183*        705 ANG=2.*PI-ANG
184*        710 CONTINUE
185*            B(LL,L,4)=ANG*57.29578
186*            FN(L)=29.9695*SQRT((WN(NF)-WNRR/2.)**2+(1./(5.08*WGW))**2)
187*            X(L)=2.203+(H(L,1)*2.203/.22)
188*            Y(L)=2.203+(H(L,2)*2.203/.22)
189*       C    PLOT CURVE WITH 9,10,11,12 GHZ MARKERS.
190*            IF(L-1)950,950,951
191*        950 CALL PLOT(X(1),Y(1),3)
192*        951 CONTINUE
193*            AL=ABS(FN(L)-9.001)
194*            IF(AL-.05)507,507,512
195*        512 AL=ABS(FN(L)-10.001)
196*            IF(AL-.05)508,508,513
197*        513 AL=ABS(FN(L)-11.001)
198*            IF(AL-.05)509,509,514
199*        514 AL=ABS(FN(L)-12.001)
200*            IF(AL-.05)510,510,506
201*        507 CALL SYMBOL(X(L),Y(L),.07,1,0.0,-1)
202*            CALL SYMBOL(X(L),Y(L),.1,8H 9.0 GHZ,0.0,8)
203*            GO TO 506
204*        508 CALL SYMBOL(X(L),Y(L),.07,1,0.0,-1)
205*            CALL SYMBOL(X(L),Y(L),.1,9H 10.0 GHZ,0.0,9)
206*            GO TO 506
207*        509 CALL SYMBOL(X(L),Y(L),.07,1,0.0,-1)
208*            CALL SYMBOL(X(L),Y(L),.1,9H 11.0 GHZ,0.0,9)
209*            GO TO 506
210*        510 CALL SYMBOL(X(L),Y(L),.07,1,0.0,-1)
211*            CALL SYMBOL(X(L),Y(L),.1,9H 12.0 GHZ,0.0,9)
212*        506 CONTINUE
213*            CALL PLOT(X(L),Y(L),2)
214*       C    END OF SMITH CHART PLOT.
215*            LE=L
216*            NF=NF-10
217*            L=L+1
218*       C  END OF REFLECTION COEFFICIENT AS A FUNCTION OF FREQ. AT DIST.YL
219*            GO TO 302
```

```
220*        301 CONTINUE
221*            IF(LL.NE.5)GO TO 5000
222*            WRITE(1,1071)LE
223*       1071 FORMAT(I2)
224*            WRITE(1,1070)(FN(I),I=LE,1,-1)
225*       1070 FORMAT(8F10.4)
226*            WRITE(1,1072)(H(I,1),I=1,LE)
227*            WRITE(1,1072)(H(I,2),I=1,LE)
228*       1072 FORMAT(8F10.6)
229*       5000 CONTINUE
230*            WRITE(6,952)
231*        952 FORMAT(1H1,10X,'FREQUENCY',10X,'MAGNITUDE OF REFLECTION COEFFICIEN
232*           1T',///)
233*            DO1010L=1,LE
234*            WRITE(6,953)(FN(L),(B(LL,L,3),LL=1,10))
235*        953 FORMAT(10X,F6.3,10X,10F10.4)
236*       1010 CONTINUE
237*            WRITE(6,960)
238*        960 FORMAT(1H1,10X,'FREQUENCY',10X,'PHASE ANGLE',///)
239*            DO1020L=1,LE
240*            WRITE(6,1021)(FN(L),(B(LL,L,4),LL=1,10))
241*       1021 FORMAT(10X,F6.3,10X,10F10.4)
242*       1020 CONTINUE
243*            DO229J=1,LE
244*            I=LE+1-J
245*            X(J)=B(5,I,3)
246*        229 CONTINUE
247*            DO231J=1,LE
248*            I=LE+1-J
249*            Y(J)=FN(I)
250*        231 CONTINUE
251*            REAL LTRSZ,LENGTH
252*            LOGICAL BOX,FIXLIM,USELIM
253*            DATA HTITLE/'FREQUENCY IN GHZ.
254*           2                    '/
255*            DATA VTITLE/'MAGNITUDE OF REFLECTION COEFFICIENT
256*           2                    '/
257*            CALL PLOT(10.,-3.,-3)
258*            MODE=1
259*            LTRSZ=.1
260*            UP=4.5
261*            OVER=0.
262*            HEIGHT=5.
263*            LENGTH=5.
264*            HLBND=Y(1)
265*            HUBND=Y(LE)
266*            ICOUNT=LE
267*            BOX=.TRUE.
268*            USELIM=.FALSE.
269*            FIXLIM=.FALSE.
270*            USELIM=.TRUE.
271*            FIXLIM=.TRUE.
272*            VLBND=0.
273*            VUBND=.2
274*            NUMINT=16
275*            PERCNT=.9
276*            CALL PLOTY(MODE,X,Y,ICOUNT,UP,OVER,HEIGHT,LENGTH,BOX,FIXLIM,USELIM
```

```
     1 ,NUMINT,VTITLE,HTITLE,LTRSZ,VLBND,VUBND,HLBND,HUBND,PERCNT)
      DO230J=1,LE
      I=LE+1-J
      X(J)=B(5,I,4)
  230 CONTINUE
      CALL PLOT(10.,-3.,-3)
      DATA HTITLE/'FREQUENCY IN GHZ.
     2                    '/
      DATA RTITLE/'ANGLE IN DEGREES
     2                    '/
      MODE=1
      LTRSZ=.1
      UP=4.5
      OVER=0.
      HEIGHT=5.
      LENGTH=5.
      HUBND=Y(LE)
      HLBND=Y(1)
      PERCNT=.9
      ICOUNT=LE
      BOX=.TRUE.
      USELIM=.FALSE.
      FIXLIM=.FALSE.
      VUBND=180.
      VLBND=-180.
      NUMINT=16
      CALL PLOTY(MODE,X,Y,ICOUNT,UP,OVER,HEIGHT,LENGTH,BOX,FIXLIM,USELIM
     1 ,NUMINT,RTITLE,HTITLE,LTRSZ,VLBND,VUBND,HLBND,HUBND,PERCNT)
 1006 DO1007LL=1,10
      DO1008L=1,LE
      J=LE+1-L
      B(LL,L,1)=B(LL,J,4)
 1008 CONTINUE
 1007 CONTINUE
      CALL PLOT(10.,-3.,-3)
      DATA PTITLE/'DISTANCE IN CM.
     2                    '/
      LTRSZ=.1
      UP=4.5
      OVER=0
      HEIGHT=5.
      LENGTH=5.
      HLBND=YL(1)
      HUBND=YL(10)
      PERCNT=.9
      ICOUNT=10
      BOX=.TRUE.
      USELIM=.TRUE.
      FIXLIM=.TRUE.
      VUBND=360.
      VLBND=0.0
      NUMINT=6
      DO1011I=1,4
      MODE=1
      IF(I.GT.1)MODE=4
      FM=9.0+I-1
      LF=5
```

```
334*            IF(I.GT.1)LF=12
335*            IF(I.GT.2)LF=16
336*            IF(I.GT.3)LF=23
337*            DO1012LL=1,10
338*            X(LL)=B(LL,LF,1)
339*       1012 CONTINUE
340*            CALL PLOTX(MODE,X,ICOUNT,UP,OVER,HEIGHT,LENGTH,BOX,FIXLIM,USELIM,
341*           1 NUMINT,RTITLE,PTITLE,LTRSZ,VLBND,VUBND,HLBND,HUBND,PERCNT)
342*       1011 CONTINUE
343*        600 CONTINUE
344*       2001 CONTINUE
345*            CALL PLOT(0.0,0.0,999)
346*            END

END OF COMPILATION:        NO  DIAGNOSTICS.
```

Matching Program

```
Statement  Label
Number     Number                    Statement
    1*                DIMENSION D(100)
    2*                DIMENSION REL(100)
    3*                DIMENSION FR(90),WN(90),WL(90),FSWL(90),DP(4),WIDTH(4),ALENGH(4)
    4*                DIMENSION AA(90),CO(90),SI(90),ARMS(3,3,3),SE(90),BETA(90)
    5*                DIMENSION XREL(90),YIMAG(90)
    6*                DIMENSION IBUF(20000),X(90),Y(90),HTITLE(12),VTITLE(12)
    7*                DIMENSION ALPHA(3,90),BETE(3,90),BESOA(3,90),BESOB(3,90),BESIA(3,9
    8*               10),BESIB(3,90),SOP(3,90),SII(3,90)
    9*                COMPLEX GAM(90),AGAM(4,90),GAMMA(90),GAMMAH,BGAM,YI,ZII,YT
   10*                COMPLEX GGAM(3,3,90,3)
   11*                COMPLEX ZI,ZT
   12*                COMPLEX XGAM(100)
   13*                COMPLEX YII
   14*      CTHIS PROGRAM DETERMINES THE DIMENSIONS OF THE DESIGNATED
   15*                CALL PLOTS(IBUF(1),20000,2)
   16*      C  MATCHING ELEMENT, IN ORDER TO IMPEDANCE MATCH THE MEASURED
   17*      C  MISMATCH.
```

```
18*      C  LIST OF CONSTANTS.
19*             PI=3.1415926536
20*             C=2.998*(10**10)
21*      C  WAVEGUIDE WIDTH IN INCHES=WGW
22*             WGW=0.9
23*             A=WGW*2.54
24*      C  WAVEGUIDE HEIGHT IN INCHES=WGH.
25*             WGH=.4
26*             B=WGH*2.54
27*      C  E IS THE BASE OF THE NATURAL LOG.
28*             E=2.7182818284
29*             SQTWO=SQRT(2.)
30*     C*************************************************************************
31*     C*************************************************************************
32*     C** THE VALUE OF THE FIRST DATA CARD IS MACHEL.                          **
33*     C** THE VALUE OF MACHEL SELECTS THE TYPE OF MATCHING ELEMENT.            **
34*     C** THE VALUE OF MACHEL MAY BE 1 OR 2 OR 3 OR 4 WHERE                   **
35*     C** 1 CORRESPONDS TO THE CAPACITIVE IRIS.                                **
36*     C** 2 CORRESPONDS TO THE ASYMMETRICAL IND. IRIS.                         **
37*     C** 3 CORRESPONDS TO THE SOLID INDUCTIVE POST.                           **
38*     C** 4 CORRESPONDS TO THE DIELECTRIC POST.                                **
39*     C*************************************************************************
40*     C*************************************************************************
41*      C  DATA CARD ORDER.
42*      C  FIRST DATA CARD=MACHEL
43*      C  SECOND DATA CARD=EPRIM
44*      C  THIRD DATA CARD=LE(NO OF DATA POINTS)
45*      C  FREQ. DATA CARDS
46*      C  REAL AND IMAGINARY PARTS OF UNMATCHED REFLECTION COEFF.
47*      C  BAND LIMITS TO BE MATCHED OVER.
48*      C  NOO'' THE NUMBER OF TIMES THE DEVICE IS TO BE MATCHED
49*      C  ALENGH THE STARTING VALUE FOR LENGTH DOWN THE GUIDE.
50*      C  NOTE'' THE NUMBER OF ALENGH DATA CARDS SHOULD BE = TO THE NO.'NOO
51*             READ(5,560)MACHEL
52*          560 FORMAT(I1)
53*      C  EPRIM IS THE RELATIVE DIELECTRIC CONSTANT FOR THE DIELECTRIC POST.
54*             READ(5,601)EPRIM
55*          601 FORMAT(F10.3)
56*             READ(5,1010)LE
57*         1010 FORMAT(I2)
58*             WRITE(6,2050)MACHEL,LE
59*         2050 FORMAT(1H1,///,10X,'MACHEL =',I1,10X,'NUMBER OF DATA POINTS =',I3)
60*             READ(5,1011)(FR(I),I=1,LE)
61*         1011 FORMAT(8F10.4)
62*             READ(5,1)(XREL(I),I=1,LE)
63*             READ(5,1)(YIMAG(I),I=1,LE)
64*           1 FORMAT(8F10.4)
65*             WRITE(6,2052)
66*         2052 FORMAT(///,10X,'REAL PART OF THE MISMATCH',///)
67*             WRITE(6,2051)(XREL(I),I=LE,1,-1)
68*         2051 FORMAT(10X,8F10.7)
69*             WRITE(6,2053)
70*         2053 FORMAT(///,10X,'IMAGINARY PART OF THE MISMATCH',///)
71*             WRITE(6,2051)(YIMAG(I),I=LE,1,-1)
72*             DO8N=1,LE
73*             GAM(N)=XREL(N)+(0,1)*YIMAG(N)
74*           8 CONTINUE
```

```
      DO1020N=1,LE
      I=LE+1-N
      XGAM(N)=GAM(I)
 1020 CONTINUE
      DO1021N=1,LE
      GAM(N)=XGAM(N)
 1021 CONTINUE
C  FRBEG AND FREND ARE THE FREQUENCY BAND LIMITS IN GHZ. OF THE MATCHING
C  BANDWIDTH OF INTEREST.
      READ(5,3)FRBEG,FREND
    3 FORMAT(2F10.3)
      DO4I=1,LE
      DIF=ABS(FRBEG-FR(I))
      IF(DIF.LE.0.07)GO TO 5
    4 CONTINUE
    5 JBEG=I
      DO6I=1,LE
      DIF=ABS(FREND-FR(I))
      IF(DIF.LE.0.07)GO TO 7
    6 CONTINUE
    7 JEND=I
      IF(JBEG.GE.JEND)JBEG=1
C  FR IS FREQUENCY IN GHZ.
C  WN IS INSUIDE WAVENUMBER IN CM.
C  WL IS INSUIDE WAVELENGTH IN CM.
C  FSWL IS FREE SPACE WAVELENGTH IN CM.
      DO2I=1,LE
      WN(I)=SQRT((FR(I)/29.9695)**2-(1./(2.*2.54*WGW))**2)
      WL(I)=1./WN(I)
      FSWL(I)=29.9695/FR(I)
      BETA(I)=2.*PI/WL(I)
    2 CONTINUE
C  INITIAL VALUES FOR THE PHYSICAL PARAMETERS OF THE MATCHING ELEMENT.
      READ(5,4001)NOO
 4001 FORMAT(I2)
      DO3002NR=1,NOO
      READ(5,4000)ALENGH(1)
 4000 FORMAT(F10.5)
      WRITE(6,5001)ALENGH(1)
 5001 FORMAT(///,10X,'STARTING VALUE OF ALENGH = ',F10.4)
      MM=0
      DP(1)=.32
      IF(MACHEL.GE.3)DP(1)=.16
      WIDTH(1)=.05
      IF(MACHEL.GE.3)WIDTH(1)=.47
C  INCREMENT PHYSICAL PARAMETERS AROUND THE (I,I,1) POINT IN
C  DIMENSION SPACE.
C  THIS PROGRAM PREFORMS AN INCREMENTING ADJUSTMENT TO ZOOM IN.
      ANCRMT=1.
      IF(MACHEL.LT.3)ANUMBR=.1
      IF(MACHEL.GE.3)ANUMBR=.05
      GO TO 250
  350 ANCRMT=ANCRMT*2.
  250 DP(2)=DP(1)-ANUMBR/ANCRMT
      FALBD=DP(1)
      FALBW=WIDTH(1)
      IF(DP(2).LT..04.AND.MACHEL.LT.3)DP(2)=FALBD
```

```
132*            IF(DP(2).LT..005.AND.MACHEL.GE.3)DP(2)=FALBD
133*            DP(3)=DP(1)+ANUMBR/ANCRMT
134*            WIDTH(2)=WIDTH(1)-.01/ANCRMT
135*            IF(WIDTH(2).LT..03.AND.MACHEL.LT.3)WIDTH(2)=FALBW
136*            IF(WIDTH(2).LT..46.AND.MACHEL.GE.3)WIDTH(2)=FALBW
137*            WIDTH(3)=WIDTH(1)+.01/ANCRMT
138*            ALENGH(2)=ALENGH(1)-.1/ANCRMT
139*            ALENGH(3)=ALENGH(1)+.1/ANCRMT
140*      C  RETURN TO RECALCULATION.
141*      C  FIXED MISMATCH IS GAM.
142*      C  THE FIXED MISMATCH AT A POINT ALENGH TOWARD THE GENERATOR IS AGAM.
143*            DO302M=1,3
144*            DO303N=JBEG,JEND
145*            AGAM(M,N)=GAM(N)*CEXP((0,-1)*2.*BETA(N)*ALENGH(M))
146*            IF(ALENGH(M).LT.0.)AGAM(M,N)=GAM(N)
147*        303 CONTINUE
148*        302 CONTINUE
149*            GO TO (399,499,599,699),MACHEL
150*      C*****************************************************************
151*        399 CONTINUE
152*      C  MATCHING ELEMENT''CAPACITIVE IRIS''COMPLEX REFLECTION COEFF.
153*      C  AS A FUNCTION OF DIMENSION SPACE AND FREQUENCY.
154*            DO300L=JBEG,JEND
155*            AB=SQRT(1.-(B/WL(L))**2)
156*            AA(L)=(1./AB)-1.
157*        300 CONTINUE
158*      C  WIDTH(I) IS EQUAL TO THE THICKNESS OF THE IRIS.
159*      C  DP(I) IS EQUAL TH TWICE THE IRIS HEIGHT.
160*            DO252J=1,3
161*            D(J)=B-DP(J)
162*            DO251I=1,3
163*            IF(I.EQ.1.AND.J.EQ.1.OR.I.EQ.1.AND.J.EQ.2.OR.I.EQ.1.AND.J.EQ.3.OR.
164*           1I.EQ.2.AND.J.EQ.1.OR.I.EQ.3.AND.J.EQ.1)GO TO 2003
165*            GO TO 251
166*       2003 CONTINUE
167*            COND=WIDTH(I)/DP(J)
168*            IF(COND.GE.1.)DP(J)=FALBD
169*            IF(COND.GE.1.)WIDTH(I)=FALBW
170*            GM=1.+(WIDTH(I)/(PI*DP(J)))*ALOG(4.*PI*DP(J)/(E*WIDTH(I)))
171*            CO(J)=COS(PI*DP(J)/(2.*B))
172*            SI(J)=SIN(PI*DP(J)/(2.*B))
173*            SE(J)=1./COS(PI*DP(J)*GM/(2.*B))
174*            DO301KK=JBEG,JEND
175*            BONE=PI*DP(J)*WIDTH(I)/(2.*B*D(J))
176*            BTWO=AA(KK)*(SI(J)**4)/(1.+AA(KK)*(CO(J)**4))
177*            BTRE=(1./16.)*((B/WL(KK))**2)*((1.-3.*(CO(J)**2))**2)*(SI(J)**4)
178*            BNORM=(2.*B/WL(KK))*(ALOG(SE(J))-BONE+BTWO+BTRE)
179*            BA=BNORM+(B/D(J))*TAN(PI*WIDTH(I)/WL(KK))
180*            BB=(B/D(J))*1./SIN(2.*PI*WIDTH(I)/WL(KK))
181*            YI=(0,1)*BA+1.
182*            ZII=((0,1)/BB)+1./YI
183*            YT=(0,1)*BA+1./ZII
184*            DO260N=1,3
185*            BGAM=(YT-1.)/(1.+YT)
186*            GGAM(I,J,KK,N)=BGAM*CEXP((0,1)*2.*BETA(KK)*ALENGH(N))
187*            IF(ALENGH(N).GE.0.)GGAM(I,J,KK,N)=BGAM
188*        260 CONTINUE
```

```
189*      C  I CORRES. TO THICKNESS OF THE IRIS.
190*      C  J CORRES TO HEIGHT OF IRIS.
191*      C  KK CORRES TO FREQUENCY.
192*      C  GGAM IS THE COMPLEX REFLECTION COEFF. AS PER. ADMITTANCE.
193*      C  SMITH CHART PLOT.
194*        301 CONTINUE
195*        251 CONTINUE
196*        252 CONTINUE
197*            GO TO 404
198*      C*************************************************************************
199*        499 CONTINUE
200*      C  MATCHING ELEMENT 'ASYMMETRICAL INDUCTIVE IRIS' COMPLEX REFLECTION
201*      C  AS A FUNCTION OF DIMENSION SPACE AND FREQUENCY.
202*            DO400I=1,3
203*            DO401J=1,3
204*            IF(I.EQ.1.AND.J.EQ.1.OR.I.EQ.1.AND.J.EQ.2.OR.I.EQ.1.AND.J.EQ.3.OR.
205*           1I.EQ.2.AND.J.EQ.1.OR.I.EQ.3.AND.J.EQ.1)GO TO 2007
206*            GO TO 401
207*       2007 CONTINUE
208*            COND=WIDTH(I)/DP(J)
209*            IF(COND.GE.1.)DP(J)=FALBD
210*            IF(COND.GE.1.)WIDTH(I)=FALBW
211*            CAPDP=(DP(J)/SQTWO)*(1.+(WIDTH(I)/(PI*DP(J)))*ALOG(4.*PI*DP(J)/(E*
212*           1WIDTH(I))))
213*            CAPD=((4./(3.*PI))*WIDTH(I)*DP(J)**3)**(1./4.)
214*            DO402KK=JBEG,JEND
215*      C  XA AND XB ARE NORMALIZED IMPEDANCES.
216*            XA=(4.*A/WL(KK))*((A/(PI*CAPDP))**2)
217*            XB=(A/(16.*WL(KK)))*((PI*CAPD/A)**2)
218*            ZI=(0,-1)*XB+1.
219*            ZII=(1./((1./((0,1)*XA))+1./ZI))
220*            ZT=(0,-1)*XB+ZII
221*            BGAM=(1.-ZT)/(1.+ZT)
222*            DO403N=1,3
223*            GGAM(I,J,KK,N)=BGAM*CEXP((0,1)*2.*BETA(KK)*ALENGH(N))
224*            IF(ALENGH(N).GE.0.)GGAM(I,J,KK,N)=BGAM
225*        403 CONTINUE
226*      C  I CORRES. TO THICKNESS OF THE IRIS.
227*      C  J CORRES. TO HEIGHT OF IRIS.
228*      C  KK CORRES. TO FREQUENCY.
229*      C  GGAM IS THE COMPLEX REFLECTION COEFF. AS PER ADMITTANCE
230*      C  SMITH CHART PLOT.
231*        402 CONTINUE
232*        401 CONTINUE
233*        400 CONTINUE
234*            GO TO 404
235*      C*************************************************************************
236*        599 CONTINUE
237*      C  MATCHING ELEMENT 'SOLID INDUCTIVE POST' COMPLEX REFLECTION COEFF.
238*      C  AS A FUNCTION OF DIMENSION P
239*      C  AS A FUNCTION OF DIMENSION SPACE AND FREQUENCY.
240*      C  DP(I) IS DEFINED TO BE THE DIAMETER OF THE POST.
241*      C  WIDTH(I) IS DEFINED TO BE THE DISTANCE OF THE CENTER LINE OF THE POST
242*      C  FROM THE SIDE-WALL.
243*            DO540I=1,3
244*            IF(WIDTH(I).GT.1.82)WIDTH(I)=FALBW
245*            DO541KK=JBEG,JEND
```

```
246*            N=2
247*            M=2
248*            XSII=0.0
249*            XSOO=0.0
250*        543 XI=SQRT(1./((N**2)-((2.*A/FSWL(KK))**2)))
251*            XSO=((SIN(N*PI*WIDTH(I)/A))**2)*(XI-1./N)
252*            XSOO=XSO+XSOO
253*            IF(XSO.LE..001)GO TO 545
254*        544 N=N+1
255*            GO TO 543
256*        545 XI=SQRT(M**2/((M**2)-((2.*A/FSWL(KK))**2)))
257*            XSI=((SIN(2.*M*PI*WIDTH(I)/A))*(XI-1.))
258*            XSII=XSI+XSII
259*            ABXSI=ABS(XSI)
260*            IF(ABXSI.LE..001)GO TO 547
261*        546 M=M+1
262*            GO TO 545
263*        547 CONTINUE
264*            SOP(I,KK)=XSOO*2.-2.*((SIN(PI*WIDTH(I)/A))**2)
265*            SII(I,KK)=XSII+(.5*(1./TAN(PI*WIDTH(I)/A))-SIN(2.*PI*WIDTH(I)/A))
266*        541 CONTINUE
267*        540 CONTINUE
268*            DO548I=1,3
269*            CT=1./TAN(PI*WIDTH(I)/A)
270*            CSS=(1./SIN(PI*WIDTH(I)/A))**2
271*            SNS=(SIN(PI*WIDTH(I)/A))**2
272*            DO549J=1,3
273*            IF(I.EQ.1.AND.J.EQ.1.OR.I.EQ.1.AND.J.EQ.2.OR.I.EQ.1.AND.J.EQ.3.OR.
274*           1I.EQ.2.AND.J.EQ.1.OR.I.EQ.3.AND.J.EQ.1)GO TO 2008
275*            GO TO 549
276*       2008 CONTINUE
277*            IF(DP(J).GE..22)DP(J)=FALBD
278*            IF(DP(J).LE..0)GO TO 200
279*            PDOA=(PI*DP(J)/A)**2
280*            PDO=(PI*DP(J)/(A*2.))**2
281*            SOPP=ALOG((4.*A/(PI*DP(J))*SIN(PI*WIDTH(I)/A)))
282*            DO550KK=JBEG,JEND
283*        C   XA AND XB ARE NORMALIZED IMPEDANCES.
284*            XB=(A/WL(KK))*PDOA*SNS
285*            XA=XB/2.+A/(2.*WL(KK))*CSS*(SOPP+SOP(I,KK)-((PI*DP(J)/(2.*A))**2)*
286*           1(((SOPP+SOP(I,KK))*CT-SII(I,KK))**2))
287*            ZI=(0.,-1)*XB+1.
288*            ZII=(1./((1./((0.,1)*XA))+1./ZI))
289*            ZT=(0.,-1)*XB+ZII
290*            BGAM=(1.-ZT)/(ZT+.1)
291*            DO551K=1,3
292*            GGAM(I,J,KK,K)=BGAM*CEXP((0.,1)*2.*BETA(KK)*ALENGH(K))
293*            IF(ALENGH(K).GE.0.0)GGAM(I,J,KK,K)=BGAM
294*        551 CONTINUE
295*        C   I CORRES TO DISTANCE OF POST FROM SIDE WALL.
296*        C   J CORRES TO DIAMETER OF POST.
297*        C   KK CORRES TO FREQUENCY.
298*        C   K CORRES TO DISTANCE BETWEEN MISMATCHES.
299*        550 CONTINUE
300*        549 CONTINUE
301*        548 CONTINUE
302*            GO TO 404
```

```
303*      C*************************************************************************
304*        699 CONTINUE
305*      C  MATCHING ELEMENT 'DIELECTRIC POST' COMPLEX REFLECTION COEFF.
306*      C  AS A FUNCTION OF DIMENSION SPACE AND FREQUENCY, GIVEN THE DIELECTRIC.
307*            SQEPRM=SQRT(EPRIM)
308*      C  DP IS DEFINED TO BE THE DIAMETER OF THE DIELECTRIC POST.
309*      C  WIDTH IS DEFINED TO BE THE DISTANCE FROM THE SIDEWALL TO THE CENTER-
310*      C  LINE OF THE POST.
311*      C  BESLA IS THE BESSEL FUNCTION WITH ALPHA AS ITS ARGUMENT.
312*      C  BESLB IS THE BESSEL FUNCTION WITH BETE AS ITS ARGUMENT.
313*            DO602J=1,3
314*            IF(DP(J).GE..342)DP(J)=FALBD
315*            DO603N=JBEG,JEND
316*            ALPHA(J,N)=PI*DP(J)/FSWL(N)
317*            BETE(J,N)=ALPHA(J,N)*SQEPRM
318*            BESOA(J,N)=BSSL(ALPHA(J,N),1)
319*            BESOB(J,N)=BSSL(BETE(J,N),1)
320*            BESIA(J,N)=BSSL(ALPHA(J,N),3)
321*            BESIB(J,N)=BSSL(BETE(J,N),3)
322*      C  J CORRES TO DIAMETER, N CORRES TO FREE-SPACE WAVELENGTH.
323*          603 CONTINUE
324*          602 CONTINUE
325*      C  CALCULATE SO THE PARTIAL SUM.
326*      C  I CORRES TO DISTANCE FROM SIDEWALL.
327*      C  L CORRES TO FREE-SPACE WAVELENGTH.
328*            DO604I=1,3
329*            IF(WIDTH(I).LT..46)WIDTH(I)=WIDTH(1)
330*            DO605L=JBEG,JEND
331*            N=2
332*            XS00=0.0
333*          606 XI=SQRT(1./((N**2)-((2.*A/FSWL(L))**2)))
334*            XSO=((SIN(N*PI*WIDTH(I)/A))**2)*(XI-1./N)
335*            XS00=XSO+XS00
336*            IF(XSO.LE..001)GO TO 608
337*          607 N=N+1
338*            GO TO 606
339*          608 CONTINUE
340*            SOP(I,L)=XS00*2.-2.*((SIN(PI*WIDTH(I)/A))**2)
341*          605 CONTINUE
342*          604 CONTINUE
343*      C  CALCULATE THE SHUNT AND SERIES IMPEDANCE FOR THE POST MODEL.
344*            DO609I=1,3
345*            DO610J=1,3
346*            IF(I.EQ.1.AND.J.EQ.1.OR.I.EQ.1.AND.J.EQ.2.OR.I.EQ.1.AND.J.EQ.3.OR.
347*           1I.EQ.2.AND.J.EQ.1.OR.I.EQ.3.AND.J.EQ.1)GO TO 2009
348*            GO TO 610
349*         2009 CONTINUE
350*      C  I CORRES TO DISTANCE FROM THE SIDEWALL.
351*      C  J CORRES TO DIAMETER OF DIELECTRIC.
352*            SOPP=ALOG((4.*A/(PI*DP(J))*SIN(PI*WIDTH(I)/A)))
353*            DO611M=JBEG,JEND
354*      C  M CORRES TO FREQ.
355*            XB=(2.*A/WL(M))*((PI*DP(J)/A)**2)*(SIN(PI*WIDTH(I)/A)**2)/(((ALPHA
356*           1(J,M)**2)*BESIB(J,M)/BESIA(J,M))+(1./(ALPHA(J,M)*BESOA(J,M)*
357*           2BESIB(J,M)-BETE(J,M)*BESOB(J,M)*BESIA(J,M)))-2.)
358*            XA=.5*XB+(A/(2.*WL(M)))*(1./(SIN(PI*WIDTH(I)/A)**2))*((BESOB(J,M)/
359*           1BESOA(J,M))*(1./(BETE(J,M)*BESOA(J,M)*BESIB(J,M)-ALPHA(J,M)*
```

```
360*          2BESOB(J,M)*RESIA(J,M)))-(SOPP+SOP(I,M))+(ALPHA(J,M)/4.))
361*           YI=1./((0,1)*XB+1.)
362*           YII=1./((0,-1)*XA)+YI
363*           YT=1./((0,1)*XB+1./YII)
364*           BGAM=(YT-1.)/(1.+YT)
365*           DO612N=1,3
366*           GGAM(I,J,M,N)=BGAM*CEXP((0,1)*2.*BETA(M)*ALENGH(N))
367*           IF(ALENGH(N).GE.0.)GGAM(I,J,M,N)=BGAM
368*       612 CONTINUE
369*     C  GGAM IS THE COMPLEX REFLECTION COEFF AS PER ADMITTANCE SMITH CHART.
370*       611 CONTINUE
371*       610 CONTINUE
372*       609 CONTINUE
373*           GO TO 404
374*     C*****************************************************************
375*       404 CONTINUE
376*     C  CALCULATE THE MISMATCH AND THE RMS OF THE MISMATCH.  THEN DETERMINE
377*     C  THE SMALLEST VALUE AND EXIT OR RETURN TO INCREMENT IN DIM. SPACE.
378*           DO201I=1,3
379*           DO202J=1,3
380*           DO203K=1,3
381*           IF(I.EQ.1.AND.J.EQ.1.AND.K.EQ.1.OR.I.EQ.1.AND.J.EQ.1.AND.K.EQ.2.OR
382*          1.I.EQ.1.AND.J.EQ.1.AND.K.EQ.3.OR.I.EQ.1.AND.J.EQ.2.AND.K.EQ.1.OR.I
383*          2.EQ.1.AND.J.EQ.3.AND.K.EQ.1.OR.I.EQ.2.AND.J.EQ.1.AND.K.EQ.1.OR.I.E
384*          3Q.3.AND.J.EQ.1.AND.K.EQ.1)GO TO 2001
385*           GO TO 203
386*      2001 CONTINUE
387*           PARTSM=0.0
388*           DO204N=JBEG,JEND
389*           GAMMAH=(AGAM(K,N)+GGAM(I,J,N,K)-2.*AGAM(K,N)*GGAM(I,J,N,K))/(1.-AG
390*          1AM(K,N)*GGAM(I,J,N,K))
391*           SNGLVL=(CABS(GAMMAH))**2
392*           PARTSM=PARTSM+SNGLVL
393*       204 CONTINUE
394*           RS=SQRT(PARTSM)
395*           ARMS(I,J,K)=(1./SQRT(JEND-JBEG))*RS
396*     C  THE ROOT MEAN SQ. OF THE MISMATCH OVER THE BAND OF INTEREST HAS BEEN
397*     C  CALCULATED.
398*       203 CONTINUE
399*       202 CONTINUE
400*       201 CONTINUE
401*     C  DETERMINE THE SMALLEST VALUE OF ARMS(I,J,K),AND SET IT EQUAL TO THE
402*     C  CENTER POINT IN DIMENSION SPACE.
403*     C  ARMS IS THE ROOT MEAN SQUARE MISMATCH OVER THE BAND OF INTEREST.
404*     C  DETERMINEATION OF THE LEAST OF THE ARMS ENSEMBLE.
405*           ATEST=ARMS(1,1,1)
406*           DO205I=1,3
407*           DO206J=1,3
408*           DO207K=1,3
409*           IF(I.EQ.1.AND.J.EQ.1.AND.K.EQ.1.OR.I.EQ.1.AND.J.EQ.1.AND.K.EQ.2.OR
410*          1.I.EQ.1.AND.J.EQ.1.AND.K.EQ.3.OR.I.EQ.1.AND.J.EQ.2.AND.K.EQ.1.OR.I
411*          2.EQ.1.AND.J.EQ.3.AND.K.EQ.1.OR.I.EQ.2.AND.J.EQ.1.AND.K.EQ.1.OR.I.E
412*          3Q.3.AND.J.EQ.1.AND.K.EQ.1)GO TO 2004
413*           GO TO 207
414*      2004 CONTINUE
415*           IF(ARMS(I,J,K).LT.ATEST)ATEST=ARMS(I,J,K)
416*       207 CONTINUE
```

```
417*        206 CONTINUE
416*        205 CONTINUE
419*            DO100I=1,3
420*            DO101J=1,3
421*            DO102K=1,3
422*            IF(I.EQ.1.AND.J.EQ.1.AND.K.EQ.1.OR.I.EQ.1.AND.J.EQ.1.AND.K.EQ.2.OR
423*           1.I.EQ.1.AND.J.EQ.1.AND.K.EQ.3.OR.I.EQ.1.AND.J.EQ.2.AND.K.EQ.1.OR.I
424*           2.EQ.1.AND.J.EQ.3.AND.K.EQ.1.OR.I.EQ.2.AND.J.EQ.1.AND.K.EQ.1.OR.I.E
425*           3Q.3.AND.J.EQ.1.AND.K.EQ.1)GO TO 2005
426*            GO TO 102
427*       2005 CONTINUE
428*            IF(ABS(ATEST-ARMS(I,J,K)).LT.1.E-20)GO TO 103
429*        102 CONTINUE
430*        101 CONTINUE
431*        100 CONTINUE
432*        103 CONTINUE
433*            MM=MM+1
434*      C  TEST FOR TERMINATION.
435*            IF(MM.EQ.1)GO TO 108
436*            IF(I.NE.1.OR.J.NE.1.OR.K.NE.1)GO TO 108
437*            IF(ANORMT.GE.8.)GO TO 200
438*            GO TO 350
439*        108 CONTINUE
440*            WIDTH(1)=WIDTH(I)
441*            DP(1)=DP(J)
442*            ALENGH(1)=ALENGH(K)
443*            IT1=ITIME(IT2,IT3)
444*            IF(IT1.LT.1.5E+5)GO TO 200
445*            GO TO 250
446*      C  RESULTANT MISMATCH PROCEEDURE IS CARRIED OUT.
447*        200 CONTINUE
448*            WRITE(6,370)I,J,K
449*        370 FORMAT(1H1,//,10X,'OPTIMUM CHOICE HAS INDICES (',I1,',',I1,',',I1,
450*           1')')
451*            WRITE(6,800)
452*        800 FORMAT(//,10X,'COORDINATE(I,J,K)',10X,'ROOT MEAN SQUARE OVER MATCH
453*           1ED BAND',//)
454*            DO802II=1,3
455*            DO803JJ=1,3
456*            DO804KK=1,3
457*            IF(II.EQ.1.AND.JJ.EQ.1.AND.KK.EQ.1.OR.II.EQ.1.AND.JJ.EQ.1.AND.KK.E
458*           1Q.2.OR.II.EQ.1.AND.JJ.EQ.1.AND.KK.EQ.3.OR.II.EQ.1.AND.JJ.EQ.2.AND.
459*           2KK.EQ.1.OR.II.EQ.1.AND.JJ.EQ.3.AND.KK.EQ.1.OR.II.EQ.2.AND.JJ.EQ.1.
460*           3AND.KK.EQ.1.OR.II.EQ.3.AND.JJ.EQ.1.AND.KK.EQ.1)GO TO 2006
461*            GO TO 804
462*       2006 CONTINUE
463*            WRITE(6,801)II,JJ,KK,ARMS(II,JJ,KK)
464*        801 FORMAT(21X,'(',I1,',',I1,',',I1,')',10X,F10.7)
465*        804 CONTINUE
466*        803 CONTINUE
467*        802 CONTINUE
468*            GO TO (398,498,598,698),MACHEL
469*      C*****************************************************************
470*        398 CONTINUE
471*            D(J)=B-DP(J)
472*            DO395KK=1,LE
473*            AB=SQRT(1.-(B/WL(KK))**2)
```

```
474*            AA(KK)=(1./AB)-1.
475*            GM=1.+(WIDTH(I)/(PI*DP(J)))*ALOG(4.*PI*DP(J)/(E*WIDTH(I)))
476*            CO(J)=COS(PI*DP(J)/(2.*B))
477*            SI(J)=SIN(PI*DP(J)/(2.*B))
478*            SE(J)=1./COS(PI*DP(J)*GM/(2.*B))
479*            BONE=PI*DP(J)*WIDTH(I)/(2.*B*D(J))
480*            BTWO=AA(KK)*(SI(J)**4)/(1.+AA(KK)*(CO(J)**4))
481*            BTRE=(1./16.)*((B/WL(KK))**2)*((1.-3.*(CO(J)**2))**2)*(SI(J)**4)
482*            BNORM=(2.*B/WL(KK))*(ALOG(SE(J))-BONE+BTWO+BTRE)
483*            BA=BNORM+(B/D(J))*TAN(PI*WIDTH(I)/WL(KK))
484*            BB=(B/D(J))*1./SIN(2.*PI*WIDTH(I)/WL(KK))
485*            YI=(0,1)*BA+1.
486*            ZII=((0,1)/BB)+1./YI
487*            YT=(0,1)*BA+1./ZII
488*            BGAM=(YT-1.)/(1.+YT)
489*            GGAM(I,J,KK,K)=BGAM*CEXP((0,1)*2.*BETA(KK)*ALENGH(K))
490*            IF(ALENGH(K).GE.0.)GGAM(I,J,KK,K)=BGAM
491*            AGAM(K,KK)=GAM(KK)*CEXP((0,-1)*2.*BETA(KK)*ALENGH(K))
492*            IF(ALENGH(K).LT.0.)AGAM(K,KK)=GAM(KK)
493*            GAMMA(KK)=(AGAM(K,KK)+GGAM(I,J,KK,K)-2.*AGAM(K,KK)*GGAM(I,J,KK,K))
494*           1/(1.-AGAM(K,KK)*GGAM(I,J,KK,K))
495*       395 CONTINUE
496*            DH=DP(J)/2.
497*            WRITE(6,226)
498*       226 FORMAT(1H1,///,10X,'CAPACITIVE IRIS IS THE MATCHING ELEMENT')
499*            WRITE(6,242)ANCRMT
500*       242 FORMAT(//,10X,'NUMBER OF INCREMENT = ',F4.0)
501*            WRITE(6,270)FR(JBEG),FR(JEND)
502*       270 FORMAT(//,10X,'MATCHED BAND IS FROM ',F7.3,' GHZ. TO ',F7.3,' GHZ.
503*           1')
504*            WRITE(6,227)WIDTH(I),DH,ALENGH(K)
505*       227 FORMAT(//,10X,'THICKNESS=  ',F6.4,1X,'IN CM',10X,'HEIGHT=  ',F6.4
506*           1,' IN CM',10X,'DISTANCE TOWARD THE GEN. FROM MISMATCH=  ',F8.4)
507*            GO TO 999
508*      C*****************************************************************
509*       498 CONTINUE
510*            CAPDP=(DP(J)/SQTWO)*(1.+(WIDTH(I)/(PI*DP(J)))*ALOG(4.*PI*DP(J)/(E*
511*           1WIDTH(I))))
512*            CAPD=((4./(3.*PI))*WIDTH(I)*DP(J)**3)**(1./4.)
513*            DO496KK=1,LE
514*        C   XA AND XB ARE NORMALIZED IMPEDANCES.
515*            XA=(4.*A/WL(KK))*((A/(PI*CAPDP))**2)
516*            XB=(A/(16.*WL(KK)))*((PI*CAPD/A)**2)
517*            ZI=(0,-1)*XB+1.
518*            ZII=(1./((1./((0,1)*XA))+1./ZI))
519*            ZT=(0,-1)*XB+ZII
520*            BGAM=(1.-ZT)/(1.+ZT)
521*            GGAM(I,J,KK,K)=BGAM*CEXP((0,1)*2.*BETA(KK)*ALENGH(K))
522*            IF(ALENGH(K).GE.0.)GGAM(I,J,KK,K)=BGAM
523*            AGAM(K,KK)=GAM(KK)*CEXP((0,-1)*2.*BETA(KK)*ALENGH(K))
524*            IF(ALENGH(K).LT.0.)AGAM(K,KK)=GAM(KK)
525*            GAMMA(KK)=(AGAM(K,KK)+GGAM(I,J,KK,K)-2.*AGAM(K,KK)*GGAM(I,J,KK,K))
526*           1/(1.-AGAM(K,KK)*GGAM(I,J,KK,K))
527*       496 CONTINUE
528*            DH=DP(J)/2.
529*            WRITE(6,405)
530*       405 FORMAT(1H1,///,10X,'INDUCTIVE ASYMMETRICAL IRIS IS THE MATCHING EL
```

```
531*          1EMENT')
532*           WRITE(6,406)ANCRMT
533*       406 FORMAT(//,10X,'NUMBER OF INCREMENT = ',F4.0)
534*           WRITE(6,470)FR(JBEG),FR(JEND)
535*       470 FORMAT(//,10X,'MATCHED BAND IS FROM ',F7.3,' GHZ. TO ',F7.3,' GHZ.
536*          1')
537*           WRITE(6,407)WIDTH(I),DH,ALENGH(K)
538*       407 FORMAT(//,10X,'THICKNESS = ',F6.4,1X,'CM.',10X,'HEIGHT = ',F6.4,'
539*          1CM.',10X,'DISTANCE TOWARD THE GEN. FROM MISMATCH = ',F8.4)
540*           GO TO 999
541*     C*****************************************COMMON*OUTPUT***************
542*       598 CONTINUE
543*     C  MATCHING ELEMENT 'SOLID INDUCTIVE POST' COMPLEX REFLECTION COEFF.
544*     C  AS A FUNCTION OF DIMENSION P
545*     C  AS A FUNCTION OF DIMENSION SPACE AND FREQUENCY.
546*     C  DP(I) IS DEFINED TO BE THE DIAMETER OF THE POST.
547*     C  WIDTH(I) IS DEFINED TO BE THE DISTANCE OF THE CENTER LINE OF THE POST
548*     C  FROM THE SIDE-WALL.
549*           DO525KK=1,LE
550*           N=2
551*           M=2
552*           XSII=0.0
553*           XSOO=0.0
554*       513 XI=SQRT(1./((N**2)-((2.*A/FSWL(KK))**2)))
555*           XSO=((SIN(N*PI*WIDTH(I)/A))**2)*(XI-1./N)
556*           XSOO=XSO+XSOO
557*           IF(XSO.LE..001)GO TO 515
558*       514 N=N+1
559*           GO TO 513
560*       515 XI=SQRT(M**2/((M**2)-((2.*A/FSWL(KK))**2)))
561*           XSI=((SIN(2.*M*PI*WIDTH(I)/A))*(XI-1.))
562*           XSII=XSI+XSII
563*           ABXSI=ABS(XSI)
564*           IF(ABXSI.LE..001)GO TO 517
565*       516 M=M+1
566*           GO TO 515
567*       517 CONTINUE
568*           SOP(I,KK)=XSOO*2.-2.*((SIN(PI*WIDTH(I)/A))**2)
569*           SII(I,KK)=XSII+(.5*(1./TAN(PI*WIDTH(I)/A))-SIN(2.*PI*WIDTH(I)/A))
570*       525 CONTINUE
571*           CT=1./TAN(PI*WIDTH(I)/A)
572*           CSS=(1./SIN(PI*WIDTH(I)/A))**2
573*           SNS=(SIN(PI*WIDTH(I)/A))**2
574*           PDOA=(PI*DP(J)/A)**2
575*           PDO=(PI*DP(J)/(A*2.))**2
576*           SOPP=ALOG((4.*A/(PI*DP(J))*SIN(PI*WIDTH(I)/A)))
577*           DO526KK=1,LE
578*     C  XA AND XB ARE NORMALIZED IMPEDANCES.
579*           XB=(A/WL(KK))*PDOA*SNS
580*           XA=XB/2.+A/(2.*WL(KK))*CSS*(SOPP+SOP(I,KK)-((PI*DP(J)/(2.*A))**2)*
581*          1(((SOPP+SOP(I,KK))*CT-SII(I,KK))**2))
582*           ZI=(0.,-1)*XB+1.
583*           ZII=(1./((1./((0,1)*XA))+1./ZI))
584*           ZT=(0.,-1)*XB+ZII
585*           BGAM=(1.-ZT)/(ZT+.1)
586*           GGAM(I,J,KK,K)=BGAM*CEXP((0,1)*2.*BETA(KK)*ALENGH(K))
587*           IF(ALENGH(K).GE.0.0)GGAM(I,J,KK,K)=BGAM
```

```
588*      C  I CORRES TO DISTANCE OF POST FROM SIDE WALL.
589*      C  J CORRES TO DIAMETER OF POST.
590*      C  KK CORRES TO FREQUENCY.
591*      C  K CORRES TO DISTANCE BETWEEN MISMATCHES.
592*           AGAM(K,KK)=GAM(KK)*CEXP((0.,-1)*2.*BETA(KK)*ALENGH(K))
593*           IF(ALENGH(K).LT.0.0)AGAM(K,KK)=GAM(KK)
594*           GAMMA(KK)=(AGAM(K,KK)+GGAM(I,J,KK,K)-2.*AGAM(K,KK)*GGAM(I,J,KK,K))
595*          1/(1.-AGAM(K,KK)*GGAM(I,J,KK,K))
596*       526 CONTINUE
597*           WRITE(6,519)
598*       519 FORMAT(1H1,///,10X,'SOLID INDUCTIVE POST IS THE MATCHING ELEMENT')
599*           WRITE(6,520)ANCRMT
600*       520 FORMAT(//,10X,'NUMBER OF INCREMENT = ',F4.0)
601*           WRITE(6,521)FR(JBEG),FR(JEND)
602*       521 FORMAT(//,10X,'MATCHED BAND IS FROM ',F6.3,' GHZ.',' TO ',F6.3,' G
603*          1HZ.')
604*           WRITE(6,522)DP(J),WIDTH(I),ALENGH(K)
605*       522 FORMAT(//,10X,'DIAMETER = ',F6.4,' CM.',10X,'SIDEWALL DISTANCE =
606*          1',F6.4,' CM.',10X,'DISTANCE TOWARD THE GEN. FROM MISMATCH = ',F8.4)
607*           GO TO 999
608*     C*****************************************************************
609*       698 CONTINUE
610*           DO620N=1,LE
611*           ALPHA(J,N)=PI*DP(J)/FSWL(N)
612*           BETE(J,N)=ALPHA(J,N)*SQEPRM
613*           BESOA(J,N)=BSSL(ALPHA(J,N),1)
614*           BESOB(J,N)=BSSL(BETE(J,N),1)
615*           BESIA(J,N)=BSSL(ALPHA(J,N),3)
616*           BESIB(J,N)=BSSL(BETE(J,N),3)
617*       620 CONTINUE
618*           DO621L=1,LE
619*           N=2
620*           XSOO=0.0
621*       622 XI=SQRT(1./((N**2)-((2.*A/FSWL(L))**2)))
622*           XSO=((SIN(N*PI*WIDTH(I)/A))**2)*(XI-1./N)
623*           XSOO=XSO+XSOO
624*           IF(XSO.LE..001)GO TO 624
625*       623 N=N+1
626*           GO TO 622
627*       624 CONTINUE
628*           SOP(I,L)=XSOO*2.-2.*((SIN(PI*WIDTH(I)/A))**2)
629*       621 CONTINUE
630*           SOPP=ALOG((4.*A/(PI*DP(J))*SIN(PI*WIDTH(I)/A)))
631*           DO625M=1,LE
632*           XB=(2.*A/WL(M))*((PI*DP(J)/A)**2)*(SIN(PI*WIDTH(I)/A)**2)/(((ALPHA
633*          1(J,M)**2)*BESIB(J,M)/BESIA(J,M))+(1./(ALPHA(J,M)*BESOA(J,M)*
634*          2BESIB(J,M)-BETE(J,M)*BESOB(J,M)*BESIA(J,M)))-2.)
635*           XA=.5*XB+(A/(2.*WL(M)))*(1./(SIN(PI*WIDTH(I)/A)**2))*((BESOB(J,M)/
636*          1BESOA(J,M))*(1./(BETE(J,M)*BESOA(J,M)*BESIB(J,M)-ALPHA(J,M)*
637*          2BESOB(J,M)*BESIA(J,M)))-(SOPP+SOP(I,M))+(ALPHA(J,M)/4.))
638*           YI=1./((0,1)*XB+1.)
639*           YII=1./((0,-1)*XA)+YI
640*           YT=1./((0,1)*XB+1./YII)
641*           BGAM=(YT-1.)/(1.+YT)
642*           GGAM(I,J,M,K)=BGAM*CEXP((0,1)*2.*BETA(M)*ALENGH(K))
643*           IF(ALENGH(K).GE.0.)GGAM(I,J,M,K)=BGAM
644*           AGAM(K,M)=GAM(M)*CEXP((0,-1)*2.*BETA(M)*ALENGH(K))
```

```
645*            IF(ALENGH(K).LT.0.)AGAM(K,M)=GAM(M)
646*            GAMMA(M)=(AGAM(K,M)+GGAM(I,J,M,K)-2.*AGAM(K,M)*GGAM(I,J,M,K))/(1.-
647*           1AGAM(K,M)*GGAM(I,J,M,K))
648*         625 CONTINUE
649*            WRITE(6,626)
650*         626 FORMAT(1H1,////,10X,'DIELECTRIC POST IS THE MATCHING ELEMENT')
651*            WRITE(6,627)ANCRMT
652*         627 FORMAT(//,10X,'NUMBER OF INCREMENT = ',F4.0)
653*            WRITE(6,628)FR(JBEG),FR(JEND)
654*         628 FORMAT(//,10X,'MATCHED BAND IS FROM ',F7.3,' GHZ. TO ',F7.3,' GHZ.
655*           1')
656*            WRITE(6,629)WIDTH(I),DP(J),ALENGH(K)
657*         629 FORMAT(//,10X,'DISTANCE FROM SIDEWALL = ',F6.4,1X,'CM.',5X,'DIAMET
658*           1ER = ',F6.4,' CM.',5X,'DISTANCE TOWARD THE GEN. FROM MISMATCH = ',
659*           2F8.4)
660*      C*****************************************************************
661*         999 CONTINUE
662*            WRITE(6,228)
663*         228 FORMAT(//,10X,'RESULTANT MISMATCH')
664*            WRITE(6,229)
665*         229 FORMAT(//,10X,'FREQUENCY IN GHZ.',10X,'MAG. REFL. COEFF.',10X,'VSW
666*           1R',10X,'MAG.REFL.COEFF.DISURB.',//)
667*            DO240N=1,LE
668*            AMAG=CABS(GAMMA(N))
669*            VSWR=(1.+AMAG)/(1.-AMAG)
670*            AMMAG=CABS(GAM(N))
671*            VSWRR=(1.+AMMAG)/(1.-AMMAG)
672*            X(N)=VSWRR
673*            WRITE(6,230)FR(N),AMAG,VSWR,AMMAG
674*         230 FORMAT(10X,F8.3,15X,F10.5,12X,F8.4,10X,F10.5)
675*         240 CONTINUE
676*            WRITE(6,231)
677*         231 FORMAT(1H1,///,45X,'MATCHING ELEMENT',38X,'UNMATCHED ELEMENT')
678*            WRITE(6,232)
679*         232 FORMAT(//,10X,'FREQUENCY',10X,'REAL REFL. COEFF.',10X,'IMAG REFL.
680*           1 COEFF.',10X,'REAL REFL. COEFF.',10X,'IMAG. REFL. COEFF.',//)
681*            DO241N=1,LE
682*            WRITE(6,233)FR(N),GGAM(I,J,N,K),GAM(N)
683*         233 FORMAT(10X,F8.3,14X,F10.6,16X,F10.6,15X,F10.6,15X,F10.6)
684*         241 CONTINUE
685*      C  PUNCH DATA CARDS.
686*            DO1001N=1,LE
687*            REL(N)=REAL(GAM(N))
688*            YIMAG(N)=AIMAG(GAM(N))
689*        1001 CONTINUE
690*            DO1003N=1,LE
691*            REL(N)=REAL(GAMMA(N))
692*            YIMAG(N)=AIMAG(GAMMA(N))
693*        1003 CONTINUE
694*            WRITE(1,1004)(REL(N),N=LE,1,-1)
695*            WRITE(1,1004)(YIMAG(N),N=LE,1,-1)
696*        1004 FORMAT(8F10.6)
697*      C  PLOT COMPARISON BETWEEN UNMATCHED AND MATCHED DISTURBANCE.
698*            DO3000N=1,LE
699*            Y(N)=FR(N)
700*         3000 CONTINUE
701*            RB=X(1)
```

```
      DO3001N=1,LE
      IF(X(N).GT.RB)RB=X(N)
 3001 CONTINUE
      VLBND=1.
      VUBND=RB
      CALL PLOT(10.,-3.,-3)
      REAL LTRSZ,LENGTH
      LOGICAL BOX,FIXLIM,USELIM
      DATA HTITLE/'FREQUENCY IN GHZ.
     2                    '/
      DATA VTITLE/'VOLTAGE STANDING WAVE RATIO
     2                    '/
      DO3002NA=1,2
      IF(NA.EQ.1)GO TO 3003
      DO3004N=1,LE
      AR=CABS(GAMMA(N))
      X(N)=(1.+AR)/(1.-AR)
 3004 CONTINUE
 3003 CONTINUE
      MODE=1
      IF(NA.EQ.2)MODE=4
      LTRSZ=.1
      UP=4.5
      OVER=0.0
      HEIGHT=4.5
      LENGTH=4.5
      HLBND=Y(1)
      HUBND=Y(LE)
      ICOUNT=LE
      BOX=.TRUE.
      USELIM=.TRUE.
      FIXLIM=.TRUE.
      NUMINT=20
      CALL PLOTY(MODE,X,Y,ICOUNT,UP,OVER,HEIGHT,LENGTH,BOX,FIXLIM,USELIM
     1 ,NUMINT,VTITLE,HTITLE,LTRSZ,VLBND,VUBND,HLBND,HUBND,PERCNT)
 3002 CONTINUE
      CALL PLOT(0.0,0.0,999)
      END

END OF COMPILATION:      NO  DIAGNOSTICS.
```

APPENDIX C

DERIVATION OF THE IMPEDANCE MATCHING EQUATION

The objective of this derivation is to establish the key equation which has been used in the impedance matching technique. Due to the comparison reflectometers' unique ability to locate discontinuities in an otherwise matched waveguide and to determine the reflection coefficient as a function of frequency for each disturbance, it will only be necessary to deal with two disturbances at a time, the original mismatch and the matching element.

The reflection coefficient measured and calculated in this thesis apply to the admittance Smith chart. The following derivation also applies to the admittance Smith chart.

The following equations will be required:

Phase propagation constant

$$\beta = 2\pi/\lambda_g \tag{C-1}$$

Current reflection coefficient

$$\Gamma_{Io} = |\Gamma_{Io}| \exp[j\theta_o] \tag{C-2}$$

Current reflection coefficient generated by the disturbance having the shunt admittance Y, where the characteristic admittance is Y_o

$$\Gamma_I = (Y-Y_o)/(Y+Y_o) \qquad \text{(C-3)}$$

Generalized current reflection coefficient

$$\Gamma_I = \Gamma_{Io}\exp[-j2BS] = |\Gamma_{Io}|\exp[j\theta_o]\exp[-j2BS] \qquad \text{(C-4)}$$

Given a transmission line:

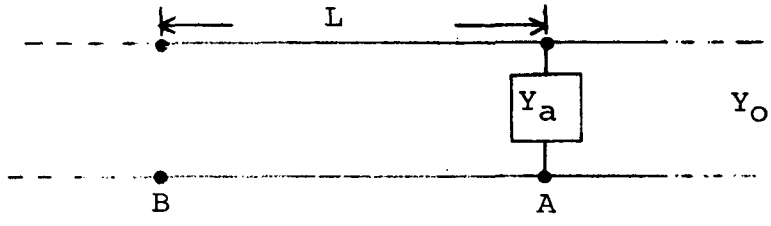

Figure 91. Transmission Line with Disturbance

The quantity Y_a is a single shunt admittance in an otherwise uniform transmission line. The total admittance at point A is that formed by Y_a and the characteristic admittance of the line, and is given by:

$$Y'_a = Y_a + Y_o \tag{C-5}$$

This admittance defines the current reflection coefficient Γ_{Ia} at A by Equation (C-3). (C-6)

$$\Gamma_{Ia} = Y_a/(Y_a+2Y_b)$$

The reflection coefficient at point B is given in terms of Γ_{Ia} and L (the distance from A to B) as:

$$\Gamma_{Iab} = \Gamma_{Ia}\exp[-j2BL] \tag{C-7}$$

Similarly, if the only disturbance in the transmission line were a shunt admittance Y_b at B, the reflection coefficient at point B is given by:

$$\Gamma_{Ib} = Y_b/(Y_b+2Y_o) \tag{C-8}$$

Consider now, both Y_a and Y_b in the transmission line as in Figure 89.

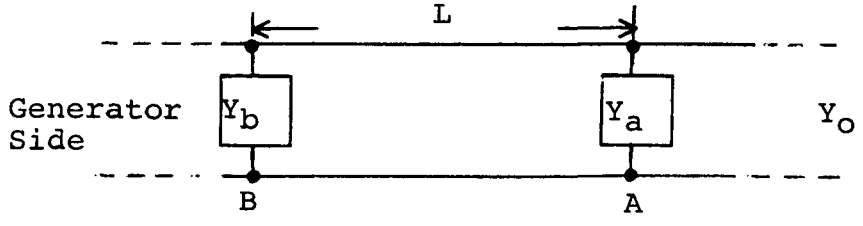

Figure 92. Transmission Line Containing a Discontinuity at Point A and Point B

The total admittance at point A looking away from the generator is given by Equation (C-5). On the load side of Y_b at point B the admittance is given by :

$$Y/Y_o = (y'_a/y_o + j \tan \beta L)/[1+j(y_a/y_o)\tan \beta L] . \quad \text{(C-9A)}$$

Defining normalized admittance $y = Y/Y_o$ and $y'_a = Y'_a/Y_o$, Equation (C-9) can be expressed as:

$$y = (y'_a + j \tan \beta L)/(1+j\, y'_a \tan \beta L) . \quad \text{(C-9B)}$$

The total admittance on the generator side of point B is given by Equation (C-10).

$$(y_t = y_b + (y_a+1+j \tan \beta L)/[1+j(y_a+1)\tan \beta L] . \quad \text{(C-10)}$$

Simplifying the above we have:

$$y_t = \frac{y_a+y_b+1+j(y_b+y_a y_b+1)\tan \beta L}{1+j(y_a+1)\tan \beta L} .$$

Substituting y_t into Equation (C-3), the reflection coefficient as pertaining to the admittance Smith chart is given by:

$$\Gamma_{It} = \frac{2y_a \exp(-j2\beta L) + y_a y_b - y_a y_b \exp(-j2\beta L) + 2y_b}{4 + 2y_a + 2y_b + y_a y_b - y_a y_b \exp(-j2\beta L)} \qquad \text{(C-11)}$$

From Equation (C-6) and (C-8), y_a and y_b can be expressed in terms of Γ_{Ia} and Γ_{Ib}.

$$y_a = -2\Gamma_{Ia}/(\Gamma_{IB}-1) \qquad \text{(C-12)}$$

$$y_b = -2\Gamma_{Ib}/(\Gamma_{IB}-1) \qquad \text{(C-13)}$$

Substituting (C-12) and (C-13) into (C-11) and simplifying:

$$\Gamma_{It} = \frac{\Gamma_{Ia}\exp(-j2\beta L) + \Gamma_{Ib} - 2\Gamma_{Ia}\Gamma_{Ib}\exp(-j2\beta L)}{1 - \Gamma_{Ia}\Gamma_{Ib}\exp(-j2\beta L)} \qquad \text{(C-14)}$$

Equation (C-14) expressed the total current reflection coefficient at point B as a result of y_a and y_b. This total current reflection coefficient is in terms of the reflection coefficient Γ_{Ia} and Γ_{Ib} which are defined by Equations (C-6) and (C-8) respectively, Γ_{It}, Γ_{Ia}, and Γ_{Ib} are reflection coefficient referenced to the admittance Smith chart.

Expressing Γ_{It} in the form of Equation (C-14) is particularly compatable with the comparison reflectometer. For example, for a positive distance L, Γ_{Ia} corresponds to

the mismatch measured by the comparison reflectometer and Γ_{Ia} corresponds to the matching element a distance L toward the generator from the mismatch. The total mismatch resulting from this match is given by Γ_{It}. The objective of this research is to reduce Γ_{It} to the lowest possible value over the bandwidth of interest.

APPENDIX D

COMPARISON REFLECTOMETER OPERATING PROCEDURE

The setup procedure is referenced to the reflectometer setup of Figure 23. In the following paragraphs it will be assumed that the operator has recently assembled the comparison reflectometer and a complete calibration of the system is required. It will also be assumed that the individual components of the system are in good condition and meet their individual specifications.

In order to reduce 60 Hz powerline ripple from interfering with the 1 KHz modulated r.f., it was found necessary to float the comparison reflectometer above ground. This was done by plugging all of the units into the powerline using two-to-three prong adaptors, leaving the pig tails ungrounded.

When energizing the comparison reflectometer it is essential to turn on the coherent synchronizer first and then the BWO. This prevents possible damage to the BWO helix. Consequently, when shutting down the units the BWO should be shut down first followed by the coherent synchronizer.

Coherent Synchronizer

The LFE Model 244 should be set up using the following procedure when used in the comparison reflectometer setup.

(1) Switch the front panel switch to multiply.

(2) Switch the reference mode to tunable.

(3) Switch the frequency tune to fixed.

(4) Turn signal level approximately 1/4 revolution from full on.

(5) Switch frequency fine tune to the 8-16 GHz range.

(6) Switch the front panel switch to 50 MHz marker position.

(7) Switch mode switch to 16-32 MHz/volt oscillator sensitivity on back panel.

(8) Connect 25 MHz tap TP1 to the input of a high impedance scope.

(9) Connect power line plug to powerline stabilizing transformer.

(10) Switch on power to unit.

(11) Turn phase lock error voltage to off.

(12) Allow approximately one hour to warm up.

This unit is now ready for the final operating procedure.

Type 210 Sweep Oscillator

The AIL BWO should be set up using the following procedure when used in the comparison reflectometer setup.

(1) Insert the 8.0-12.4 GHz plugin.

(2) Push sweep select button to slow.

(3) Turn rate inner knob clockwise, sweeper will stop after a single sweep.

(4) Outer rate knob is used for fine rate adjust.

(5) Push off button under AM.

(6) Depress blank button.

(7) Depress XTAL button.

(8) Attach output from crystal detector on directional coupler C2 to input of oscillator plugin, Figure 23.

(9) Connect 200 micro farad external capacitor to range ext. BNC on back panel.

(10) Plug in power line connector.

(11) Depress line button and wait for the r.f. light to go on.

(12) Switch r.f. knob on plugin to on position.

(13) Adjust level control to obtain -10 dBm (.1 mw) power level at the output of directional coupler C3, Figure 23.

The unit is now set up for final operating procedure.

Audio Oscillator

Set audio oscillator to 1 KHz. This can be done by connecting the output of the audio oscillator to the input of the Hewlett-Packard 5211A electronic counter and adjusting the oscillator for a 1 KHz counter reading.

Turn the gain down on the audio oscillator and connect its output to the bias connector of the waveguide modulator. Connect a high impedance oscilloscope's input to the crystal detector on C3, Figure 23. Increase the audio oscillator gain until a square wave is observed on the scope. Care must be taken not to exceed the maximum

rating on the bias level of the modulator.

Ratio Meter

The Hewlett-Packard Model 416B ratio meter should be set up using the following procedure when used in the comparison reflectometer setup. The reference step should be terminated in a matched load.

(1) Turn the error voltage gain up until a phase lock is registered on the level meter of the coherent synchronizer. This will stabilize the frequency, and therefore, also the amplitude of the reflected wave.

(2) Connect the incident and reflected inputs to detectors on C_3 and C_4 respectively.

(3) Plug in ratio meter power line using adapter.

(4) Switch detector to XTAL.

(5) Switch excess incident attenuation to 10 db.

(6) Switch reference attenuator to -30 db.

(7) Switch on power to the unit.

(8) Allow unit to warm up for one hour.

(9) Adjust reference adjust for a 100% scale reading.

(10) Measure voltage at output using the Dymec voltage measuring system.

(11) Adjust output voltage, using the control on the back panel, to 6.928 volts. This voltage is Emax.

(12) Readjust reference adjust to center of scale. This unit is now set up for the final operating procedure.

Voltage Measurement System

The Dymec model DY-552A voltage measuring and recording system is comprised of the model DY-2210 voltage-to-frequency converter, the H.P. model 5211A/B electronic counter, the model DY-2540 scanner/coupler, and the motorized tape punch. This system should be set up according to the following procedure when used as part of the comparison reflectometer setup.

(1) Switch on power to voltage-to-frequency converter.

(2) Switch range switch to 10 volt.

(3) Connect output of ratio meter to input of voltage-to-frequency converter.

(4) Connect output of voltage-to-frequency converter to input of electronic counter.

(5) Make proper zero adjustment and calibrate voltage-to-frequency converter.

(6) Switch on power to electronic counter.

(7) Turn sample rate to the hold position.

(8) Turn sensitivity half way.

(9) Switch function switch to frequency/second position.

(10) Switch on power to scanner/coupler.

(11) Switch start switch to automatic.

(12) Switch decay switch on back of panel to fast.

(13) Switch back panel switch to tape.

(14) Plug in push button to remote reset according to the diagram on back panel of electronic counter.

(15) Switch on tape punch.

This unit is now set up and ready for the system final operating procedure.

Coherent Synchronizer Spectrum Test

If a reliable phase lock is to be made at 50 MHz intervals, the coherent synchronizer must be in good operating condition. It is important that the spectrum be relatively flat and that all phase lock points be achievable. This is checked by tapping the 25 MHz signal from the 25 MHz amplifier and displaying it on a high impedance oscilloscope. A representation of the varactor spectrum can be then observed by sweeping the leveled RF input of the BWO and observing the IF signal on an oscilloscope. A small wire was replaced in the coaxial varactor mount, shorting the center post to the grounded outer conductor. The distributive inductance and capacitance of this wire serves to impedance match the varactor to the varactor mount.

The coherent synchronizers RF input was initially connected to the directional coupler by a type N adapter and a type N cable to the type N connector of the coherent synchronizer. It was experimentally determined that the frequency response of the cable interferred with the operation of the varactor. A solid type N coaxial line replaced the cable, and the varactor spectrum was then

adjusted so as to provide a flat harmonic spectrum from 8.0 GHz to 12.4 GHz. These adjustments allow phase lock points from 7.975 GHz to 12.425 GHz.

Adjust the lock range to zero on the front panel of the coherent synchronizer. Depress the fast button on the AIL BWO sweeper and turn the sweep knob to the clockwise position for repetitive sweep. Use the sweep output of the swept oscillator to trigger the oscilloscope and depress the blanking button on the sweep oscillator plugin.

Adjust the oscilloscopes' time sweep until one full sweep of the BWO fits within the scope, Figure 93. What is actually seen is the level of the 25 MHz signal as the RF to the input of the coherent synchronizer is swept. Therefore, the characteristics of the bandpass of the I.F. amplifier is reproduced every time the BWO frequency is within

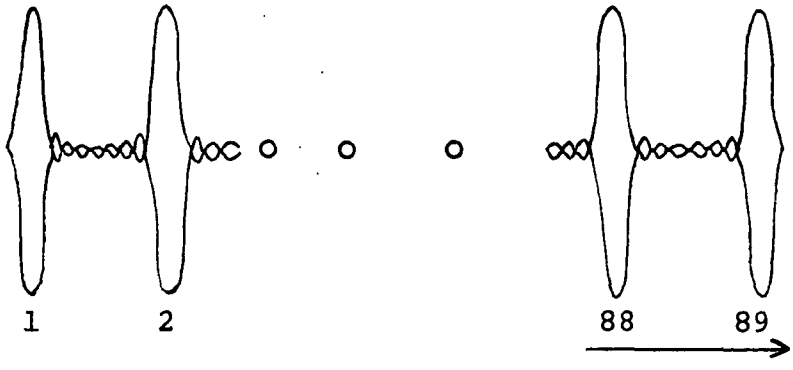

Figure 93. Display Showing the I.F. Band Pass as the RF Input is Swept

25 MHz of a varactor harmonic, Figure 25. The level control on the front panel of the coherent synchronizer should be adjusted to achieve as much gain as possible and yet to keep the noise level down. This can easily be done, since there is a point where increasing the gain increases the noise level sharply. The varactor should be adjusted such that the amplitude level of the peaks of the response of Figure 90 are relatively constant. Since this adjustment for the model 244 is a tedious one of trial and error, it is suggested that as much care as possible be taken with this instrument.

System Operating Procedure. With all individual instruments operating according to the previously discussed procedures, the system is now ready to be set up for measurements.

(1) Depress the slow button on the sweep oscillator.

(2) Turn the rate inner knob clockwise, to single sweep and stop position.

(3) Turn outer knob half way.

(4) Attach the test element to the comparison reflectometer as in Figure 23.

(5) Depress sweep button on sweep oscillator.

(6) While oscillator is in the process of a slow sweep, monitor the meter on the ratio meter and adjust reference control to ensure that the needle remains in the range of the meter scale. Steps 5 and 6 may need repeating

so that in a single sweep, without changing controls, the needle swings symmetrically on the scale.

(7) Reduce the sweep rate such that it takes approximately 15 minutes to sweep the band one time. This time can be reduced as the operator gains experience with the equipment.

(8) Set the oscilloscope to internal trigger and set the sweep rate to maximum. Adjust the scope gain such that the 25 MHz wave will half fill the screen when a phase lock has occured. This can be done by turning the lock range to maximum. When the scope adjustment has been made return the lock range to zero.

(9) Adjustment of the lock range determines the phase lock duration. During the phase lock duration a measurement is taken with a normally closed push button. On the particular model 224 used in this research the control was set approximately 1/64 inch above the zero volt line. This setting is best made after working with the control while making a sweep.

(10) Depress the front panel start button. This starts the slow sweep. As the frequency increases the waveform will increase on the oscilloscope and the level on the level meter will increase. When a phase lock is made the phase of the sine wave on the oscilloscope will change phase by 180° and will remain very stable in amplitude and phase. The level meter will jump as the phase is locked

and remain at that level. The phase meter on the coherent synchronizer which is an indication of the error voltage on the helix of the BWO, will begin to move, as the internal sweep attempts to change the BWO frequency. At this time a measurement is taken by depressing the hand held push button, Figure 23. When the error voltage is at its maximum setting and can no longer hold the BWO, the phase lock is broken. The phase meter centers, the level drops to zero and the sine wave disappears from the scope. The BWO jumps to a higher frequency and continues to increase slowly until again phase locked automatically. This is done 89 times and gives one set of measurements.

The second set of measurements is taken with the reference step terminated in the matched load, Figure 23. The procedure is the same as that described in the above paragraphs. It is important not to change any adjustment on the ratiometer or measuring equipment during the two sets of measurements, since the two will be compared during the calculations (III-31).

When measurements are completed, the information on the tapes is punched on data cards by a tape to card converter. These data cards are then used as data in the reflectometer computer programs, Appendix B.

BIBLIOGRAPHY

1. Hollway, D. L., "The Comparison Reflectometer," I.E.E.E. Transactions Microwave Theory and Technique, Vol. MTT-15, No. 4, April 1967.

2. Paris, D. T. and Hurd, F. K., Basic Electromagnetic Theory, McGraw-Hill, Inc., 1969.

3. Krutter, H., "Explanation of Impedance Matching," M.I.T. Radiation Laboratory Report T-6, 250-259, 1942.

4. Engen, G. F. and Beatty, R. W., "Microwave Reflectometer Techniques," I.R.E. Transactions Microwave Theory and Technique, pp. 351-355, July 1959.

5. Operating and Service Manual, Ratio Meter Model 416B, Hewlett-Packard, Section IV, Paragraphs 4-1 to 4-15.

6. de Ronde, F. C., "A Precise and Sensitive K-Band Reflecto "meter" Providing Automatic Full-Band Display of Reflection Coefficient," I.E.E.E. Transactions Microwave Theory and Techniques, pp. 435-440, July 1965.

7. Hewlett-Packard, Microwave Theory and Measurements, Prentice-Hall, Englewood Cliffs, N. J., 1962.

8. Ginzton, E. L., Microwave Measurements, McGraw-Hill, 1957

9. Hewlett-Packard, "Cable Testing with Time Domain Reflectometry," Application Note 67, May 1968.

10. Hewlett-Packard, "Narrowband TDR Locates Waveguide Faults," Microwave Journal, Vol. 13, pp. 16, December 1970.

11. Hewlett-Packard, "Microwave Network Analyzer Applications," Application Note 117-1, June 1970.

12. Hollway, D. L., "The Comparison.Reflectometer: Operation and Maintenance," National Standards Laboratory Division of Applied Physics, December 1967, (Internal Report).

13. Marcuvitz, N., Waveguide Handbook, Dover Publications, Inc., 1965.

14. Hewlett-Packard Co., "Ratiometer Model 416B, Operating and Service Manual", June 1968.

15. de Ronde, F. C., "Full-Band Matching of Waveguide Discontinuities," Rough draft of a paper to be presented at the G-MTT 1966 International Microwave Symposium, May 16-19 1966.

16. Detlefsen, J., "Frequency Response of Input Impedance Implies the Distribution of Discontinuities of a Transmission-Line System," Electronic Letter, Vol. 6, February 1970, pp. 67-69.

17. Kraus, John D., Electromagnetics, McGraw-Hill, Inc., 1953.

18. Lewin, L., "Reflection Cancellation in Waveguides," Wireless Engineer, Vol. 26, No. 311, pp. 258-264, 1949.

19. Moreno, T., Microwave Transmission Design Data, Dover Publications, Inc., 1958.

20. Muehe, C. E., "Band-Pass Time-Domain Reflectometry, "I.E.E.E. Internation Convention Record, 1969, pp. 416-417.

21. Parr, J. C., "Matching Discontinuities in Waveguides," Wireless Engineer, Vol. 30, pp. 243-249, 1953.

22. Somlo, P. I., "The Locating Reflectometer," I.E.E.E. Transactions on Microwave Theory and Techniques, Vol. MTT-20, No. 2, February 1972.

23. Whinnery, J. R., and Jamieson, H. W., "Equivalent Circuits for Discontinuities in Transmission Lines," Proceedings of I.R.E., pp. 98-114, February 1944.

VITA

Robert Stephen Gordy was born on [redacted], in [redacted], the son of Lily Anparo Duke and the stepson of John Gilbert Duke. He was married to Donna Kathryn Bostian of Tampa, Florida, in March, 1963, and has two daughters.

He attended public schools in Tampa, Florida, and graduated from H. B. Plant High School in June 1960. In March, 1963, he received an honorable discharge from the United States Navy and in June, 1968, received a B.S.E. degree from the University of South Florida.

In September, 1968, Mr. Gordy entered the Electrical Engineering graduate school at the Georgia Institute of Technology. He received the M.S.E.E. degree in June, 1970. He held a position of graduate research assistant from January, 1969, to June, 1972.

From 1968 to 1971 he held a National Aeronautics and Space Administration Trainee Fellowship.